THE DEVELOPMENT AND APPLICATION OF ANALYTICAL METHODS FOR THE IDENTIFICATION OF DYES ON HISTORICAL TEXTILES

DAVID ALEXANDER PEGGIE

DOCTOR OF PHILOSOPHY

THE UNIVERSITY OF EDINBURGH

FEBRUARY 2006

DECLARATION

I declare that this thesis is my own composition, that the work described herein has been carried out by me, unless otherwise stated, and that it has not been submitted in any previous application for a higher degree.

This thesis describes the results of research carried out since the 1st October 2002, the date of my admission as a research student. The work was conducted in the School of Chemistry, The University of Edinburgh, under the supervision of Prof. Hamish McNab and Dr Alison Hulme, and in the Conservation and Analytical Research department of the National Museums of Scotland, under the supervision of Dr Anita Quye.

To my parents

Thank you

We shall not cease from exploration
And the end of all our exploring
Will be to arrive where we started
And know the place for the first time

From *Little Gidding* (Four Quartets)
T.S. Eliot

ACKNOWLEDGEMENTS

I would like to thank my supervisors, Prof. Hamish McNab, Dr Alison Hulme and Dr Anita Quye, for their wisdom, encouragement and boundless enthusiasm throughout the past three years. I am much indebted.

I would also like to thank the technical staff of the University of Edinburgh for all their help and advice, in particular, Alan Taylor (Mass Spectrometry), Juraj Bella (Nuclear Magnetic Resonance) and Lorna Eades (Inductively Coupled Plasma Mass Spectrometry / Optical Emission Spectroscopy). In addition, I would like to thank Dr Jo Kirby-Atkinson (National Gallery, London) and Dr David Saunders (British Museum, formerly at the National Gallery, London) for access to their accelerated ageing chamber.

I am much obliged to both the current and former members of the Hulme and McNab research groups, many of whom gave up their valuable time, often at short notice, to help me out (even after discovering that I would be visiting yet another European city).

To all the MODHT project partners from different disciplines and institutions throughout Europe who have been my constant companions on this journey, I am most grateful. I had plenty of fun and learned much from you all.

Thanks are also due to my friends and colleagues from the National Museums of Scotland, in particular, the staff and students (both past and present) from the Conservation and Analytical Research department, too numerous to mention individually here. I would like to wish them (and any new family members) good luck for the future and sincerely hope that we will keep in touch.

Finally, I am grateful to the European Commission (Grant number EVK4-CT-2001-00048) and The University of Edinburgh for funding.

LECTURES AND MEETINGS ATTENDED

- Microscopy and Imaging, Dr McDougall, Dr Mount and Dr Jones (10 lectures)
- Chemistry In Action – Advanced Mass Spectrometry, Dr Barran (5 lectures)
- Postgraduate Course in Nuclear Magnetic Resonance. High resolution NMR Spectroscopy for Small and Large molecules, School of Chemistry, The University of Edinburgh, 20th-21st April 2005
- The Royal Society of Chemistry Organic Division, Scottish Regional Perkin Meetings. Three years attendance; The University of Dundee (2002), The University of Edinburgh (2003), The University of St. Andrews (2004)
- Regular MODHT project partner meetings (Spain, Belgium, UK)
- Organic Research Seminars and Colloquia, School of Chemistry, The University of Edinburgh
- Conservation and Analytical Research Seminars (including the Plenderleith lectures) organised by the National Museums of Scotland and the Scottish Conservation Bureau

PRESENTATIONS

- Dyes in History and Archaeology, 22nd annual meeting, Switzerland 23rd-24th October 2003
- Scientific Analysis of Ancient And Historic Textiles: Informing Preservation, Display and Interpretation, Research Centre for Textile Conservation and Textile Studies 1st annual conference, Southampton, 13th-15th July 2004
- National Museums of Scotland & Scottish Conservation Bureau Seminar Series, Edinburgh, 28th October, 2004
- ICOM-CC (International Council of Museums – Committee for Conservation), 14th triennial meeting, The Hague, 13th-17th September, 2005

POSTERS

- Dyes in History and Archaeology, 23rd annual meeting, Montpelier, 4th-5th November 2004

ABSTRACT

The analytical investigation of several historically important natural yellow and red dye sources is presented, extending previous work on the chemical characterisation of the acid hydrolysed extracts from dyed yarns.

The PDA HPLC studies of weld (*Reseda luteola* L.) dyed yarn extracts found that neither the substrate nor additional steps in the dyeing process significantly altered the relative ratio of the main flavonoid components. Furthermore, their relative photo-degradation rates on the dyed yarns were similar, presenting few problems in the identification of the biological source. In contrast, the relative ratio of the main flavonoid components in dyer's greenweed (*Genista tinctoria* L.) dyed yarn extracts was highly dependent on the dyeing process. The identification of this biological source was, however, aided by the relatively slow photo-degradation rate of the characteristic genistein component compared with the photo-degradation rates of the other dye components on the yarn.

The PDA HPLC and HPLC ESI MS^n investigation of the acid hydrolysed extracts of yarn dyed with the *Serratula* species, sawwort (*Serratula tinctoria* L.) and *Serratula coronata* L., identified their characteristic dyeing components to be luteolin, apigenin, quercetin, kaempferol and 3-*O*-methylquercetin. Similar studies performed on young fustic (*Cotinus coggygria* Scop.) dyed yarn extracts identified the main colouring components to be fisetin and sulfuretin. Fragmentation of sulfuretin under negative ion electrospray conditions proceeded *via* a retro-cheletropic mechanism. Due to the relatively high photo-degradation rates of many of the characteristic components in both sawwort and young fustic, the identification of historical yarns dyed with these sources was problematic.

The dye components characteristic for Mexican cochineal (*Dactylopius coccus* Costa) were all found to be structurally related anthraquinones, with similar photo-degradation rates on the dyed yarns. An additional phenolic group was present on

the anthraquinone core of carminic acid compared with the dcII component, while the dcIV and dcVII components were isomers of carminic acid, most probably differing only in the stereochemistry of the sugar moiety. The aglycones of both anthraquinone cores, flavokermesic acid and kermesic acid, were also observed in the acid hydrolysed extracts of the dyed yarns.

Analysis of the principal dye components from brazilwood (*Caesalpinia sappan* L.) and logwood (*Haematoxylon campechianum* L.) using negative ion ESI MS^n enabled the identification of new, structure dependent, mass spectrometric breakdown pathways. The mechanisms were supported by deuterium labelling experiments and the results were shown to be useful for the structural determination of previously unidentified components. An elimination product observed in the PDA HPLC analysis of hematein dyed yarn extracts was structurally characterised using NMR techniques. A similar component, derived from brazilein, was also observed in brazilwood dyed yarn extracts.

A novel approach towards mordant identification using inductively coupled plasma techniques was investigated. ICP MS analysis was successful in identifying the metallic ions present in the acid hydrolysed extracts from both reference and historical yarns. However, interpretation of the results from historical samples was challenging due the observation of large amounts of both aluminium and iron in the sample extracts.

Within the Monitoring of Damage to Historic Tapestries (MODHT) project, yellow and green yarns from a selection of 15^{th}-17^{th} century tapestries were investigated. Analysis of the yarn extracts identified weld and dyer's greenweed as the most prevalent yellow dye sources, with young fustic frequently identified in the metal thread core extracts.

Keywords: Natural dyes; chemical characterisation; accelerated ageing; MODHT

TABLE OF CONTENTS

1 INTRODUCTION.....2

1.1 The Monitoring of Damage to Historic Tapestries (MODHT) project 3

1.2 Historic tapestries 3

1.3 Chemistry of proteinaceous fibres 7

1.4 Damage assessment 15

1.5 Natural dye sources.....24

1.6 Dye source identification.....32

1.7 Summary.....40

1.8 References.....42

2 THE ANALYTICAL INVESTIGATION OF SELECTED NATURAL YELLOW DYE SOURCES AND THEIR MORDANTS.....51

2.1 The use of flavonoids in the identification of several historically important natural yellow dye sources.....51

2.2 Initial investigations into the use of Inductively Coupled Plasma (ICP) techniques for the analysis of mordants.....89

2.3 References.....106

3 THE ANALYTICAL INVESTIGATION OF SELECTED NATURAL RED DYE COMPONENTS BY PDA HPLC, ESI MS AND NMR 111

3.1 Studies on the main components found in the cochineal insect dyes 111

3.2 Studies on the main components found in the soluble redwood and logwood dyes 133

3.3 References.....158

4 ACCELERATED LIGHT AGEING.....163

4.1 Introduction.....163

4.2 Yarn degradation.....167

4.3 Weld (*Reseda luteola* L.) 169
4.4 Dyer's greenweed (*Genista tinctoria* L.) 177
4.5 Sawwort (*Serratula tinctoria* L.) 181
4.6 Young fustic (*Cotinus coggygria* Scop.) 186
4.7 Cochineal (*Dactylopius coccus* Costa) 189
4.8 Brazilwood (*Caesalpinia sappan* L.) 192
4.9 Summary 194
4.10 The Monitoring of Damage to Historic Tapestries 194
4.11 Conclusion 196
4.12 References 198

5 DYE ANALYSIS OF HISTORICAL YARN SAMPLES 201
5.1 The historic tapestries 201
5.2 Historical yarn samples 211
5.3 Yellow dyes identified in MODHT historical samples 221
5.4 Summary of red dyes identified in MODHT historical samples 238
5.5 Conclusion 239
5.6 References 240

6 EXPERIMENTAL 242
6.1 Preparation of dyed yarn references 242
6.2 Dye extraction 247
6.3 Chromatographic methods 248
6.4 Mass spectrometry conditions 251
6.5 PDA HPLC 256
6.6 Structural characterisation of diosmetin and chrysoeriol 268
6.7 Structural characterisation of minor components in cochineal (*Dactylopius coccus* Costa) extracts 270
6.8 Structural characterisation of hematein and its elimination product 272
6.9 Mordant identification 274

6.10 Accelerated light ageing 280
6.11 Sampling from the tapestries 299

7 APPENDIX 307
7.1 MODHT PARTNERS 307
7.2 MODHT DYE RECIPES 309
7.3 PUBLICATIONS 325

Chapter 1

1 INTRODUCTION

Most surviving pieces of original hand-woven tapestry art date from the 16th century to the 19th century, with examples in European Royal palaces, historic houses, castles, cathedrals and major galleries. They are amongst the most valuable testimonies of European cultural heritage, due to both the intrinsic value of the tapestries as objects of art and to the fact that renowned artists and their workshops were often involved in their pictorial aspects. However, to formulate plans for the future care of these important cultural objects, the issue of damage assessment must be addressed.

It is important to have a quantifiable assessment of the condition of an object, such as a tapestry, to enable recommendations to be made regarding the most appropriate conservation measures that should be undertaken. This also enables the rate of change in the condition of the tapestry to be monitored, allowing the risks to the structural integrity of the object, which may change with its condition, to be assessed. For instance, a tapestry that has been protected from the light may be very vulnerable to fading, but quite robust for handling. In contrast, a faded tapestry may be quite unaffected by moderate light levels, but fall apart when moved.[1] It is also necessary to ascertain the present condition of objects, such as tapestries, so that the need for their conservation can be prioritised systematically and impartially. To do this effectively, it is vital to obtain a comprehensive understanding of the degradation processes involved in their constituent components.

The evaluation of potential indicators of damage was conducted using both model samples and historical yarns, sampled from a number of tapestries from sites in both northern and southern European locations. The work was performed as part of a multi-disciplinary study; 'The Monitoring of Damage to Historic Tapestries' (MODHT) project, which has been outlined below. A summary of the construction and manufacturing techniques of historical tapestries is then followed by an

introduction to the chemistry of the wool and silk fibres and the main methods employed for the assessment of damage.

An integral part of the MODHT study was the chemical investigation of natural dyes, which forms the main subject of this thesis. The different natural dye sources have therefore been introduced, followed by a description of the analytical procedures most successfully employed in the investigation of characteristic dye components from historical yarns.

1.1 The Monitoring of Damage to Historic Tapestries (MODHT) project

The Monitoring of Damage to Historic Tapestries (MODHT) project was dedicated to addressing the issue of damage assessment in historic tapestries. Its main aim was to obtain an understanding of the degradation processes in the wool, silk, metal threads (metal strips wound around a fibrous core), dyes and mordants, all integral components of the woven structure.

Initially, model tapestries based on traditional materials and weaving techniques were prepared (Appendix 7.2). These were subjected to accelerated ageing conditions and the aged and unaged samples characterised using appropriate analytical techniques. This provided information on the mechanical integrity of the materials that could then be correlated with chemical information obtained from both the surface and bulk of the yarn fibres. Thus, sensitive indicators of damage could be produced and evaluated using yarns sampled from historical tapestries, woven in renowned European weaving centres between the 15th century and the 18th century.

1.2 Historic tapestries

To understand fully the main aims of the MODHT project, an appreciation of the construction and manufacture of tapestries is essential. Tapestries have an extremely strong weave structure and experiments using the woven model samples have shown that the historic tapestries sampled during this project would originally have been

very strong.[2] However, today many are in danger of failing to support their own weight (typically 50-100 kg) when hung for display.[3]

The word 'tapestry' is used loosely to refer to various kinds of textiles, with the classic misnomer, always cited, being the 'Bayeux Tapestry', which is technically not a tapestry, but a large piece of embroidery, worked in coloured wools on coarse linen. The design of a true tapestry is built up in the course of the weaving; the fabric has no existence independent of the design.[4]

However, the design of a tapestry often has a previous and independent existence in another medium. It is first a drawing or painting, then a full-scale pattern or 'cartoon' (the word cartoon is borrowed from the Italian 'cartone', a large piece of paper) before being translated into a weaving. The construction of a tapestry can therefore be divided between a painter, who made the drawing or model, and the weaver, who executed it. This separation of function was maintained by custom and enforced by law.[4] Still another artist, the cartoon designer, usually intervened between the painter and the weaver, enlarging the painter's model to the full size of the weaving and making other changes dictated by his understanding of the weaving technique to assist in the translation from one medium to another. Thus, the cultural significance of these historic tapestries transcends their description as 'objects of art', encompassing a broader artistic context.

When weaving, a 'grill' of strong vertical threads is established called the warps. Working from one side to the other, the weaver's needle, carrying the weft thread, fills in the warp grill, passing over and under alternate warps. When the needle reaches the edge, it is doubled back and the direction reversed to pass under those threads it had passed over on the previous passage (Figure 1.1).

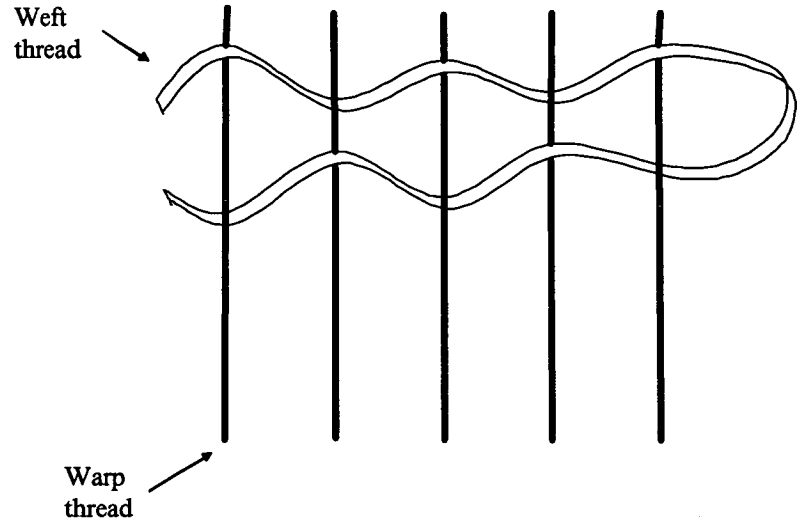

Figure 1.1: The passage of the weft thread between the warp threads during the weaving process

The two sets of interlacing yarns are unequal in character and weight, with the warp yarns usually coarse, undyed and widely spaced, while the wefts are usually fine and coloured. As the web builds, the wefts are packed densely together until they cover the warps completely so that the coloured weft alone appears on the face of the tapestry, the warps being hidden beneath the surface and their presence sensed from the visible ridges.[4]

On exhibition, the ridges of the tapestry run parallel with the floor *i.e.* horizontally, as the design would have been weaved 'sideways on' for both practical and aesthetic reasons. Firstly, the dimensions of tapestries appropriate for castle or cathedral were often vast, for example, 'Raphael presented by Tobias to his father' (PNM 7, Chapter 5) is 454 cm × 665 cm (length × breadth).[5] These dimensions are typical for the tapestries sampled during the project and to weave such a tapestry in the direction of the design would have required an impossibly big loom. Secondly, vertical elements such as trees and standing figures, if executed in the direction of the warp, would result in many long, vertical slits. These would be undesirable both from the viewpoint of the strength of the tapestry and its appearance.

The introduction of a new colour means a discontinuing of the previous weft. Where this change occurs, the strong interlacing action of the weft in binding together the warp grill is interrupted. In addition, 'loose ends' are produced on the reverse of the tapestry (Figure 1.2) which, if left by the weaver, provide convenient yarn samples that can be removed without further compromising the structural integrity of the object (Chapter 6). The availability of such samples has allowed the use of destructive chemical and physical techniques that may not have otherwise been considered. These have been employed in an effort to assess the condition of the tapestries and reveal possible indicators of damage.

Figure 1.2: A section of the reverse of a tapestry, showing the loose ends left by the weaving process. 'The Sacrifice of Polyxena' (PNM 5, Chapter 5), woven in Brussels, *ca.* 1545, and now in the Spanish Royal collection

Historic tapestries on display often appear to have maintained their mechanical strength, despite their usually faded appearance. However, when they are removed for repair, for transport to exhibitions, or for cleaning, they can undergo total structural failure due to loss of fibre and inter fibre strength. This lack of fibre strength is often difficult to assess visually, requiring knowledge of the actual physical and chemical state of the dyed, proteinaceous yarns.[6]

The physical and chemical properties of wool and silk yarns have therefore been summarised (Section 1.3). This is followed by descriptions of the different damage indicators used to assess the mechanical strength of the fibres within the MODHT project (Section 1.4.1), together with the chemical techniques utilised; amino acid analysis (Section 1.4.2) and Size Exclusion Chromatography (SEC) (Section 1.4.3).

1.3 Chemistry of proteinaceous fibres

The two fibre types most commonly used in the construction of tapestries are wool and silk. The mechanical properties of the historical yarns, and thus the structural integrity of the tapestries, are dependent on the chemical composition and macro-structure of the fibres. These are introduced in the following sections, although it should be appreciated that both wool and silk are incredibly complex, polymeric materials and a brief summary of relevant properties necessitates the exclusion of a considerable amount of fine detail.

1.3.1 Wool

The structure of wool and other mammalian fibres has been extensively studied,[7] however, wool fibres can be most simply described as consisting of two types of cells. The first make up the bulk (*ca.* 90% by mass) of the fibre in fine wools, such as those obtained from Merino sheep, and are called cortical cells. The second, which encase the cortex and make up the remaining portion (*ca.* 10% by mass), are called cuticle cells.[7] A surface lipid layer is also present on the wool, although this is mostly removed in the scouring process, where wool is agitated with non-ionic surfactant solutions.

The cuticle cells are separated from the underlying cortical cells by a cell membrane complex, which also surrounds individual cortical cells. The cuticle cells overlap one another, with the exposed scale edges pointing towards the tip and forming a protective sheath around the cortical cells. When viewed under magnification, these scales easily distinguish wool fibres from the smooth fibres of silk. However, this

difference is less apparent when aged or damaged wool fibres are inspected, since damage to the cuticle may cause the fibre to appear smooth under magnification.

The chemical constituents of the wool cells are predominantly keratin proteins, although lipids and carbohydrates are also present in significant quantities.[7] A complex mixture of three main protein groups, commonly referred to as low-sulfur proteins (LSF), high-sulfur proteins (HSP) and high-tyrosine proteins (HTP) is present,[8] although the exact composition and structure of the fibres is species specific.[9] The keratin in fine Merino wool has been found to contain up to 12% of the high-tyrosine protein type.[10]

The structures of some of the important amino acids that make up the keratin proteins are indicated below (Figure 1.3). The α-helical protein backbone, comprising three polypeptide chains twisted together, and the side chains of the different types of amino acid residues determine the mechanical characteristics and chemical reactivity of wool yarns.[7] Thus, modification of almost any side-chain affects both the mechanical and sorption properties, with the modification of basic or acidic side chains significantly influencing the dyeing properties of the yarn.

Mordanting conditions of hot, acidic solutions, such as those found in many of the recipes used during this project (Appendix 7.2) are often encountered during the colouring of wool yarns with natural dye sources. The acid binding capacity of wool at pH 1 is *ca.* 0.8 mol g^{-1}, consistent with the estimated contents of aspartic and glutamic acid residues and carboxyl-terminii.[11] At the more acid pH values, peptide bond hydrolysis will occur in the dyebath, weakening the fibres. In addition, acid uptake reduces the cohesion of the wool fibre and affects tensile properties, since the fibre cohesion is partly due to electrostastic interactions between oppositely charged groups ('salt links').

Changes in the mechanical properties of wool are also observed with the uptake of aluminium salts. This is of particular relevance for the historical dyes investigated

during this project, many of which were used as mordant dyes (Section 1.5). The carboxyl groups were found to be the main binding sites in untreated wool.[8]

Proteins containing cystine residues, such as keratin, are particularly susceptible to degradation by alkali due to a series of reactions that destroy the disulfide bonds and alter the mechanical properties of the fibre.[7,12,13] Therefore, the alkaline conditions necessary for the application of vat dyes can also be particularly damaging to wool fibres, although this can be kept to a minimum provided the conditions are carefully controlled.[8] The uptake of alkali into wool also reduces the 'salt links' in a similar manner to the uptake of acid, affecting tensile properties.

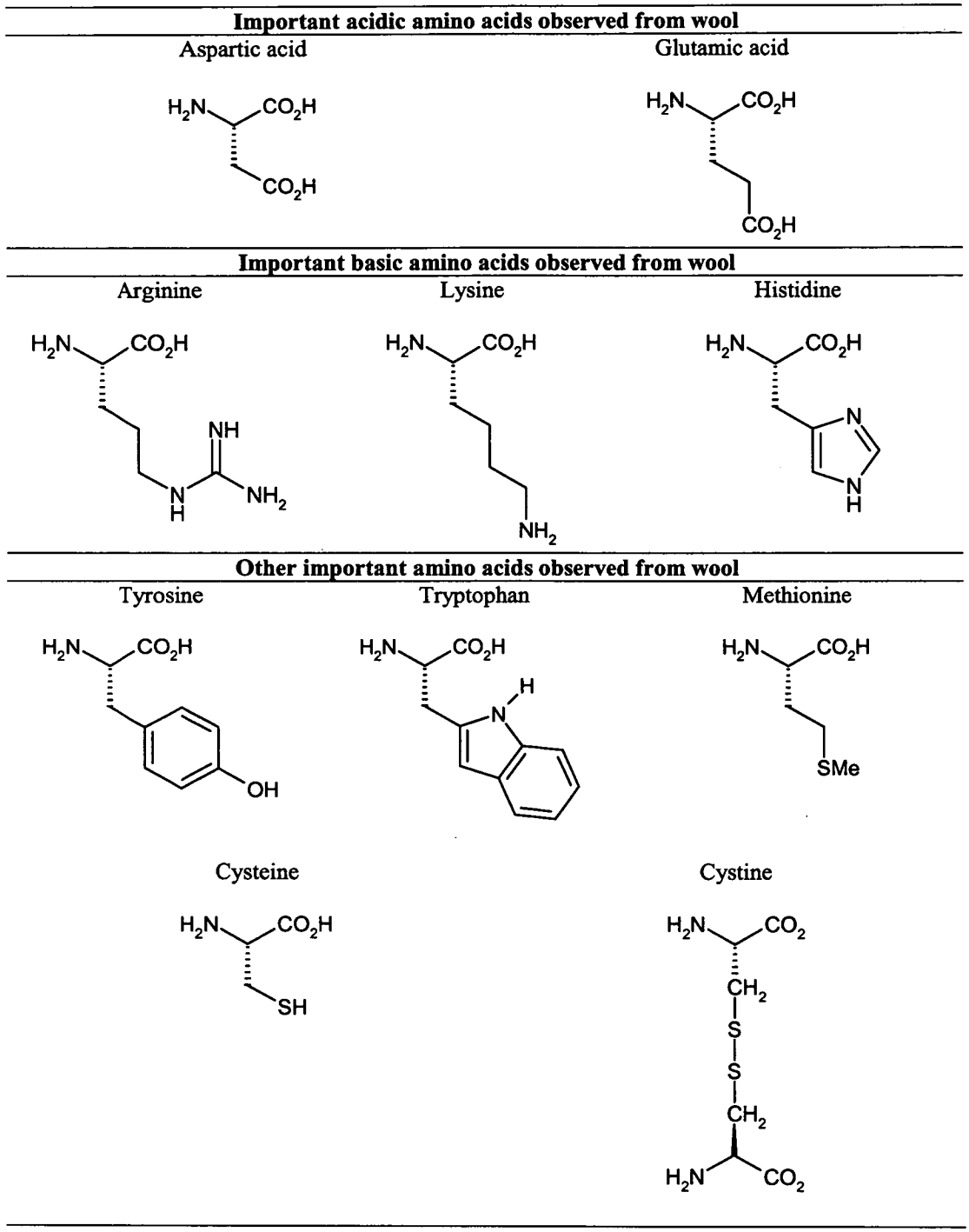

Figure 1.3: Important amino acids observed from wool

Cystine, cysteine and tryptophan are the residues most susceptible to oxidation in wool, and of these, cystine residues are the most abundant. Consequently, oxidants exert their major effect on wool by modifying cystine residues to cysteic acid (Figure

1.4). The cystine residues are of particular significance in the overall structural integrity of the wool proteins, since the disulfide groups, especially those which bridge half-cystine residues in different protein chains (cross-links) retard conformational changes. Furthermore, these cross-links are largely responsible for the difficulties experienced in solubilizing wool. As a consequence of this, investigations into the reduction of the molecular weight of keratin protein upon photo-degradation (see below) using size exclusion chromatography, a technique which requires the wool to be in solution, were not possible.

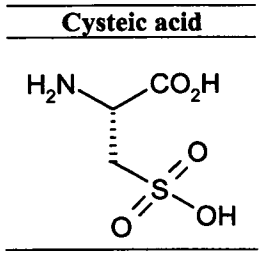

Figure 1.4: Cysteic acid, formed by the oxidation of cystine residues

The mechanical characteristics of wool vary upon absorption of moisture, with the work required to extend wool fibres decreasing with increasing humidity and moisture content, *i.e.* it is much harder to extend dry wool fibres than it is to extend the fibres in water.[7] In addition, it is easier to extend wool fibres in acid or alkaline solutions than in neutral solutions, due to the fewer number of 'salt links' opposing the extension, while the breaking of the disulfide crosslinks by oxidation also makes extension of the fibre easier.[7]

Prolonged irradiation with light is known to cause both physical and chemical damage to wool,[14,15,16] with the loss in fibre strength particularly significant when considering the effect of ageing on the historical tapestries. Studies of the chemical changes upon prolonged exposure to light indicate that cleavage of the main peptide chain almost certainly contributes towards the relatively large strength loss in irradiated yarns.[8] Although the extent of polymer degradation in aged silk has been measured using size exclusion chromatography (Section 1.4.3), this technique was

not suitable for the study of aged wool. Solubilization of the keratin protein would require cleavage of the intermolecular disulfide bonds, altering its molecular weight and thus making the extent of degradation impossible to assess.

The prolonged exposure of wool to light may also cause the fibre to yellow or bleach, with the rate increasing in the presence of moisture.[8] Neither the chromophores responsible for the initial colour of natural wool, or those produced by irradiation, are known, however, maximum yellowing is observed during irradiation at 290-320 nm and maximum bleaching at 400–460 nm.[8] The photo-degradation of wool is a complex process, affecting many amino acid residues and is still not fully understood.[16,17]

The peptide bonds in the keratin protein can be completely hydrolysed upon treatment with concentrated acid, allowing the majority of the constituent amino acids to be analysed quantitatively. This approach has enabled a comparison of selected amino acid constituents in unaged and aged reference yarns to be investigated to indicate the extent of oxidative damage to both wool and silk yarns. However, due to differences in the amino acid content of the two proteins, the degradation was measured using slightly different parameters in each case (Section 1.4.2).

1.3.2 Silk

Over the centuries, silk has been highly valued as a textile fibre due to its qualities of strength, elasticity, softness, absorbency, and affinity for dyes. Silk is produced by the larvae of a variety of insects and spiders, with the most useful silks coming from the protein secretions of the Bomycinae family. Worldwide, the larvae of *B. mori* are the most widely exploited and most important source of silk.[18]

The silk cocoon is formed gradually over a period of 3-6 days by the simultaneous extrusion of silk filaments and the figure-of-eight motion of the silkworm's head. On exposure to air, protein from two separate glands hardens into a silk thread

consisting of two fibroin filaments surrounded by a cementing layer of sericin. In contrast to wool, silk fibres do not have cuticles and appear smooth when viewed under magnification. The removal of sericin from raw silk, known as degumming, is a simple but important process in the preparation of fibres before dyeing and is usually achieved with hot dilute soap or alkaline solutions.

The fibroin protein contains a variety of amino acids, including a high proportion of glycine, alanine, serine and tyrosine (Figure 1.5). The fibroin from *B. mori* consists of two major polypeptide components, a heavy component (H-chain) and a light component (L-chain) linked by disulfide bonds.[19]

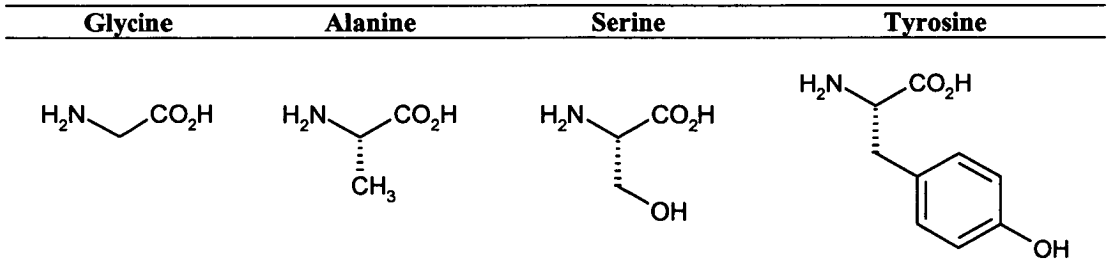

Figure 1.5: Importance amino acids observed from silk

In contrast to the keratin of wool, only minor amounts of cystine exist in silk and are considered to play a small, but significant, role in the secondary structure of fibroin. In addition, there is a much lower proportion of the acidic and basic amino acids in fibroin than in keratin and the total number of acidic groups in fibroin is, on average, about two to three times that of basic groups.[18]

Tendering of silk by mineral acids and alkalis occurs as a result of fission of the polypeptide chains of the fibroin. The degree of hydrolysis is much greater with acid than with alkali, while the rate increases with increasing temperature and agitation. Thus, hot concentrated acids and alkalis readily decompose silk. The degradative effect of boiling water on silk is also thought to involve hydrolysis. In addition, cations of various inorganic salts have been shown to increase alkaline hydrolysis.[18]

While the oxidation of silk is very complex, experiments with oxidising agents such as hydrogen peroxide indicate that the breakage of the peptide bond occurs at tyrosine residues and that tyrosine side-chains are oxidised to acidic groups.[20]

The exact composition and structure of fibroin appears to be species specific,[21] however, the preponderance of small amino acid residues permit the arrangement of the protein chains into crystalline regions with a pleated β-sheet structure, held together by hydrogen bonds.[18] Together with a more amorphous region, this structure accounts for many of the chemical and mechanical properties of silk.

In general, when tension is applied to silk, the initial deformation occurs primarily in the amorphous regions. The extent to which the randomly arranged chains are bound to each other, their interaction with the crystallites, and the proportion of crystalline and amorphous material present will determine the overall behaviour. Mechanical characteristics of silk also vary upon absorption of moisture and are related to the 'fineness' of the fibre, with finer silk generally having a greater degree of crystallinity.[18]

Silk is more susceptible to photo-degradation than any other natural fibre, with yellowing generally accompanying photochemical degradation.[18] The sensitivity of silk to light can also be altered by the presence of metal cations. Reaction mechanisms involved in photo-degradation and yellowing are complex and little understood, although UV radiation appears to be particularly damaging.[22,23] The mechanism of degradation is thought to begin in the amorphous region, with the breaking of hydrogen bonds. This is followed by the oxidation of tyrosine and the eventual hydrolytic fission of the polypeptide chains at the tyrosine residues.[18] As with wool, loss in fibre strength caused by the cleavage of the main peptide chain is particularly significant when considering the structural integrity of the historical tapestries.

Peptide bonds in the silk fibroin protein can, like the wool keratin, be hydrolysed upon treatment with concentrated acid. This allows the quantitative analysis of the majority of the constituent amino acids and thus the investigation of oxidative damage to silk due to accelerated and natural ageing of the yarns (Section 1.4.2). Furthermore, size exclusion chromatography has been successfully applied to silk samples for determination of polymer degradation in aged yarns (Section 1.4.3).

1.4 Damage assessment

Initial studies into degradation phenomena of the distinct wool and silk components within the MODHT project were conducted on the reference dyed yarns and woven models (Appendix 7.2). These were subjected to accelerated ageing conditions (Xenotest light ageing instrument, 400 h, estimated illuminance at sample surface using blue wool standards *ca.* 150 000 lux). Based on archival research and current illumination levels of many of the tapestries, this approximated the total light exposure which they may have received over *ca.* 400 years.[3]

Results from analyses of the yarns using different physical and chemical techniques indicated that in the majority of cases, a measurable amount of damage occurred in the aged yarns when compared with their unaged equivalents.[2] Furthermore, the dyeing procedures, together with the natural dye sources used, were found to have a significant influence on the results. This further complicated efforts to relate the mechanical breakdown of the tapestries to quantifiable indicators of damage and reinforced the need for the accurate identification of the dye sources on the yarns sampled from the selected historical tapestries.

Before proceeding to the main subject of this thesis, the studies into the accurate determination of dye sources from historical yarns (Chapters 2-5), the associated work conducted by the MODHT partners (Appendix 7.1) has been summarised (Sections 1.4.1-1.4.3).

1.4.1 Surface and mechanical properties

Scanning Electron Microscopy (SEM) is a widely used technique for studies on morphology and surface topography of yarn fibres.[24,25,26] Unaged and aged woven model samples from the MODHT project, together with some of the historical wool and silk yarns, were therefore analysed by SEM. This elucidated the types of physical damage characteristic of both accelerated and natural ageing. Wool and silk samples subjected to accelerated ageing conditions showed longitudinal cracks, especially on the weave crowns.[27] The nature of these cracks is unclear and they are not observed on the historical wool samples, which in contrast frequently show transverse cracks. Transverse cracks are a typical indicator of severe fibre embrittlement and were also observed on the aged yarns after tensile strength testing.[27]

X-Ray Photoelectron Spectroscopy (XPS) is a complementary technique to SEM and is used to probe the chemical nature of the yarn surface.[28,29,30,31,32] The surface chemical analysis of the wool fibres from both the aged MODHT reference samples and the historical yarns using XPS found evidence for oxidative damage.[27] A decrease in the sulfur(II)/sulfur(VI) ratio was observed in the aged wool samples compared with the unaged samples, indicating the formation of cysteic acid.[27] The cleaving of cystine bonds in the wool keratin can be ascribed to oxidative degradation, contributing to the loss of strength in aged wool (Section 1.3.1).

Variations in the sulfur(II)/sulfur(VI) ratio were also observed in the unaged MODHT wool samples dyed with different natural sources and was attributed to oxidative modification on the wool surface during the dyeing procedures.[27] Results from the XPS analysis of the yarns could not, however, be used as markers for damage, as they were not easily correlated with the reduction of tensile strength observed in the aged yarns when compared with their unaged equivalents. In addition, the low levels of sulfur containing amino acids in silk fibroin prevented the application of the method for determination of surface oxidation on silk fibres.

Physical properties of yarns, such as tensile strength, are vital when assessing the condition of an historic tapestry.[33] The tensile strength of the aged MODHT woven models, orientated to replicate the direction of force in a hanging tapestry, was found to correlate linearly with the tensile strength of the single yarns which had been identically dyed and subjected to the same ageing conditions.[34] This suggested that measurements obtained from single yarns would be representative of the structural integrity of historical tapestries. When relative tensile strength measurements of the model references dyed with different natural sources were compared, it was found that the dyeing processes altered the initial tensile strength of the yarns.[3] Furthermore, when data from the aged yarns was evaluated, the susceptibility of the fibres to degradation was also found to be dependent on the dyeing procedure and natural dye sources employed.[3] The most significant results regarding the degradation of yarns dyed with different natural sources have been summarised in Chapter 4.

Colorimetry has also been applied to the study of dyed yarn fibres.[35,36] The colour of both the unaged and aged MODHT reference fibres, measured using a Minolta spectrophotometer with CIE tristimulus values L*,a* and b*, was obtained and the overall colour change calculated using the CIEDE2000 equation (ΔE_{00}).[3] A relationship between the colour difference (ΔE_{00}) and physical properties for each dye source and dye recipe was found.[3] However, colour difference is not, in itself, a good indicator of fibre damage within a structure as complex as a tapestry. This is because the nature and rate of colour change is intrinsic to the dye and dyeing process utilized. Although exact information regarding the dyeing conditions of historical yarn samples cannot be obtained, accurate identification of the original dye source and mordant is still useful for damage assessment because the general dyeing process for different dyes was relatively consistent (Appendix 7.2). Thus, identification of yarns dyed with particular natural sources may help to identify potentially weak sections in tapestry structures.

Thermo-dynamical properties of dyed wool and silk yarns can be investigated using techniques such as Dynamic Mechanical Thermal Analysis (DMTA),[37] Differential Scanning Calorimetry (DSC),[38] and Thermogravimetry (TGA).[39,40] These techniques are also of value when monitoring effects of accelerated ageing on materials, for example, unprimed and primed canvas.[41] Thus, to obtain further information regarding differences in the mechanical properties of the MODHT reference yarns dyed with the different recipes, thermal analysis techniques were employed.[42,43] In all cases, measurements were made directly on the yarns and did not involve any pre-treatment of the samples. Dynamic mechanical thermal analysis (DMTA) was conducted to measure the stress/strain and the amount of displacement (or creep) of the yarns in both dry and wet conditions. In general, both dyeing and light ageing appeared to reduce fibre stiffness and associated strength compared with undyed or unaged equivalents.[43]

Thermal stability measurements using thermogravimetry (TGA) differentiated the model wool samples into two groups, based on whether the sample had a higher or lower thermal degradation profile compared with an undyed sample.[42] Additionally, most aged samples had a decreased thermal stability compared with the corresponding unaged samples. Thermal stability experiments using Differential Scanning Calorimetry (DSC) were also performed on both model and historic samples.[43] This was the preferred thermal analysis technique for historic samples, as only very small sample sizes were required. Compared with their unaged equivalents, a decrease in the enthalpy was measured in the reference samples subjected to accelerated ageing conditions.[43] In general, measurements on the historic samples suggested that these were more degraded than the reference samples subjected to accelerated light ageing.

The above experiments on the MODHT reference yarns, conducted by various partners within the project (Appendix 7.1) all highlight that both the dyeing process and natural or accelerated ageing, produce damage in the yarns that will ultimately affect the structural integrity of the tapestries themselves. Therefore, to identify

chemical indicators of damage that may be applicable to historical yarn samples, the tensile strength data from the MODHT models was correlated with the data obtained from other analytical techniques utilised and developed during the project. The most important of these were amino acid analysis (Section 1.4.2) and size exclusion chromatography (Section 1.4.3).

1.4.2 Calibrated amino acid analysis

The calibrated amino acid analysis of proteinaceous materials is frequently employed during the scientific investigation of significant cultural heritage items. Information can be obtained regarding the materials used in the construction of the objects, for example, binding media, varnishes or adhesives.[44,45,46] Studies have also examined the constituent amino acids obtained from aged yarn fibres.[47,48,49,50]

Calibrated amino acid analysis was used within the MODHT project to reveal the extent of oxidative degradation to the proteinaceous fibres in both the unaged MODHT reference samples, dyed using different natural sources, and the samples subjected to accelerated ageing conditions.[51] This information was then correlated with the tensile strength data and used to evaluate the amino acid results from the analysis of the historical yarns.

The quantitative analysis of the constituent amino acids requires the samples to be acid hydrolysed under non-oxidative conditions.[52] The samples were therefore placed in airtight vessels, together with the hydrolysis medium and frozen in liquid nitrogen (-190 °C). A vacuum was then applied with an oil pump, before flushing with nitrogen. This evacuating/flushing sequence was repeated five times before the vessels were placed in an oven, under vacuum, for hydrolysis (20 h, 110 °C). The test tubes were dried in a desiccator and the residues dissolved and analysed using a modified 'Waters AccQ.Tag amino acid analysis' method.[53]

As expected, changes in the amino acid composition of the aged wool samples were signalled by a decrease in the amounts of arginine, lysine and histidine (basic amino

acids), tyrosine, methionine, cystine and cysteine, together with an increase in the amounts of the acidic amino acids (aspartic and glutamic acid) and cysteic acid.[51] These results were then refined to allow fibre degradation to be expressed in terms of ratios of specific amino acids.

The relation between basic and acid amino acids, known as B/A, is a good marker for oxidative degradation and has already been used for the investigation of the degradation in other materials, such as leather.[54] In general, B/A can be defined as follows;

$$B/A = \frac{\text{basic amino acids}}{\text{acidic amino acids}}$$

Thus, for wool, B*/A was defined as;

$$B^*/A = \frac{\text{lysine} + \text{histidine}}{\text{aspartic acid} + \text{glutamic acid}}$$

In addition, a specific wool degradation parameter, KOF (Keratin Oxidation Factor) was also utilised to capture the changes occurring in the amounts of cysteic acid and the other amino acids from the aged yarns.[51] This KOF factor was defined as follows;

$$\text{KOF factor} = \frac{\text{lysine} + \text{histidine} + \text{tyrosine} + \text{methionine}}{\text{aspartic acid} + \text{glutamic acid} + \text{cysteic acid}}$$

The B*/A and KOF values obtained from analysis of the unaged, untreated wool were used as a reference and were taken to be the base level with which to compare the values obtained from the model aged and historical samples *i.e.* the B*/A and KOF values obtained from the unaged, untreated wool were considered to be 100% and the results from the reference and historical samples expressed as percentages relative to the reference.[51]

Changes in the amino acid composition of aged silk were also detected, however, the B*/A factor was neither relevant nor sensitive enough to reveal the extent of oxidative degradation in the silk fibroin. This was due to only small quantities of the specified basic and acidic amino acids being present in fibroin, producing an inherent variation associated with their quantification. Thus, only the decrease in tyrosine, reported in a similar manner to the results from the analysis of the wool yarns, was used as a marker for oxidative degradation in the silk samples.[51]

The KOF and B*/A parameters for wool and the tyrosine levels in silk were successfully employed to investigate the extent to which oxidative degradation affected the chemical components of both aged wool and aged silk fibres. The effects of the dyeing processes (pre-ageing) were also studied using the dyed model yarns, providing a context within which the historical sample results could be interpreted.[51] The most significant results regarding the correlation between the tensile strength of yarns dyed with different natural sources and the calibrated amino acid analysis results have been summarised in Chapter 4.

1.4.3 Size Exclusion Chromatography (SEC)

Size exclusion chromatography is a well-established technique for determining molecular weight distributions of polymers and is therefore an ideal analytical technique with which to investigate the reduction in the molecular weight of polymers caused by chain scission. Although SEC has been widely applied to the study of cellulosic materials in conservation,[55,56,57,58,59] there are fewer instances where it has been used to analyse proteinaceous materials.[60,61]

The photo-degradation of wool and silk yarns results in cleavage of the main peptide chains, contributing towards the strength loss observed in yarns subjected to prolonged exposure to light (Section 1.3). SEC was therefore used within the MODHT project to compare the reduction in the molecular weight of aged silk reference samples, dyed with different natural sources, to their unaged equivalents and the historical silk samples.[3]

SEC is performed by high performance liquid chromatography (HPLC) (Section 1.6.1) but with a column containing finely divided, porous particles of varying diameter.[62] Polymers of large molecular weight are unable to interact with the pores, so travel quickly through the column. However, polymers of smaller molecular weight pass in and out of the pores to a degree determined by the hydrodynamic volume (the volume occupied by the polymer when in solution), and thus travel through the column more slowly. This is largely an entropically governed phenomenon and, in contrast to reverse-phase HPLC, where the partitioning mechanism utilises interactions and weak bonding between the analytes and the stationary phase, the separation efficiency in SEC comes only from the stationary phase.[63]

Analysis by SEC requires the sample to be in solution. Consequently, silk yarn could be examined using this technique but not wool yarn, due to the differences within the protein structures of fibroin and keratin. The hydrogen bonds holding together the β-pleated sheets of silk fibroin are relatively easy to disrupt, but the tertiary structure of wool is held together by stronger covalent bonds, including disulfide links (Section 1.3.1). The sample preparation for wool would require the disulfide links to be cleaved, altering its molecular weight and thus making the extent of degradation impossible to assess.

Although the problem regarding the solubility of wool undoubtedly limits the applicability of SEC to the analysis of aged historical yarns, silk is usually considered to be particularly vulnerable to damage caused by ageing.[18] Additionally, where silk is present in a tapestry, it forms part of the woven image and is therefore located in the load bearing weft direction (Section 1.2), so its condition is of great importance when assessing the ability of a tapestry to support its own weight during display.

The complete dissolution of sample material is important when determining the molecular weight distribution of polymers. The chosen solvent must also be suitable

for use in the HPLC system. Although a concentrated aqueous lithium thiocyanate solution is generally believed to be the most appropriate solvent for solubilizing silk, the HPLC system was unable to resolve the silk and solvent peaks completely, making quantification problematic.[2] To achieve complete resolution of the peaks, denaturing conditions were used to disrupt the intramolecular bonds holding the tertiary structure of the protein in place, without affecting the polymer chain lengths. The denatured molecules therefore have a greater hydrodynamic volume and pass through the column more rapidly than the untreated sample. Urea was used as the denaturing agent for this project and optimisation of the peak resolution consequently improved the sensitivity of the technique, allowing smaller samples than previously possible (*ca.* 0.5 mg) to be accurately analysed and thus permitting the investigation of silk from both model and historical samples.[2,3]

The weight-average molecular weight (M_w) of each sample was determined from the SEC data. The tensile strength is often most influenced by the large molecules in the material and this value is biased towards the heavier molecules, since these contribute more to the total mass of the polymer sample than smaller molecules. The alternative number average molecular weight (M_n) is not as suitable, since it is biased towards the smaller molecules.[62]

The ratio of the mass average and number average molecular weight gives rise to the polydispersity index (PDI), often called the molecular weight distribution (MWD).[62] However, a novel method for quantifying the molecular weight distribution was developed for the purposes of the present study.[34] The molecular weight distribution was quantified by a 'Hi/Lo index', defined as follows;

$$\text{Hi/Lo index} = \frac{\text{area under chromatogram for high molecular weight fractions}}{\text{area under chromatogram for low molecular weight fractions}}$$

The same retention time fractions for the 'high' and 'low' molecular weights were used each time, adjusted for any alterations in flow rate.[34]

This index provided a useful indicator of damage for each sample and together with the weight-average molecular weight (M_w), was successfully employed to investigate the effects of light ageing on the molecular weights of model silk yarns, dyed with different natural sources.[3] The extent of damage observed in the aged model silk fibres could also be compared with the results obtained from the analysis of the historical samples.[3] The most significant results regarding the correlation between the tensile strength of yarns dyed with different natural sources and the SEC results have been summarised in Chapter 4.

1.5 Natural dye sources

Studies into the chemical and mechanical properties of the MODHT dyed reference materials indicate that the dyeing methods influence the strength properties of both the unaged and aged fibres. As the dyeing method is dependent on the natural source, accurate identification of the original dye source is therefore an important factor when assessing damage to historic tapestry structures.

Development of the first synthetic dyes, from the mid-19th century onwards, eventually made the use of natural dyes all but obsolete. By the beginning of the 20th century, synthetic dyes were manufactured relatively easily and could produce virtually any colour, shade or hue. Furthermore, they could often be formulated with handling properties tailored to specific applications. However, before the mid-19th century, only colouring components obtained from natural materials were available for the dyeing of textile yarns.

The best natural dyes in terms of resistance to fading by light and washing were either vat dyes, for example, indigo (see below) or mordant dyes such as madder, where the dye molecule is bound to the fibre by a metallic salt such as alum [$AlK(SO_4)_2.12H_2O$] or ferric sulphate [$Fe_2(SO_4)_3$]. Organic compounds like tannins were also sometimes used. Many natural dyes require a mordant because the dye components from most natural sources have little affinity with the protein side chains of the wool or silk. The mordant is absorbed by the yarn fibres and, during the

dyeing process, reacts with the dye components to form an insoluble, coloured complex. The mordant improves the fastness of the dye, but also influences the final colour obtained. The majority of reference yarns prepared for the MODHT project used an alum mordant, as the dyes of interest were most usually applied in this way.

Two of the most historically important blue vat dyes were indigo and woad (Section 1.5.2). In their oxidised form, their dyeing components are coloured but water insoluble. Under reducing conditions, the dye components, principally indigotin, are converted into non-coloured *leuco* forms, but are soluble in alkaline aqueous solutions. The yarn fibres are introduced into the alkaline solution and when removed and exposed to air, the components oxidise back to their insoluble form and the pigment aggregates are trapped within the yarn fibres.

So-called direct dyes, such as saffron (*Crocus sativus* L.)[a] and turmeric (from various *Curcuma* spp.) do not require a mordant and, as their name suggests, are applied directly to the yarn fibre. They are usually less wash-fast and light-fast than mordant dyes.

The natural dye sources of most interest within the MODHT project can be classified by the chemical components 'fixed' onto the dyed yarns. For the MODHT samples, as for most historical and archaeological textiles, analytical preparation necessitated extracting the dye-related compounds and several different methods are commonly used.[64,65,66] Chemical analysis is then used to distinguish the different natural dye sources.[67,68,69]

[a] The first part of the name indicates the genus to which the plant belongs, distinguishing a group of related species or an isolated, distinctive species. The second part is the species, distinguishing several species within a genus. The abbreviated name that follows the Latin names indicates the botanist responsible for the recognition of the plant as a hitherto unknown species, and is used as a further safeguard against confusion in the application of the name.

Some of the sources most frequently observed in historic tapestries, together with their main colouring components, are outlined below.

1.5.1 Yellows

The flavonoids are the main yellow colouring components found on historically dyed yarns and have usually been applied with a mordant.[70,71] Many different flavonoids can be obtained from natural dye sources,[72] but the occurrence of specific flavonoids in particular species has allowed their use as chemotaxonomic markers, which is now well established.[73,74,75,76,77]

Flavonoid

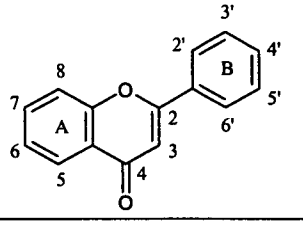

Figure 1.6: The general structure of flavonoids

The main flavonoid components from several of the most frequently used plant sources for the historical dyeing of textile yarns are detailed below. Weld *(Reseda luteola* L.) is known to contain the flavones luteolin and apigenin,[78,79] while dyer's greenweed *(Genista tinctoria* L.*)* contains the isoflavone genistein in addition to apigenin and luteolin.[80] The main dyeing components in young fustic *(Cotinus coggygria* Scop.*)* are the flavonol fisetin, together with the aurone sulfuretin.[81] Sawwort *(Serratula tinctoria* L.*)* dyed yarns are believed to contain the flavones luteolin and apigenin and the flavonols quercetin, 3-*O*-methylquercetin and kaempferol (Figure 1.7).[70,79,82]

These components are often found in the plant together with their *O*-glycosides, which can sometimes be fixed onto the dyed yarn along with the aglycones.[64,83] However, if a highly acidic dyeing or extraction procedure is utilised, the glycosides will be hydrolysed to their constituent aglycone and sugar components.

Flavones

Luteolin
5,7,3',4'-tetrahydroxyflavone

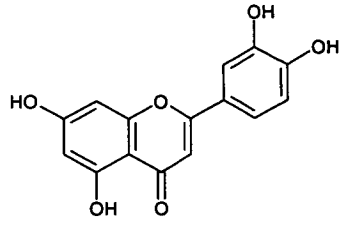

Apigenin
5,7,4'-trihydroxyflavone

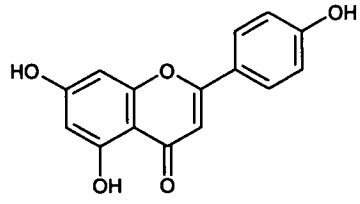

Isoflavone

Genistein
5,7,4'-trihydroxyisoflavone

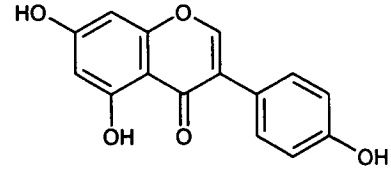

Flavonols

Quercetin
3,5,7,3',4'-pentahydroxyflavone

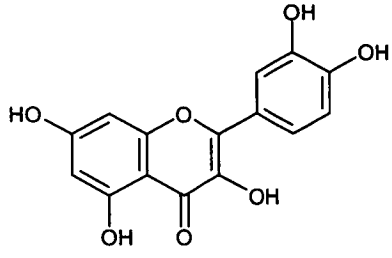

Kaempferol
3,5,7,4'-tetrahydroxyflavone

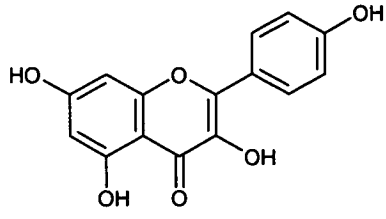

Fisetin
3,7,3',4'-tetrahydroxyflavone

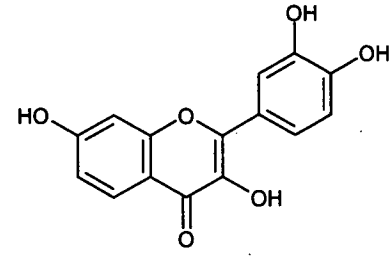

3-*O*-Methylquercetin
3-methyl-3,5,7,3',4'-pentahydroxyflavone

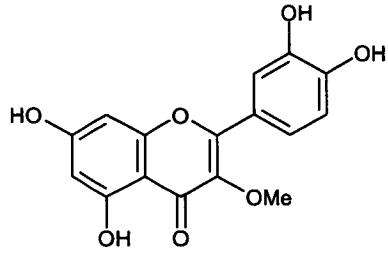

Related component (Aurone)

Sulfuretin
3'4'6-trihydroxyaurone

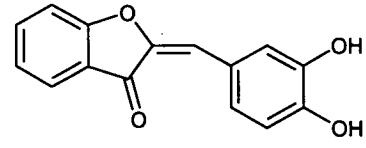

Figure 1.7: The main flavonoids and a related, aurone component from several natural sources frequently used historically to produce a yellow colour on dyed textiles

The components observed in the acid hydrolysed extracts of yarns dyed with the above mentioned sources have been explored in more detail in Chapter 2, while the effects of light ageing on the relative ratios of the aglycones observed in the yarn extracts have been examined in Chapter 4.

1.5.2 Blues

Indigotin (Figure 1.8) can be obtained from several plant sources, for example, the indigo plant (*Indigofera tinctoria* L.) and woad (*Isatis tinctoria* L.).[80] Yarns dyed with these natural sources will also contain minor amounts of indirubin, as will yarns dyed with a synthetic source.[80] Although indigotin is also present in some purple dyes obtained from shellfish, for example, spiny dye murex (*Bolinus brandaris* L.) and banded dye murex (*Hexaplus trunculus* L.), these also contain bromo-substituted indigotin and indirubin derivatives (Figure 1.8).[84]

Indigotin and its main isomers

Indigotin

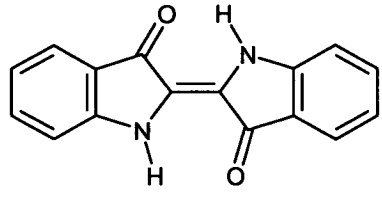

6-Bromoindigotin

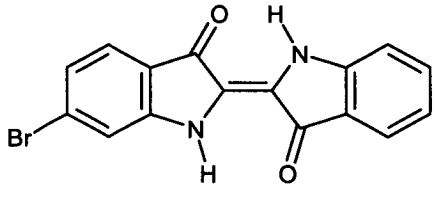

Indirubin

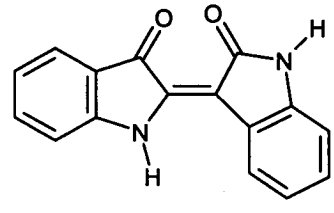

6,6'-Dibromoindigotin

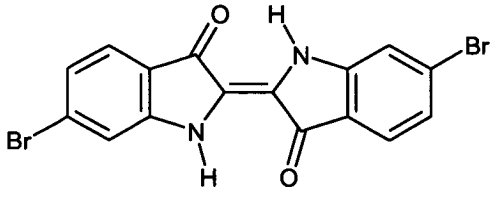

6,6'-Dibromoindirubin

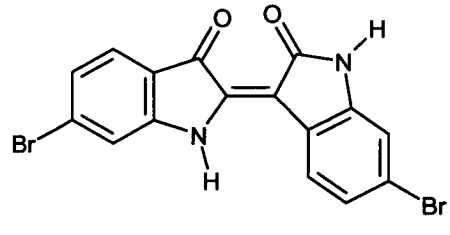

Figure 1.8: The indigoid dye components

The indigoids are vat dyes (Section 1.5), thus, upon oxidation in air, the pigment aggregates are trapped in the yarn fibres. When the indigo plant or woad is used in

combination *i.e.* overdyed or underdyed, with red, yellow or brown sources, purple, green and black yarns can be obtained.

1.5.3 Reds

The main group of natural dye sources for colouring yarns red, and the most important historically, are the anthraquinone plant dyes, particularly those obtained from the roots of different *Rubiaceae* spp. Commonly used sources for mordant dyeing include madder (*Rubia tinctorum* L.), wild madder (*Rubia peregrina* L.) and munjeet (*Rubia cordifolia* L.). Some of the main colouring components from these sources have been detailed below (Figure 1.9). Although the anthraquinone contents of the madder roots can be complex, the occurrence of specific anthraquinones in the extracts of dyed yarns can sometimes indicate the use of a particular species.[85,86]

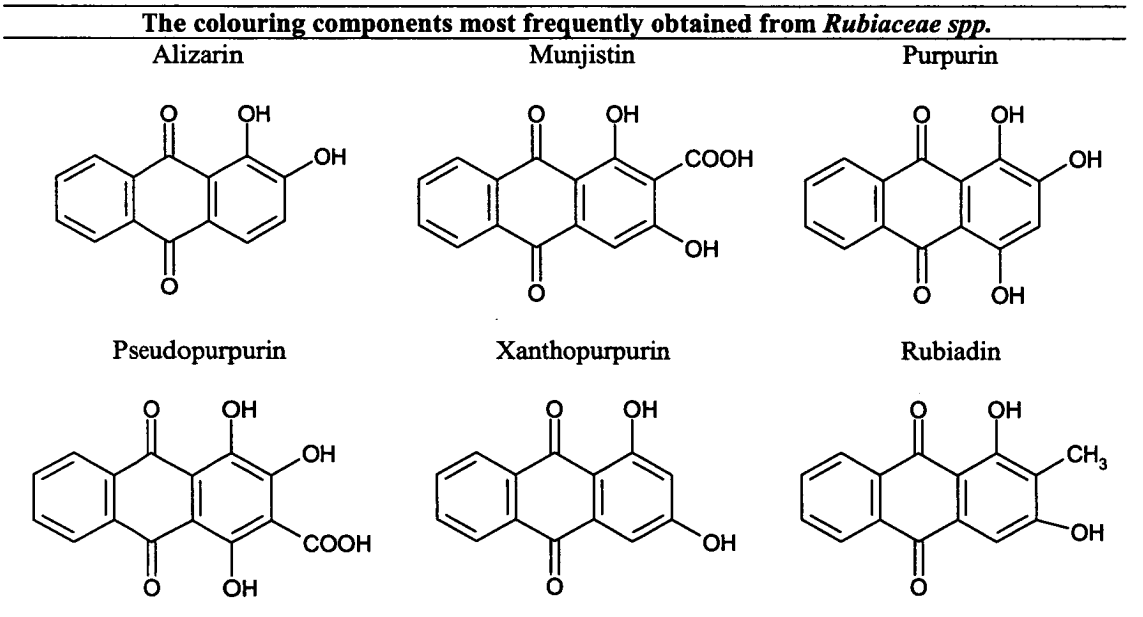

Figure 1.9: The anthraquinone dye components from *Rubiaceae* spp.

Another important natural source of red anthraquinone components is from the coccid insect dyes, including Mexican cochineal (*Dactylopius coccus* C.), kermes (*Kermes vermilio* P.) and lac dye (*Kerria lacca*). A variety of anthraquinone colouring components can be obtained from these insects (Figure 1.10), although

some of their minor components remain to be identified. The identification of the unknown components from Mexican cochineal (*Dactylopius coccus* C.), has been addressed in Chapter 3, while the effects of light ageing on the relative ratios observed in the yarn extracts have been explored in Chapter 4. As with the madder plant sources, they are generally used as mordant dyes and the presence and relative ratios of the components from the dyed yarn extracts can sometimes allow species identification.[85,87,88,89]

The colouring components most frequently obtained from the coccid insect dyes

Carminic acid

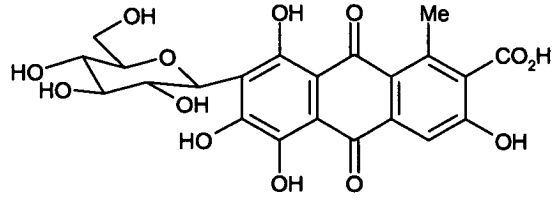

Kermesic acid

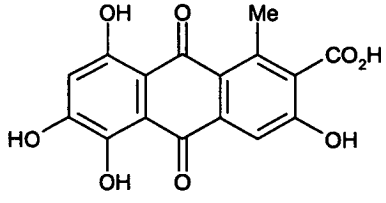

Flavokermesic acid

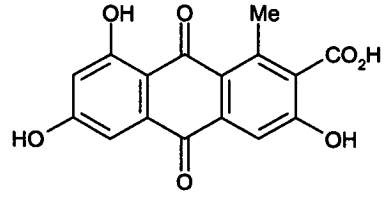

Laccaic acid A

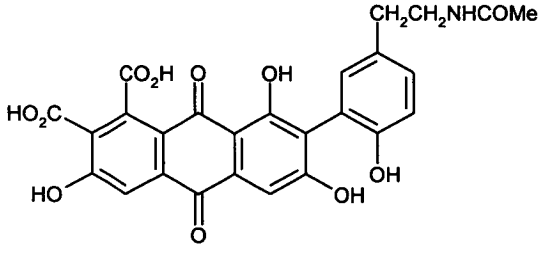

Laccaic acid B

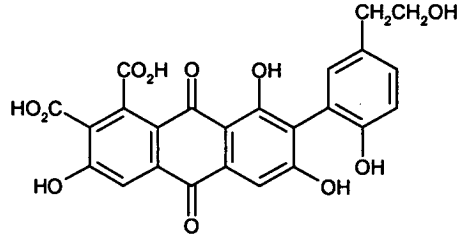

Figure 1.10: The main anthraquinone dye components from coccid insect dyes

Other historically important red dye plant sources include the soluble redwoods, in which the principal colourants can be extracted by soaking the heartwood in water. These have received much less attention than the root and insect reds because the

fugitive nature of the colouring components, even on mordanted yarns, was well known historically.[81] The main colouring component, brazilein, is formed by the oxidation of brazilin (Figure 1.11). Compounds of this structural class were originally termed neoflavonoids, however, recent developments indicate that a more appropriate designation is in fact homoisoflavonoids.[90,91,92]

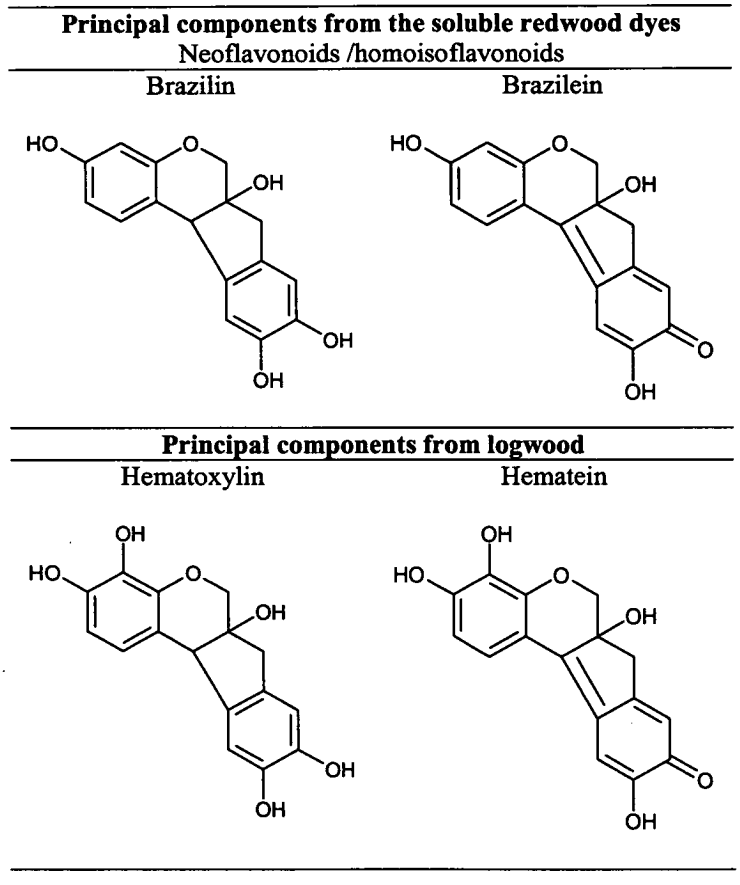

Figure 1.11: The neoflavonoid, or homoisoflavonoid, components from the soluble redwoods and logwood

There are a number of botanical sources of soluble redwood dyes, the main being *Caesalpinia brasiliensis* L., *Caesalpinia echinata* Lam., *Caesalpinia sappan* L. and *Caesalpinia crista* L. Their common names include brazilwood, peachwood, sappanwood, limawood and pernambuco wood, but these and the specific botanical sources have been much confused, both historically and in recent times.[92]

A dye source containing a related neoflavonoid/homoisoflavonoid component to that obtained from brazilwood is logwood *(Haematoxylon campechianum* L.), which was often used in combination with other dye sources to produce purple or black coloured yarns.[81] The components observed in the acid hydrolysed extracts of yarns dyed with the both brazilwood and logwood have been examined in more detail in Chapter 3, while the effects of light ageing on the relative ratios of the components observed in the yarn extracts have been explored in Chapter 4.

1.6 Dye source identification

Colour is one of the most important elements in the pictorial art of tapestry. However, fading of many of the original colours, leaving little or no visible trace of the dye, often occurs (Figure 1.12).

Figure 1.12: The front of 'The Story of St. Piatus and Eleutherius' (TOU 1, Chapter 5), woven in Arras in 1402 and housed in the cathedral of Tournai, Belgium

Wherever possible, historical textiles are sampled from discrete areas, for example, the ends of yarns within seams or from the reverse side of the tapestry. This produces minimal damage to the textile structure and the sampled yarns have reduced damage from exposure to light. Biological sources of textile dyes are usually determined by relative quantification of several chemical components. If a dye has faded, source identification can be complicated because the ageing process can alter the species-specific chemical composition. Recently, several characteristic

degradation pathways and products have been successfully identified for aged historical natural yellow flavonoid dyes.[80]

For the MODHT project, several analytical techniques and methodologies used for flavonoid ageing studies have been applied to investigate the characteristic components obtained from yarns dyed with different sources. The effects of prolonged exposure to light on the characteristic components have also been studied. The most important of the techniques applied to the study of the natural dye sources was PDA HPLC (Section 1.6.1), which has become an established analytical tool for the analysis of historical textiles in museums. Further investigative work was performed using mass spectrometry (Section 1.6.3).

1.6.1 Photo Diode Array High Performance Liquid Chromatography (PDA HPLC)

Partition chromatography is an important analytical technique for separating components in mixtures to aid in their identification and quantitation. In conjunction with a photo diode array (PDA) detector, a powerful separation and detection system is created.[93,94,95,96] This was the main method employed to identify the dye sources used on the historical yarns, sampled during the current project.

High performance liquid chromatography (HPLC) is a separation technique based on the relative affinity of the analytes for two phases; the stationary phase of the column and the mobile phase, also known as the eluent, which is pumped through the column at a regulated velocity. The analysis of natural dye extracts are best conducted on a reverse phase (RP) chromatography system, where the stationary phase is non-polar and the mobile phase is polar, resulting in polar analytes eluting before non-polar materials. The following discussions will therefore be confined to RP HPLC systems.

In all modern RP HPLC systems, a liquid stationary phase is chemically bonded to a solid support, typically silica. Two RP HPLC columns containing a chemically

bonded stationary phase are shown (Figure 1.13). The larger internal diameter of the semi-preparative column (Figure 1.13, top) allows a larger amount of material to be separated than with the analytical column and consequently was used for the investigation of the minor cochineal dye components (Chapter 3). The analytical column (Figure 1.13, bottom) was used for the investigation of the reference and historical samples.

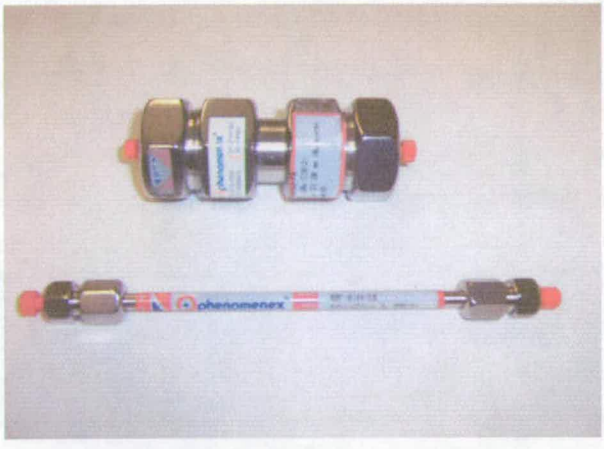

Figure 1.13: A semi-preparative RP column (top) and an analytical RP column (bottom). The larger internal diameter of the semi-preparative column compared with the analytical column allows a larger amount of material to be separated

As a consequence of the liquid stationary phase being chemically bound, it no longer behaves as a true liquid and has properties that could be described as 'mid-way' between those of a solid and a liquid. This is significant because the solid stationary phase separates analytes by adsorption onto its surface, while the chemically bonded liquid stationary phase separates analytes *via* a partitioning mechanism.[97]

This partitioning mechanism is based on the degree to which an analyte 'mixes with' the stationary and mobile phases, which can be thought of as immiscible liquids of different polarities. A large difference in the polarities of the mobile and stationary phases is undesirable, as good chromatography *i.e.* effective separation, is produced when the residence times of each analyte in the stationary phase are different.

Ideally, an analyte would therefore travel through the system continually passing between the two phases.

The composition of the mobile phase is usually aqueous with a miscible organic solvent (modifier) added to increase the partitioning behaviour of the system. The modifier is also added to allow some mixing between the mobile and stationary phases, as water does not mix with octyl or octadecyl (C_8 or C_{18} stationary phases). The differing polarities of the mobile and stationary phases cause the analytes to experience retention to a lesser or greater extent, depending on whether they are highly polar or non-polar respectively. Selectivity is also partially due to the stationary phase, with non-specific adsorption of modifier onto the stationary phase and specific interactions between analyte functional groups and residual silanol groups.

With the correct mobile phase composition and elution conditions, it is possible to separate many of the important dye source components from one another, thus aiding biological species identification in dye analysis. A solvent gradient, where the proportion of modifier is gradually increased, is often used to optimise the resolution and detection of sample analytes having a wide range of retention times, while also producing shorter analysis times and maintaining good chromatographic characteristics.

Additional variables that must be optimised include the column length, since the separating power of a column increases as its length increases. However, the analysis time is also proportional to the length, with a shorter column providing faster analysis times. Column ovens are often used to stabilise the temperature and increase the life of the column. Temperature does not have a dramatic effect on the retention process of a reverse phase system, but it can alter other variables, including mobile phase viscosity.

The dye analytes are chromophoric and often have characteristic UV-Vis spectra, so the most appropriate detection system is one based on UV-Vis. Once the analytes have been separated, they are therefore detected using a Photo Diode Array (PDA) detector. This incorporates a row of photo diodes, each of which is sensitive over a small wavelength range. After software manipulation, their combined information is used to form a UV-Vis spectrum. Detection by PDA allows peaks to be identified using retention time (R_t) and spectral (UV-Vis) data. The spectral purity of each peak can also be determined, indicating when co-elution of two or more components is taking place.[98]

The amount of light absorbed by an analyte is related to the incident intensity and the transmitted intensity by the Beer-Lambert Law;

$$A = Log\frac{I_0}{I} = \varepsilon c l_{Path}$$

Where A = Absorption

I_0 = Incident Intensity of radiation

I = Transmitted Intensity of radiation

ε = Molar extinction coefficient of analyte (l mol^{-1} cm^{-1})

c = Concentration of analyte in mobile phase passing through detector flow cell (mol l^{-1})

l_{path} = Path length of detector flow cell (cm)

As can be seen from the above expression, the absorption is also related to the concentration of the analyte in the mobile phase. At dilute concentrations, this relationship is usually linear, allowing quantification. The degree to which the radiation is absorbed is also dependent on the wavelength of the radiation and on the molar extinction coefficient of the analyte.

1.6.2 3-D Fluorescence Spectroscopy

Fluorescence detection can also be used as a sensitive tool for the analysis of dyed yarns, sometimes without the need for chromatographic separation of the analytes.[99,100] The characteristic dye components can absorb light of a specific wavelength, the excitation wavelength (λ_{ex}), to reach a higher energy state. This

energy is usually lost *via* vibration and heat, however, it can also be lost by emitting light, the emission wavelength (λ_{em}). Both the excitation and emission wavelengths are dependent on the molecular structure, so the fluorescence detector scans between a range of excitation wavelengths, producing a characteristic contour plot for each component, expressing the intensity of fluorescence (emission wavelength) produced from each excitation wavelength.

To predict the presence of broad dye classes, for example, flavonoid or anthraquinone, non-destructive screening of some of the historical yarns was performed, with no prior sample preparation, using 3-D fluorescence spectroscopy.[51] The dyed yarns were irradiated with different wavelengths of light, producing 3-D fluorescence spectra. Although this was a useful method to identify yarns possibly dyed with brazilwood, the resulting spectra were often complicated and difficult to interpret.

1.6.3 Mass Spectrometry

As indicated in the previous section, the use of PDA HPLC provides a powerful separation and detection system for natural dyes. However, coupled to mass spectrometry, a powerful investigative system for the characterisation of unknown components is created.[101,102,103,104] An atmospheric pressure ionisation method, such as electrospray, allows the eluent from the HPLC to be fed into a mass spectrometer, often revealing the mass to charge (*m/z*) value of unknown components. Furthermore, the use of an ion trap device can sometimes provide additional structural data by analysis of the breakdown patterns.[105,106,107,108,109]

The formation of the required gas-phase ions during electrospray ionisation takes place outside the vacuum system. The sample is introduced into the ionisation source through a high voltage (3-4 kV) stainless steel capillary, which aids in nebulising the HPLC eluent and promotes ionisation. The resulting spray contains micron-sized droplets of solvated analyte ions, which become even smaller as they evaporate further. The droplets are thought to reach a point where charge repulsion

between like-charged ions causes disintegration of the droplet (Coulombic fission), although the exact process by which the ions in the charged droplets are ultimately converted to gas-phase ions is not known.[110]

The electrospray process usually operates only at low (5-10 μl min^{-1}) flow rates and therefore needs to be modified to accommodate HPLC flows (*ca.* 300 μl min^{-1}). This is done by employing a co-axial flow of high purity nitrogen gas to assist the nebulisation process, together with a counter current auxiliary gas flow to aid desolvation and to prevent re-deposition of droplets on the outside of the sprayer. A heated capillary also assists the desolvation process and is the interface between the ion source and the high vacuum region of the mass spectrometer, acting as a nozzle for the expansion of the gas into the next chamber. This system is capable of handling flows of up to *ca.* 300 μl min^{-1}, allowing the eluent from an HPLC system using a narrow bore analytical column to be directly injected into the mass spectrometer. Systems using larger bore columns can also be used in combination with a post-column flow-splitter. This has only a small effect on sensitivity due to the fact that ESI appears to be concentration dependent, rather than mass flow sensitive, as is the more usual case with mass spectrometry.[111]

The ions are then sampled *via* a 'skimmer', collected by the first octopole and transmitted to the second octopole through the interoctopole lens (Figure 1.14). Octopoles are used because they transmit the ions efficiently through a region of relatively high pressure directly into the ion trap. Significantly, these parameters can be adjusted, tuning the mass spectrometer for the detection of a particular component or class of components. However, it should also be appreciated that adjusting these parameters to provide a signal maximum for a particular component may be at the expense of the signal from a second component of interest. Thus, the detection of unknowns is sometimes problematic.

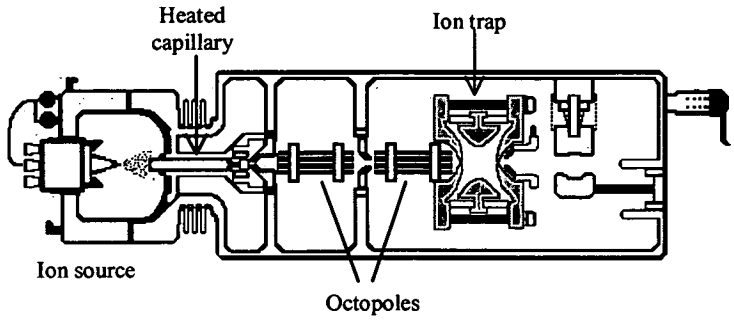

Figure 1.14: Diagram of an LCQ ion trap mass analyser (from reference 80)

The ions are then introduced into the trap by a 'gate' mechanism. Once inside, they are confined to roughly circular orbits by voltages applied to end caps. Helium (1 mTorr) is introduced to reduce the kinetic energy of the ions and contract their trajectory to the centre of the trap. This improves the sensitivity and resolution of the instrument by allowing the ions to be ejected in dense ion packets.[112] The trap itself is essentially a stainless steel cylinder, a few cm high and *ca.* 10 cm in diameter, with holes in the end-caps to admit the sample and allow the ejection of ions. It is evacuated to a high vacuum by a combination of rotary and turbomolecular pumps.

An MS/MS (or MS^2) experiment can now be performed to gain structural information. First, a waveform is applied to eject all ions except the precursor of interest. The trapped precursor ions are then accelerated to a higher kinetic energy by applying another RF pulse or waveform. The radius traced out by the path of the precursor ion also increases, thus the maximum kinetic energy that can be achieved is limited and decreases with increasing mass-to-charge ratio (*m/z*). The precursor ions are accelerated in the presence of a collision gas (helium). When an ion collides with a neutral atom or molecule, some of its kinetic energy can be converted into internal energy (collisional activation). If there is enough excess internal energy to break chemical bonds, the ions will decompose (collisionally induced dissociation, or CID). If an activated ion has a broad internal energy distribution, many different kinds of fragmentations will result, while a narrow internal energy distribution will result in efficient conversion of the precursor ions to only a few specific products.[113]

In addition, a low, narrow internal energy distribution will favour bond rearrangements, while a high, narrow internal energy distribution will favour simple bond cleavage.[114]

Collision activation in an ion trap is somewhat different from collisional activation in other mass spectrometers. The ions can be momentarily accelerated to a higher kinetic energy, but then decelerated by the 'excitation' waveform. This acceleration/deceleration process is allowed to continue in the presence of a collision gas for periods of ms or longer, thus the collision energy is not a single value and the collision process involves multiple collisions.[114] A few, low-energy reaction processes, such as rearrangement reactions, are therefore favoured. These may, however, be difficult to interpret in terms of the original precursor ion structure. As it is common to observe only a few fragment-ion types in an ion trap MS^2 spectrum, multi-stage experiments, where the product ion is itself trapped then excited (MS^n), are often required to obtain structural information.

1.6.4 Nuclear Magnetic Resonance (NMR)

Structural information on characteristic dye components can also be obtained using Nuclear Magnetic Resonance (NMR) spectroscopy. This is a common technique routinely used for the structural determination of organic molecules and in general, is conducted on mg amounts of material.[115] Although NMR techniques are being exploited for use within the cultural heritage sector,[116,117] their applicability for the identification of unknown dye components is limited by the relatively small quantities of the unknown minor components found within an often complex mixture (generally μg amounts or smaller). However, NMR techniques have increasingly been used in combination with chromatographic and mass spectrometric analysis for the identification of minor components in plant and insect extracts.[118,119]

1.7 Summary

The dyeing procedures, together with the natural dye sources used, have been shown to play a significant role in the results obtained from the chemical and physical

analysis of unaged and aged reference samples within the MODHT project. This complicated efforts to relate the mechanical breakdown of the tapestries to quantifiable indicators of damage. Accurate identification of the dye sources on the yarns sampled from the selected historical tapestries is therefore necessary for an effective assessment of damage.

1.8 References

[1] Howell, D. *'Prioritising interventive treatments for textile materials'*, Postprints to the AHRB Research Centre for Textile Conservation and Textile Studies 1st Annual Conference, **2005,** 69-70

[2] Hallet, K.; Howell, D., *'Size exclusion chromatography as a tool for monitoring silk degradation in historic tapestries'*, Postprints to the AHRB Research Centre for Textile Conservation and Textile Studies 1st Annual Conference, **2005,** 143-150

[3] Hallet, K.; Howell, D., *'Size exclusion chromatography of silk – inferring the tensile strength and assessing the condition of historic tapestries'*, Preprints to the ICOM Committee for Conservation, 14th Triennial meeting, The Hague, **2005**, 2, 911-919

[4] Bennett, A.G., *'Five Centuries of tapestry'*, **1976**, The Fine Arts Museum of San Francisco and Charles E. Tuttle Co.

[5] Carretero, C.H., *'Colección real espanola, Patrimonio Nacional'*, Report prepared for the Monitoring of Damage in Historic Tapestries (MODHT) project, **2002**

[6] Timár-Balázsy, Á.; Eastop, D., *'Chemical Principles of textile conservation'*, **1998**, Butterworth-Heinemann

[7] Jones, L.N.; Rivett, D.E.; Tucker, D.J., *'Wool and related mammalian fibers'*, in, 'The Handbook of Fiber Chemistry'; Lewin, M and Pearce E.M., (eds), **1998**, Marcel Dekker Inc, 2nd edition, 356-413

[8] Milligan, B.; Maclaren, J.A., *'Wool science, the chemical reactivity of the wool fibre'*, **1981**, Australian Science Free Press, Marrackville, Australia

[9] Parsons, Y.M.; Cooper, D.W.; Piper, L.R., *'Evidence of linkage between high-glycine-tyrosine keratin gene loci and wool fiber diameter in a Merino half-sib family'* Anim Genet, **1994**, 25, 2, 105-108

[10] Gillespie, J.M.; Darskus, R.L., *'Relation between the tyrosine content of various wools and their content of a class of proteins rich in tyrosine and glycine'*, Aust J Biol Sci, **1971**, 24, 1189

[11] Crewther, W.G.; Fraser, R.D.B.; Lennox, F.G.; Lindley, H., *'The chemistry of keratins'*, Adv Protein Chem, **1965**, 20, 191

[12] Steenken, I.; Zahn, H. *'Investigation of the alkaline modification of wool using new analytical methods for the determination of degradation'*, J Soc Dyers Colour, **1986**, 102, 9, 269-73

[13] Hill, R.R.; Ghadimi, M.J, *'Alkali-promoted yellowing of wool. Yellow degradation products from a model for protein-bound cystine'*, Soc Dyers Colour, **1996**, 112, 5/6, 148-152

[14] Inglis, A.S.; Leaver I.H.; Lennox, F.G., *'Studies in wool yellowing. XI. Changes in the composition of components due to UV irradiation'*, Proc Int wool textile research conf, **1965**, 2, 1210129

[15] Weatherall, I.L., *'The tendering of wool by light'*, Proc Int Wool Textile Research conf, **1975**, 2, 580-589

[16] Holt, L.A.; Milligan, B., *The formation of carbonyl groups during irradiation of wool and its relevance to photoyellowing'*, Tex Res J, **1977**, 47, 620-624

[17] Church, J.S.; Millington, K.R., 'Photodegradation of wool keratin: Part 1. Vibrational spectroscopic studies', Biospectroscopy, **1996**, 2, 4, 249-258

[18] Robson, R.M., *'Silk: Composition, Structure, and Properties'*, in, 'The Handbook of Fiber Chemistry'; Lewin, M and Pearce E.M., (eds), **1998**, Marcel Dekker Inc, 2nd edition, 416-463

[19] Gamo, T.; Inokuchi, T.; Laufer, H., *'Polypeptides of fibroin and sericin secreted from the different sections of the silk gland in* Bombyx mori', Insect Biochem, **1977**, 7, 285

[20] Masayoshi, N.; Kobayashi, K., *'Fine structure of silk fibroin. VI. Difference in the disintegration of silk fibroin by hydrogen peroxide and by dilute alkali solution'*, J Soc Textile Cellulose Ind (Japan), **1954**, 10, 131-134

[21] Zurovec, M.; Sehnal, F., *'Unique molecular architecture of silk fibroin in the waxmoth,* Galleria mellonella', J Biol Chem, **2002**, 277, 25, 22639-22647

[22] Tsukada, M.; Hirabayashi, K., *'Change of silk fibroin structure by ultraviolet radiation'*, J Polym Sci Pol Lett, **1980**, 18, 507-511

[23] Baltova, S.; Vassileva, V., *'Photochemical behaviourof natural silk – II. Mechanism of fibroin photodestruction'*, Polymer degrad stab, **1998**, 60, 61-65

[24] Sikorski, J.; Hepworth, A.; Buckley, T., *'Scanning electron microscope techniques in wool research and processing'*, Appl Polym Symp, **1971**, 18, 2, 887-93

[25] Ballard, M.; Koestler, R.J.; Blair, C.; Indictor, N., *'Historical silk flags studied by scanning electron microscopy-energy dispersive x-ray spectrometry'* Adv Chem Ser, **1989**, 220, 419-28

[26] Angel, A.; Jakes, K.A., *'Preparing and analyzing fractured archaeological fibers'*, J Electron Micr Tech, **1990**, 14, 1, 1-5

[27] Hacke, A-M., PhD Thesis, **2006**, The University of Manchester

[28] Carr, C.N.; Ho, S.F.; Lewis, D.M.; Owen, E.D.; Roberts, M.W., *'Photoelectron spectroscopy and the surface chemistry of wool'*, J Text I, **1985**, 76, 6, 419-424

[29] Carr, C.M.; Leaver, I.H.; Hughes, A.E., *'Detection and analysis by XPS of sulfhydryl groups at the surface of wool fibers'*, Text Res J, **1986**, 56, 3, 216-217

[30] Carr, C.M.; Leaver, I.H.; Hughes, A.E., *'X-ray photoelectron spectroscopic study of the wool fiber surface'*, Text Res J, **1986**, 56, 7, 457-461

[31] Shao, J.; Jones, D.C.; Mitchell, R.; Vickerman, J.C.; Carr, C.M., *'Time-of-flight secondary-ion-mass spectrometric (ToF-SIMS) and X-ray photoelectron spectroscopic (XPS) analyses of the surface lipids of wool'*, J Text I, **1997**, 88, 4, 317-324

[32] Shao, J.; Liu, J.; Zheng, J.; Carr, C.M., *'X-ray photoelectron spectroscopic study of silk fibroin surface'*, Polym Int, **2002**, 51, 12, 1479-1483

[33] Karsten, I.F.; Kerr, N., *'The properties and light stability of silk adhered to sheer silk and polyester support fabrics with poly(vinyl acetate) copolymer'*, Stud Conserv, **2002**, 47, 3, 195-210

[34] Hallet, K., *Unpublished data*, **2005**, Historic Royal Palaces, Conservation and Collections Care, Hampton Court Palace, London

[35] Betcheva, R.; Konstantinova, T.; Spirieva, A., *'Colorimetric study on the textile application of some benzanthrone dyes'*, Fibres text east eur, **2001**, 9, 3, 41-44

[36] Montazer, M.; Parvinzadeh, M.; Kiumarsi, A., *'Colorimetric properties of wool dyed with natural dyes after treatment with ammonia'*, Color Technol, **2004**, 120, 4, 161-166

[37] Bora, M.N.; Baruah, G.C.; Talukdar, C.L., *'Investigation on the thermodynamical properties of some natural silk fibers with various physical methods'*, Thermochim Acta, **1993**, 218, 425-434

[38] Huson, M.G., *'DSC investigation of the physical aging and deaging of wool'*, Polym Int, **1991**, 26, 3, 157-161

[39] Beck, P.J.; Gordon, P.G.; Ingham, P.E., *'Thermogravimetric analysis of flame-retardant-treated wools'*, Text Res J, **1976**, 46, 7, 478-483

[40] Zhang, H.; Magoshi, J.; Becker, M.; Chen, J.Y.; Matsunaga, R., *'Thermal properties of Bombyx mori silk fibers'*, J Appl Polym Sci, **2002**, 86, 8, 1817-1820

[41] Odlyha, M.; Foster, G.M.; Townsend, J.; Hackney, S., *'Dynamic mechanical thermal analysis for the evaluation of deacidification treatment of painting canvases'*, J Therm Anal Calorim, **1997**, 50, 191-202

[42] Odlyha, M.; Wang, Q., Foster, G.M., de Groot, J.; Horton, M.; Bozec, L., *'Monitoring of damage to historic tapestries: the application of dynamic mechanical thermal analysis to model and historic tapestries'*, Postprints to the AHRB Research Centre for Textile Conservation and Textile Studies 1st Annual Conference, **2005,** 126-134

[43] Odlyha, M.; Wang, Q.; Foster, G.M.; de Groot, J.; Horton, M.; Bozec, L., *'Thermal analysis of model and historic tapestries'*, J Therm Anal Calorim, **2005**, 82, 3, 627-636

[44] Halpine, S., *'Amino acid analysis of proteinaceous media from Cosimo Tura's "The Annunciation with Saint Francis and Saint Louis of Toulouse"'*, Stud Conserv, **1992**, 37, 22-38

[45] Ronca, F., *'Protein determination in polychromed stone sculptures, stuccoes and gesso grounds'*, Stud Conserv, **1994**, 39, 107-120

[46] Wouters, J.; Van Bos, M.; Lamens, K., *'Baroque Stucco Marble Decorations. I. Preparation of Laboratory Replicas and Establishment of Criteria for Analytical Evaluation of Organic Materials'*, Studi Conserv, **2000**, 45, 106-116

[47] Csapo, J.; Csapo-Kiss, Z.; Martin, T.G.; Folestad, S.; Orwar, O.; Tivesten, A.; Nemethy, S., *'Age estimation of old carpets based on cystine and cysteic acid content'*, Anal Chim Acta, **1995**, 300, 1-3, 313-320

[48] Becker, M.A.; Magoshi, Y.; Sakai, T.; Tuross, N.C., *'Chemical and physical properties of old silk fabrics'*, Stud Conserv, **1997**, 42, 1, 27-37

[49] Csapo, J.; Csapo-Kiss, Z..; Csapo, J., Jr, *'Use of amino acids and their racemization for age determination in archaeometry'*, Trends Anal Chem, **1998**, 17, 3, 140-148

[50] Yanagi, Y.; Kondo, Y.; Hirabayashi, K.., *'Deterioration of silk fabrics and their crystallinity'*, Text Res J, **2000**, 70, 10, 871-875

[51] Lamens, K.; Vanden Berghe, I.; Wouters, J., *Unpublished data*, **2005**, The Royal Institute for Cultural Heritage (KIK), Belgium

[52] Knecht, R. and Chang, J.-YY., *'Liquid chromatographic determination of amino acids after gas-phase hydrolysis and derivitization with (dimethylamino)-azobenzene-sulfonyl chloride'*, Anal Chem, **1986**, 58, 2375-2379

[53] Waters AccQ.Tag Chemistry Package, **1993**, Instruction Manual, Millipore Corporation, Milford, USA, manual number WAT052874, Rev. 0

[54] Larsen, R.; Vest, M.; Nielsen, K; Jensen, A.L., *'Amino acid analysis'* in 'STEP Leather Project: Evaluation of the correlation between natural and artificial ageing of vegetable tanned leather and determination of parameters for standardization of an artificial ageing method', Larsen, R., **1994**, Royal Danish Academy of Fine Arts, School of Conservation, Copenhagen, 39-57

[55] Burgess, H., *'The use of gel permeation chromatography in investigating the degradation of cellulose during conservation bleaching'*, Preprints of the contributions to the Washington congress, 3-9 September, Brommelle, N.; Thomson, G. (eds.), **1982**, London: International Institute for Conservation, 85-88

[56] Emsley, A.; Ali, M.; Heywood, R., *'A size exclusion chromatography study of cellulose degradation'*, Polymer, **2000**, 41, 24, 8513-8521

[57] Dupont, A-L, *'The role of gelatine/alum sizing in the degradation of paper: a study by size exclusion chromatography in lithium chloride/N,N-dimethylacetamide using multiangle light scattering detection'*, **2002**, Works of Art on paper, books, documents and photographs: techniques and conservation, contributions to the Baltimore congress, Daniels, V; Donnithorne, A; Smith, P. (eds.), International Institute for Conservation, London, 59-64

[58] Jerosch, H.; Lavédrine, B.; Cherton, J-C, *'Study on the correlation between SEC and mechanical tests of different paper types for degradation state evaluation'*, Restaurator, **2002**, 23, 4, 222-239

[59] Jerosch, H.; Lavédrine, B.; Cherton, J-C, *'The use of size exclusion chromatography (SEC) for the evaluation of paper degradation caused by nitrogen oxides in comparison with other methods'*, Works of Art on paper, books, documents and photographs: techniques and conservation, contributions to the Baltimore congress, **2002**, Daniels, V; Donnithorne, A; Smith, P. (eds.), International Institute for Conservation, London, 108-113

[60] Howell, D.; *'Silk degradation studies'*, Silk: Harper's Ferry Regional Textile Group, 11th Symposium, **1992**, National museum of American History, 11-12

[61] Tse, S.; Dupont, A-L., *'Measuring silk deterioration by high-performance size-exclusion chromatography, viscometry and electrophoresis'*, ACS Symp Ser, **2001**, 779, 98-114

[62] Sperling, L.H., *'Gel Permeation Chromatography and High Performance Liquid Chromatography: Modern Terminology and Usage'*, ACS Division of Polymeric Materials: Science and Engineering (PMSE), **1999**, 81, 569

[63] Trathnigg, B., *'Size-exlusion chromatography of polymers'*, in 'Encyclopaedia of analytical chemistry', Meyers, R.A. (ed), **2000**, John Wiley & Sons Ltd., 8008-8034

[64] Zhang, X.; Laursen, R.A., *'Development of Mild Extraction Methods for the Analysis of Natural Dyes in Textiles of Historical Interest Using LC-Diode Array Detector-MS'*, Anal Chem, **2005**, 77, 2022-2025

[65] Koren, Z.C., *'An efficient HPLC analysis scheme for plant and animal red, blue and purple dyes'*, Dyes Hist Arch, **1995**, 13, 27-37

[66] Wouters, J., *'High Performance Liquid Chromatography of anthraquinones: analysis of plant and insect extracts and dyed textiles'*, Stud Conserv, **1985**, 30, 119-128

[67] Verhecken, A., *'A concise History of Dye Analysis'*, Dyes Hist Arch, **2005**, 20, 1-22

[68] Ferreira, E.S.B.; Quye, A.; Hulme, A.N.; McNab, H., *'The Natural constituents of historical textile dyes'*, Chem Soc Rev, **2004**, 33, 329 - 336

[69] Schweppe. H., *'Handbuch der Naturfarbstoffe'*, **1993**, Verlagsgesellschatf, Landsberg

[70] Cardon, D., *Le monde des teintures naturelles'*, **2003**, Éditions Belin, 141-195

[71] Quye, A.; Cheape, H.; Burnett, J.; Ferrira, E.S.B.; Hulme, A.N.; McNab, H., *'An historical and analytical study of red, pink, green and yellow colours in quality 18th and early 19th century Scottish tartans'*, Dyes Hist Arch, **2003**, 19, 1-12

[72] Goto, T.; Kondo, T., *'Structure and molecular stacking of anthocyanins – flower colour variation'*, Angew Chem Int Ed Engl, **1991**, 30, 17-33

[73] Swain, T., *'Flavonoids as chemotaxonomic Markers in Plants'*, in 'Pigments in plants', Czygan, F.C. (ed), **1980**, Gustav-Fisher-Verlag, 2nd edition, 224-236

[74] Williams, C.A.; Greenham, J.; Harborne, J.B., *'The role of lipophilic and polar flavonoids in the classification of temperate members of the Anthemideae'*, **2001**, Biochem Syst Ecol, 29, 929-945

[75] Tomás-Barberán, F.A.; Martos, I.; Ferreres, F.; Radovic, B.S.; Anklam, E., *'HPLC flavonoid profiles as markers for the botanical origin of European unifloral honeys'*, J Sci Food Agr, **2001**, 81, 485-496

[76] Roseiro, L.B.; Viala, D.; Besle, J.M.; Carnat, A.; Fraisse, D.; Chezal, J.M.; Lamaison, J.L., *'Preliminary observations of flavonoid glycosides from the vegetable coagulant* Cynara *L. in protected designation of origin cheeses'*, Int Dairy J, **2005**, 15, 579-584

[77] Wollenweber, E.; Stevens, J.F.; Dörr, M.; Rozefelds, A.C., *'Taxonomic significance of flavonoid variation in temperate species of* Nothofagus*'*, Phytochemistry, **2003**, 62, 1125–1131

[78] Yuldashev, M.P.; Batirov, É.Kh.; Malikov, V.M.; Yuldasheva, N.P. *'Flavonoids of* Psoralea drupaceae *and* Reseda luteola*'*, Chem Nat Compd, **1996**, 32, 6, 923-924

[79] Kaiser, R.; *Quantitative Analysis of Flavonoids in Yellow Dye Plant Species Weld (*Reseda luteola *L.) and Sawwort (*Serratula tinctoria *L.)'*, Angew Bot, **1993**, 67, 128-131

[80] Ferreira, E.S.B., *'New Approaches Towards the identification of yellow dyes in ancient textiles'*, PhD Thesis, **2002**, The University of Edinburgh

[81] Hofenk de Graaff, J.H., *'The Colourful Past'*, **2004**, Abegg-Stiftung and Archetype Publications, 1st edition, 175-181

[82] Andary, C.; Prunac, S., *'Yellow Dyes of Historical Importance: A Multi-Disciplinary Study. II: Chemical Analysis of Weld and Saw-wort'*, Dyes Hist Arch, **1996**, 14, 33-38

[83] Cristea, D.; Bareau, I.; Vilarem, G., *'Identification and quantitative HPLC analysis of the main flavonoids present in weld (*Reseda luteola *L.)'*, Dyes Pigments, **2003**, 57, 267-272

[84] Cooksey, C.J.; Sinclair, R.S., *'Colour variation in Tyrian Purple Dyeing'*, Dyes Hist Arch, **2005**, 20, 127-135

[85] Wouters, J., *'High Performance Liquid Chromatography of Anthraquinones: Analysis of Plant and Insect Extracts and Dyed Textiles'*, Stud Conserv, **1985**, 30, 119-128

[86] Wouters, J., *'The Dye of* Rubia peregrine. *I. Preliminary Investigations'*, Dyes Hist Arch, **2001**, 16/17, 145-157

[87] Wouters, J.; Verhecken, A., *'The Coccid Insect Dyes: HPLC and computerized Diode Array Analysis of Dyed Yarns'*, Stud Conserv, **1989**, 34, 189-200

[88] González, M.; Méndez, J.; Carnero, A.; Lobo, M.G.; Afonso, A., *'Optimizing Conditions for the Extraction of Pigments in Cochineals (*Dactylopius coccus *Costa) using Response Surface Methodology'*, J Agr Food Chem, **2002**, 50, 6969-6974

[89] Wouters, J.; Verhecken, A., *'The Scale Insect Dyes (*Homoptera: Coccoidea*). Species Recognition by HPLC and Diode-Array Analysis of the Dyestuffs'*, Annals Soc Ent Fr (N.S.), **1989**, 25, 4, 393-410

[90] Reddy, V.L.N.; Ravikanth, V.; Lakshmi, V.V.N.S.J.; Murty, U.S.; Venkateswarlu, Y., *'Inhibitory activity of homoisoflavonoids from* Caesalpinia sappan *against* Beauveria bassiana*'*, Fitoterapia, **2003**, 600-602

[91] Camarda, L.; Merlini, L.; Nasini, G., *'Dragon's blood from* Dracaena draco*, structure of novel homoisoflavonoids'*, Heterocycles, **1983**, 20, 1, 39-43

[92] Nowik, W., *'The possibility of differentiation and identification of red and and blue 'soluble' dyewoods: Determination of species used in dyeing and chemistry of their dyestuffs'*, Dyes Hist Arch, **2001**, 16/17, 129-144

[93] Mattila, P.; Astola, J.; Kumpulainen, J., *'Determination of flavonoids in plant material by HPLC with Diode-Array and Electro-Array Detections'*, J Agr Food Chem, **2000**, 48, 5834-5841

[94] Trojanowicz, M.; Orska-Gawryś, J.; Surowiec, I.; Szostek, B.; Urbaniak-Walczak, K.; Kehl, J.; Wrobel, M., *'Chromatographic investigation of dyes extracted from Coptic textiles from the national museum in Warsaw'*, Stud Conserv, **2004**, 49, 115-130

[95] Crozier, A.; Jensen, E.; Lean, M.E.J.; MccDonald, M.S., *'Quantitative analysis of flavonoids by reversed-phase high-performance liquid chromatography'*, J Chromatogr A, **1997**, 761, 315-321

[96] Waksmundzka-Hajnos, M., *'Chromatographic separations of aromatic carboxylic acids'*, J Chromatogr B, **1998**, 717, 93-118

[97] Consultants in Chromatographic Training, *'An introduction to HPLC techniques for AstraZeneca Pharmaceuticals'*, **2000**, Version 2.2; CCT, 6 Hattons Park, Longstanton, Cambridge, CB4 5DL

[98] Huber, L.; George, S.A. (eds), *'Diode Array Detection in HPLC'*, **1993**, Marcel Dekker, Inc., 1st edition

[99] Shimoyama, S.; Noda, Y., *'Non-destructive determination of plant dyestuffs used for ancient madder dyeing, employing a three-dimensional fluorescence spectrum technique'*, Dyes Hist Arch, **1995**, 13, 14-26

[100] van Bommel, M.R., *'The analysis of dyes with HPLC coupled to Photodiode Array and Fluorescence detection'*, Dyes Hist Arch, **2005**, 20, 30-38

[101] Stobiecki, M., *'Application of mass spectrometry for identification and structural studies of flavonoid glycosides'*, Phytochemistry, **2000**, 54, 237-256

[102] Mämmelä, P.; Savolainen, H.; Lindroos, L.; Kangas, J.; Vartiainen, T., *'Analysis of oak tannins by liquid chromatography-electrospray ionisation mass spectrometry'*, J Chromatogr A, **2000**, 891, 75-83

[103] Careri, M.; Elviri, L.; Mangia, A., *'Validation of a liquid chromatography ionspray mass spectrometry method for the analysis of flavanones, flavones and flavonols'*, Rapid Commun Mass sp, **1999**, 13, 2399-2405

[104] Puchalska, M.; Poleć-Pawlak, K.; Zadrozna, I.; Hryszko, H.; Jarosz, M., *'Identification of indigoid dyes in natural organic pigments used in historical art objects by high-performance liquid chromatography coupled to electrospray ionisation mass spectrometry'*, J Mass Spectrom, **2004**, 39, 1441-1449

[105] Justesen, U., *Collision-induced fragmentation of deprotonated methoxylated flavonoids, obtained by electrospray ionisation mass spectrometry'*, J Mass Spectrom, **2001**, 36, 169-178

[106] Fabre, N.; Rustan, I.; de Hoffmann, E.; Quetin-Leclercq, J.; *'Determination of flavone, flavonol and flavanone aglycones by negative ion liquid chromatography electrospray ion trap mass spectrometry'*, J Am Soc Mass Spectr, **2001**, 12, 707-715

[107] Cuyckens, F.; Claeys, M.; *'Mass spectrometry in the structural analysis of flavonoids'*, J Mass Spectrom, **2004**, 39, 1-15

[108] de Rijke, E.; Zappey, H.; Ariese, F.; Gooijer, C.; Brinkman, U.A.Th., *'Liquid chromatography with atmospheric pressure chemical ionisation and electrospray ionisation mass spectrometry of flavonoids with triple-quadrupole and ion-trap instruments'*, J Chromatogr A, **2003**, 984, 45-58

[109] Davis, B.D.; Brodbelt, J.S., *'Determination of the glycosylation site of flavonoid monoglucosides by metal complexation and tandem mass spectrometry'*, J Am Soc Mass Spectr, **2004**, 15, 1287-1299

[110] Ikonomou, M.G.; Blades, A.T.; Kebarle, P., *'Electrospray-Ion spray: A comparison of mechanisms and performance'*, Anal Chem, **1991**, 63, 1989-1998

[111] Catlow, D.W., *'Mass spectrometry: Level one training course'*, Astrazeneca training manual, **1998**

[112] McLuckey, S.A.; Glish, G.L.; Kelley, P.E., *'Collision-activated dissociation of negative ions in an ion trap mass spectrometer'*, Anal Chem, **1987**, 59, 1670-1674

[113] Wysocki, V.H.; Kenttämaa, H.I.; Cooks, R.G., *'Internal energy distributions of isolated ions after activation by various methods'*, Int J Mass Spectrom, **1987**, 75, 181-208

[114] Jeol Mass Spectrometer – Product Notes; http://www.jeolusa.com/ms/docs/ms-ms.pdf; accessed on 30th January **2006**

[115] Lambert, J.B.; Shurvell, H.F.; Lightner, D.A.; Cooks, R.G., *'Organic Structural Spectroscopy'*, **1998**, Prentice-Hall, Inc., 8-152

[116] Lambert, J.B.; Shawel, C.E.; Stearns, J.A., *'Nuclear Magnetic Resonance in Archaeology'*, Chem Soc Rev, **2000**, 29, 175-182

[117] Blűmich, B; Anferova, S.; Sharma, S.; Segre, A.L.; Federici, C., *'Degradation of historical paper: Nondestructive analysis by the NMR-MOUSE'*, J Magn Reson, **2003**, 161, 204–209

[118] Rauter, A..; Martins, A.; Borges, C.; Ferreira, J.; Jorge, J.; Bronze, M-R.; Coelho, A.V.; Choi, Y.H.; Verpoorte, R., *'Liquid chromatography-diode array detection-electrospray ionisation mass spectrometry/nuclear magnetic resonance analysis of the anti-hyperglycemic flavonoid extract of* Genista tenera. *Structure elucidation of a flavonoid-C-glycoside'*, J Chromatogr, **2005**, 1089, 59-64

[119] Gronquist, M.; Meinwald, J.; Eisner, T.; Schroeder, F.C., *'Exploring Uncharted Terrain in Nature's Structure Space Using Capillary NMR Spectroscopy: 13 Steroids from 50 Fireflies'*, J Am Chem Soc, **2005**, 127, 10810-10811

Chapter 2

2 THE ANALYTICAL INVESTIGATION OF SELECTED NATURAL YELLOW DYE SOURCES AND THEIR MORDANTS

The analytical investigation of several historically important natural yellow dye sources is presented. This extends previous work on the characterisation of acid hydrolysed extracts of natural yellow dye sources,[1] providing information on the flavonoid components of authentically dyed reference material.

Furthermore, a novel approach towards mordant identification using Inductively Coupled Plasma (ICP) techniques is presented. The mordant, usually a metal salt such as alum [$AlK(SO_4)_2.12H_2O$], forms a complex between the fibre and the dye molecule, altering the colour and increasing the fastness of the dye. The identification of the mordant-dye composition of historical yarns can provide information regarding manufacture and provenance, while also aiding in the assessment of actual, or potential, damage to the object.

2.1 The use of flavonoids in the identification of several historically important natural yellow dye sources

2.1.1 Introduction

The characteristic flavonoid components obtained from the acid hydrolysed extracts of dyed yarns can be used to identify the probable biological sources employed in the dyeing of the historical samples (Chapter 5). In addition to providing important empirical evidence for the use of certain dye sources, species identification allows grouping of 'similar' historical yarns *i.e.* those likely to have undergone comparable dyeing procedures. This information can aid in the analysis of data obtained from other chemical and physical tests, designed to provide an overall damage assessment for the object (Chapter 1).

Identification of the dye sources used on historical tapestries first requires the characterisation of the chemical components from yarns dyed with authentic reference sources. The reference sources should be dyed onto the yarn in a manner as similar as possible to the procedures described in historical dyeing manuals.[2] A series of 'historically accurate' reference samples was therefore produced as part of the Monitoring of Damage to Historic Tapestries (MODHT) project (Appendix 7.2).

The most likely biological sources used to produce yellows (and greens when used with a blue dye source such as indigo or woad) within the period of interest were identified as weld, dyer's greenweed, sawwort and young fustic.[3] Authentic plant material was sourced, and then dyed onto wool and silk yarns, following historical procedures as far as possible. The dyeing of weld and dyer's greenweed onto both wool and silk was performed by one of the project members,[4] (Appendix 7.2) while the sawwort and young fustic samples were dyed at the National Museums of Scotland (Chapter 6). The yarn specifications for all the references produced were carefully selected to compare favourably with the yarn in the historical tapestries sampled during the project (Chapter 5) and were English sheep wool (3-ply, 158 Tex) and Italian spun *Bombyx mori* silk (2-ply, 66 Tex). The ply of a yarn is the number of fibre strands and the Tex is a measure of the weight (g) of 1 km of yarn.

The dye components on the reference yarns should be extracted using an identical procedure to that chosen for the analysis of the historical yarns. Several different extraction methods have been documented,[5,6,7] however, the sample preparation for the extraction of dye components from historical textiles within the present study is based on the commonly used hydrolysis procedure with hydrochloric acid (Chapter 6).[8] To identify these components and thus the biological source, the acid hydrolysed extracts are analysed using PDA HPLC (Chapter 1). The chromatographic method was based on one developed to separate as many of the important natural dye components as possible (Chapter 6).[1] The components can often be characterised by comparison of retention time (R_t) and UV-Vis spectral information with known standards. However, additional information from

Electrospray Ionisation (Ion Trap) Mass Spectrometry (ESI MS^n) is sometimes required to enable characterisation of unknown components.

The PDA HPLC spectra obtained from the acid hydrolysed extracts of historical textile yarns can thus be compared with spectra from authentically dyed reference material. The dye source is usually successfully identified when relatively unaged material is used.

2.1.2 Results and Discussion

2.1.2.1 Weld (*Reseda luteola* L.)

The yellow dye component most commonly detected in acid hydrolysed extracts from historical European textiles is luteolin, a flavone with perhaps the best light fastness of all the flavonoids found in yellow plant dyes. When luteolin is detected along with relatively minor amounts of apigenin and a luteolin methyl ether, the dye source is usually reported as weld (*Reseda luteola* L.), regarded as the most widely used of all European yellow dye plants (Figure 2.1).

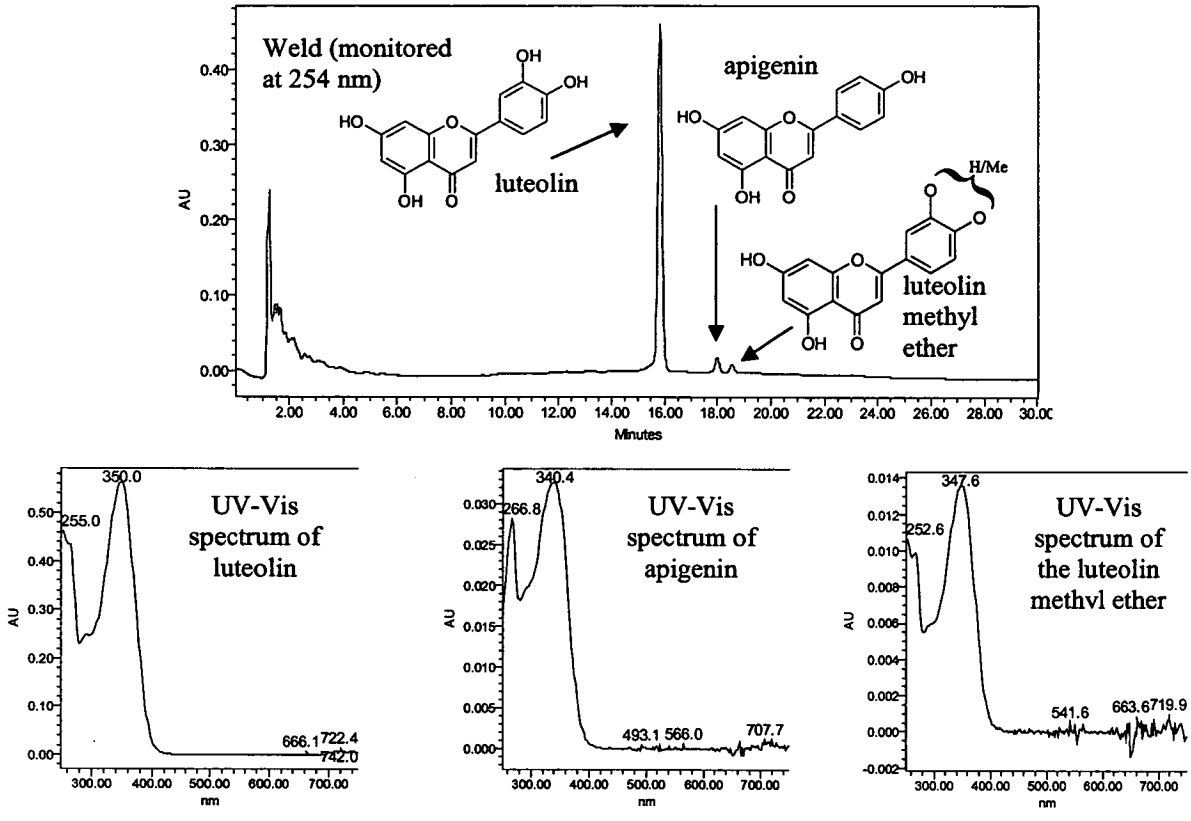

Figure 2.1: The chromatogram (monitored at 254 nm) of the acid hydrolysed extracts of weld, showing the structure of the characteristic components and their UV-Vis spectra

Although the constituents of weld are well documented,[1,9,10,11] the identity of the luteolin methyl ether in the acid hydrolysed extracts has not been confirmed. Previous research using negative ion HPLC ESI MS^n techniques found that the Collisionally Induced Dissociation (CID) of this unknown component was best explained with the methoxy group present on the B-ring (Scheme 2.1).[1]

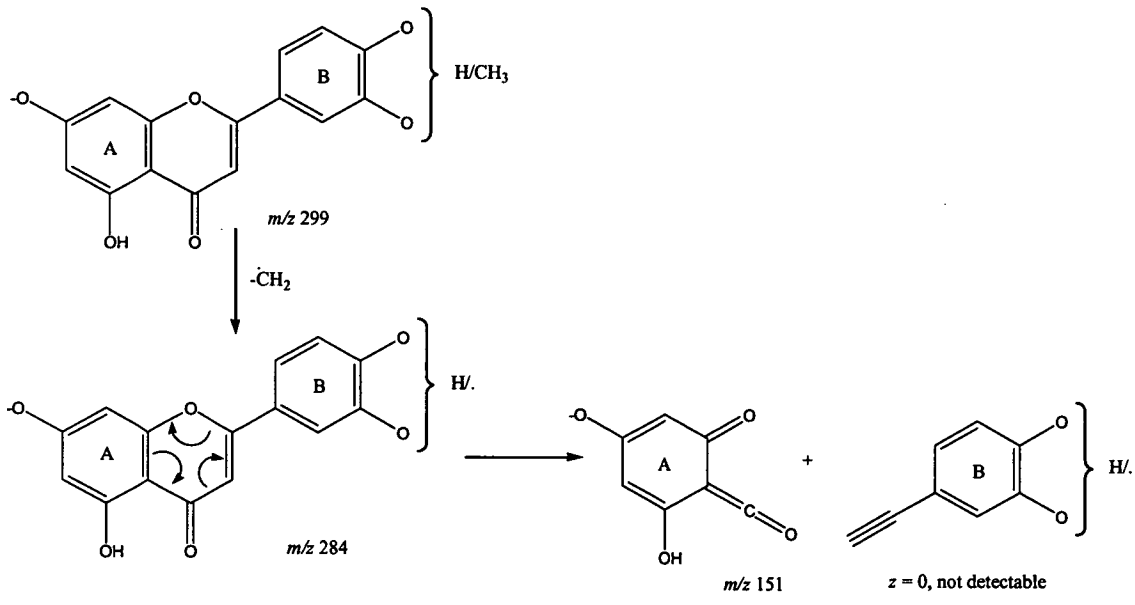

Scheme 2.1: The suggested breakdown path of the *m/z* 299 ion in the ion trap mass spectrometric analysis of the acid hydrolysed extracts from a weld dyed yarn (from reference 1)

Reference samples of the two possible flavonoid isomers, chrysoeriol (3'-methoxy-5,7,4'-trihydroxyflavone) and diosmetin (4'-methoxy-5,7,3'-trihydroxyflavone) were therefore purchased (Figure 2.2) and their identity confirmed by Nuclear Magnetic Resonance (NMR) spectroscopy (Chapter 6).

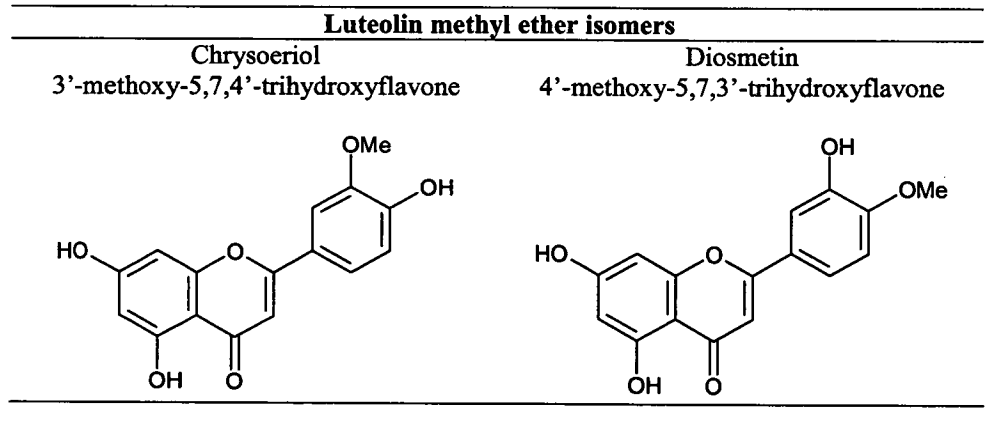

Figure 2.2: The two possible flavonoid isomers, diosmetin (4'-methoxy-5,7,3'-trihydroxyflavone) and chrysoeriol (3'-methoxy-5,7,4'-trihydroxyflavone)

A solution of each was chromatographed under identical conditions to that of the weld reference. A comparison of retention time and UV-Vis spectra suggested that

the luteolin methyl ether present in the acid hydrolysed extracts of weld dyed yarn was chrysoeriol. This was confirmed by spiking experiments, where a solution of either chrysoeriol or diosmetin was used to reconstitute the dry residue from the acid hydrolysis of a weld dyed yarn and compared with an un-spiked weld extract (Figure 2.3).

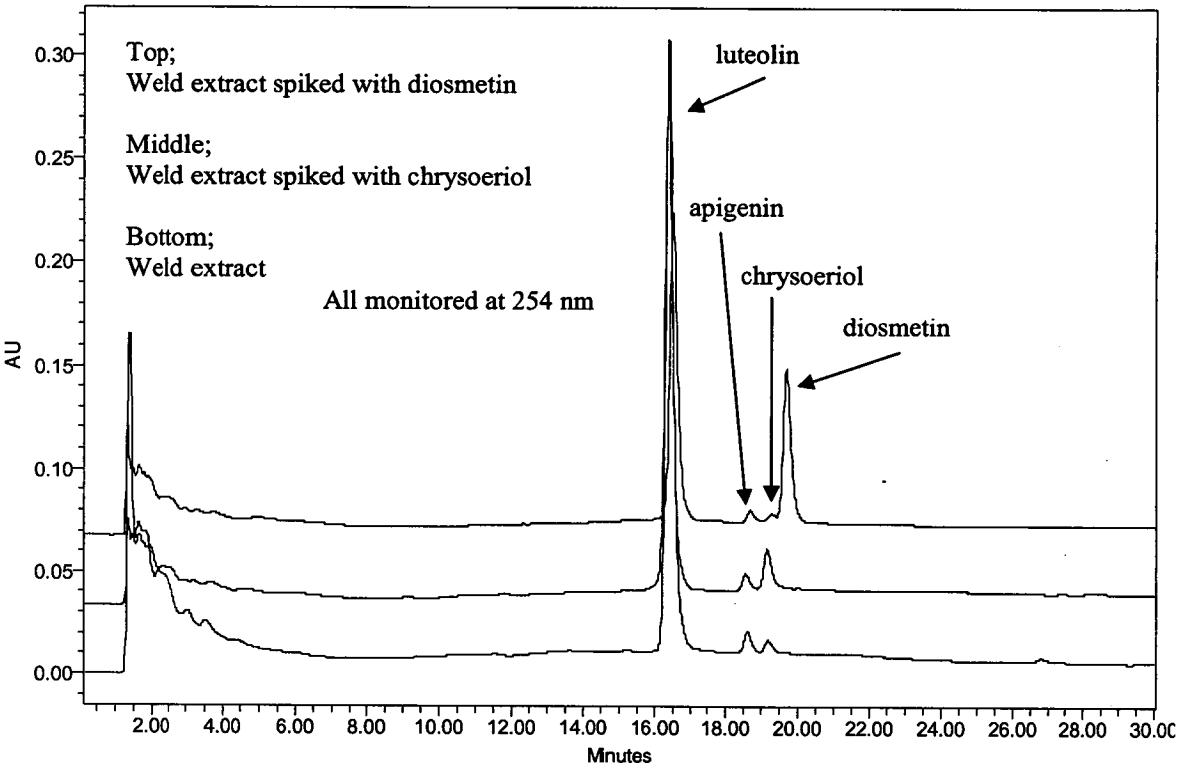

Figure 2.3: The identity of the luteolin methyl ether component in the weld extracts was confirmed as chrysoeriol by comparing an un-spiked weld extract (bottom) with weld extracts spiked with either diosmetin (top) or chrysoeriol (middle)

The weld extract (Figure 2.3, bottom) contains three peaks, luteolin, apigenin and a luteolin methyl ether. In the weld extract reconstituted with a spiked chrysoeriol solution (Figure 2.3, middle), no new peaks are visible, however, the area of the peak corresponding to the luteolin methyl ether increased. Furthermore, the spectral purity of this peak remained constant. In contrast, an additional peak, with a retention time corresponding to the diosmetin isomer, is present in the diosmetin spiked solution (Figure 2.3, top). Thus, the luteolin methyl ether isomer in the acid hydrolysed extracts from weld dyed yarn is chrysoeriol.

The use of acid hydrolysis conditions to extract the dye components from the yarn converts any flavonoid-*O*-glycosides present into their parent aglycones. For example, the presence of several luteolin-*O*-glucosides, including luteolin-7-glucoside, luteolin-3'-glucoside and luteolin-3',7-diglucoside, have been observed in weld plant extracts (Figure 2.4).[11] However, under the chosen extraction conditions, these will all be hydrolysed to luteolin.

Luteolin glucosides

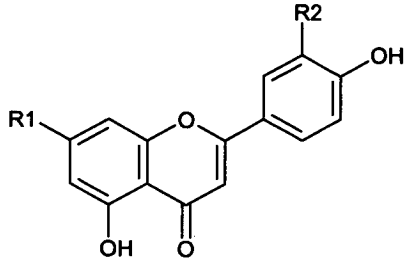

Luteolin-7-glucoside	R1 = *O*-glucose and R2 = OH
Luteolin-3'-glucoside	R1 = OH and R2 = *O*-glucose
Luteolin-3'7-diglucoside	R1 = R2 = *O*-glucose

Figure 2.4: Some luteolin-*O*-glycosides observed in weld plant extracts

A systematic investigation was undertaken to study the effects of different substrates (wool or silk) and additional steps in the dyeing process (over/under-dyeing with indigo to produce a green yarn) on the ratio of the three characteristic components observed in the acid hydrolysed extracts. A summary of the reference weld samples can be found in Table 2.1, while full details of the mordanting and dyeing procedures can be found in Appendix 7.2. The acid hydrolysed extracts of the MODHT reference dyeings were analysed using PDA HPLC and comparisons made between the peak areas (monitored at 254 nm) of the main flavonoid components in each reference sample. The weight of all yarn samples was between 0.5 and 2.5 mg.

Table 2.1: Summary of weld reference dyeings (recipes in Appendix 7.2)

Code	Yarn	Colour	Description
Y/W1	wool	yellow	alum mordanted wool dyed with weld
G/W1	wool	green	Y/W1 overdyed with woad
G/W2	wool	green	woad overdyed with weld
Y/S1a	silk	yellow	alum (boil) mordanted silk dyed with weld
Y/S1b	silk	yellow	alum mordanted silk dyed with weld
G/S1	silk	green	Y/S1a overdyed with woad
G/S2	silk	green	Y/S1b overdyed with woad
G/S3	silk	green	alum (boil) mordanted silk, dyed with woad then overdyed with weld
G/S4	silk	green	alum mordanted silk, dyed with woad then overdyed with weld

Four wool samples, mordanted with alum and dyed with weld (Y/W1) were extracted using the standard acid hydrolysis procedure. For each extract, the relative percentage area (monitored at 254 nm) of the three main flavonoid components was tabulated (Table 2.2). The mean and 95% confidence intervals for each component have also been reported.

Table 2.2: Relative peak areas (monitored at 254 nm) of the main flavonoid components in the acid hydrolysed extracts of alum mordanted wool dyed with weld

Y/W1	Relative peak area (monitored at 254 nm) / %		
Weld on wool	Luteolin	Apigenin	Chrysoeriol
Sample 1	94.3	3.5	2.1
Sample 2	94.4	3.6	2.0
Sample 3	94.5	3.5	2.0
Sample 4	94.3	3.6	2.1
MEAN ± 95% confidence interval	94.4 ± 0.15	3.5 ± 0.09	2.1 ± 0.09

The reproducibility of the relative percentages of the components, monitored at a wavelength of 254 nm and calculated using automatic integration software, was excellent. The relative percentages of the three main flavonoid components were almost identical in each of the four samples. Thus, uneven dyeing of the yarn or small differences in extraction conditions have had a negligible effect on the results.

Two different green wool reference samples were prepared by performing multiple dyeings. The first utilised a yellow wool sample dyed with weld (Y/W1) which was overdyed with woad to give a green yarn (G/W1). The second reference yarn was prepared by reversing the above procedure and using woad to dye a wool yarn blue, then overdying this with weld (G/W2). To evaluate the effect of an additional dye component on the relative amounts of the three main flavonoid components, four samples of each of the green wool reference dyeings (G/W1 and G/W2) were extracted. For each extract, the relative peak areas (monitored at 254 nm) of the three main flavonoid components have been tabulated (Table 2.3 and Table 2.4). The mean and 95% confidence intervals for each component have also been reported.

Table 2.3: Relative peak areas (monitored at 254 nm) of the main flavonoid components in the acid hydrolysed extracts of alum mordanted wool dyed with weld then woad

G/W1	**Relative peak area (monitored at 254 nm) / %**		
Weld overdyed with woad	**Luteolin**	**Apigenin**	**Chrysoeriol**
Sample 1	96.3	1.8	1.9
Sample 2	96.8	1.9	1.3
Sample 3	96.6	2.0	1.4
Sample 4	96.4	2.1	1.6
MEAN ± 95% confidence interval	96.5 ± 0.35	1.9 ± 0.21	1.5 ± 0.42

Table 2.4: Relative peak areas (at 254 nm) of the main flavonoid components in the acid hydrolysed extracts of wool dyed with woad then mordanted with alum and dyed with weld

G/W2	**Relative peak area (monitored at 254 nm) / %**		
Woad overdyed with weld	**Luteolin**	**Apigenin**	**Chrysoeriol**
Sample 1	95.4	2.8	1.7
Sample 2	95.4	2.9	1.8
Sample 3	94.7	3.3	1.9
Sample 4	94.8	3.3	1.9
MEAN ± 95% confidence interval	95.1 ± 0.60	3.1 ± 0.42	1.8 ± 0.15

As observed for the yellow wool reference sample (Y/W1), the reproducibility of the relative flavonoid percentages in both green wool reference samples (G/W1 and G/W2) was very good. Furthermore, the additional dyeing procedures in the green samples have had little impact on the ratios of the main components. Although a

marginal increase in the relative amount of luteolin was observed in the extracts from green yarns compared with the yarn dyed only with weld, the addition of a blue dye, either underdyed or overdyed onto a weld dyed yarn, has not significantly affected the characteristic ratio of the main flavonoid components used for dyestuff identification.

The green yarns were dyed with woad, in a manner conforming as closely as possible to medieval practice (45-50 °C and a pH of *ca.* 8.2-8.5). It is interesting that these conditions, which differ substantially from those of the weld dyebath (100 °C and a pH of *ca.* 10.2), have had only a minimal effect on the ratio of the main flavonoid components observed in the acid hydrolysed extracts. This relative stability is in stark contrast to the flavonoid components observed in the acid hydrolysed extracts from yarn dyed with dyer's greenweed (Section 2.1.2.2).

The peak area, monitored at 254 nm, of the main flavonoid colouring component, luteolin, changes linearly within the concentration range of interest (unpublished data). However, meaningful comparisons between the luteolin concentration (per mg of yarn) in the yellow and green extracts cannot be easily achieved. This is due to the addition of the indigo pigment in the green samples, which aggregates between yarn fibres, increasing the mass of a given length of yarn. This increase in mass may not be uniform throughout the length of the dyed yarn, thus quantitative comparisons between yellow and green yarns are difficult.

The effect of the substrate and mordanting procedure on the relative ratios of the three main flavonoid components observed in the acid hydrolysed extracts was also investigated. The extracts from two different reference yarns of weld dyed on alum mordanted silk (Y/S1a and Y/S1b) were analysed by PDA HPLC. The preparation of these two reference materials differed only in their respective mordanting procedures (Appendix 7.2); the silk used for the Y/S1a sample was immersed in alum dissolved in hot water (38 °C) and left for 20 h, while the silk used for the Y/S1b reference was boiled in the alum mordanting solution for 10 min, then

removed while the solution cooled to room temperature, before being re-immersed for 10 h.

The relative percentages of the three main flavonoid components from four extracts of the first reference (Y/S1a) have been tabulated in Table 2.5. The mean and 95% confidence intervals for each component have also been reported.

Table 2.5: Relative peak areas (monitored at 254 nm) of the main flavonoid components in the acid hydrolysed extracts of alum (boil) mordanted silk dyed with weld

Y/S1a	**Relative peak area (monitored at 254 nm) / %**		
Weld on silk	**Luteolin**	**Apigenin**	**Chrysoeriol**
Sample 1	92.1	4.7	3.3
Sample 2	92.9	4.2	2.9
Sample 3	92.5	4.3	3.2
Sample 4	92.8	4.2	3.0
MEAN ± 95% confidence interval	92.5 ± 0.57	4.4 ± 0.38	3.1 ± 0.29

The relative percentages of the flavonoid components from four extracts of the second silk sample (Y/S1b) (Table 2.6) were found to be very similar to that of the first. Again, the mean and 95% confidence intervals for each component have been reported.

Table 2.6: Relative percentage area (monitored at 254 nm) of the main flavonoid components in the acid hydrolysed extracts of alum mordanted silk dyed with weld

Y/S1b	**Relative peak area (monitored at 254 nm) / %**		
Weld on silk	**Luteolin**	**Apigenin**	**Chrysoeriol**
Sample 1	91.0	5.4	3.6
Sample 2	91.6	4.9	3.5
Sample 3	91.6	4.8	3.5
Sample 4	91.7	4.8	3.4
MEAN ± 95% confidence interval	91.5 ± 0.51	5.0 ± 0.46	3.5 ± 0.13

Thus, the mordanting procedure has a minimal effect on the relative percentages of the characteristic components used to identify the use of weld as the biological dye source.

Green silk samples were prepared by the over or under dyeing of both mordanted silk yarns, producing four samples, G/S1-4 (see Table 2.1). To evaluate the effect of multiple dyeings on the relative amounts of the three main flavonoid components, four samples of each of the green silk reference dyeings (G/S1-4) were extracted. For each extract, the relative peak areas (monitored at 254 nm) of the three main flavonoid components have been tabulated (Table 2.7). The mean and 95% confidence intervals have also been reported for each component.

Table 2.7: Relative percentage area (monitored at 254 nm) of the main flavonoid components in the acid hydrolysed extracts G/S1-G/S4

	Relative peak area (monitored at 254 nm) / %		
G/S1 Weld overdyed with woad (boil mordant)	**Luteolin**	**Apigenin**	**Chrysoeriol**
Sample 1	92.2	4.5	3.2
Sample 2	92.9	4.2	2.9
Sample 3	93.0	3.9	3.1
Sample 4	92.4	4.4	3.1
MEAN ± 95% confidence interval	92.6 ± 0.61	4.3 ± 0.42	3.1 ± 0.20
G/S2 Weld overdyed with woad	**Luteolin**	**Apigenin**	**Chrysoeriol**
Sample 1	91.9	4.8	3.3
Sample 2	92.6	4.4	3.0
Sample 3	92.0	4.5	3.5
Sample 4	92.6	4.3	3.0
MEAN ± 95% confidence interval	92.3 ± 0.60	4.5 ± 0.34	3.2 ± 0.39
G/S3 Woad overdyed with weld (boil mordant)	**Luteolin**	**Apigenin**	**Chrysoeriol**
Sample 1	93.0	4.2	2.8
Sample 2	91.7	4.9	3.4
Sample 3	91.1	5.3	3.6
Sample 4	93.4	3.9	2.7
MEAN ± 95% confidence interval	92.3 ± 1.7	4.6 ± 1.02	3.1 ± 0.70
G/S4 Woad overdyed with weld	**Luteolin**	**Apigenin**	**Chrysoeriol**
Sample 1	89.7	6.3	4.0
Sample 2	89.8	6.2	4.0
Sample 3	90.6	5.6	3.8
Sample 4	90.4	5.7	3.9
MEAN ± 95% confidence interval	90.1 ± 0.70	6.0 ± 0.56	3.9 ± 0.15

The additional dyeing procedures employed in the green silk samples, like in their wool counterparts, have had little impact on the ratios of the main components. The addition of a blue dye, either underdyed or overdyed onto a weld dyed yarn, has not significantly affected the characteristic ratio of the main flavonoid components used for dyestuff identification.

The total concentration of flavonoid components, per mg of yarn (related to the total peak area monitored at 254 nm), is greater when silk rather than wool is used as a substrate (Chapter 6). This difference arises from the use of wool and silk yarns with different tex values, as the larger the tex value, the heavier the yarn (Section 2.1.1). However, the different morphologies of the wool and silk fibres (Chapter 1) may also affect the ability of mordants and dyes to penetrate into the fibre bulk.

The above experiments indicate that there is very little change in the relative ratios of the main flavonoid components observed upon chromatographic analysis of the acid hydrolysed extracts from weld dyed silk or wool reference materials. The similarity of the relative percentages of the three main components from all the weld dyed references has been summarised in Figure 2.5.

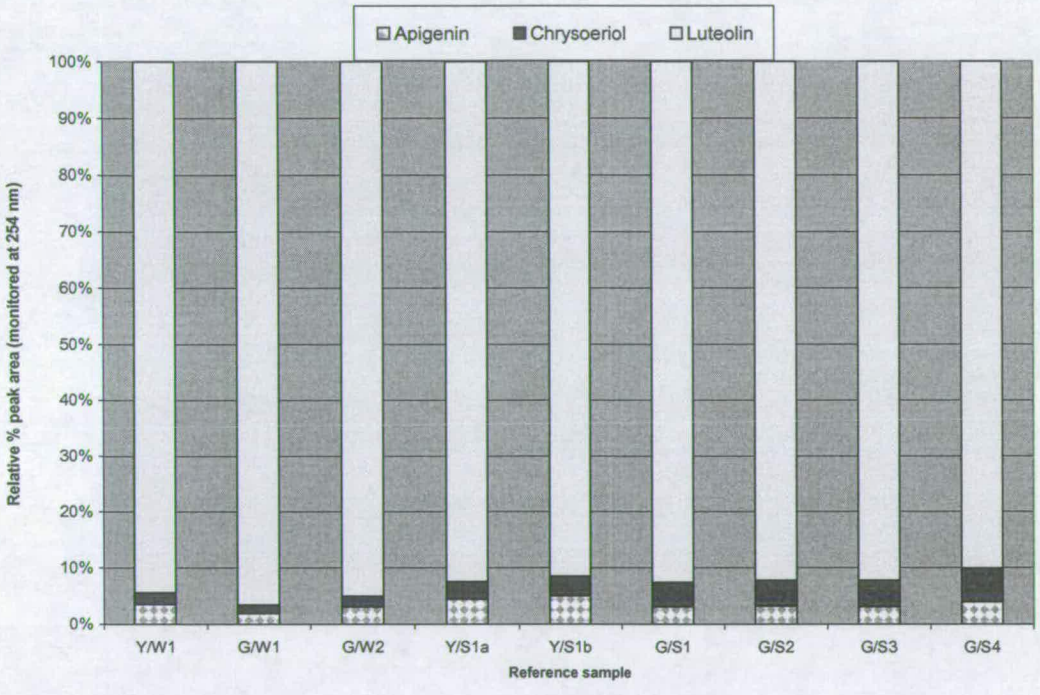

Figure 2.5: The relative percentages of the three main components observed upon chromatographic analysis of the acid hydrolysed extracts from all weld dyed references, monitored at 254 nm. Y/W1 = wool dyed with weld, G/W1 = weld dyed yarn overdyed with woad, G/W2 = woad dyed yarn overdyed with weld, Y/S1a = silk dyed with weld, G/S1-4 = silk dyed with weld and over or under-dyed with woad

It can be observed that none of the variables so far considered (substrate, mordanting or dyebath conditions, or additional woad dyeings) have appreciably altered the ratio of the main flavonoid components in the acid hydrolysed extracts of weld. The combined apigenin and chrysoeriol percentage in each of the sample extracts never exceeds 10% of the total flavonoid components when monitored at 254 nm. Interestingly, this is in contrast to the ratio of the main flavonoid components observed in the acid hydrolysed extracts of dyer's greenweed (Section 2.1.2.2), which fluctuate upon additional dyeings.

However, when comparing the data from freshly dyed reference samples with data obtained from historical samples of unknown provenance, a further variable should also be considered. The natural variation of the relative flavonoid abundances found in the dye plant material may also effect the relative ratio of colouring components observed in the extracts of dyed yarns. Although flavonoids in plants can often be used as chemotaxonomic markers,[12] making them ideal for dyestuff identification, differences in the flavonoids found in plant material from the same species can arise.[9,13-15] These differences may be due to several factors, including; geographical location, as observed in populations of the sunflower family (*Asteraceae*), for example;[14] the time (season or year) of harvesting;[15] or the use of different areas of the plant in the dyebath *i.e.* leaves and/or stems.[9]

A detailed analysis of the effect of these variables upon the flavonoid ratios observed in the acid hydrolysed extracts of dyed yarns is beyond the scope of the present study. However, it is likely that small differences in the flavonoid content of plant materials would have only a minor impact on the concentration of the main dye components in the dyebath and consequently only a small effect on the relative ratios of the flavonoid species mordanted onto the yarn. Furthermore, the extraction protocol will also minimise any natural variation in the glycosidic components, since any flavonoid-*O*-glycosides present on the yarn will be hydrolysed to their respective aglycones upon acid hydrolysis.

The exact dyeing conditions for each historical sample will never be known, but significantly, these experiments highlight that different mordanting or dyebath conditions, different substrates or additional dyeings, do not appreciably alter the ratio of the main flavonoid components found in the acid hydrolysed extracts of weld dyed yarn. A much greater problem in the identification of weld on historical samples is the potential loss of characteristic components due to photo-degradation reactions. These may alter the flavonoid 'fingerprint' used for identification and have been investigated using accelerated ageing techniques (Chapter 4).

2.1.2.2 Dyer's greenweed (*Genista tinctoria* L.)

When the isoflavone genistein is detected along with the flavones luteolin and apigenin, the dye source is usually reported as dyer's greenweed (*Genista tinctoria* L.) (Figure 2.6). Genistein does not contribute directly to the yellow colour of yarn dyed with dyer's greenweed, as it does not absorb an appreciable amount of light in the 300-400 nm region (although a small 'shoulder' is still apparent in the UV-Vis spectrum in this region). The UV-Vis absorbance spectrum is thus very different to that of the other flavonoid components, all of which have a λ_{max} value in the 300-400 nm region. Consequently, yarn 'dyed' only with pure genistein remains colourless, even when mordanted with alum.

A previous investigation of the flavonoid components found in the acid hydrolysed extracts of dyer's greenweed dyed yarn, utilising PDA HPLC and LC ESI MS techniques, provided useful fingerprint information for additional minor components.[1] However, none of these minor components were completely characterised, thus, only the relative ratios of the fully characterised flavonoids from the extracts of the unaged reference samples of dyer's greenweed (genistein, luteolin and apigenin) were investigated. This was conducted in a similar manner to the investigation of the components in weld dyed yarns *i.e.* by chromatographic analysis of the acid hydrolysed extracts, utilising the peak area response at 254 nm. However, with the current chromatographic method, the genistein and luteolin components are

only partially separated and are not completely baseline resolved. This necessitated a more qualitative approach than that used for the investigation of weld.

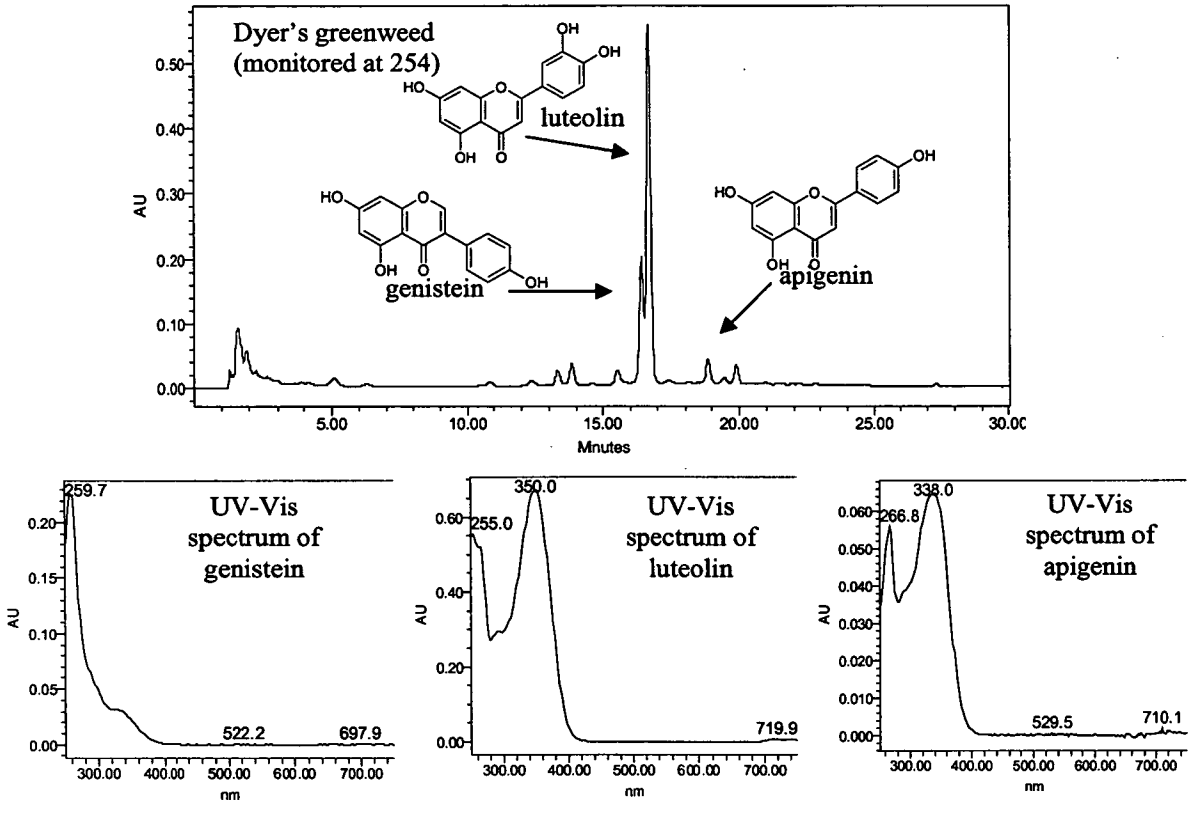

Figure 2.6: The HPLC chromatogram (monitored at 254 nm) of the acid hydrolysed extracts of dyer's greenweed, showing the structure of the characteristic components and their UV-Vis spectra

A summary of the reference dyer's greenweed samples can be found in Table 2.8. There is one sample dyed on wool (Y/W2), while five samples have been dyed on silk (Y/S3a-e). The different dyeing procedures employed in the production of these five silk samples significantly altered the colour of the dyed yarns.

Table 2.8: Summary of dyer's greenweed reference dyeings (recipes can be found in Appendix 7.2)

Code	Yarn	Colour	Description
Y/W2	wool	yellow	alum mordanted wool dyed with dyer's greenweed
Y/S3a	silk	yellow	alum mordanted silk dyed with dyer's greenweed
Y/S3b	silk	yellow	alum (boil) mordanted silk dyed with dyer's greenweed (×2)
Y/S3c	silk	yellow	alum mordanted silk dyed with dyer's greenweed (×2)
Y/S3d	silk	yellow	alum (boil) mordanted silk dyed with dyer's greenweed (×3)
Y/S3e	silk	yellow	silk dyed with dyer's greenweed (no mordant)

Four samples of wool mordanted with alum and dyed with dyer's grenweed (Y/W2) were extracted. For each extract, the relative percentage area (monitored at 254 nm) of the three main flavonoid components was tabulated (Table 2.9). Again, the peak area of each component was calculated using the automatic integration software, however, it must be remembered that the genistein and luteolin components are not baseline resolved. The relative percentage area should therefore be used as a qualitative indication of the relative ratio of the components and not as a quantitative result. The mean and 95% confidence interval have also been reported for each component, although in this case should only be taken as an indication of the repeatability of the sample extraction. The values do not represent the accuracy of the relative percentages due to the inherent error associated with the quantification of co-eluting components.

Table 2.9: Relative percentage area (monitored at 254 nm) of the main flavonoid components in the acid hydrolysed extracts of alum mordanted wool dyed with dyer's greenweed

Y/W2	Relative peak area (monitored at 254 nm) / %		
Dyer's greenweed on wool	Genistein	Luteolin	Apigenin
Sample 1	49.7	41.3	8.9
Sample 2	50.1	41.0	8.9
Sample 3	50.8	40.0	9.2
Sample 4	50.6	40.6	8.8
MEAN ± 95% confidence interval	50.3 ± 0.79	40.7 ± 0.89	9.0 ± 0.28

The acid hydrolysed extracts from dyer's greenweed dyed wool yarns (Y/W2) have a greater genistein peak area relative to the area of luteolin (monitored at 254 nm).

However, this ratio appears to be highly dependent on the dye process, as the tabulated results of dyer's greenweed on silk indicate (Table 2.10). Each of the silk yarns (Y/S3a-e) were sampled and analysed twice rather than four times, so the mean and 95% confidence intervals have not been reported. The results are in contrast to those from textile yarns dyed with weld, where the relative ratio of the main components in the dyed yarn extracts remained similar with varying dyeing conditions (Section 2.1.2.1). Furthermore, it also implies that unlike the relative ratios of the major and minor components from the acid hydrolysed extracts of yarns dyed with the coccid insect dye sources (Chapter 3) the ratios cannot be used for species determination.[16]

Table 2.10: Relative percentage area (monitored at 254 nm) of the main flavonoid components in the acid hydrolysed extracts of alum mordanted silk dyed with dyer's greenweed

Dyer's greenweed on silk	Relative peak area (monitored at 254 nm) / %		
	Genistein	Luteolin	Apigenin
Y/S3a	44	48	8
	43	48	9
Y/S3b	26	67	7
	24	71	5
Y/S3c	28	66	6
	23	69	8
Y/S3d	10	86	4
	9	86	5
Y/S3e	49	42	9
	49	42	9

The extracts from alum mordanted silk yarns dyed with dyer's greenweed (Y/S3a) have a slightly higher ratio of luteolin to genistein, in contrast to the extracts from the equivalent alum mordanted wool sample. The following two samples (Y/S3b and Y/S3c) differ from one another only in their mordanting procedure and have both undergone a second dyeing in the dyer's greenweed dyebath. This has resulted in a dramatic change in the relative ratio of the main flavonoid components in the extracts compared with the extracts from the silk yarn dyed only once (Y/S3a), with luteolin becoming the dominant component in the chromatogram when monitored at 254 nm.

This trend continues with a third dyeing in the dyer's greenweed dyebath (Y/S3d), with the proportion of luteolin in the extracts again increasing compared with genistein. When no mordant is used (Y/S3e) the ratio of the three components in the extracts are similar to that observed in the dyed wool extracts.

The large differences in the flavonoid ratios observed in the extracts of reference samples prepared using different dyeing procedures or yarn substrates can be illustrated graphically (Figure 2.7). Although genistein and luteolin co-eluted in the chromatographic method, analysis of the 'peak purity' data confirmed that differences in the ratios were not due to instrumental variation.

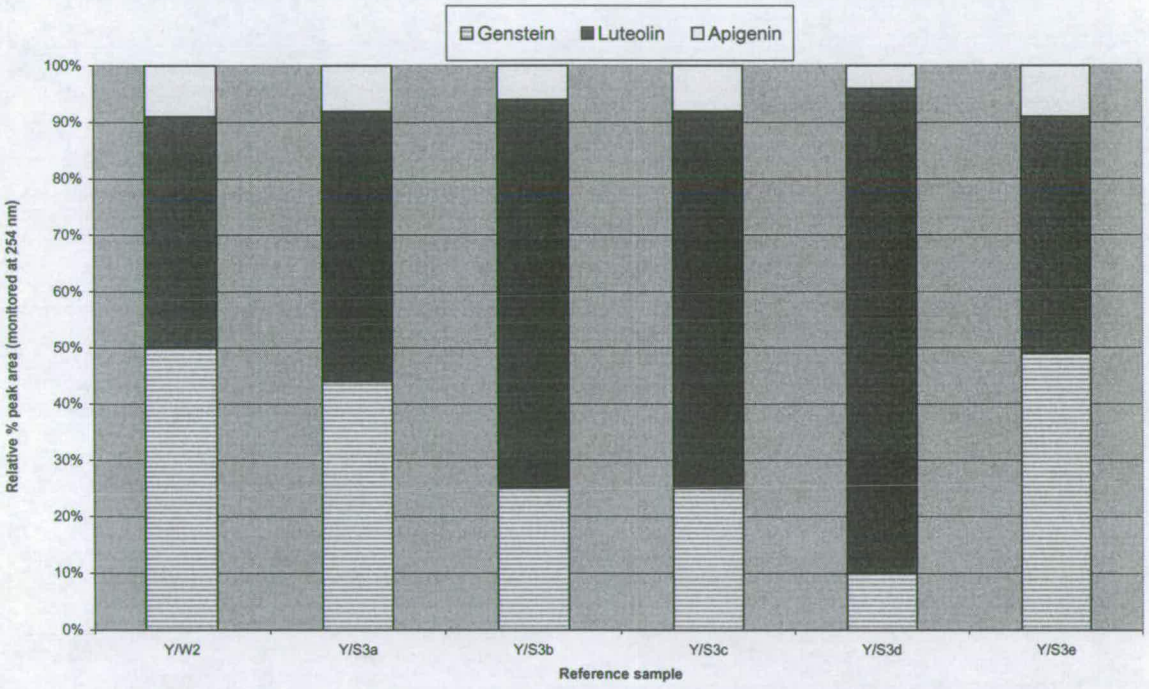

Figure 2.7: The varying flavonoid ratios observed in the extracts of reference samples dyed with dyer's greenweed and prepared using different dyeing procedures or yarn substrates. Y/W2 = dyer's greenweed on wool, Y/S3a-e = dyer's greenweed on silk, prepared using different mordanting or dyeing procedures

The loss of genistein relative to luteolin in samples which have undergone two or three dyeings is possibly the result of a competitive binding process. The structure of luteolin (a flavone) may be less sterically hindered than genistein (an isoflavone)

upon binding with the mordant. Thus, with each additional dyeing, luteolin is able to displace more of the genistein. Alternatively, the conditions of the dyebath may preferentially degrade genistein, as several studies have shown that isoflavones such as genistein thermally degrade at elevated temperatures in the processing of soy products.[17,18]

The presence of the uncoloured genistein molecule results in less luteolin being present on the yarn, 'diluting' the colour of the yarn to a light yellow. However, with multiple dyeings the relative amount of genistein present on the dyed yarn decreases compared with luteolin, considerably altering the yarn colour to produce a much brighter yellow. The need for multiple dyeings may explain why the quality of the dyestuff was judged to be lower than that of weld.[19,24] The presence of genistein in the acid hydrolysed extracts from an historical sample is the main indicator employed to distinguish this biological source from many other common alternatives. However, the relative ratio of genistein, luteolin and apigenin has been shown to be highly dependent on the dyeing procedure, so only its qualitative (rather than quantitative) detection should be employed to indicate the possible use of dyer's greenweed.

A further problem in source identification may arise due to photo-degradation reactions altering the characteristic flavonoid profile of the acid hydrolysed extracts. The consequences of prolonged exposure to light for the identification of yarns dyed with dyer's greenweed have been investigated using accelerated ageing techniques (Chapter 4).

2.1.2.3 Sawwort (*Serratula tinctoria* L.)

Although weld was probably the most widely used of all European yellow dye plants, other biological sources, including dyer's greenweed (*Genista tinctoria* L.) and sawwort (*Serratula tinctoria* L.) were acknowledged substitutes.[3,19] The use of both weld and dyer's greenweed is often reported in the dye source analysis results

for yellow historical textiles, but it is perhaps surprising that no analytical evidence for sawwort in such samples has been reported.

The literature on the chemical constituents of sawwort is sparse. One previous paper reported the presence, by Thin Layer Chromatography (TLC), of luteolin and 3-*O*-methylquercetin in the acid hydrolysed extracts of dyed yarns.[20] The presence of other flavonoids in the sawwort plant, including apigenin and kaempferol, has also been reported.[9,21] A study to identify the characteristic colouring components, utilising modern analytical methodology, was therefore undertaken on freshly dyed reference yarns. Authentic sawwort reference material, harvested from two different geographical locations, was sourced. A related species, *Serratula coronata* L. was also used for comparison, allowing a more complete characterisation of the flavonoid composition expected from the acid hydrolysed extracts of *Serratula* species. Unlike the weld and dyer's greenweed reference yarns, both the *Serratula tinctoria* L. and *Serratula coronata* L. reference yarns were dyed at the National Museums of Scotland (Chapter 6).

The chemical characterisation of the acid hydrolysed extracts from all three samples was performed using PDA HPLC and, where further investigative work was required, HPLC ESI MS^n. The chromatograms (monitored at 254 nm) of the three freshly dyed reference samples were qualitatively similar (Figure 2.8).

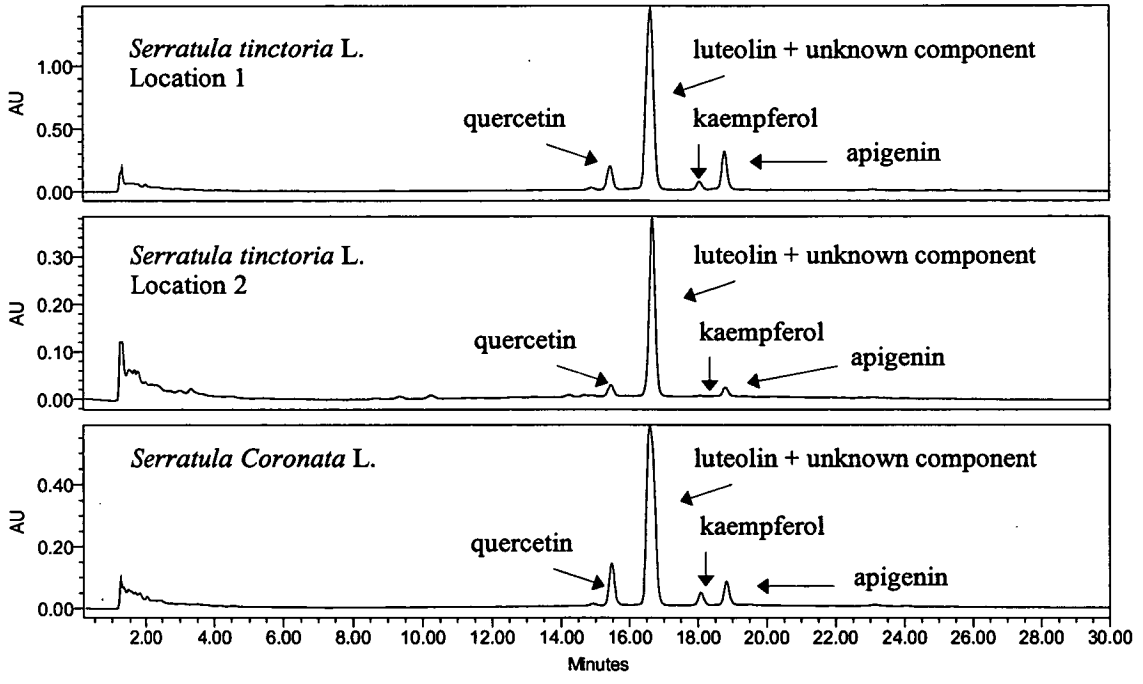

Figure 2.8: Chromatograms (monitored at 254 nm) of the three *Serratula* species (a) *Serratula tinctoria* L. from Lanquedoc-Roussillon, (b) *Serratula tinctoria* L. from Mount Aigoual (c) The related species *Serratula coronata* L.

The main constituent in both sawwort (*Serratula tinctoria* L.) samples was luteolin. However, the PDA data suggested that the luteolin peak was not spectrally pure and was therefore co-eluting with another component. The extracts from the related *Serratula coronata* L. appeared to contain a greater amount of this unknown component relative to luteolin, as the peak's UV-Vis spectrum no longer matched with that expected for luteolin. Minor amounts of the flavonols quercetin and kaempferol, and the flavone apigenin were also observed in all three extracts, although at different relative percentages in each reference sample. The main constituents are shown in Figure 2.9 and were identified by matching their retention time and spectral information to an in-house library of standard compounds.

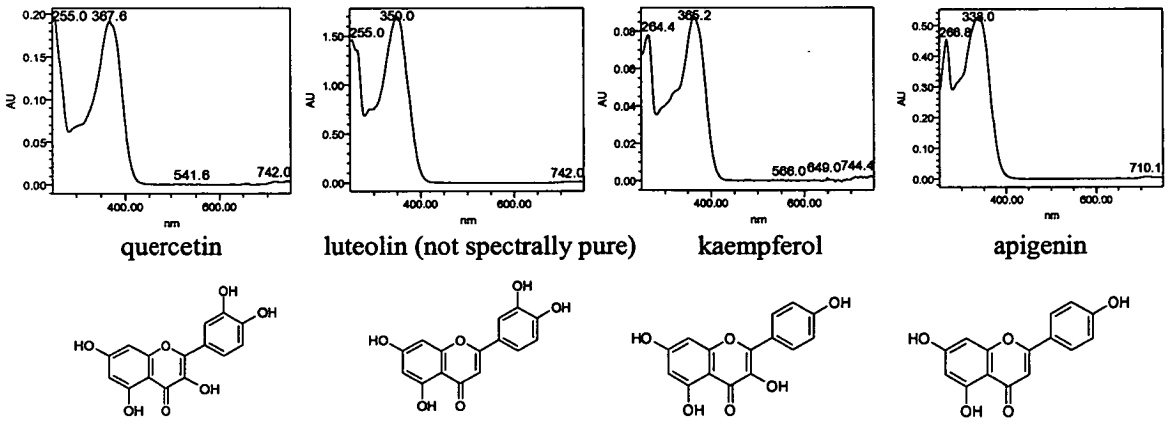

Figure 2.9: The UV-Vis spectra and structures of the main flavonoid constituents found in yarns dyed with *Serratula tinctoria and Serratula coronata* species

Further investigation of the flavonoid composition in the acid hydrolysed extracts from the sawwort (*Serratula tinctoria* L.) dyed yarns using LC ESI MS^n suggested the presence of 3-*O*-methylquercetin (*m/z* 315*)*. A deprotonated molecular ion, $[M-H]^-$, at *m/z* 315 was observed co-eluting with luteolin (Figure 2.10). A deprotonated molecular ion at *m/z* 315 was also observed co-eluting with luteolin in the acid hydrolysed extracts of the *Serratula coronata* L. dyed yarn.

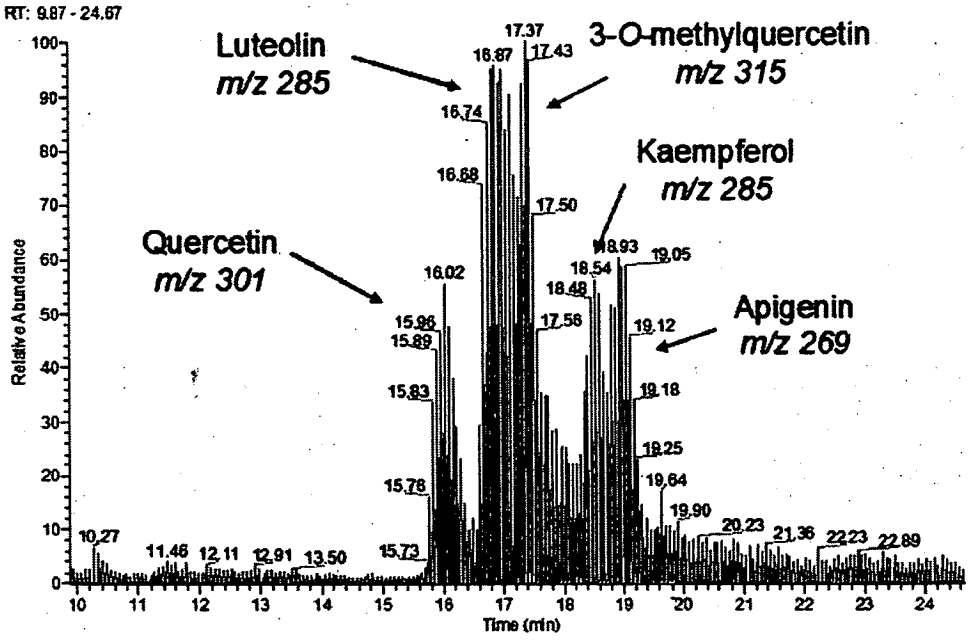

Figure 2.10: The 'base peak' chromatogram from the HPLC ESI MS of the acid hydrolysed extract of a sawwort (*Serratula tinctoria* L.) dyed yarn, clearly showing the 3-*O*-methylquercetin component co-eluting with luteolin

Tandem mass spectrometric analysis of this deprotonated molecular ion (*m/z* 315) in all samples produced a single breakdown peak at *m/z* 300 ($-CH_3$), suggesting replacement of one of the hydroxyl functional groups of quercetin with a methoxy group.[22] Compared with quercetin, the unidentified component has a longer retention time, suggesting greater hydrophobicity; also consistent with the methylation of a hydroxyl group. The MS^3 analysis of the fragment ion at *m/z* 300 gave two peaks, *m/z* 271 (-29 Da) and *m/z* 255 (-45 Da) (Figure 2.11). These are consistent with small fragments observed in the breakdown pathways of other flavonoid components and did not provide any further structural information.[23]

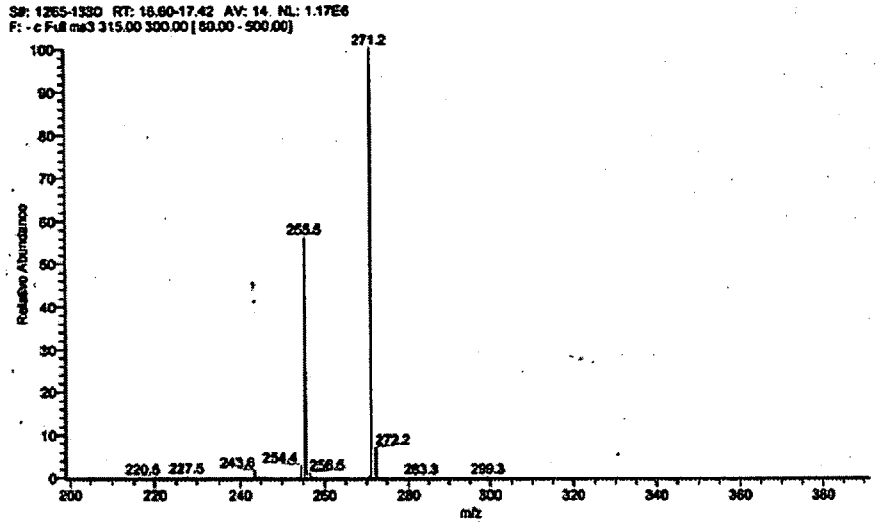

Figure 2.11: The MS^3 (315, 300) CID 'fingerprint' of 3-*O*-methylquercetin in the acid hydrolysed extracts of sawwort (*Serratula tinctoria* L.)

A pure reference sample of 3-*O*-methylquercetin was therefore analysed under identical conditions by PDA HPLC and HPLC ESI MS^n. The retention time of the 3-*O*-methylquercetin standard matched with that expected for the unknown component in the *Serratula tinctoria* L. and *Serratula coronata* L. extracts (Figure 2.12). However, due to co-elution with luteolin, the UV-Vis spectrum of the unknown component from these samples could not be compared with that obtained from the 3-*O*-methylquercetin reference.

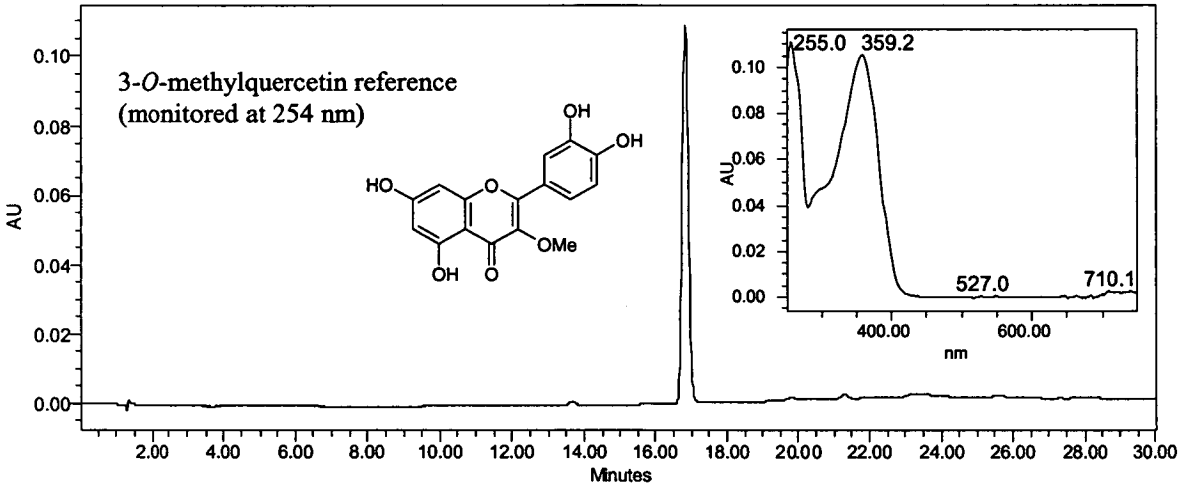

Figure 2.12: PDA HPLC of the 3-O-methylquerceetin reference component (monitored at 254 nm) with its UV-Vis spectrum

The identity of the unknown component in both *Serratula tinctoria* L. extracts and in the *Serratula coronata* L. sample was, however, confirmed as 3-*O*-methylquercetin by the HPLC ESI MS^n analysis. The deprotonated molecular ion and subsequent fragmentation pattern of the unknown component was identical to that obtained from the reference 3-*O*-methylquercetin.

To gain further information regarding the CID breakdown of 3-*O*-methylquercetin, the reference sample was dissolved in deuteriated methanol (MeOD) and directly injected into the mass spectrometer (Figure 2.13). This allowed the number of exchangeable protons on each of the fragments, produced during CID breakdown, to be calculated and thus the number, and sometimes position, of the hydroxyl groups to be inferred.

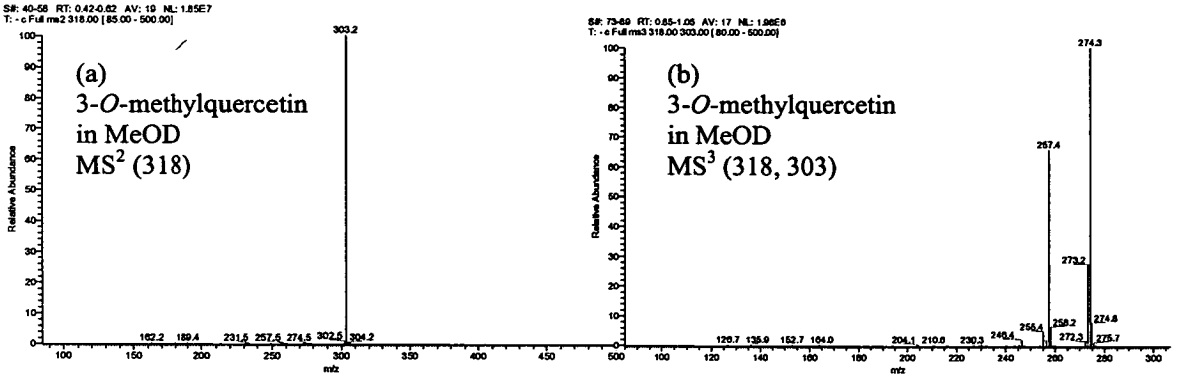

Figure 2.13: The (a) MS^2 (318) and (b) MS^3 (318, 303) spectra of a 3-*O*-methylquercetin reference in MeOD directly injected into the mass spectrometer

As expected, fragmentation of the fully deuteriated molecular ion (*m/z* 318) produced a breakdown peak at *m/z* 303 ($-CH_3$) due to the fragmentation of the ether moiety. This *m/z* 303 peak was trapped and subjected to further CID (Table 2.11).

Table 2.11: MS^3 (315, 300) Collision Induced Dissociation (CID) of 3-*O*-methylquercetin (*m/z* 315) under negative ion conditions

***m/z*: MS^3 315, 300 (relative abundance)**	**Neutral fragment lost (possible species)**	**Information from deuteriated studies**
271 (100%)	29 (CHO; C_2H_5)	Base peak. Observed fragment has 4 exchangeable protons, while the neutral fragment has none.
255 (58%)	45 (CO_2H; OC_2H_5)	Observed fragment has 3 exchangeable protons, while the neutral fragment has one.

In both the deuteriated and non-deuteriated case, the highest mass fragment, and base peak, was due to loss of 29 Da (probably CHO). A significant peak is also observed from the loss of a 45 Da fragment (probably CO_2H), however, these fragments are common breakdown peaks in the negative ion ESI mass spectra of flavonoids and provided little further structural information.[1]

The acid hydrolysed extracts from sawwort (*Serratula tinctoria* L.) and *Serratula coronata* L. dyed yarn were thus shown to contain the flavonols quercetin, and kaempferol, the related flavonol component 3-*O*-methylquercetin and the flavones luteolin and apigenin. The PDA HPLC elution programme used for this analysis did

not separate the luteolin and 3-*O*-methylquercetin components. The routine separation of these flavonoids would require development of the current chromatographic method, however, the use of HPLC ESI MS^n confirmed the presence of both compounds.

The characteristic components were observed at different relative amounts in each sample (Table 2.12), despite identical dyeing conditions. The relative amount of luteolin and 3-*O*-methylquercetin (monitored at 254 nm) had to be calculated together, as they co-eluted in the PDA HPLC method. Close examination of the PDA results for the combined (luteolin + 3-*O*-methylquercetin) peak in the *Serratula coronata* L. showed that the UV-Vis spectrum no longer matched that expected for luteolin. This suggests that the *Serratula coronata* L. extract contains a greater amount of 3-*O*-methylquercetin relative to luteolin than the sawwort extracts from either location 1 (Lanquedoc-Roussillon region, France) or location 2 (Mount Aigoual, France).

Table 2.12: Relative peak areas (monitored at 254 nm) of the five main components in the acid hydrolysed extracts of sawwort (*Serratula tinctoria* L.) from two different geographical locations. A related species, *Serratula coronata* L. was also analysed. The relative area of luteolin and 3-*O*-methylquercetin was calculated together in each case

Location	Relative peak area (monitored at 254 nm) / %			
	Quercetin	Luteolin + 3-*O*-methylquercetin	Kaempferol	Apigenin
Location 1 Lanquedoc-Roussillon	8.0	76.2	3.0	12.8
Location 2 Mount Aigoual	6.0	89.0	0.3	4.7
Related species *Serratula coronata* L	12.8	75.4	4.1	7.7

The relative amounts of all the characteristic components appeared to vary considerably between the dyed yarn extracts, with a greater relative amount of apigenin observed in the extract from location 1 (Lanquedoc-Roussillon) and only a relatively small amount of the flavonol kaempferol observed in the sample from location 2 (Mount Aigoual, France).

Despite these differences, the presence of the flavonols quercetin and kaempferol in *Serratula tinctoria* L. and *Serratula coronata* L. extracts immediately distinguishes their PDA HPLC chromatograms from those of other flavonoid sources, such as weld or dyer's greenweed. However, previous work has indicated that due to their relatively high sensitivity to photo-degradation,[1] flavonols are not ideal for identifying the biological species used in the dyeing of historical samples.

Degradation of the flavonols would leave only the two common flavones, luteolin and apigenin, with which to identify sawwort in the acid hydrolysed extracts of historical samples. However, both of these components are also found in the extracts of weld or dyer's greenweed dyed yarns. This may go some way in accounting for the infrequency with which sawwort is identified on historical samples. A fuller discussion on the flavonoid components observed in extracts after the accelerated ageing of yarns dyed with sawwort is presented in Chapter 4.

Extracts from all three samples also contained trace amounts of unidentified colouring components. However, these were close to the detection limit of the PDA HPLC instrumentation and therefore not suitable for use as characteristic markers for the identification of sawwort in historical samples. Detailed spectral information for all components can be found in Chapter 6.

2.1.2.4 Young fustic (*Cotinus coggygria* Scop.)

Young fustic (*Cotinus coggygria* Scop.) is a yellow mordant dyestuff, obtained from the heartwood or inner part of the bark of the tree. Due to its poor light fastness, the dye source was often forbidden and only used for cheaper textile products or for dyeing the silk cores of metal threads (Chapter 5). Several flavonoid aglycones have been reported in the dye source, including fisetin and myricetin.[21] In addition, the aurone sulfuretin is also present.[24] The acid hydrolysed extract of a silk yarn dyed with young fustic at the National Museums of Scotland (Chapter 6) was chemically characterised using PDA HPLC and HPLC ESI MS techniques.

The PDA HPLC analysis of the acid hydrolysed extracts is shown in Figure 2.14. The retention time and UV-Vis spectrum of the main component matches with the aurone sulfuretin (λ_{max} = 399 nm, R_t 15.6 min). Further identifiable peaks were the flavonol fisetin [λ_{max} = 361, 319(sh) nm, R_t 13.6 min] and the related dihydrofisetin [λ_{max} = 279, 312(sh) nm, R_t 4.5 min].

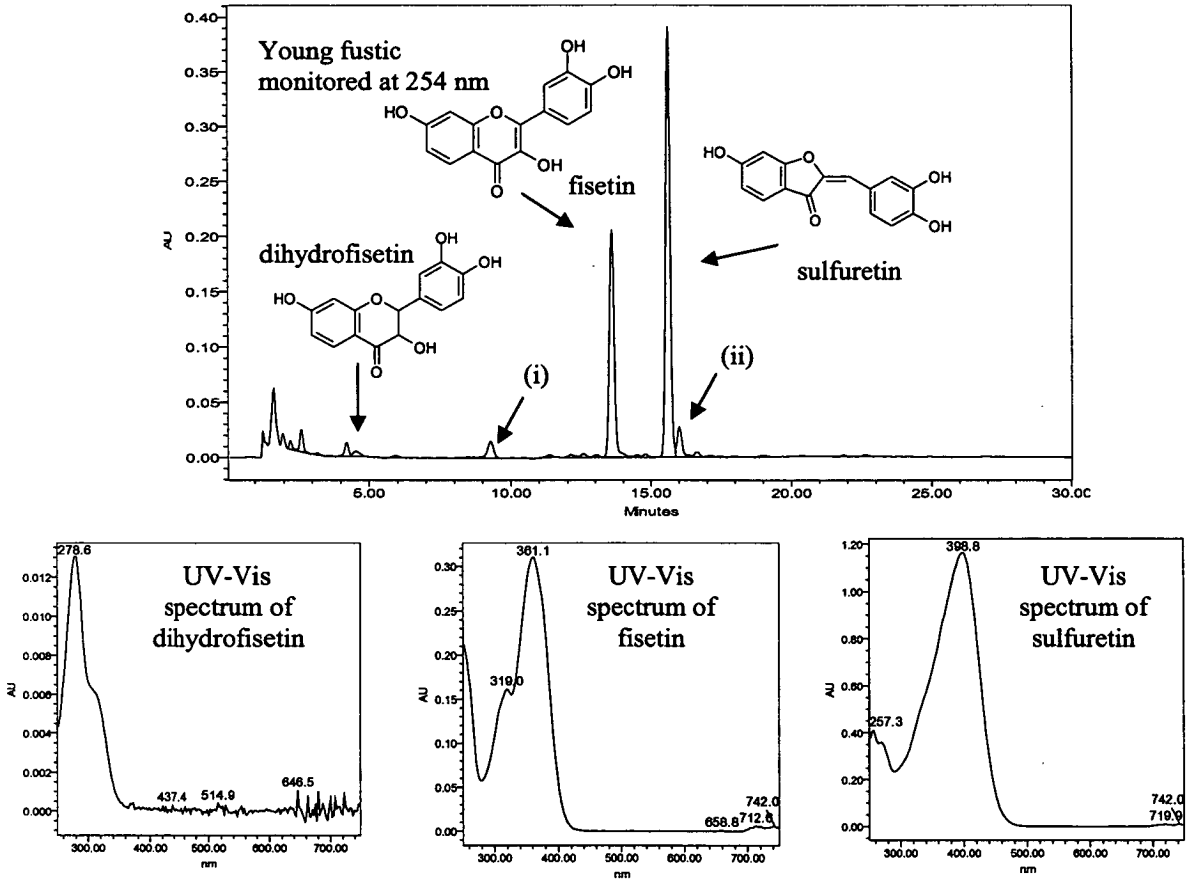

Figure 2.14: PDA HPLC of the acid hydrolysed extracts of Young fustic (*Cotinus coggygria* Scop.)

No peak was observed corresponding to the myricetin standard (λ_{max} = 375 nm, R_t 12.3 min). Several other minor components could not be identified from authentic standards. The most prominent, (i) had λ_{max} = 279, 312(sh) nm, R_t 9.3 min, and by inspection, appeared to be related to dihydrofisetin [λ_{max} = 279, 312(sh) nm]. The second peak, (ii) had λ_{max} = 368 nm, R_t 16.0 min. The results from the mass

spectrometric investigations of the components are detailed below, while spectral information has also been provided (Chapter 6).

The negative ion HPLC ESI MS^n analysis of the acid hydrolysed extracts confirmed the presence of both sulfuretin, with a deprotonated molecular ion, $[M-H]^-$ at *m/z* 269, and fisetin, with a deprotonated molecular ion, $[M-H]^-$ at *m/z* 285. The CID fragmentation of the aurone, sulfuretin, was investigated by directly injecting a sulfuretin reference sample dissolved in methanol or deuteriated methanol, allowing the number of exchangeable protons on each fragment to be deduced (Figure 2.15). The CID fragmentation of the flavonol, fisetin, has been investigated elsewhere.[1]

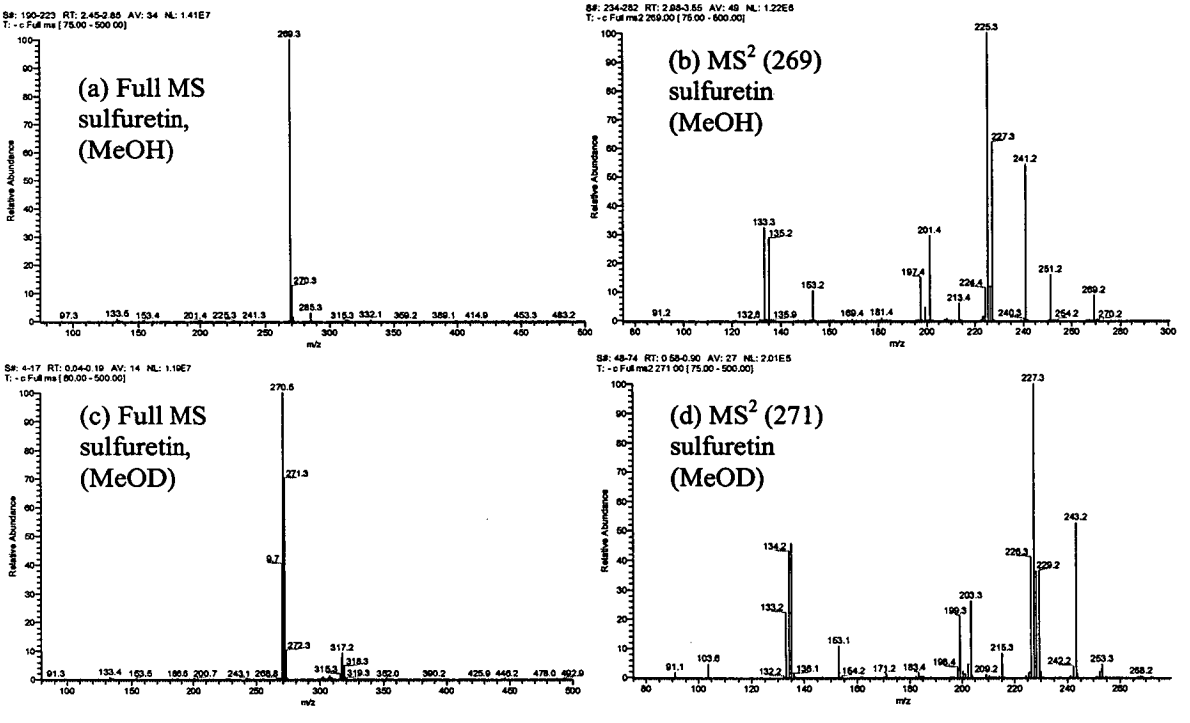

Figure 2.15: The direct injection and CID of the aurone, sulfuretin (*m/z* 269). (a) The Full mass spectrum of sulfuretin in MeOH, (b) The MS^2 (269) spectrum of sulfuretin in MeOH, (c) The Full mass spectrum of sulfuretin in MeOD, (d) The MS^2 (271) spectrum of the fully deuteriated sulfuretin in MeOD

The sulfuretin results have been tabulated (Table 2.13) and although an aurone, many of the small fragments were consistent with the observed breakdown pathways of

reference flavonoid components under similar conditions (for example, those from 3-*O*-methylquercetin).

Table 2.13: MS^2 fragmentation of the deprotonated molecular ion of sulfuretin in MeOH and MeOD

Sulfuretin in MeOH *m/z*: MS^2 **269** (relative abundance)	**Sulfuretin in MeOD** *m/z*: MS^2 **271** (relative abundance)	**Neutral fragment lost**	**and possible structure**
251 (16%)	253 (4%)	18	H_2O
241 (56%)	243 (52%)	28	CO
227 (62%)	229 (36%)	42	CH_2CO
	228 (36%)	43	CHDCO
225 (100%)	227 (100%)	44	CO_2
	226 (42%)	45	--
213 (8%)	215 (8%)	56	--
201 (30%)	203 (26%)	68	C_4H_4O or C_3O_2
197 (16%)	199 (22%)	72	--
153 (10%)		116	--
	153 (12%)	118	--
135 (28%)		134	See Scheme 2.2
133 (32%)	135 (46%)	136	
	134 (42%)	137	
	133 (22%)	138	

In both the deuteriated and non-deuteriated case, the highest mass fragment, though of low relative abundance, is due to loss of 18 Da (H_2O). The deuteriated sample also contains a very small 19 Da fragment (HOD). This is followed by a more abundant peak corresponding to the loss of a 28 Da fragment (probably CO).

A significant peak is also observed from the loss of a 42 Da fragment (probably CH_2CO). In the case of the deuteriated species the situation is complicated by peaks due to loss of 42 Da (*i.e.* the fragment contains no deuterium) and 43 Da (*i.e.* the fragment contains one deuterium). Furthermore, a 45 Da fragment is also observed. The base peak in both the non-deuteriated and deuteriated samples is due to the loss of 44 Da (CO_2), further complicating analysis of the deuteriated fragmentation

pattern. All of these fragments are common breakdown peaks in the negative ion ESI mass spectra of flavonoids.[1]

The major low-mass fragment ions are found at *m/z* 135 and *m/z* 133 in the non-deuteriated species, corresponding to the loss of 134 Da and 136 Da respectively. This suggests a retro-cheletropic mechanism (Scheme 2.2) similar to the retro-Diels Alder mechanism encountered in the CID fragmentation of the flavonoids.[1] This mechanism is supported by the deuteriated experiment, with the *m/z* 135 fragment remaining unaltered (as it has no remaining exchangeable proton sites), while the *m/z* 133 fragment becomes *m/z* 134 due to proton/deuterium exchange at one remaining site. The presence of sulfuretin in the acid hydrolysed extracts of historical samples can thus be confirmed by the MS^2 fragmentation of its deprotonated molecular ion (*m/z* 269).

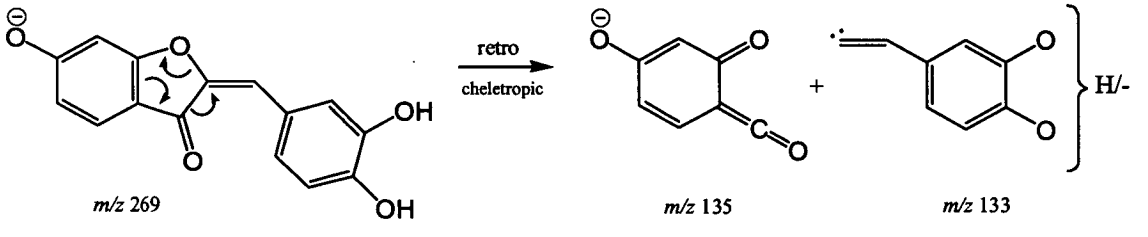

Scheme 2.2: The retro-cheletropic CID fragmentation of the aurone, sulfuretin

Due to the large number of closely eluting minor components in the acid hydrolysed extracts of young fustic, the PDA HPLC and HPLC ESI MS results were difficult to compare. The HPLC ESI MS base peak chromatogram and UV-signal at 254 nm are shown in Figure 2.16.

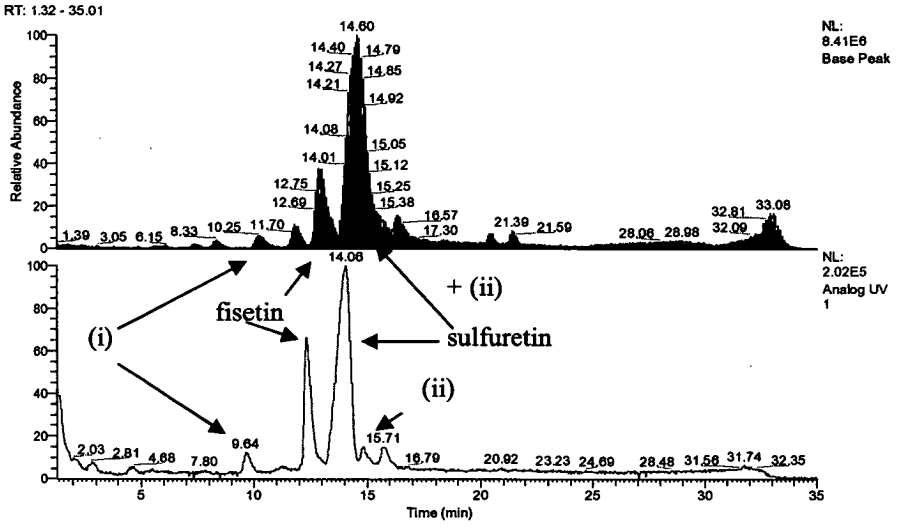

Figure 2.16: The HPLC ESI MS base peak chromatogram and UV-signal, monitored at 254 nm from the acid hydrolysed extracts of young fustic. As the detectors are connected in series, the UV-signal of each component is slightly off-set compared with the base peak signal from the mass spectrometer

The mass spectra of the unknown peaks (i) and (ii) are shown in Figure 2.17.

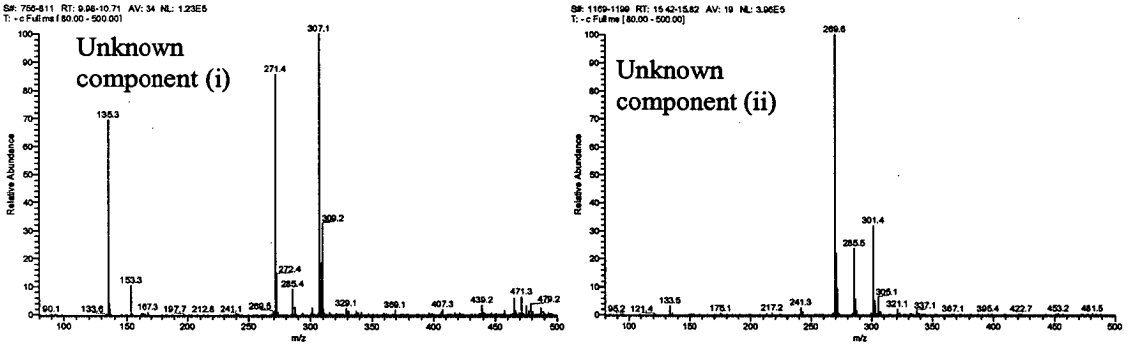

Figure 2.17: The HPLC ESI MS of the two most prominent unknown components in the acid hydrolysed extracts of yarn dyed with young fustic (*Cotinus coggygria* Scop.)

The mass spectrum of peak (i) contained a 3:1 peak pattern at *m/z* 307/309 (Figure 2.17). This distinctive isotope pattern is usually characteristic for compounds containing a single chlorine atom, suggesting that it may have been formed during the acid hydrolysis extraction protocol. This unknown component may have been derived from a fisetin related compound, leuco-fisetinidin (Figure 2.18).

Flavan
leuco-fisetinidin

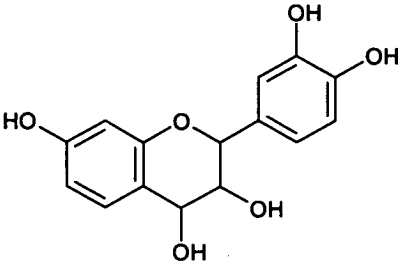

Figure 2.18: A possible structure for the precursor of the unknown component (i), observed in the HPLC ESI MS analysis of acid hydrolysed extracts from yarn dyed with young fustic

Many flavans such as this have been isolated from biological species,[25,26,27] and under acid conditions they can lose water, enabling the formation of HCl addition products (Scheme 2.3).[28]

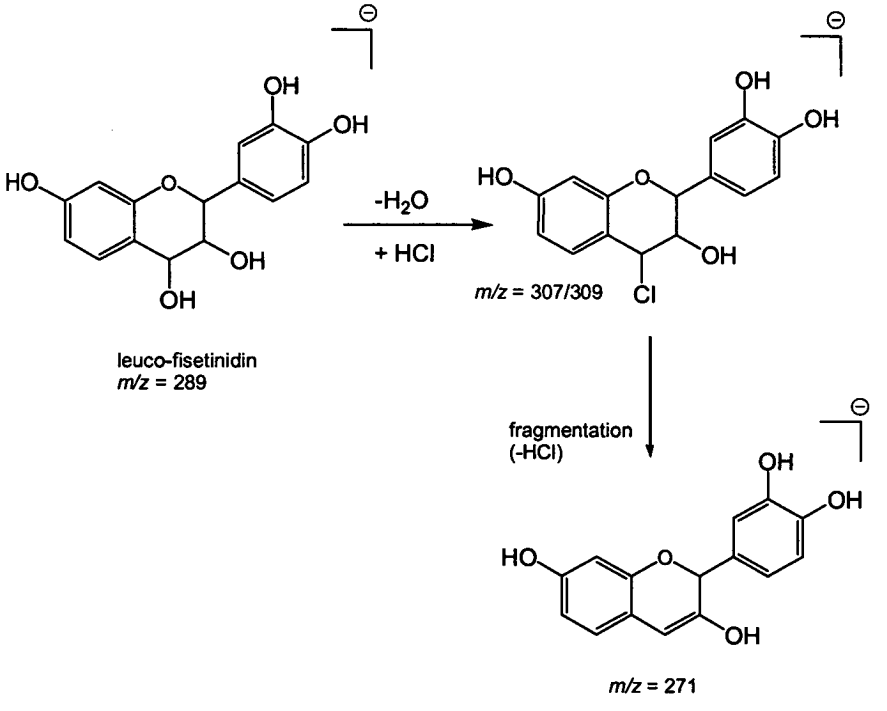

Scheme 2.3: In acidic conditions, flavans such as leuco-fisetinidin can lose water, enabling the formation of HCl addition products. The addition (and subsequent loss) of HCl may explain the mass spectrum of the unknown component, (i)

The presence of chlorine would explain the characteristic 3:1 peak pattern at *m/z* 307/309, while the *m/z* 271 peak can be explained by the subsequent loss of HCl from the molecule. This would also explain the different chromatographic behaviour but similar UV characteristics of this component compared with dihydrofisetin (Chapter 6).

The base peak in the mass spectrum of the second unknown component, (ii), is observed at *m/z* 270. The structure of this component could not be elucidated, however, a smaller peak at *m/z* 301 corresponds to the mass of an *O*-methyl analogue of dihydrofisetin (Figure 2.19). Compounds such as 3-*O*-methyldihydrofisetin have been isolated from a number of natural products,[29,30] however it has never been reported in extracts from young fustic plant material. Furthermore, the UV-Vis spectrum of this peak does not resemble that of diydrofisetin (Chapter 6) thus, structural elucidation of this component requires further investigative work.

***O*-methyl analogue of dihydrofisetin**
3-*O*-methyldihydrofisetin

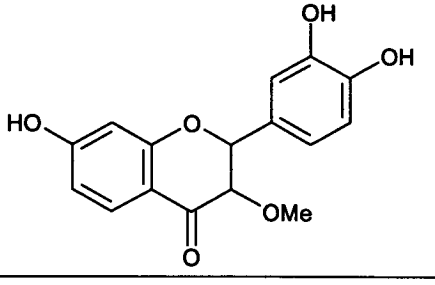

Figure 2.19: 3-*O*-methyldihydrofisetin, a possible component in the acid hydrolysed extracts from yarn dyed with young fustic

An aliquot of the young fustic dyebath was also hydrolysed and a peak corresponding to ellagic acid (Figure 2.20) was observed.

Ellagic acid

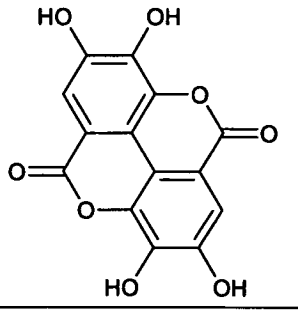

Figure 2.20: Ellagic acid, observed in the acid hydrolysed extracts of the young fustic dyebath

As the heartwood of young fustic was used in the dyebath preparation (Chapter 6), the presence of ellagic acid, which is often observed in the wood of trees,[31,32] is unsurprising. The use of this component, together with the other characteristic species identified above, may be used for the detection of young fustic as the dye source on historical samples. However, fisetin is known to be highly light fugitive, so a freshly dyed sample was subjected to accelerated ageing conditions to investigate the consequence for the identification of yarns dyed with young fustic (Chapter 4).

2.1.3 Conclusion

Systematic investigation of the main flavonoid components from different weld reference samples found that neither the substrate nor additional steps in the dyeing process significantly altered the relative ratio of the main components observed in dyed yarn extracts. In contrast, the ratio of the main flavonoid components found in extracts of unaged reference samples of dyer's greenweed were found to be highly dependent on the dyeing process. Relative amounts of the isoflavonoid genistein decreased with respect to the other components with the introduction of subsequent dyeing steps. Although natural variation of the relative flavonoid abundances found in the dye plant material may also affect the relative ratios of colouring components observed in the extracts of dyed yarns, different batches of dyestuff were not examined in this study.

PDA HPLC and HPLC ESI MS studies on the acid hydrolysed extracts of yarn dyed with the *Serratula* species, sawwort (*Serratula tinctoria* L.) and *Serratula coronata* L., provided important information regarding the identity of their characteristic minor components. Both quercetin and 3-*O*-methylquercetin were unambiguously detected in the extracts from freshly dyed yarns, together with kaempferol, luteolin and apigenin.

Similar characterisation studies performed on the acid hydrolysed extracts of young fustic identified the main colouring components to be the aurone sulfuretin and the flavonol fisetin. Fragmentation of sulfuretin under negative ion electrospray conditions was shown to proceed *via* a retro-cheletropic mechanism. Two further unidentified components were observed in the acid hydrolysed extracts and using data from HPLC ESI MS analysis, it was speculated that these might be related to dihydrofisetin, another minor component observed in the extracts of young fustic. However, before this can be confirmed, further investigative work is required

2.2 Initial investigations into the use of Inductively Coupled Plasma (ICP) techniques for the analysis of mordants

2.2.1 Introduction

Previous attempts to investigate the mordants on historical textile samples have utilised several different techniques, for example, X-Ray Fluorescence (XRF),[33] Scanning Electron Microscopy with Energy Dispersive X-Ray detection (XRF EDX),[34,35,36,37] and Particle-Induced X-Ray Emission (PIXE).[38] Although showing promise, surface techniques such as these are particularly sensitive to contamination. The presence of metallic elements from dust, dirt, soil, stains or past treatments, for example, may all constitute a source of metallic elements not associated with the mordanting process.[39,40,41,42]

Further limitations of surface techniques such as XRF or SEM EDX include non-uniformity of sample (uneven mordanting and dyeing or deterioration through wear

or handling) and instrument sensitivity (significant elements can often be present at concentrations close to the limits of detection). Furthermore, the interpretation of data from historical yarns can be complex, due to the presence of several ions including iron, which often appears as a trace element even when not used as a mordant, and other metallic ions such as aluminium, copper or cobalt.[43]

In an effort to address some of the problems associated with mordant identification, the use of Inductively Coupled Plasma (ICP) techniques was investigated. A short introduction to these techniques has been provided in Chapter 6. Surface impurities such as dirt and grime should become less significant when homogenised into a bulk solution, such as the acid hydrolysed extracts already prepared for dye analysis. Thus, when analysed using ICP techniques, a large concentration of a particular metal could indicate that it was used in the mordanting species. In addition, a portion of the acid hydrolysed extracts used for dye analysis can be diluted and fed into the plasma, thus a complete dye and mordant profile may be obtained from one small sample.

2.2.2 Results and Discussion

2.2.2.1 Inductively Coupled Plasma Optical Emission Spectroscopy (ICP OES)

An initial study was conducted to assess the suitability of Inductively Coupled Plasma Optical Emission Spectroscopy (ICP OES) for the identification of aluminium mordants. Selected MODHT reference samples (Table 2.14), prepared with an alum mordant, were chosen. A mordanted but undyed wool yarn (R/W3 mordant), and the same mordanted yarn dyed with brazilwood (R/W3) were extracted using the acid hydrolysis method. This allowed a comparison of the mordanted yarn with a dyed equivalent. For a similar investigation, but with a silk substrate, a mordanted but undyed silk yarn (Y/S1,3 mordant) was extracted, together with the same yarn but dyed this time with weld (Y/S1a). In addition to these samples, three 'reagent blanks' containing no yarn were prepared. This ensured that any metallic ions were from the mordanted yarns and not present due to

the sample preparation. All yarn samples were between 0.5 and 3.0 mg in weight and were hydrolysed and reconstituted as for dye analysis (Chapter 6).

An accurately measured aliquot of each reconstituted acid hydrolysed extract was then diluted with deionised water. Aluminium standards were also prepared and used to calibrate the instrument (Chapter 6). The diluted extracts of the selected reference samples were analysed in triplicate and the mean amounts of aluminium in each solution (per mg of yarn) calculated in ppm (Table 2.14). These values have also been expressed as the concentration of aluminium in the original extracts (per mg of yarn) to allow the amount of aluminium in each of the samples to be compared with one another. An example calculation has been provided (Chapter 6).

Table 2.14: Selected alum mordanted reference samples, analysed by Inductively Coupled Plasma Optical Emission Spectroscopy. All values quoted are per mg of yarn

Sample	Description	Al (mean) / ppm	Al (mean) / mM	% RSD of three replicate injections
R/W3 mordant	Wool yarn mordanted with alum	0.3781	2.1	0.8
R/W3	Above yarn dyed with brazilwood	0.2887	1.6	3.2
Y/S1,3 mordant	Silk yarn mordanted with alum	0.4873	2.8	2.8
Y/S1a	Above yarn dyed with weld	0.3605	2.0	0.4
Blank 1	Reagent blanks	0.0479	--	30.3
Blank 2	(containing no yarn)	0.0292	--	29.9

Aluminium was detected in all the alum mordanted samples, although at values of less than 1 ppm. The results suggested that the dyeing process reduces the amount of mordant on both the wool and silk yarns when compared with their undyed, but mordanted, equivalents.

Although the amounts of aluminium identified in the samples were all above the limit of detection for aluminium, the sample concentration could not be increased

further due to practical considerations regarding the minimum amount of solution required for the introduction of samples into the instrument. In addition, the instrument was unable to scan for a wide range of elements in a single run. Thus, ICP OES is a very convenient method for investigations into the effects of different mordanting procedures using model references, where large sample sizes are readily available. However, a more sensitive technique is likely to be required for the analysis of historical samples, where small sample sizes are required and the extent of mordant loss due to wear and handling or cleaning treatments is unknown.

2.2.2.2 Inductively Coupled Plasma Mass Spectrometry (ICP MS)

Inductively Coupled Plasma Mass Spectrometry (ICP MS) is a highly sensitive technique, with detection limits in the parts-per-billion (ppb) to parts-per-trillion (ppt) range. It has multi-elemental detection capability, allowing qualitative, semi-quantitative and quantitative determinations to be achieved over a large concentration range. A fully quantitative scan, using appropriate standards, can provide an exact concentration of the relevant metallic ions. Alternatively, a semi-quantitative scan, utilises a predefined calibration curve to give an indication of the relative amounts of detected species. In addition, 5-7 replicate measurements are usually performed to increase the reliability of the data.

The suitability of ICP MS for the identification of aluminium mordants was assessed using a further selection of MODHT reference samples (Table 2.15). To compare a mordanted yarn silk yarn with a dyed equivalent, a silk sample (Y/S2 mordant) and the same yarn dyed with young fustic (Y/S2a) were extracted using the acid hydrolysis method. A second mordanted but undyed silk yarn (Y/S1,3 mordant) and the same yarn dyed with dyer's greenweed (Y/S3b) were also extracted using the acid hydrolysis procedure, but the reconstituted extracts were stored in a freezer for *ca.* 6 months. This was to illustrate the applicability of the method to samples that had undergone mid to long term storage. A silk yarn dyed with dyer's greenweed but without a mordant provided a suitable unmordanted control sample, ensuring that any metallic components detected did not originate from the yarn, while two 'reagent

blanks' containing no yarn were also prepared to confirm the sample preparation did not influence the results. A mordanted but undyed wool yarn (R/W4,5 mordant), and a mordanted wool yarn dyed with weld (Y/W1) were also extracted for comparison. All yarn samples were between 0.5 and 3.0 mg in weight and were hydrolysed and reconstituted as for dye analysis (Chapter 6).

Table 2.15: Selected alum mordanted reference samples, analysed by Inductively Coupled Plasma Mass Spectrometry. The mordanting and dyeing of the samples has been described in Appendix 7.2

Sample	Description
Y/S3e	Silk yarn dyed with dyer's greenweed (no mordant). Extract freshly prepared.
Y/S2 mordant	Alum mordanted silk. Extract freshly prepared.
Y/S2a	Above yarn dyed with young fustic. Extract freshly prepared.
Y/S1,3 mordant (frozen)	Alum (boil) mordanted silk. Extract frozen for *ca.* 6 months before use.
Y/S3b (frozen)	Silk yarn (boil) mordanted then dyed with dyer's greenweed. Extract frozen for *ca.* 6 months before use.
R/W4,5 mordant	Alum mordanted wool. Extract freshly prepared.
Y/W1 (frozen)	Alum mordanted wool dyed with weld. Extract frozen for *ca.* 6 months before use.
Reagent blank (fresh)	Acid hydrolysis procedure employed, but with no yarn present. Extract freshly prepared.
Reagent blank (frozen)	As above, but extract frozen for *ca.* 6 months before use.

Solutions for ICP MS analysis are often prepared in high-purity nitric acid (2%) to prevent precipitation or adsorption of the trace analyte species onto the interior walls of the sample container. An acidic solution can also help to stabilise any metallic species present, leading to smaller concentration variations between replicate injections. However, the presence of nitric acid can sometimes lead to increased background noise from polyatomic interference ions formed from the matrix. This may be especially pronounced in the acid hydrolysed yarn extracts that contain a large amount of organic matter, leading to interference of the *m/z* 27 ($^{27}Al^{+}$) signal from polyatomic ions such as $^{1}H^{12}C^{14}N^{+}$. Standards and samples were therefore diluted in water rather than a nitric acid solution.

An aliquot of each reconstituted acid hydrolysed extract was accurately weighed, then diluted with water before the weight of the resulting solution was obtained. Aluminium standards were accurately prepared and used to calibrate the instrument (Chapter 6). The diluted extracts of the selected reference samples were then analysed and the mean amounts of aluminium in each solution (per mg of yarn) from five replicate injections calculated in ppb (Table 2.16). These values have also been expressed as the concentrations of aluminium in the original extracts (per mg of yarn), allowing the concentration of aluminium in each of the samples to be compared.

Table 2.16: Fully quantitative ICP MS results for $^{27}Al^+$ (five replicate injections). All values quoted are per mg of yarn

Sample	Description	$^{27}Al^+$ (mean) / ppb	$^{27}Al^+$ (mean) / mM	% RSD of five replicate injections
Y/S3e	silk dyed with dyer's greenweed (no mordant)	9	0.2	3.3
Y/S2 mordant	alum mordanted silk	167	3.5	1.5
Y/S2a	above yarn dyed with young fustic	78	1.4	3.5
Y/S1,3 mordant (frozen)	alum mordanted silk	116	2.2	2.0
Y/S3b (frozen)	above yarn dyed with dyer's greenweed	32	0.6	2.3
R/W4,5 mordant	alum mordanted wool	41	0.8	1.5
Y/W1 (frozen)	alum mordanted wool, dyed with weld	52	1.1	2.3
Reagent blank (fresh)	No yarn present during extraction procedure	18	--	8.7
Reagent blank (frozen)		4	--	7.1

The percentage relative standard deviations (% RSD) for the five replicate injections of each diluted extract were less than 4%. An RSD of less than 2% is usually expected for samples diluted with 2% nitric acid. However, without the stabilising effect conferred by the presence of the acid, this was deemed to be acceptable. The detector response at *m/z* 27, related to the amount of $^{27}Al^+$ ions detected, was an

order of magnitude less in the unmordanted reference (Y/S3e) than in the alum mordanted samples. Thus, the aluminium detected in the alum mordanted samples is likely to originate from the mordanting procedure.

Significantly, the concentrations of aluminium in the acid hydrolysed extracts of mordanted samples were, in all cases, larger than in the extracts from samples that had subsequently been dyed. For example, the extract from alum mordanted silk dyed with young fustic (Y/S2a) contained less than half the concentration of aluminium as the undyed equivalent (Y/S2 mordant). The (frozen) extract from alum mordanted silk, dyed twice with dyer's greenweed (Y/S3b) also had a considerably smaller aluminium concentration than the (frozen) extract from the equivalent undyed sample (Y/S1,3). This suggests that the dyeing process removes excess mordant from the yarn. Therefore, the assessment of techniques for mordant identification should always be performed on mordanted and dyed reference samples.

The aluminium concentrations (per mg of yarn) in the alum mordanted, but undyed silk extracts (Y/S2 mordant and Y/S1,3 mordant) were 3.5 mM and 2.2 mM respectively. Although the same amount of alum per weight of silk was used in both mordanting procedures, it is impossible to conclude whether the observed difference is due to the slightly different mordanting procedures (Appendix 7.2) or whether it is the result of cold storage. In addition, the aluminium concentration (per mg of yarn) in the mordanted, but undyed wool sample (R/W4,5 mordant) was less than the aluminium concentration obtained from either of the mordanted, but undyed silk samples (Y/S2 mordant and Y/S1,3 mordant). A considerably smaller amount of aluminium was used during this mordanting procedure compared with the silk procedures (Appendix 7.2), but the inherent differences in the weight of the two substrates makes a direct comparison impossible.

The results outlined above suggested that Inductively Coupled Plasma Mass Spectrometry (ICP MS) would be a suitable technique with which to investigate the

metallic mordants on historical samples. Thus, eight yarns from the MODHT sampling campaign (Chapter 6) were selected for analysis (Table 2.17).

Table 2.17: Historical samples selected for analysis by Inductively Coupled Plasma Mass Spectrometry (ICP MS)

Sample	Yarn	Colour	Yellow dye source	Period
BXL 3/13	wool	yellow	dyer's greenweed	Brussels, 1500-1550
TOU 1/11	wool	yellow	weld	Arras, <1500
BXL 3/09	wool	green	dyer's greenweed	Brussels, 1500-1550
BRU 2/29	wool	green	weld	Bruges, 1600-1650
PNM 2/09	silk	yellow	dyer's greenweed	Brussels, 1500-1550
PNM 8/12	silk	yellow	weld	Bruges, 1600-1650
BRU 1c/16	silk	green	dyer's greenweed	Bruges, 1500-1550
PNM 1/32	silk	green	weld	Arras, <1500

Four of the historical samples were wool and four were silk. Two samples from each yarn type were dyed green (as indicated by the presence of indigotin in the dye analysis)[6] and two were dyed yellow (as indicated by the absence of indigotin). In each case, one sample was chosen where the yellow dye source was identified as weld and another where the source used to dye the textile yellow was dyer's greenweed. The tapestries from the MODHT sampling campaign can be arranged into five distinct historical groupings based on their place and date of manufacture (Arras, <1500; Brussels, 1500-1550; Bruges, 1500-1550; Bruges, 1600-1650 and Antwerp, 1650-1700) and the first four are represented in this study. The most likely mordant to have been used in all the above samples is alum, since the use of an iron mordant with weld or dyer's greenweed would produce a yarn with a rather dull colour.

A further six MODHT reference samples were selected for analysis, corresponding, where available, to the substrate/dye combinations of the chosen historical samples (Table 2.18).

Table 2.18: Further MODHT reference samples chosen for analysis using Inductively Coupled Plasma Mass Spectrometry

Reference	Yarn	Colour	Yellow dye source
Y/W2	wool	yellow	dyer's greenweed
Y/W1	wool	yellow	weld
G/W1	wool	green	weld
Y/S3a	silk	yellow	dyer's greenweed
Y/S1a	silk	yellow	weld
G/ S4	silk	green	weld

All historical and reference yarn samples were between 0.3 and 2.7 mg in weight and were hydrolysed and reconstituted as for dye analysis (Chapter 6). Several 'reagent blanks' were also analysed, including one reconstituted 'blank' extract which had been in the freezer for *ca.* one year. This was analysed to ensure that the background count was stable for this length of storage. The samples described above, together with six aluminium standards, were then prepared for ICP MS analysis as described for the previous set of samples (Chapter 6).

The mean amounts of aluminium in each of the solutions (per mg of yarn) from five replicate injections were calculated in ppb (Table 2.19). These values have also been expressed as the concentration of aluminium in the original extracts (per mg of yarn) to allow the aluminium concentrations in each of the samples to be compared.

Table 2.19: Fully quantitative ICP MS results for $^{27}Al^{+}$ (five replicate injections) in the selected historical samples and their equivalent reference samples. All results are per mg of yarn

Sample	$^{27}Al^{+}$ (mean) / ppb	$^{27}Al^{+}$ (mean) / mM	% RSD of five replicate injections
BXL 3/13	204	2.6	3.2
Y/W2	49	0.5	5.8
TOU 1/11	148	1.8	5.2
Y/W1	134	1.3	3.9
BXL 3/09	64	1.0	2.7
No equivalent ref.	--	--	--
BRU 2/29	99	1.1	1.7
G/W1	131	1.3	4.3
PNM 2/09	535	5.3	6.6
Y/S3a	246	2.4	5.1
PNM 8/12	138	1.8	2.7
Y/S1a	216	2.1	5.1
BRU 1c/16	137	2.1	4.2
No equivalent ref.	--	--	--
PNM 1/32	101	0.9	4.7
G/S4	154	1.5	2.2
Reagent blank (frozen)	7	--	2.8
Reagent blank 1	23	--	25.1
Reagent blank 2	18	--	3.5

A significant amount of aluminium was detected in all the sample extracts. The percentage relative standard deviation (% RSD) of the five replicate injections of each sample varied between 1.7% and 6.6%. This was slightly larger than expected, although without the stabilising presence of the nitric acid, perhaps unsurprising.

The concentrations of aluminium (per mg of yarn) in the extracts from all the historical samples are consistent with the use of an alum mordant. The aluminium concentrations were between 0.9 mM and 5.3 mM in the historical samples, compared with aluminium concentrations between 0.5 mM and 2.4 mM in the alum

mordanted references. However, in some instances, the concentrations of aluminium were very similar to the equivalent reference samples (for example, TOU1/11 and Y/W1), while in other cases there were large discrepancies (for example, BXL3/13 and Y/W2).

To enable a fuller interpretation of the above data, the metallic ion 'profiles' in the acid hydrolysed extracts of both the historical samples and the reference yarns mordanted with alum were examined. As a fully-quantitative calibration curve had only been prepared for aluminium, the semi-quantitative data, utilising a predefined calibration curve, was used to give an indication of the relative amounts of selected ions (Table 2.20).

Comparing the relative amounts of the selected ions in each historical sample showed that in every case, aluminium and iron ions were the most prevalent species. However, the relative concentrations of iron compared with aluminium were higher in half of the historical samples (BXL 3/09, PNM 2/09, PNM 8/12 and PNM 1/32), while the concentrations of aluminium were greater than iron in the remaining samples (BXL 3/13, TOU 1/11, BRU 2/29, BRU 1c/16). Furthermore, the concentration of the most prevalent species was usually less than twice the concentration of the second most concentrated species.

These results were surprising, as it was hoped that a large concentration of a particular species in the extracts would allow the mordanting species to be clearly distinguished. This did prove to be the case in the alum mordanted reference samples, where, in contrast to the historical samples, the relative amounts of aluminium compared with iron were considerably greater in all cases.

Table 2.20: Semi-quantitative ICP MS results for selected ions in the historical samples and their equivalent reference samples

Sample	$^{24}Mg^+$ (mean) / mM	$^{27}Al^+$ (mean) / mM	$^{52}Cr^+$ (mean) / mM	$^{56}Fe^+$ (mean) / mM	$^{65}Cu^+$ (mean) / mM	$^{206}Pb^+$ (mean) / mM
BXL 3/13	0.7	2.6	0.1	1.4	0.1	0.1
Y/W2	0.5	0.5	0.0	0.2	0.0	0.0
TOU 1/11	0.4	1.8	0.1	1.1	0.0	0.0
Y/W1	0.3	1.3	0.0	0.1	0.0	0.0
BXL 3/09	0.4	0.9	0.1	1.4	0.0	0.1
No equiv. ref.	--	--	--	--	--	--
BRU 2/29	0.6	1.1	0.0	0.6	0.0	0.0
G/W1	0.3	1.3	0.0	0.3	0.0	0.0
PNM 2/09	2.2	5.3	0.8	8.0	0.1	0.0
Y/S3a	3.8	2.4	0.0	0.4	0.0	0.0
PNM 8/12	0.7	1.8	0.1	2.5	0.0	0.0
Y/S1a	0.3	2.1	0.0	0.5	0.0	0.0
BRU 1c/16	0.5	2.1	0.0	1.0	0.1	0.0
No equiv. ref.	--	--	--	--	--	--
PNM 1/32	0.8	0.9	0.1	1.4	0.1	0.0
G/S4	1.4	1.5	0.0	0.9	0.1	0.1

Although the alum mordanted reference samples contained a relatively small amount of iron (<1.0 mM), they were prepared in a modern laboratory using laboratory grade chemicals, minimising sample contamination. It is therefore difficult to speculate on whether the source of the iron in the historical extracts, present at concentrations between 0.6 mM and 8.0 mM, is due to impurities within the constituents used in the mordanting and dyeing processes, or whether it is from subsequent contamination of the yarns due to soiling.

However, the importance of the purity of the alum with respect to the final colour of the dyed yarn was well known to ancient dyers,[44] suggesting that the iron is unlikely to have been deliberately added and that great care would have been taken to limit iron contamination as much as was practically possible. The iron may therefore be

present as a post-manufacturing contaminant, perhaps from dirt or dust.[39,40,41,42] The above data are therefore inconclusive and suggest that mordant identification in historical samples may, in many cases, prove to be problematic due to the ubiquitous presence of iron.

A further challenge in distinguishing the use of different mordants with ICP MS is the occurrence of 'interference peaks' from the plasma support gas, affecting the detection of the two main elements of interest (Al and Fe). For example, two species are commonly observed at *m/z* 56, the major isotope of iron, $^{56}Fe^{+}$, and the diatomic molecular species $^{40}Ar^{16}O^{+}$. Although this problem can be minimised with careful sample and instrument preparation and the use of appropriate standards in fully-quantitative procedures, it can sometimes be difficult to assess the reliability of the data from semi-quantitative scans.

Three historical yarn samples (BRU 2/29, PNM 2/09 and PNM 8/12) were therefore also examined by scanning electron microscopy coupled with energy dispersive X-ray spectrometry (SEM EDX) (Chapter 6). The 'smooth' nature of the fibres in the SEM images of both PNM 2/09 and PNM 8/12 identifies them as silk, while the 'scaly' fibres observed in the SEM image of BRU 2/29 is indicative of wool (Figure 2.21).

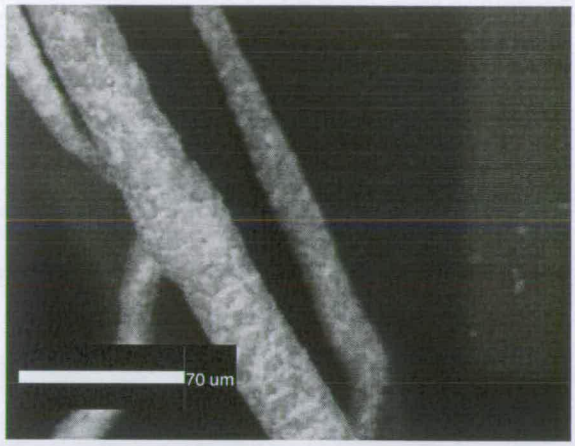

(a) BRU 2/29, Green wool (weld)

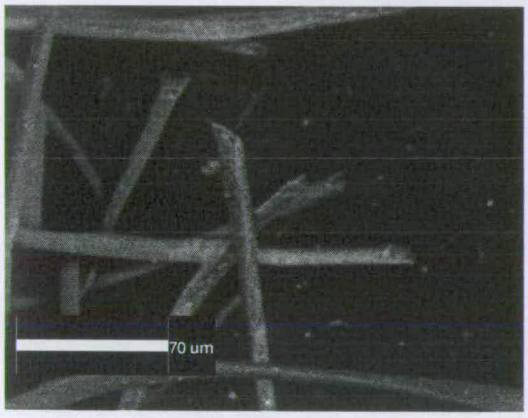

(b) PNM 2/09, Yellow silk (dyer's greenweed)

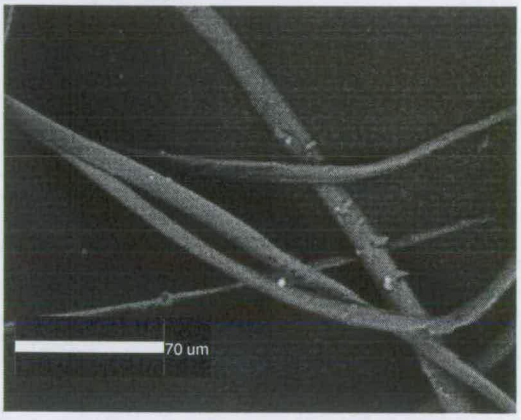

(c) PNM 8/12, Yellow silk (weld)

Figure 2.21: SEM images of three historical samples, (a) BRU 2/29 (wool), (b) PNM 2/09 (silk) and (c) PNM 8/12 (silk)

Aluminium is clearly observed in the SEM EDX analysis on the fibres from all three samples (Figure 2.22). However, despite ICP MS analysis of the bulk sample identifying significant amounts of iron in both PNM 2/09 and PNM 8/12, the SEM EDX analysis of the fibre surface found only trace amounts of iron on the PNM 2/09 sample and no iron on the PNM 8/12 sample. This highlights the potential limitations of the (surface) SEM EDX technique, but also suggests that the iron from the PNM 2/09 sample might be due to post-mordanting and dyeing surface contamination.

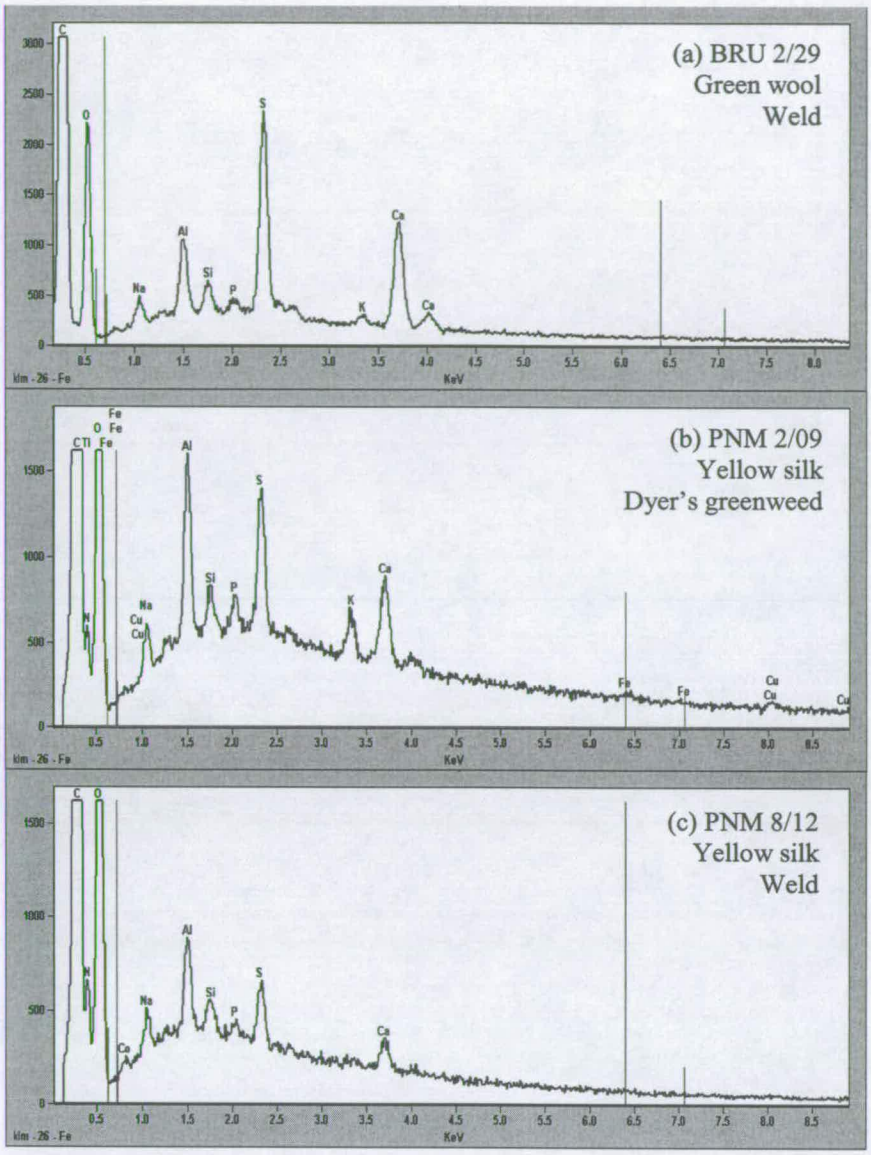

Figure 2.22: SEM EDX analysis of three historical samples, (a) BRU 2/29, (b) PNM 2/09 and (c) PNM 8/12

Relative to aluminium and iron, all the reference and historical yarn extracts contained only a small amount of the other selected ions; magnesium, chromium, copper and lead. Thus, it is likely that either aluminium or iron was present in the main mordanting species used in the historical samples.

Stable lead isotopes are increasingly used in environmental science as tracers of natural and anthropogenic lead sources.[45,46] Thus, lead isotope information may help

to indicate if contamination of the sample is likely to have occurred during the production of the dyed yarns or as a result of modern pollution sources. Possible modern sources of lead contamination include the additives from paint, which contribute to lead levels in dust,[39] or the lead additives in petrol, which were a major source of atmospheric lead pollution until the 1990s, when their use declined.[47] These two sources can be distinguished using isotope ratio analysis, as the lead used as an additive in petrol has a signature $^{206}Pb/^{207}Pb$ ratio.[47] An exploratory study conducted using another set of historical samples from the MODHT sampling campaign was therefore initiated and the lead isotope ratios tabulated below (Table 2.21).[48]

Table 2.21: Lead isotope analysis of the extracts from five historical yarn samples using ICP MS

Sample	Description	Lead isotope ratios		
		^{208}Pb / ^{207}Pb	^{208}Pb / ^{206}Pb	^{206}Pb / ^{207}Pb
TOU 1/12	wool / weld	2.412 ± 0.0112	2.104 ± 0.0068	1.146 ± 0.0025
PNM 1/13	silk /dyer's greenweed	2.402 ± 0.0078	2.139 ± 0.0043	1.123 ± 0.0038
BXL 1/2	silk /dyer's greenweed	2.441 ± 0.0064	2.093 ± 0.0052	1.166 ± 0.0028
PNM 5/13	wool / weld	2.404 ± 0.0111	2.096 ± 0.0087	1.147 ± 0.0096
BRU 1a/6	wool / weld	2.431 ± 0.0073	2.087 ± 0.0071	1.165 ± 0.0058

For the lead to have been solely from petrol sources, the $^{206}Pb/^{207}Pb$ ratio would have to be in the region of 1.04-1.09, indicating that this was not the case in any of the historical samples. However, the $^{206}Pb/^{207}Pb$ ratio in samples containing lead from a mixture of sources rarely reaches the 1.04-1.09 region due to the averaging effect of the mixed sources. The $^{206}Pb/^{207}Pb$ ratio in PNM 1/13 is particularly low compared with the other samples, suggesting that lead from petrol additives might have contributed to the result. Although the lead ratios from the samples proved to be inconclusive regarding the lead source, they clearly demonstrated that lead contamination was not solely due to the additives from petrol.

In a recently published work, mordant analysis using ICP MS was described and similar results regarding the presence of both aluminium and iron reported.[49] These authors were unaware of our preliminary dissemination on this topic.[50]

2.2.3 Conclusion

ICP MS analysis was successful in identifying the metallic ions present in the acid hydrolysed extracts of reference yarns, with the results reflecting differences in the substrate and mordanting procedures undergone by each sample. However, interpretation of the results from the analysis of the historical sample extracts proved problematic, due to the observation of large amounts of both aluminium and iron. The relatively small amount of other metallic ions present in the extracts makes their use as the main mordanting species unlikely.

2.3 References

[1] Ferreira, E.S.B, *'New Approaches towards the identification of yellow dyes in ancient textiles'*, PhD Thesis, **2002**, The University of Edinburgh

[2] Edelstein, S.M.; Borghetty, H.C., *'The Plictho of Gioanventura Rosetti. Instructions in the art of the dyers which teaches the dyeing of woolen cloths, linens, cottons, and silk by the great art as well as by the common'*, translation of the 1548 (first) edition, **1969**, *The M.I.T. Press*, Cambridge. MA., 131-152, 186-199

[3] Cardon, D., *'Yellow Dyes of Historical Importance: Beginnings of a Long-Term Multi-Disciplinary Study'*, Dyes Hist Arch, **1995**, 13, 59-73

[4] Hacke, A-M., PhD Thesis, **2006**, University of Manchester

[5] Zhang, X.; Laursen, R.A., *'Development of Mild Extraction Methods for the Analysis of Natural Dyes in Textiles of Historical Interest Using LC-Diode Array Detector-MS'*, Anal Chem, **2005**, 77, 2022-2025

[6] Koren, Z.C., *'An efficient HPLC analysis scheme for plant and animal red, blue and purple dyes'*, Dyes Hist Arch, **1995**, 13, 27-37

[7] Surowiec, I.; Nowik, W.; Trojanowicz, M., *'Optimization of solvent extraction of dyes for their identification in archaeological textiles'*, Dyes Hist Arch, 22, *in press*

[8] Wouters, J., *'High Performance Liquid Chromatography of anthraquinones: analysis of plant and insect extracts and dyed textiles'*, Stud Conserv, **1985**, 30, 119-128

[9] Kaiser, R., *'Quantitative analyses of flavonoids in yellow dye plant species weld (*Reseda luteola *L.) and Sawwort (*Serratula tinctoria *L.)'*, Angew Bot, **1993**, 67, 128-131

[10] Yuldashev, M.P.; Batirov, E. Kh.; Malikov, V.M.; Yulasheva, N.P., *'Flavonoids of* Psoralea drupaceae *and* Reseda luteola*'*, Chem Nat Compd, **1996**, 32, 923-924

[11] Cristea, D.; Bareau, I.; Vilarem, G., *'Identification and quantitative HPLC analysis of the main flavonoids present in weld (*Reseda luteola *L.)'*, Dyes Pigments, **2003**, 267-272

[12] Swain, Tony, *'Flavonoids as chemotaxonomic markers in plants'*, in 'Pigments in Plants', F.C. Czygan (ed.), **1980,** Gustav, Fischer Verlag, 2nd edition, 224-236

[13] Stevens, J.F.; Hart, H.; Elema, E.T.; Bolck, A., *'Flavonoid variation in* Eurasian Sedum *and* Sempervivum*'*, Phytochemistry, **1996**, 41, 2, 503-512

[14] Bohm, B.A.; Stuessy, T.F., *'Flavonoids and Population variation'*, in 'Flavonoids of the sunflower family (*Astraceae*)', **2001**, Springer Wien, New York, , 545-560

[15] Nakatsuka, T.; Nishihara, M.; Mishiba, K.; Yamamura, S., *'Temporal expression of flavonoid biosynthesis-related genes regulates flower pigmentation in* gentian *plants'*, Plant Sci, **2005**, 168, 1309–1318

[16] Wouters, J.; Verhecken, A., *'The Scale Insect Dyes (Homoptera: Coccoidea). Species Recognition by HPLC and Diode-Array Analysis of the Dyestuffs'*, Annals Soc Ent Fr (N.S.), **1989**, 25, 4, 393-410

[17] Wang, G.; Kuan, S.S.; Francis, O.J.; Ware, G.M.; Carman, A.S., *'A Simplified HPLC method for the determination of phytoestrogens in soybean and its processed products'*, J Agr Food Chem, **1990**, 38, 185-190

[18] Ungar, Yael; Osundahunsi, O.F.; Shimoni, E., *'Thermal stability of genistein and daidzein and its effect on their antioxidant activity'*, J Agr Food Chem, **2003**, 51, 4394-4399

[19] Bancroft, E., *'Experimental Refearches concerning the philosophy of permanent colours'*, **1794**, Vol. 1, London, 410-415

[20] Andary, C.; Prunac S., *'Yellow Dyes of Historical Importance: A multi-Disciplinary Study'*, Dyes Hist Arch, **1995**, 14, 33-38

[21] Cardon, D. and du Chatenet, G. *'Guide des Teintures naturelles'*, **1990**, Delachaux et Niestlé, 1st edition, 66

[22] Ferreira, E.S.B.; Quye, A.; McNab, H.; Hulme, A.N., *'Photo-oxidation Products of Quercetin and Morin as Markers for the Characterisation of Natural Flavonoid Yellow Dyes in Ancient Textiles'*, **2002**, Dyes Hist Arch, 18, 63-72

[23] Justesen, U., *'Collision-induced fragmentation of deprotonated methoxylated flavonoids, obtained by electrospray ionization mass spectrometry'*, J Mass Spectrom, **2001**, 36, 169-178

[24] Hofenk de Graaff, J.H., *'The Colourful Past'*, **2004**, Abegg-Stiftung and Archetype Publications, 1st edition, 175-181

[25] Park, K-Y.; Jung, G-O.; Lee, K-T.; Choi, J.; Choi, M-Y.; Kim, G.; Jung, H-J.; Park, H-J., *'Antimutagenic activity of flavonoids from the heartwood of* Rhus vericiflua*'*, J Ethnopharmacol, **2004**, 90, 1, 73-79

[26] Roux, D.; Paulus, E., *'Condensed tannins. XII. Polymeric leucofisetinidin tannins from the heartwood of* Acacia mearnsii*'*, Biochem J, **1962**, 82, 320-324

[27] Botha, J.J.; Young, D.A.; Ferreira, D.; Roux, D.G., *'Synthesis of condensed tannins. Part 1. Stereoselective and stereo-specific syntheses of optically pure 4-arylflavan-s-ols and assessment of their absolute stereochemistry at C-4 by means of circular dichroism'*, J Chem Soc Perkin Trans I, **1981**, 1213-1219

[28] Slabbert, N.P., *'Ionisation of some flavanols and dihydroflavonols'*, Tetrahedron, **1977**, 33, 821-824

[29] Drewes, S.E.; Ilsley, A.H., *'Isolation of 3-methoxyfisetin from* Acacia mearnsi', Chem Commun, **1968**, 20, 1246-1247

[30] Barba, B.; Diaz, J.G.; Herz, W., *'Anthraquinones and other constituents of two* Senna *species'*, Phytochemistry, **1992**, 31, 12, 4374-4375

[31] Takashi, T.; Jiang, Z-H.; Kouno, I., *'Distribution of ellagic acid derivatives and a diarylheptanoid in wood of* Platycarya strobilacea', Phyochemistry, **1998**, 47, 5, 851-854

[32] El-Toumy, S.A.A.; Marzouk, M.S.; Rauwald, H.W., *'Ellagi- and gallotannins from* Punica granatum *heartwood*', Pharmazie, **2001**, 56, 10, 823-824

[33] Masschelin-Kleiner, L.; Maes, L.R.J., *'Ancient dyeing techniques in eastern Mediterranean regions'*, Preprints to the ICOM Committee for Conservation, 5th Triennial meeting, Zagreb, **1978**

[34] Indictor, N.; Koestler, R.J.; Sheryll, R., *'The Detection of Mordants by Energy Dispersive X-Ray Spectrometry Part I. Dyed Woolen Textile Fibres'*, J Am Inst Conserv, **1985**, 24, 104-109

[35] Koestler, R.J.; Indictor, N.; Sheryll, R., *'The Detection of Metallic Mordants by Energy Dispersive X-Ray Spectrometry Part II. Historical Silk Textiles'*, J Am Inst Conserv, **1985**, 24, 110-115

[36] Koestler, Sheryll, R.; R.J.; Indictor, N., *'Identification of dyeing mordants and related susbstances on textile fibers: A preliminary study using energy dispersive X-Ray spectrometry'*, Stud Conserv, **1985**, 58-62

[37] Ballard, M.; Koestler, R.J.; Indictor, N., *'Weighted silks observed using Energy Dispersive X-Ray spectrometry'*, Scan Electron Micros, **1986**, 499-506

[38] Williams, E.T.; Indictor, N., *'Detection of metallic mordants on textiles by Particle-Induced X-Ray Emission'*, Scan Electron Micros, **1986**, 847-850

[39] Butte, W.; Heinzow, B., *'Pollutants in house dust as indicators of indoor contamination'*, Rev Environ Contam T, **2002**, 175, 1-46

[40] Millette, J.R., *'Early studies characterising household dirt'*, Microscope, **2001**, 49, 4, 201-208

[41] Bradl, H.B., *'Adsorption of heavy metal ions on soils and soils constituents'*, J Colloid Interf Sci, **2004**, 277, 1-18

[42] Lithgow, K.; Lloyd, H.; Brimblecombe P.; Yoon, Y.H.; Thickett, D., *'Managing dust in historic houses – a visitor/conservator interface'*, Preprints to the ICOM Committee for Conservation, 14th Triennial meeting, The Hague, **2005**, 2, 662-669

[43] Trojanowicz, M.; Orsks-Gawrys, J.; Surowiec, I.; Szostek, B.; Urbaniak-Walczak, K.; Kehl, J.; Wróbel, M., *'Chromatographic investigation of dyes extracted from Coptic textiles from the National Museum in Warsaw'*, Stud Conserv, **2004**, 49, 2, 115-131

[44] Verhecken, A., *'The history of alum production in Belgium'*, Dyes Hist Arch, 23, in press

[45] Sangster, D.F.; Outridge, P.M.; Davis, W.J., *'Stable lead isotope characteristics of lead ore deposits of environmental significance'*, Environ Rev Dossiers Environ, **2000**, 8, 2, 115-147

[46] Sugden, C.L., *'Isotopic studies of the environmental chemistry of lead'*, PhD Thesis, **1993**, The University of Edinburgh

[47] Eades, L.J.; Farmer, J.G.; MacKenzie, A.B.; Kirika, A.; Bailey-Watts, A.E., *'Stable lead isotopic characterisation of the historical record of the environmental lead contamination in dated freshwater lake sediment cores from northern and central Scotland'*, Sci Total Environ, **2002**, 292, 55-67

[48] Hulme, A.N.; McNab, H.; Peggie, D.A.; Quye, A; Roberts, A., *Unpublished data*, **2005**

[49] Dussubieux, L.; Naedel, D.; Cunningham, R.; Alden, H.; Ballard, M.W., *'Accuracy, precision and investigation: mordant analysis on antique textiles by various methods'*, Preprints to the ICOM Committee for Conservation, 14th Triennial meeting, The Hague, **2005**, 2, 898-903

[50] Hulme, A.N.; McNab, H.; Peggie, D.A.; Quye, A., *'A novel approach to mordant identification using Inductively Coupled Plasma – Mass Spectrometry'*, poster at the 23rd annual meeting of Dyes Hist Arch, **2004**

Chapter 3

3 THE ANALYTICAL INVESTIGATION OF SELECTED NATURAL RED DYE COMPONENTS BY PDA HPLC, ESI MS AND NMR

The analytical investigation of cochineal (anthraquinone), and soluble redwood and logwood (neoflavonoid/homoisoflavonoid) dyes is presented. This extends the scope and nature of the characterisation work in Chapter 2, while building on the methodology previously developed within the group to characterise unknown components found in the acid hydrolysed extracts of yarns dyed with natural yellow (flavonoid) dye sources.[1,2,3]

3.1 Studies on the main components found in the cochineal insect dyes

3.1.1 Introduction

Mexican cochineal (*Dactylopius coccus* Costa) is one of the coccid dye sources. The term 'coccid dyes' encompasses all the different scale insect dyes, obtained from female beetles of different families.[4] These insects contain a variety of anthraquinone colouring components (Figure 3.1), and in many cases, species can be distinguished from one another by the relative amounts of each component in the acid hydrolysed extracts of dyed yarns.[5,6] The small differences found in the overall chemical composition of the extracts from yarns dyed with different species does not significantly alter the colour of the yarn. Thus, the identification of a particular species used to dye an historical textile is impossible by simple colour matching techniques.

Anthraquinone components from the 'coccid' insect dyes

Carminic acid

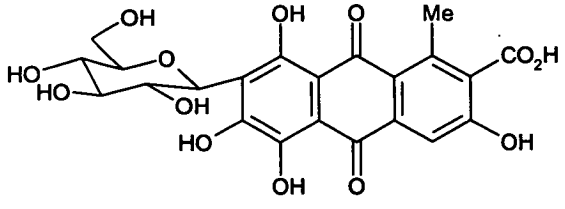

Kermesic acid

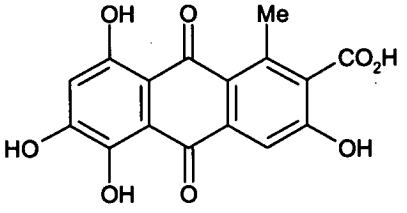

Laccaic acids A and B

Laccaic acid A: R=$CH_2NHCOMe$
Laccaic acid B: R = CH_2OH

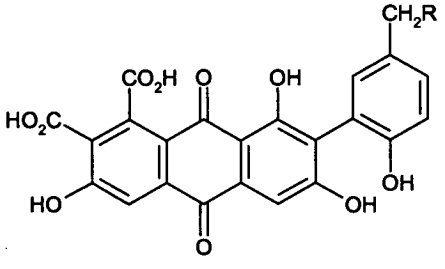

Flavokermesic acid (laccaic acid D)

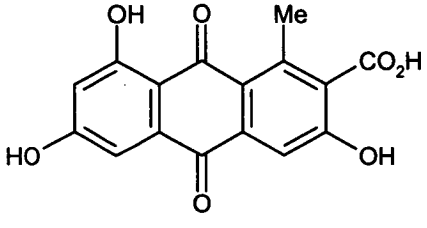

Figure 3.1: Common colouring components found in the Coccid dye sources

From the variety of scale insects that have been used as a dye source, five species in particular have been previously investigated; kermes (*Kermes vermilio* Planchon); Polish Cochineal, (*Porphyrophora polonica* Linnaeus); Armenian cochineal (*Porphyrophora hameli* Brandt); Mexican cochineal (*Dactylopius coccus* Costa) and lac dye (*Kerria lacca*).[7,8] Although much research has been devoted to distinguishing these different coccid dyestuffs from one another, many of their minor components remain to be identified. Furthermore, in contrast to compounds such as the flavonoids, only a few publications are available on the HPLC ESI MS of anthraquinones.[9,10]

The dyes source used for the model tapestries within the MODHT project was Mexican cochineal (*Dactylopius coccus* Costa). In the middle of the 16th century, the Spanish imported a new coccid dyestuff from South America (particularly Mexico),

and it was this species that was found on some of the historical samples analysed within the project (Chapter 5).

3.1.2 Results and Discussion

3.1.2.1 PDA HPLC analysis of acid hydrolysed extracts of yarn dyed with *Dactylopius coccus* Costa

A PDA HPLC chromatogram was obtained from the acid hydrolysed extract of a wool sample dyed with Mexican cochineal (*Dactylopius coccus* Costa) (R/W5). To allow the chromatographic method to be used on the HPLC ESI MS system without alteration, the ortho-phosphoric acid in the standard chromatographic method was replaced with formic acid (Chapter 6). This ensured that the retention times of the components under investigation would be similar on both systems, thus allowing minor components to be more readily identified. The chromatogram (monitored at 430 nm) of the freshly dyed samples is shown in Figure 3.2 with the anthraquinone constituents and their relative percentages (at both 430 nm and 275 nm) summarised in Table 3.1.

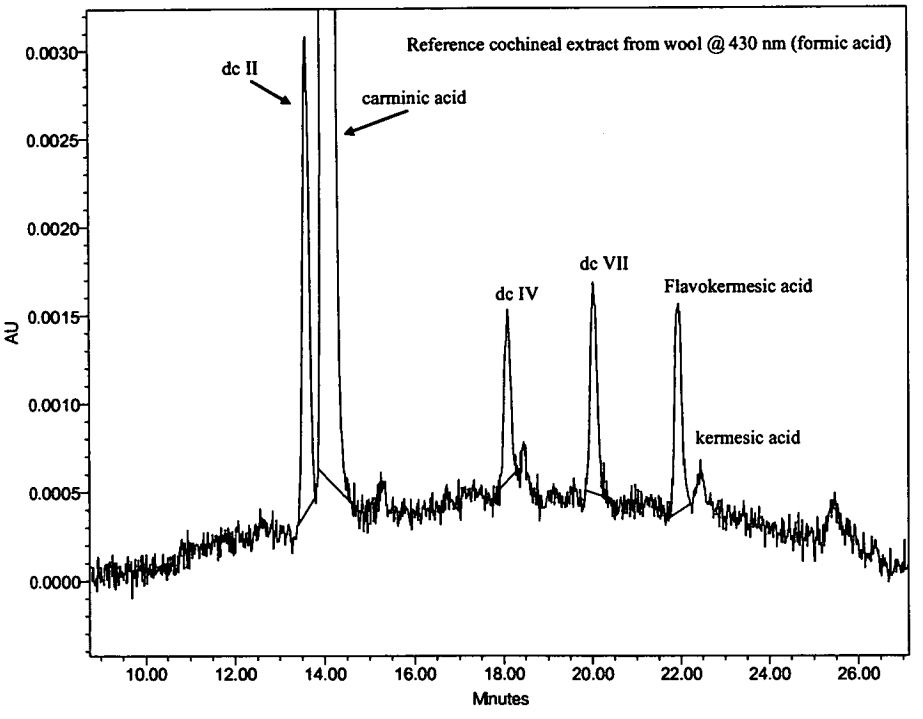

Figure 3.2: PDA HPLC chromatogram (monitored at 430 nm) of a cochineal dyed wool extract (R/W5)

The main colouring component was identified as carminic acid, while flavokermesic acid was the only other previously characterised component observed.[11] A small amount of kermesic acid also appeared to be eluting slightly later than flavokermesic acid, constituting less than 0.05% of the dye components at 430 nm. Although not sufficiently resolved from baseline noise to be confidently assigned in the above sample, its presence was later confirmed by mass spectrometry (Section 3.1.2.3). Three additional components were observed in the extracts. The names of these structurally unknown components from the *Dactylopius coccus* Costa. (dc) species are, in order of elution, dcII, dcIV and dcVII, following the nomenclature scheme adopted by Wouters and Verhecken.[7] All the components were identified by matching their retention times and spectral information to either an in-house library of standard compounds or with previously published data.

Table 3.1: Retention times (R_t) and relative peak areas (at both 430 nm and 275 nm) of the main anthraquinone components of the acid hydrolysed extracts of cochineal (*Dactylopius coccus* Costa) dyed wool (R/W5)

Peak	R_t	Relative peak area (monitored at 430 nm) / %	Relative peak area (monitored at 275 nm) / %
dcII	13.6	4.3	2.5
Carminic acid	14.1	90.3	93.0
dc IV	18.1	1.5	1.4
dc VII	20.0	1.9	2.2
Flavokermesic acid	22.0	2.0	0.8

The UV-Vis spectra of the components are shown in Figure 3.3. By inspection, the dcII component (λ_{max} = 285.7 and 435.0) appears to be related to flavokermesic acid (λ_{max} = 285.7 and 432.6), while dcIV (λ_{max} = 276.3 and 493.1) and dcVII (λ_{max} = 276.3 and 490.6) have UV-Vis spectra similar to that of carminic acid (λ_{max} = 276.3 and 495.5).

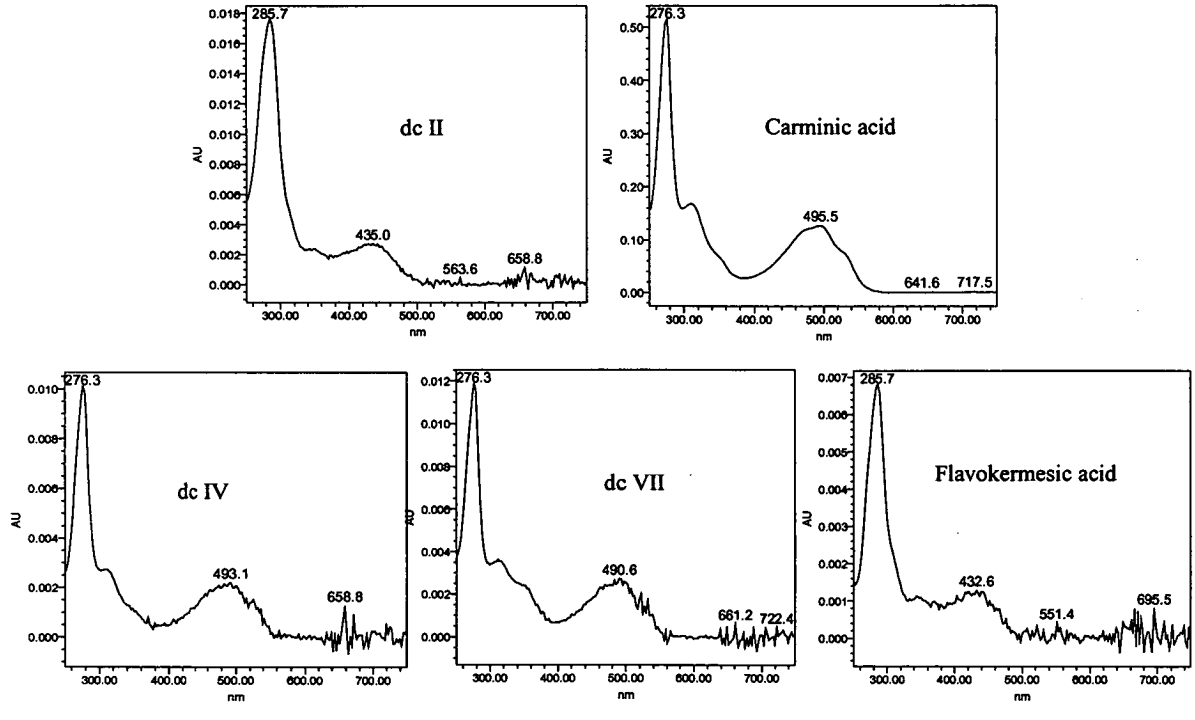

Figure 3.3: UV-Vis spectra of the main constituents of cochineal (*Dactylopius coccus* Costa)

Initial HPLC ESI MS investigations of the acid hydrolysed extracts of cochineal dyed yarn under negative ion conditions confirmed the base peak, $[M-H]^-$, to be carminic acid (*m/z* 491). The minor components, however, were more difficult to

detect due to their relatively small abundance. Careful analysis of the mass spectra revealed a component with a mass consistent with carminic acid minus an oxygen (*m/z* 475) and eluting at the dcII position (Figure 3.4).

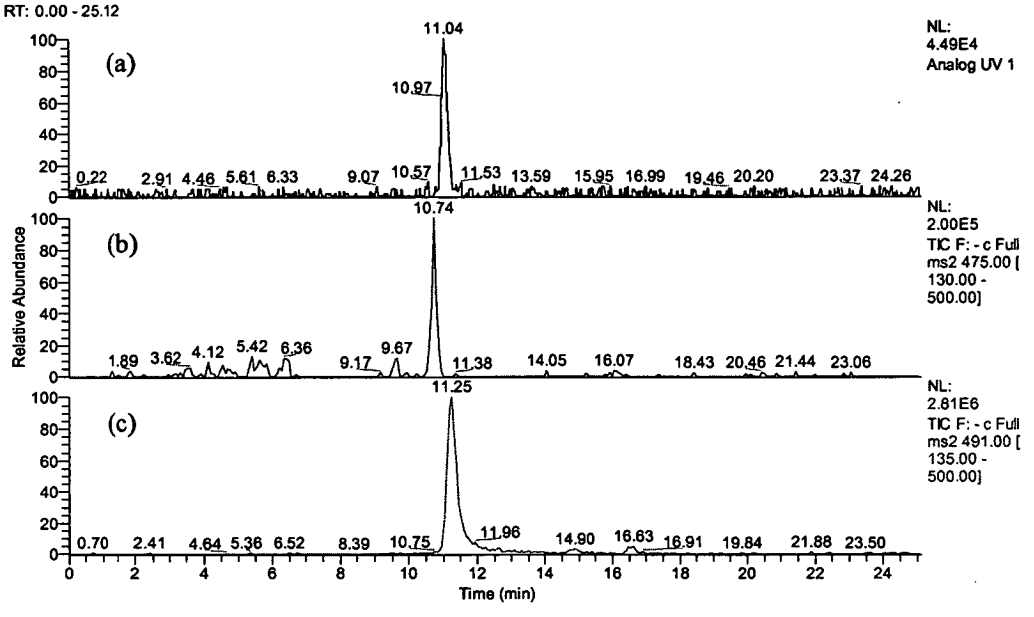

Figure 3.4: Negative ion LC ESI MS of extracts from acid hydrolysed cochineal dyed yarn. (a) UV signal at 430 nm, (b) MS^2 chromatogram for *m/z* 475 and (c) MS^2 chromatogram for *m/z* 491

The UV-Vis spectra and longer retention of the two additional unknown components, dcIV and dcVII, initially suggested that they might be methyl ether derivatives (similar to chrysoeriol, the luteolin methyl ether derivative characterised in weld). However, further analysis showed this not to be the case (Section 3.1.2.3).

3.1.2.2 Direct injection ESI MS^n analysis of *Dactylopius coccus* Costa

To investigate the natural constituents of *Dactylopius coccus* Costa further, a freshly prepared methanolic solution of the 'raw cochineal' used for the dyeing of the model tapestries was prepared. The directly injected solution gave a good mass spectrum under negative ion electrospray conditions. Collision Induced Dissociation (CID) experiments were performed in an effort to reveal structural information, while spectra were also recorded using deuteriated methanol (MeOD) as a solvent. Under these conditions, molecular ion clusters were observed corresponding to sequential

replacement by deuterium of the hydrogen atom in each of the OH groups (with the exception of the ionised OH). In each case, the ion corresponding to the most fully deuteriated species was chosen for CID experiments. Thus fragmentation pathways under CID conditions could be investigated.

The base peak in the raw cochineal extract was, as expected, the deprotonated molecular ion of carminic acid (*m/z* 491), the major component observed on textile fibres dyed with cochineal. The results of the MS^2 (MeOH) and MS^2 (MeOD) experiments on this component are summarised in Table 3.2 below.

Table 3.2: Collision Induced Dissociation (CID) of carminic acid (*m/z* 491) under negative ion conditions

***m/z*: MS^2 491 (relative abundance)**	**Neutral fragment lost (possible species)**	**Information from deuteriated studies**
447 (100%)	44 (CO_2)	Base peak. Observed fragment has 8 exchangeable protons, while the neutral fragment has none.
357 (5%)	134	Observed fragment has 6 exchangeable protons, while the neutral fragment has 2.
327 (3%)	164	Observed fragment has 5 exchangeable protons, while the neutral fragment has 3.

Significantly, both the *m/z* 357 and *m/z* 327 ions were again observed in further (MS^3) experiments performed on the *m/z* 447 base peak (Table 3.3).

Table 3.3: MS^3 fragmentation of [carminic acid-H-44]$^-$ (*m/z* 447)

***m/z*: MS^3 491, 447 (relative abundance)**	**Neutral fragment lost (possible species)**	**Information from deuteriated studies**
429 (28%)	18 (H_2O)	Observed fragment has 6 exchangeable protons, while the neutral fragment has 2. However, the neutral species H_2O and HOD were also lost.
357 (100%)	90 ($C_3H_6O_3$)	Base peak. Observed fragment has 6 exchangeable protons, while the neutral fragment has 2.
327 (52%)	120 ($C_4H_8O_4$)	Observed fragment has 5 exchangeable protons, while the neutral fragment has 3.

As both *m/z* 357 and *m/z* 327 ions were observed after CID fragmentation of the isolated *m/z* 447 component, they must originate from an initial loss of a carboxylic

acid moiety from the carminic acid, followed by the loss of a neutral fragment of 90 Da (containing 2 exchangeable protons) and 120 Da (containing 3 exchangeable protons) respectively. This information can be used to rationalise the fragmentation of carminic acid under the chosen CID conditions (Scheme 3.1) and suggests that the loss of the carboxylic acid moiety (producing the *m/z* 447 fragment) is followed by the fragmentation of the sugar residue, resulting in the *m/z* 357 and *m/z* 327 peaks.

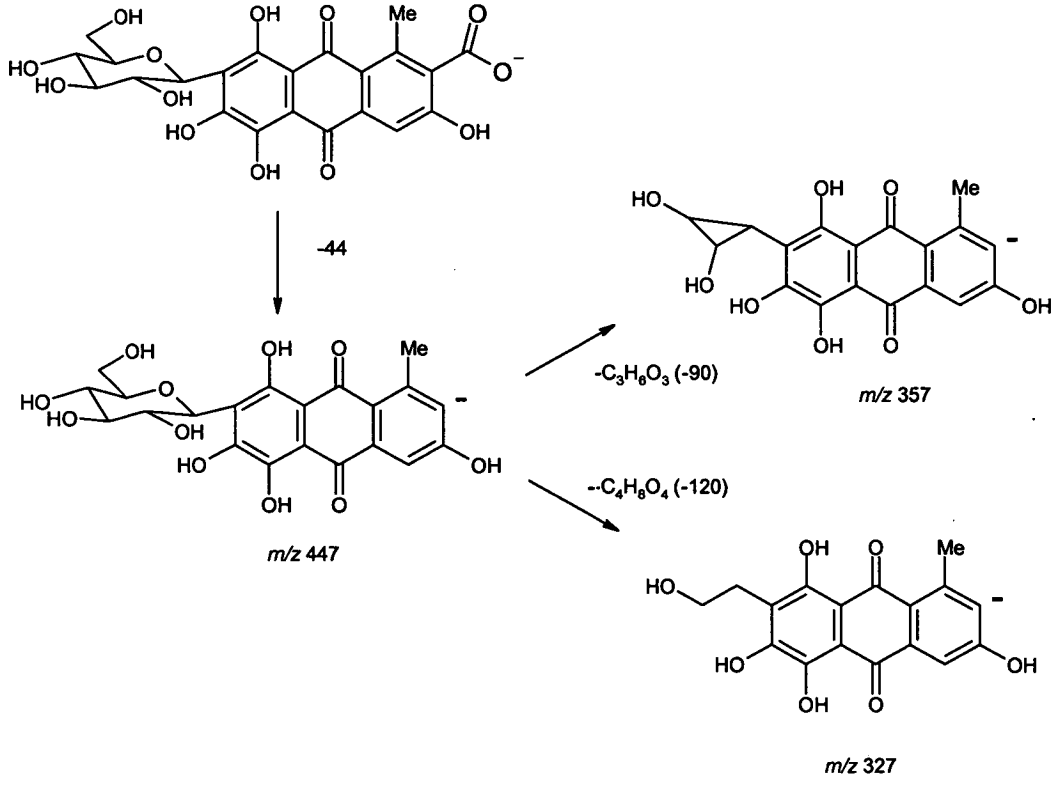

Scheme 3.1: Possible CID fragmentation of carminic acid (*m/z* 491)

Identical losses have also been reported in recent studies of flavonoid C-glycoside fragmentation under negative ion conditions.[12,13,14] The observed product ions, formed by cross-ring cleavage, are characteristic for a hexose (Figure 3.5).

Hexose cleavage during Collisionally Induced Dissociation (CID)

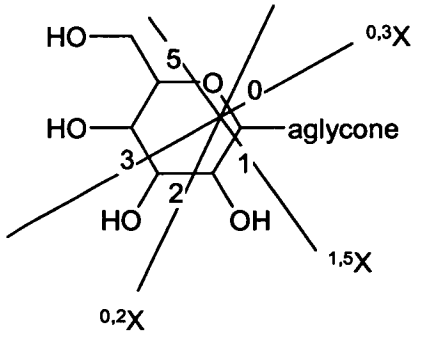

$^{0,2}X$: [M-H-120]
$^{0,3}X$: [M-H-90]
$^{1,5}X$: [M-H-134]

Figure 3.5: Characteristic product ions formed by cross-ring cleavages () in a hexose residue

A similar series of experiments was conducted on the deprotonated molecular ion of dcII (*m/z* 475) in an effort to elucidate the structure of this unknown component. The results from the MS^2 (MeOH) and MS^2 (MeOD) experiments suggest that the unknown dcII component is structurally similar to carminic acid, but with one less hydroxyl group on the core anthraquinone ring (Table 3.4).

Table 3.4: Collision Induced Dissociation (CID) of the unknown dcII component (*m/z* 475) under negative ion conditions

***m/z*: MS^2 475 (relative abundance)**	**Neutral fragment lost (possible species)**	**Information from deuteriated studies**
431 (100%)	44 (CO_2)	Base peak. Observed fragment has 7 exchangeable protons, while the neutral fragment has none.
413 (5%)	62	Observed fragment has 5 exchangeable protons, while the neutral fragment has two. Possibly *m/z* 431 [(base peak) – 18]$^-$.
385 (4%)	90	Observed fragment has 5 exchangeable protons, while the neutral fragment has 2. Possibly *m/z* 431 [(base peak) – 46]$^-$.
355 (2%)	120	--
341 (26%)	134	Observed fragment has 5 exchangeable protons, while the neutral fragment has 2.
311 (7%)	164	Observed fragment has 4 exchangeable protons, while the neutral fragment has 3.

Significantly, the major fragmentation products (relative abundance >5%) of the unknown dcII component are comparable to that of carminic acid. In both cases, the base peak is due to the loss of the carboxylic acid, followed by loss of a 90 Da or 120

Da fragment. The deuteriated experiments confirm that the deprotonated molecular ion of dcII (*m/z* 475) contains one less exchangeable proton than carminic acid (*m/z* 491), while the corresponding fragments observed in the MS^2 experiments also contain one less exchangeable proton. Further (MS^3) experiments performed on the base peak (*m/z* 431) (Table 3.5), also confirm the structural similarities between the unknown dcII component and carminic acid, indicating a hexose sugar moiety.

Table 3.5: MS^3 fragmentation of $[dcII\text{-}H\text{-}44]^-$ (*m/z* 475)

***m/z*: MS^3 475, 431 (relative abundance)**	**Neutral fragment lost (possible species)**	**Information from deuteriated studies**
413 (7%)	18 (H_2O)	Observed fragment has 6 exchangeable protons, while the neutral fragment has 1. However, the neutral species H_2O and D_2O were also lost.
371 (3%)	60	--
353 (5%)	78	--
341 (100%)	90 ($C_3H_6O_3$)	Base peak. Observed fragment has 5 exchangeable protons, while the neutral fragment has 2. However, the neutral species with 1 exchangeable proton is also observed (66%).
311 (27%)	120 ($C_4H_8O_4$)	Observed fragment has 4 exchangeable protons, while the neutral fragment has 3.
269 (23%)	162 ($C_6H_{10}O_5$)	Observed fragment has 4 exchangeable protons, while the neutral fragment has 3.
268 (3%)	163	--

The mass spectral data shows, unequivocally, that the dcII component is structurally related to carminic acid. The MS^n and deuteriated experiments indicate that dcII has only 3 phenolic groups on the anthraquinone core (compared with 4 on the carminic acid core). Additionally, the fragmentation of the sugar moiety proceeds in an identical manner in both compounds, suggesting a hexose structure. However, mass spectrometry cannot provide detailed information regarding stereochemistry, either of the glycosidic linkage or of the sugar itself.

Due to the structural similarities between dcII and carminic acid indicated by mass spectrometry, information regarding the position of substituents can be obtained by a comparison of their UV-Vis spectra. Several systematic investigations of the electronic spectra of substituted anthraquinones have been undertaken,[15,16,17,18] and it

has been shown that the longest $\pi \rightarrow \pi^*$ absorption band must be due to an intramolecular electron transfer transition from the substituent to the anthraquinone nucleus.[15]

Furthermore, the spectra of 1-substituted anthraquinones are shifted to longer wavelengths compared with their 2-substituted analogues by *ca.* 50-60 nm due to the presence of intramolecular hydrogen-bonding between the substituent and the adjacent carbonyl group of the quinone.[15] For the numbering sequence of anthraquionones, see Figure 3.6. By comparing the λ_{max} values of the intramolecular electron transfer band in carminic acid with the equivalent absorption band in dcII (Table 3.6) it is apparent that the phenolic group adjacent to the quinone must be absent from the dcII component.

Table 3.6: λ_{max} (Intramolecular electron transfer band) in substituted anthraquinones

	λ_{max} (intramolecular electron transfer band) / nm	Difference / nm
Carminic acid	496	
dcII	433	63
	Adapted from Ref 15	
1-substituted anthraquinone (OH)	406	
2-substituted anthraquinone (OH)	354	52

Although two possible structures for dcII remain (Figure 3.6), the structure can be conjectured, but not confirmed, by analogy with flavokermesic acid.

Two proposed structures for the dc II component

Most likely dcII structure (based on flavokermesic acid)

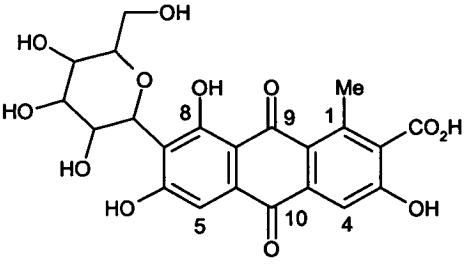

Alternative dcII structure

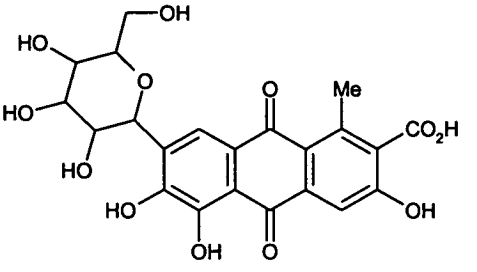

Figure 3.6: Proposed structures for the unknown dcII component in cochineal (*Dactylopius coccus* Costa)

It is therefore proposed that the core anthraquinine structure of dcII is based on flavokermesic acid, a known constituent of cochineal, rather than the unknown isomeric compound. This hypothesis is also corroborated by examining the biosynthetic route to carminic acid. All pigments of the scale insects are polyketide anthraquinones and are present *in vivo* as the potassium salts.[19]

There are two types of polyketide synthase (PKS) enzymes.[20] In type II polyketide synthases, the whole polyketide chain is first formed and then cyclised, oxidised or reduced as necessary. In contrast, each acetate unit in a type I polyketide is altered (reduced, dehydrated *etc.*) as it is added. Thus, the starting polyketide in the biosynthetic route to carminic acid (Scheme 3.2) is a formal intermediate, not necessarily having a 'real' existence. However, given the structure of a substance, in this case, carminic acid, the starting polyketide can usually be derived. In addition, side chains are always derived from the 'tail' of the polyketide, never the carboxylic acid 'head' and the carbonyl oxygen nearest the carbonyl group in the polyketide is usually retained (to activate the α-CH_2 for cylisation).

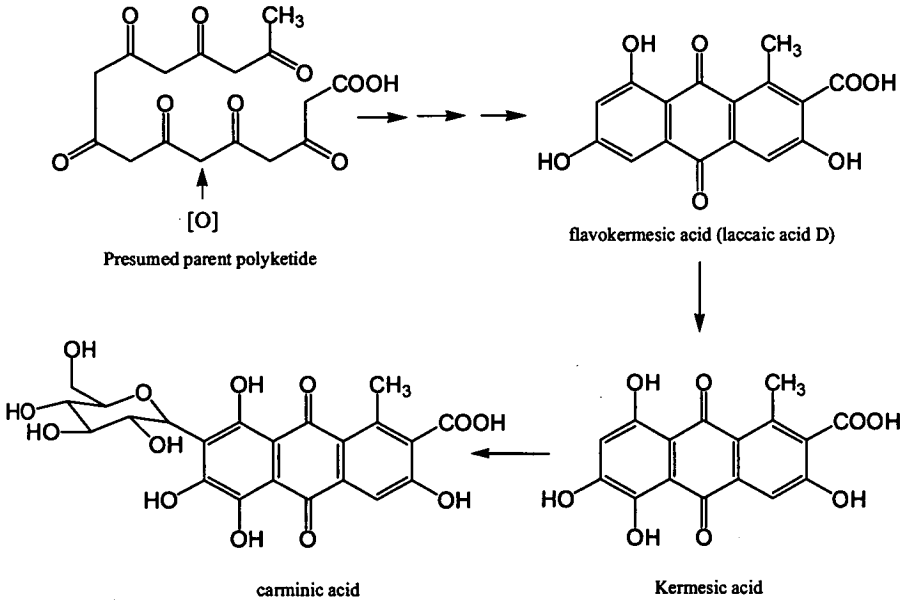

Scheme 3.2: The biosynthetic route to the polyketide anthraquinone pigments of the scale insects (adapted from reference 19)

Thus, the biosynthetic route to carminic acid proceeds *via* the polyketide to flavokermesic acid (laccaic acid D) and then kermesic acid, before a C-glucoside is added to form the final product. It is highly feasible that the C-glucoside may also be added to the flavokermesic acid precursor, producing the proposed dcII structure. In contrast, the alternative dcII structure would require a different biosynthetic route.

This structure is also substantiated by the chromatographic behaviour of the compounds, correlating the pairing of carminic acid and its aglycone (kermesic acid) with dcII and its proposed aglycone (flavokermesic acid) (Figure 3.7).

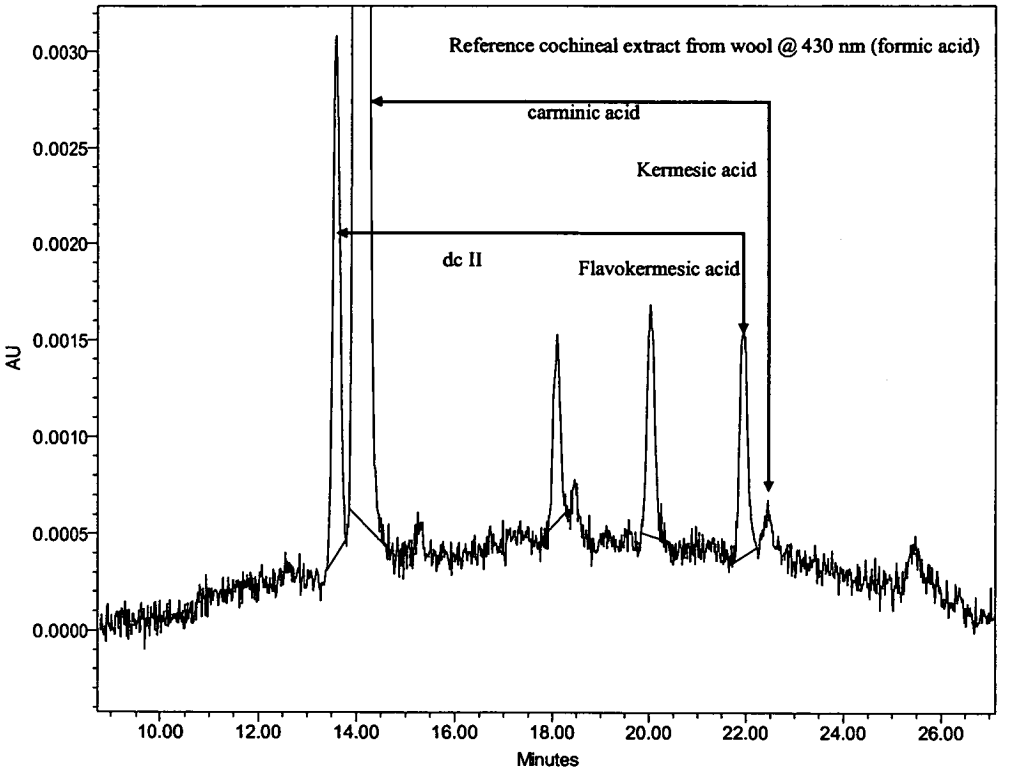

Figure 3.7: PDA HPLC chromatogram (monitored at 430 nm) of cochineal dyed wool extracts with the pairing of carminic acid and its aglycone (kermesic acid) and dcII and its proposed aglycone (flavokermesic acid) indicted

To identify the structure and stereochemistry of the dcII component unambiguously, 2D NMR techniques could be employed. However, the preparative scale isolation of this minor product from the major carminic acid component using the current chromatographic method was not possible.

3.1.2.3 Structural analysis of the unidentified components of *Dactylopius coccus Costa* by LC ESI MS^n

To investigate the remaining unknown constituents of *Dactylopius coccus* Costa. (dcIV and dcVII), a solution of the 'raw' cochineal used for the dyeing of the model tapestries was hydrolysed, as this was shown to increase marginally the recoveries of flavokermesic acid and the two unknown components.[6] In an attempt to separate the minor components from carminic acid, the solution was then chromatographed on a semi-preparative scale (Chapter 6). Three separate fractions, corresponding approximately with dcIV, dcVII and flavokermesic acid, were collected. The

respective fractions from nine injections were then combined and evaporated to dryness. Re-injection of the reconstituted fractions onto the analytical column confirmed the enrichment of the minor components and the removal of carminic acid (and dcII) (Figure 3.8).

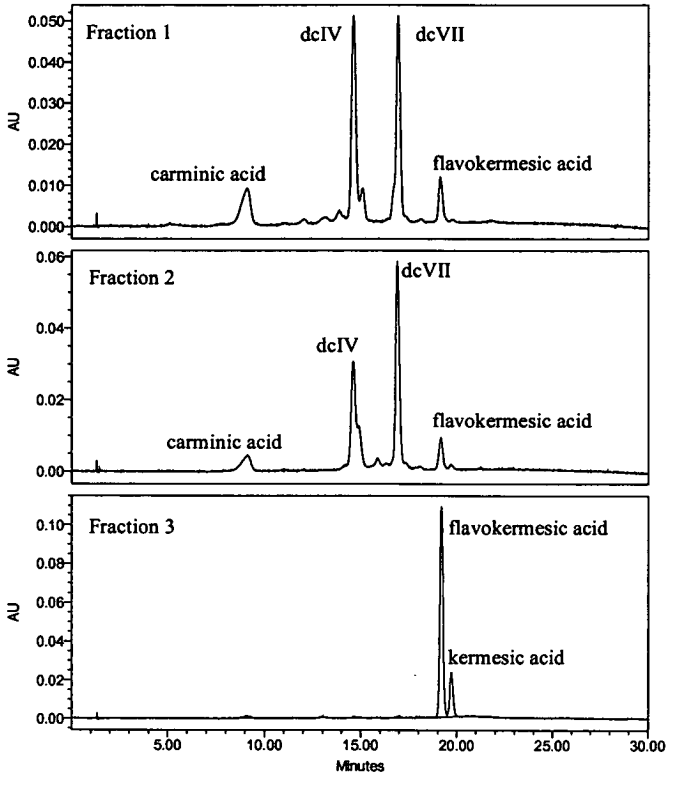

Figure 3.8: The PDA HPLC spectra (monitored at 430 nm) of the three fractions. The dry residue of each was diluted with methanol and chromatographed using the formic acid method

The fractions were also analysed using the HPLC ESI MS system. The unknown dcIV and dcVII peaks (present in both fraction 1 and fraction 2) were found to be isomeric with carminic acid, with all three components producing a deprotonated molecular ion of *m/z* 491 (Figure 3.9).

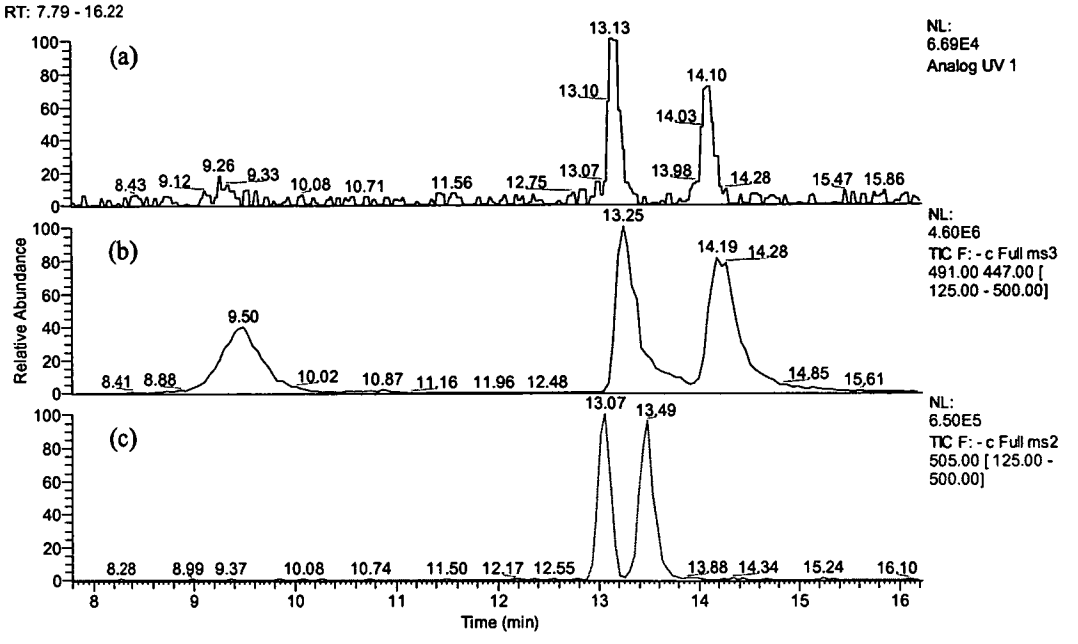

Figure 3.9: Negative ion HPLC ESI MS analysis of fraction 1. (a) The UV signal (monitored at 430 nm), (b) MS^3 chromatogram for *m/z* 491, 447 and (c) MS^2 chromatogram for *m/z* 505

Furthermore, no significant differences were observed in the MS^n fragmentation patterns of the two unknown components (dcIV and dcVII) when compared with the fragmentation of carminic acid (Figure 3.10). The UV-Vis and mass spectral data therefore indicate that dcIV and dcVII must differ from carminic acid only in the nature of the sugar moiety. This difference may be stereochemical, since mass spectrometry does not usually provide information regarding the α/β geometry of the glycosidic linkage, nor can it usually distinguish diastereomeric sugar units.

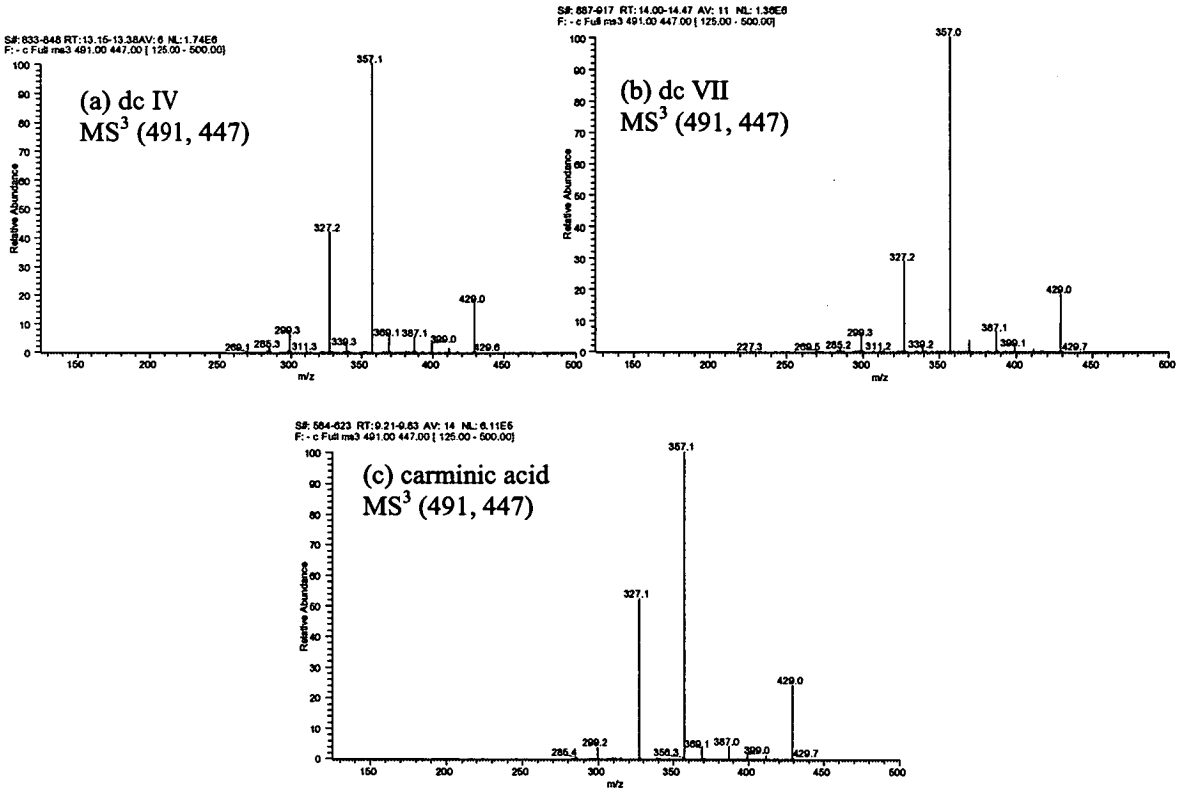

Figure 3.10: The MS^3 fragmentation patterns (*m/z* 491, 447) of the two unknown components dc IV and dcVII and carminic acid from HPLC ESI MS^n analysis of fraction 1

As the analysed fractions were obtained by hydrolysing the 'raw' cochineal extract, some components may be present in the fractions that are not necessarily observed in the acid hydrolysed extracts from a dyed yarn. The HPLC ESI MS analysis of fraction 1 revealed two minor components, both with a deprotonated molecular ion at *m/z* 505, [carminic acid–H+14]$^-$, eluting just before and just after the dcIV peak (Figure 3.9). Although there is no evidence for the presence of the first of these peaks in the acid hydrolysed yarn extracts, a trace amount of an unidentified component eluting after dcIV was observed in the cochineal dyed yarn extract (Figure 3.2). It was conjectured that these might be methyl ether derivatives of carminic acid, similar to chrysoeriol, the luteolin methyl ether derivative characterised in weld.

Furthermore, the first of these, eluting just before dcIV at a retention time of 13.1 min (Figure 3.9c) breaks down under CID conditions to produce a base peak at *m/z*

461 (-44). The two characteristic breakdown peaks of carminic acid, *m/z* 327 and *m/z* 357, are also present at low intensity. In contrast, however, the second peak, eluting just after dcIV at a retention time of 13.5 min (Figure 3.9c) breaks down under CID conditions to produce a base peak at *m/z* 473 (–32).

The initial loss of 32 (MeOH) rather than the more usual 44 (CO_2) in the negative ion CID fragmentation of this component suggests that the carboxylic acid functionality may have been replaced with an ester functionality (Figure 3.11).

Proposed structure for the unknown component eluting after dcIV

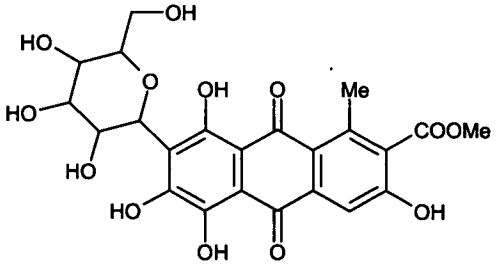

Figure 3.11: The proposed structure for the unknown component, eluting after dcIV and with a *m/z* value of 505

The HPLC ESI MS analysis of fraction 3 confirmed the presence of both flavokermesic acid and kermesic acid (Figure 3.12). However, further (MS^3) analysis provided little additional structural information.

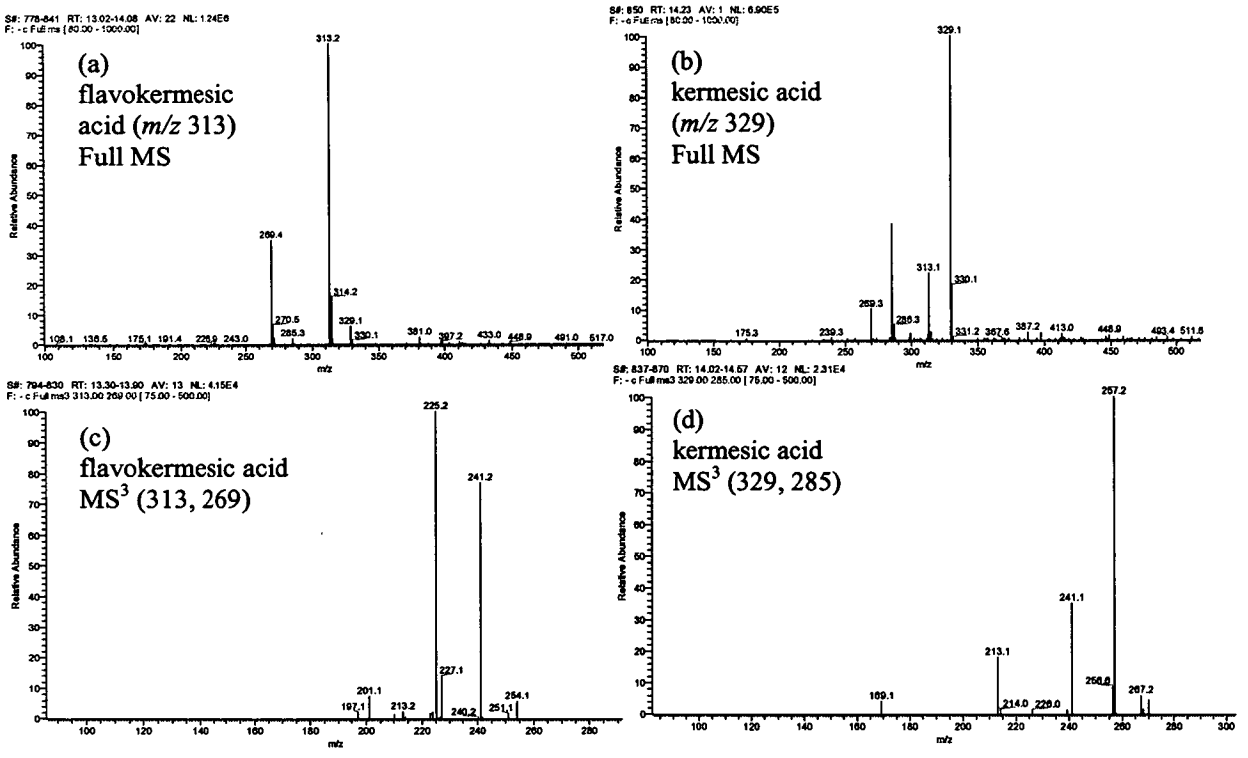

Figure 3.12: The Full MS and MS^3 of flavokermesic acid (*m/z* 313) and kermesic acid (*m/z* 329)

In an attempt to gain stereochemical information regarding the dcIV and dcVII components, 1D and 2D NMR techniques were employed (Chapter 6). The 1D proton spectrum of fraction 2 revealed a highly complex spectrum (Figure 3.13). However, the anomeric proton signal from carminic acid could be identified by comparing the NMR spectrum with that obtained from a pure carminc acid reference material. In addition, two further proton signals, possibly arising from the anomeric protons from two additional sugar systems were also identified.

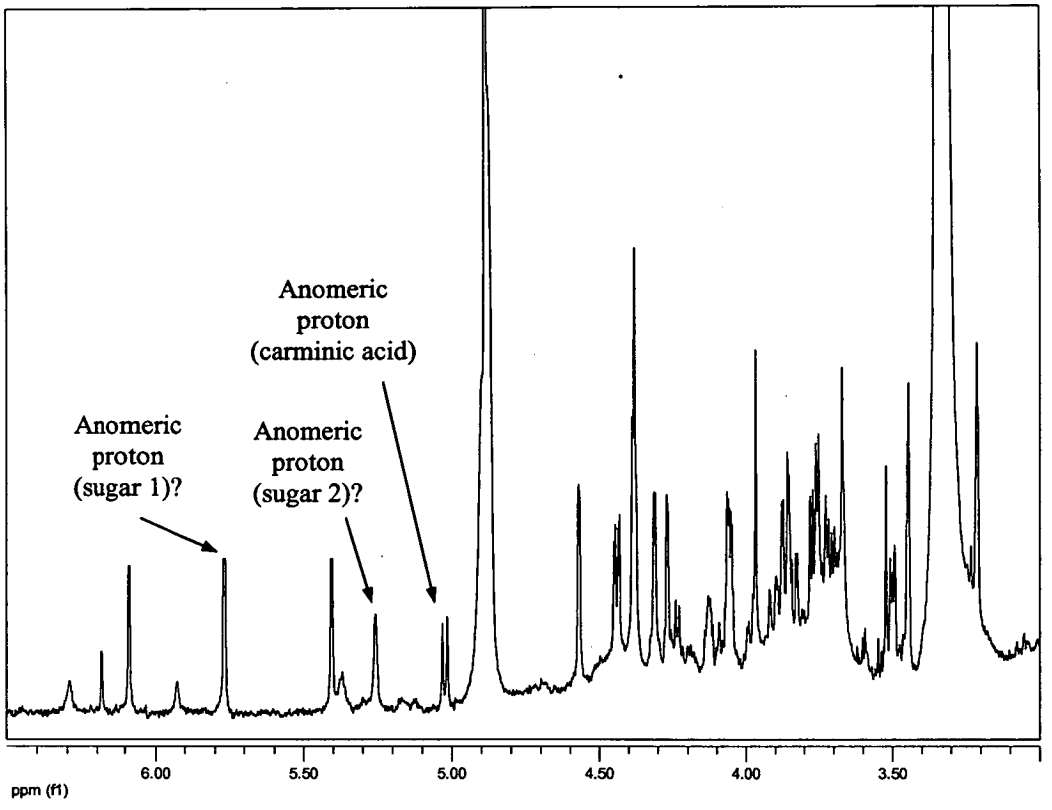

Figure 3.13: 1D proton NMR of fraction 2. The anomeric proton signal from carminic acid is visible, together with the anomeric proton signals from two other possible sugar systems

A 2D Total Correlation Spectroscopy (TOCSY) experiment was conducted on fraction 2 (Figure 3.14). This experiment correlates protons within a spin system, thus, seven protons should be observed in the spin system from a hexose sugar attached to an anthraquinone core. As expected, three sugar spin systems appeared to be visible, one of which could be identified as that of carminic acid, by comparison with the TOCSY spectrum obtained from a pure carminc acid reference material. As the presence of a hexose ring in both the dcIV and dcVII components was suggested by HPLC ESI MS analysis, these are most likely to be the source of the two additional sugar spin systems observed.

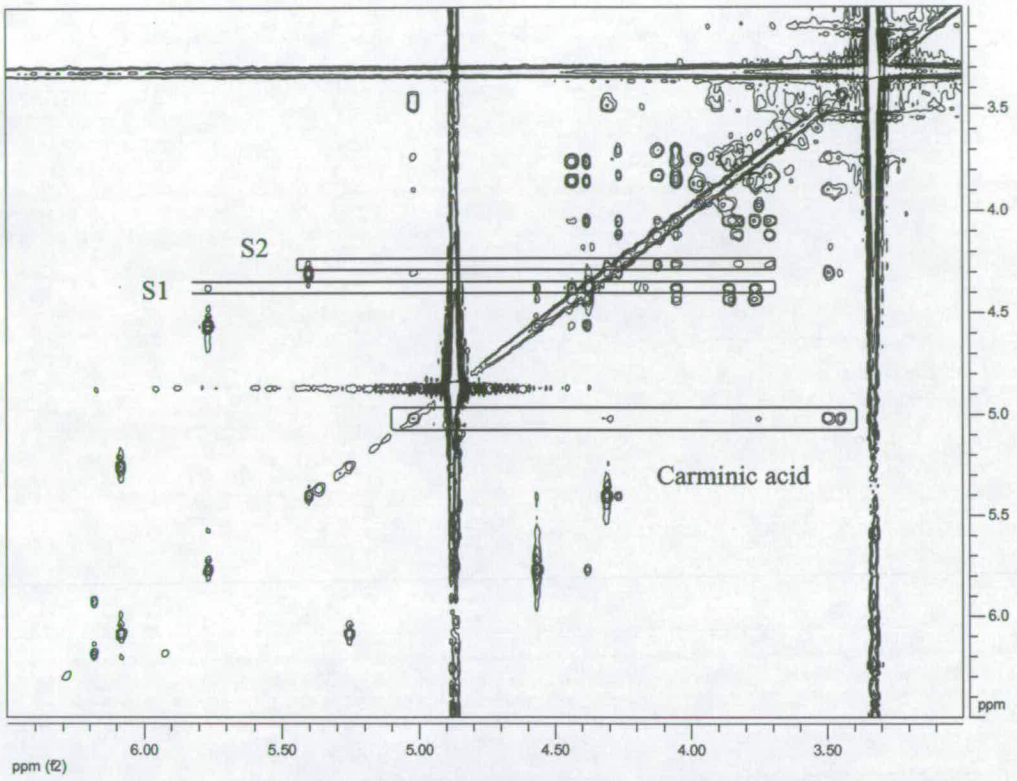

Figure 3.14: A 2D TOCSY experiment to correlate the proton signals within the different spin systems generated by the different sugar residues

Having identified the proton signals from the three separate hexose spin systems, the relative stereochemistry, and thus the identity of the sugars, can often be deduced from the size of their coupling constants. This is because the magnitude of the coupling constant varies depending on the size of the dihedral angle between the adjacent protons.[21] The relative size of the coupling constants for six common sugars is indicated below (Figure 3.15).

The coupling constant pattern for some common sugars

The β-sugars

Glucose	Galactose	Manose
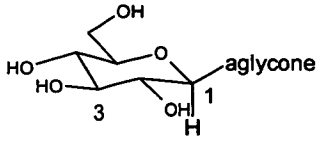	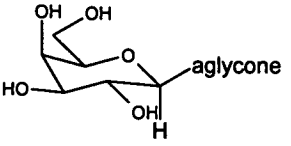	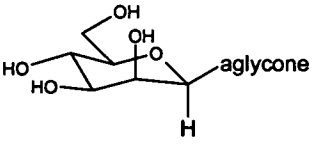
Relative size of coupling constants		
1 ←→ 2 large (anomeric)	1 ←→ 2 large (anomeric)	1 ←→ 2 small (anomeric)
2 ←→ 3 large	2 ←→ 3 large	2 ←→ 3 small
3 ←→ 4 large	3 ←→ 4 small	3 ←→ 4 large
4 ←→ 5 large	4 ←→ 5 small	4 ←→ 5 large

The α-sugars

Glucose	Galactose	Manose
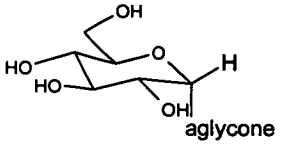	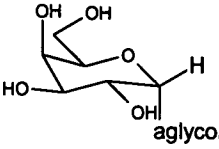	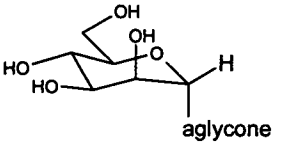
Relative size of coupling constants		
1 ←→ 2 small (anomeric)	1 ←→ 2 small (anomeric)	1 ←→ 2 small (anomeric)
2 ←→ 3 large	2 ←→ 3 large	2 ←→ 3 small
3 ←→ 4 large	3 ←→ 4 small	3 ←→ 4 large
4 ←→ 5 large	4 ←→ 5 small	4 ←→ 5 large

Figure 3.15: The relative size of the proton coupling constants in the hexose ring of six common sugars

The coupling constant of the anomeric proton from carminic acid, containing a β-glucose, was relatively large (Chapter 6). In contrast, the coupling constants of the anomeric protons in both of the unknown sugars were small and thus do not originate from a β-glucose or β-galactose moiety.

Further analysis was hindered due to the complexity of the proton spectrum, so a series of 1D TOCSY experiments was conducted in an effort to simplify the spectrum and obtain the coupling constants from the protons in each spin system. However, due to the small amount of material present, no further structural information regarding the sugar moieties could be obtained.

3.1.3 Conclusion

The series of analytical studies reported herein have provided a more complete structural characterisation of the minor components found in the acid hydrolysed extracts of cochineal dyed yarn. In addition to the main carminic acid component, the presence of flavokermesic acid and kermesic acid was confirmed. Furthermore, the dcII component was found to be structurally related to carminic acid, with a UV-Vis spectrum related to flavokermesic acid, thus enabling a possible structure to be proposed. The dcIV and dcVII components were found to be isomers of carminic acid, most probably differing only in the stereochemistry of the sugar moiety.

3.2 Studies on the main components found in the soluble redwood and logwood dyes

3.2.1 Introduction

The soluble redwood dye sources, often collectively known as 'brazilwoods' and logwood dyes, have been studied much less than the ubiquitous anthraquinone plant and insect dyes. However, results from the historical sample analysis (Chapter 5) have shown the presence of brazilwood in a small, but significant number of historical yarns, while the identification of logwood has helped to confirm early restoration yarns from the tapestries under investigation.

Brazilin and hematoxylin (Figure 3.16) are well-known constituents of redwood and logwood species, for example, *Caesalpinia sappan* L. and *Haematoxylon campechianum* L. respectively.[39] Originally termed neoflavonoids, recent developments indicate that a more appropriate designation is in fact homoisoflavonoids.[22,23,39] The structures of these compounds are very similar, with hematoxylin possessing an extra OH group in the A ring. In their oxidised forms, brazilein and hematein have been used for centuries as dye sources, and more recently, hematein has been utilised as a nuclear stain for animal tissues.[24] The characterisation of brazilin by NMR spectroscopy has been previously reported,[25] but

there is little mass spectral information in the literature, except for an isolated report of fragmentation under electron impact conditions.[24]

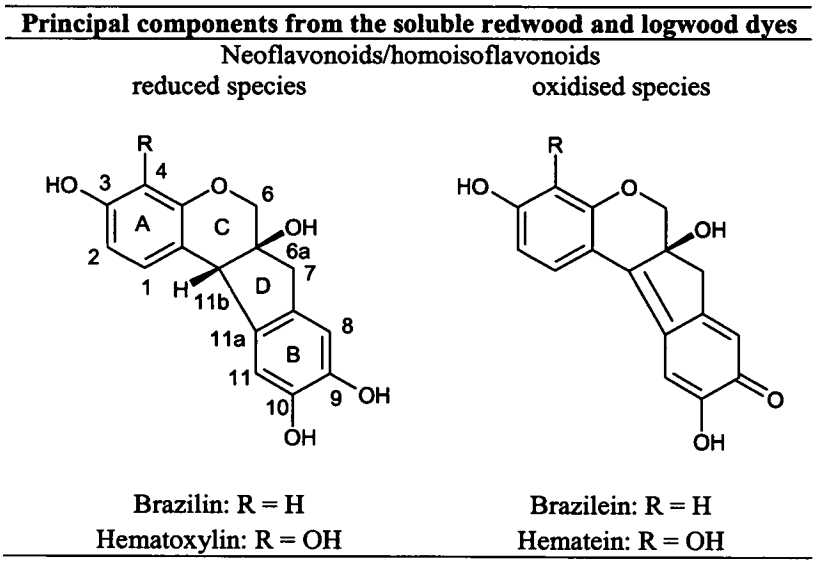

Figure 3.16: Neoflavonoid/homoisoflavonoid derivatives such brazilin and hematoxylin (reduced) and brazilein and hematein (oxidised)

The absolute stereochemistry of brazilin was established by several groups, leading to a (6a*S*,11b*R*) assignment, while the relative stereochemistry at C-6a and C-11b of brazilin and hematoxylin was also established as *cis* by synthetic, spectral and chemical evidence.[26,27] The metal complexes most usually utilized for dyeing applications have also been investigated.[28,29,30,31] These studies indicate that hematoxylin and brazilin compounds have a non-planar configuration, however, the structure of the hematein-aluminium complex has not been unambiguously elucidated. The kinetics of hematein fading have been investigated in acid solutions,[32] but there has been little research on the fading of the neoflavonoids/ homoisoflavonoids when used as mordant dyes.

Braziliein and hematein are weak acids and are adsorbed by wool appreciably only from acid solutions. The solution chemistry of these compounds is not, however, straightforward. [24,29,33] Hematein is unstable in both strongly acidic media and in strongly basic media, where it rapidly undergoes irreversible changes.[34] The UV-Vis

spectrum of hematein in methanol shows a weak absorption at *ca.* 560 nm, due to its anion (with which it is in equilibrium at a very low concentration). This equilibrium is strongly pH dependent and is most obvious in aqueous solution.

The analysis of historical yarn samples dyed with redwood or logwood dyes containing neoflavonoid/homoisoflavonoid components is thus somewhat problematic. These difficulties are compounded by the fact that the standard sample preparation for the extraction of dye components on historical textiles is a hydrolysis procedure involving hydrochloric acid.[5] Any acid-sensitive dye molecules, such as those described above, may decompose under these conditions. The UV-Vis spectra of some of these 'marker components' have already been reported,[39] but no attempt has been made to structurally characterise them.

3.2.2 Results and Discussion

3.2.2.1 Characterisation of the neoflavonoids/homoisoflavonoids by ESI MS^n

The escalating use of techniques such HPLC ESI MS for the identification of dyes on historical textiles has increased the need for an understanding of the behaviour of the neoflavonoid/homoisoflavonoid components under electrospray ionisation conditions. Furthermore, partial structural information on the ring systems (in either the reduced or the oxidised forms) may be revealed *via* ion trap mass spectrometry studies. This would improve the ability to both identify and characterise neoflavonoid/homoisoflavonoid analogues,[35,36,37,38] and could facilitate species identification, where difficulties have been encountered,[39] or allow the identification of possible photo-degradation mechanisms.

Freshly prepared methanolic solutions of the reduced neoflavonoid/ homoisoflavonoid components (hematoxylin and brazilin) gave good mass spectra under negative ion electrospray conditions, with the deprotonated molecule $[M-H]^-$ obtained in all cases. Surprisingly, however, the base peak in the brazilin reference solution was a component at *m/z* 303. The CID fragmentation of this component was

therefore investigated in methanol and deuteriated methanol in an effort to establish information regarding its structure (Table 3.7).

Table 3.7: Collision Induced Dissociation (CID) of the unknown component (*m/z* 303) in the methanolic brazilin under negative ion conditions

***m/z*: MS^2 303 (relative abundance)**	**Neutral fragment lost (possible species)**	**Information from deuteriated studies**
285 (8%)	18 (H_2O)	Observed fragment has 4 exchangeable protons, while the neutral fragment has 1.
273 (14%)	30 (CH_2O; C_2H_6)	Observed fragment has 4 exchangeable protons, while the neutral fragment has 1.
255 (10%)	48 (C_2H_8O)	--
243 (66%)	60 (C_3H_8O)	Observed fragment has 4 exchangeable protons, while the neutral fragment has 1.
231 (100%)	72 ($C_3H_4O_2$)	Base peak. Observed fragment has 3 exchangeable protons, while the neutral fragment has 2.

The deuteriated studies suggested that the unknown component had five sites where proton/deuterium exchange was readily possible. This implies that the unknown component contains five hydroxyl groups, one more than brazilin. Although not conclusive, the base peak in the brazilin reference solution may therefore be due to sappanol, a known biological precursor of brazilin (Figure 3.17).[39]

Sappanol

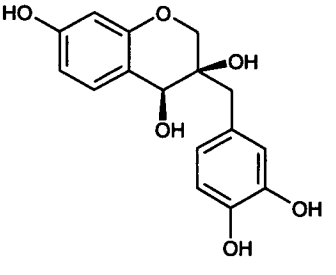

Figure 3.17: Sappanol, a biological precursor of brazilin with *m/z* 303

The expected $[M-H]^-$ base peak at *m/z* 301 was observed in the hematoxylin reference solutions, although peaks corresponding to dimers and trimers of hematoxylin, $[2M-H]^-$ and $[3M-H]^-$ were also observed.

In addition, all the solutions contained deprotonated ions of the corresponding oxidised species. These were present in the starting material as impurities and not formed *in situ* within the mass spectrometer. This was confirmed by the selection, then fragmentation, of the deprotonated molecular ions of the reduced forms, which did not lead to formation of the corresponding oxidised species. To provide further evidence of the nature of the CID breakdown pathways, spectra were also recorded using deuteriated methanol (MeOD) as solvent.

The CID mass spectra of the reduced components, brazilin and hematoxylin, showed only two breakdown peaks (>10% relative abundance). The maximum number of exchangeable protons on the observed fragments was also ascertained from the MeOD experiments (Table 3.8). As expected, there were three sites on the Brazilin molecule where hydrogen could be easily exchanged with deuterium, while the extra hydroxyl provided a total of four sites in hematoxylin.

The first of the breakdown peaks was a minor peak due to loss of H_2O. When dissolved in MeOD, loss of H_2O was observed, together with HOD, indicating that at least one of the hydrogen atoms lost did not originate at the phenol group. It is therefore not possible to identify the position of this cleavage with any certainty, a situation also commonly encountered in H_2O loss from the phenol groups of flavonoids.[40]

Table 3.8: Negative ion ESI mass spectra of brazilin and hematoxylin (reduced forms) under CID conditions. $[M-H]^-$, where M is the molecular ion of the non-deuteriated species, $[M_D-D]^-$, and where M_D is the molecular ion of the fully deuteriated species

Brazilin (MeOH)	**Brazilin (MeOD)**	**Hematoxylin (MeOH)**	**Hematoxylin (MeOD)**	**Fragment lost**
		***m/z* (relative %)**		
285 (64%)	288 (8%)	301 (100%)	305 (14%)	
$[M-H]^-$	$[M_D-D]^-$	$[M-H]^-$	$[M_D-D]^-$	
267 (8%)	270 (10%)	283 (19%)	287 (8%)	H_2O
$[M-H-18]^-$	$[M_D-D-18]^-$	$[M-H-18]^-$	$[M_D-D-18]^-$	
	269 (11%)		286 (16%)	HOD
	$[M_D-D-19]^-$		$[M_D-D-19]^-$	
163 (100%)	164 (100%)	179 (100%)	181 (100%)	See Scheme 3.3
$[M-H-122]^-$	$[M_D-D-124]^-$	$[M-H-122]^-$	$[M_D-D-124]^-$	
	165 (40%)		182 (21%)	
	$[M_D-D-123]^-$		$[M_D-D-123]^-$	
	163 (16%)		180 (49%)	
	$[M_D-D-125]^-$		$[M_D-D-125]^-$	

The major peak in the spectra of both brazilin and hematoxylin is due to loss of a neutral fragment of 122 Da from the deprotonated molecular ion. This neutral fragment must originate from the C/D/B ring sections, which are the same in both precursors. These results are best explained if the A-ring is the initial ionisation site, giving the deprotonated molecular ions depicted in Scheme 3.3.

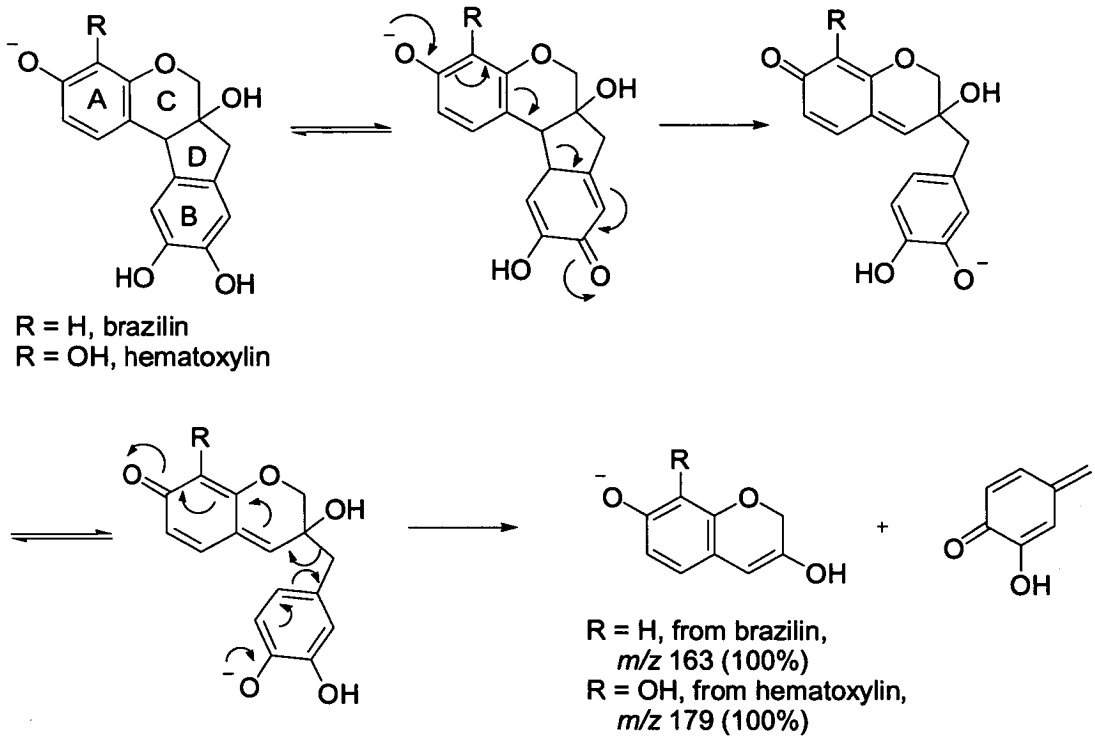

Scheme 3.3: Possible CID fragmentation of the reduced neoflavonoid/ homoisoflavonoid species brazilin and hematoxylin

This mechanism is supported by CID of the fully deuteriated species, which shows that the major observed ion in both deuteriated samples corresponds to the A/C ring fragment with the available hydroxyl group(s) retaining their deuterium atoms. Thus, the CID mass spectra of the reduced neoflavonoids/homoisoflavonoids provide direct information on the substituents of rings A and C, while the mass of the neutral fragment lost gives supporting information on the substituents of ring B and those of the methylene group of ring D.

The CID mass spectra of the oxidised forms, brazilein and hematein, show many breakdown peaks (relative abundance >10%) which can act as useful fingerprints for these compounds (Figure 3.18 and Table 3.9).

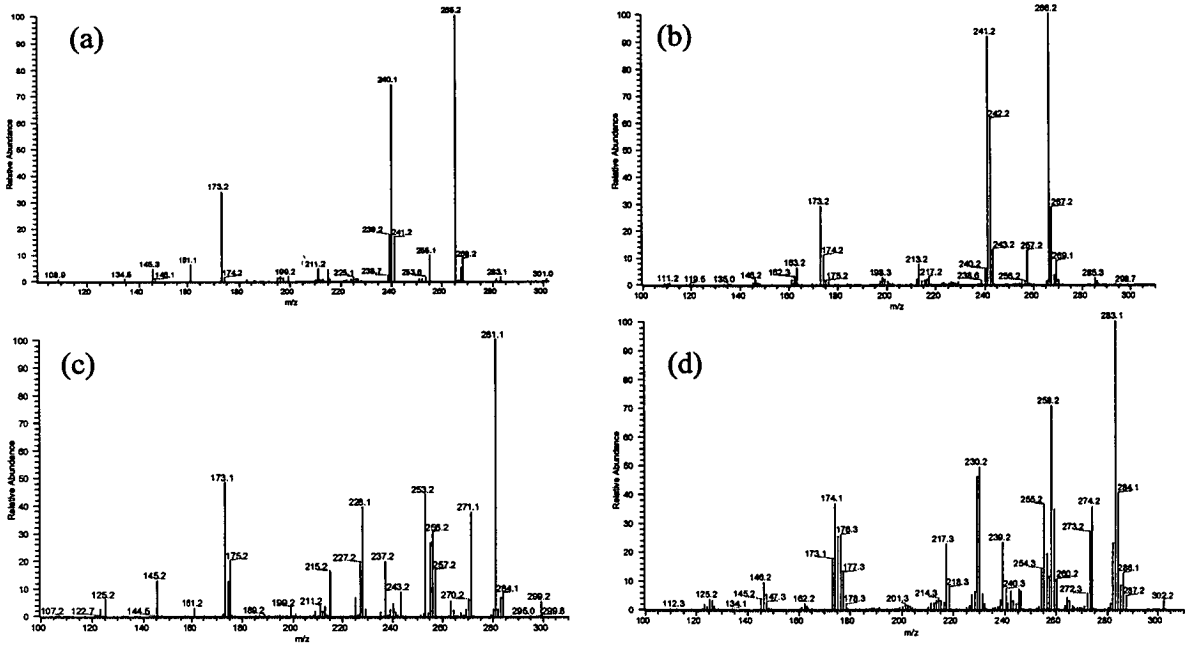

Figure 3.18: (a) CID mass spectrum (MS^2) of brazilein (*m/z* 283) in MeOH; (b) CID mass spectrum (MS^2) of deuteriated brazilein (*m/z* 285) in MeOD; (c) CID mass spectrum (MS^2) of hematein (*m/z* 299) in MeOH; (d) CID mass spectrum (MS^2) of deuteriated hematein (*m/z* 302) in MeOD

In both cases, the highest mass fragment, though of low relative abundance, was due to loss of CH_3 (15 Da). When the spectrum was recorded in MeOD, these fragments clearly corresponded to loss of CH_2D. It is therefore likely that the carbon atom derives from that at C(6) or C(7), together with the deuterium from the 6a-OH group. The most intense breakdown peaks were found to be due to loss of H_2O. In the deuteriated case, the major peak was due to loss of HOD, but some loss of H_2O was also observed. Some loss of CO (28 Da) was also observed in both cases. These are all common breakdown peaks in negative ion ESI mass spectra of flavonoids.[41,42]

Table 3.9: Negative ion ESI mass spectra of brazilein and hematein (oxidised forms) under CID conditions. $[M-H]^-$, where M is the molecular ion of the non-deuteriated species, $[M_D-D]^-$, and where M_D is the molecular ion of the fully deuteriated species. A blank in the table implies that the ion in question is present in <5% relative abundance

Brazilein (MeOH)	**Brazilein (MeOD)**	**Hematein (MeOH)**	**Hematein (MeOD)**	**Fragment lost**
		***m/z* (relative %)**		
283 (77%) $[M-H]^-$	285 (100%) $[M_D-D]^-$	299 (100%) $[M-H]^-$	302 (100%) $[M_D-D]^-$	
268 (8%) $[M-H-15]^-$	269 (8%) $[M_D-D-16]$	284 (8%) $[M-H-15]^-$	286 (12%) $[M_D-D-16]^-$	CH_3/CH_2D
265 (100%) $[M-H-18]^-$	267 (29%) $[M_D-D-18]^-$	281 (100%) $[M-H-18]^-$	284 (38%) $[M_D-D-18]^-$	H_2O
	266 (100%) $[M_D-D-19]^-$		283 (100%) $[M_D-D-19]^-$	HOD
			282 (23%) $[M_D-D-20]^-$	D_2O
255 (9%) $[M-H-28]^-$	257 (13%) $[M_D-D-28]^-$	271 (38%) $[M-H-28]^-$	274 (36%) $[M_D-D-28]^-$	CO
241 (17%) $[M-H-42]^-$	243 (13%) $[M_D-D-42]^-$	257 (16%) $[M-H-42]^-$	260 (10%) $[M_D-D-42]^-$	CH_2CO
240 (74%) $[M-H-43]^-$	242 (62%) $[M_D-D-43]^-$	256 (30%) $[M-H-43]^-$	259 (35%) $[M_D-D-43]^-$	CH_3CO
	241 (92%) $[M_D-D-44]^-$		258 (71%) $[M_D-D-44]^-$	CH_2DCO
239 (18%) $[M-H-44]^-$		255 (26%) $[M-H-44]^-$		CO_2
	174 (11%) $[M_D-D-111]^-$			Scheme 3.4
173 (34%) $[M-H-110]^-$	173 (29%) $[M_D-D-112]^-$	173 (48%) $[M-H-126]^-$	173 (17%) $[M_D-D-129]^-$	

More unusually, a significant peak, due to the loss of a 43 Da fragment (probably CH_3CO) was observed in the spectra of both brazilein and hematein. The deuteriated species show peaks due to loss of both 43 Da (*i.e.* the fragment contains no deuterium) and 44 Da (*i.e.* CO_2 or CH_2DCO).

In the range *m/z* 180-240, the CID spectrum of hematein is much more complex than that of brazilein, presumably due to the juxtaposition of hydroxyl groups in ring A. Thus, peaks at *m/z* 253 $[M-H-H_2O-CO]^-$, 237 $[M-H-H_2O-CO_2]^-$, 228 $[M-H-C_3H_3O_2]^-$, 227 $[M-H-C_3H_4O_2]^-$ are only found in the spectrum of hematein.

The major low-mass fragment ion is found at *m/z* 173 in both oxidised species. To ensure that this peak was a fragment from the deprotonated molecular ion and not caused by further breakdown of the MS^2 CID base peaks within the mass spectrometer, the MS^2 *m/z* 281 peak from the hematein sample and the *m/z* 265 peak from the brazilein sample were isolated then fragmented in an MS^3 experiment. No peak at *m/z* 173 was observed in either case. Since the same fragment is produced from both species, it is clear that in contrast to the spectra of the reduced forms, the observed fragment cannot be derived from ring A. It is likely that that the 10-hydroxyl group of the B-ring is the initial ionisation site,[33] providing the deprotonated molecular ions of the oxidised neoflavonoid/homoisoflavonoid species. A suggested mechanism is shown in Scheme 3.4.

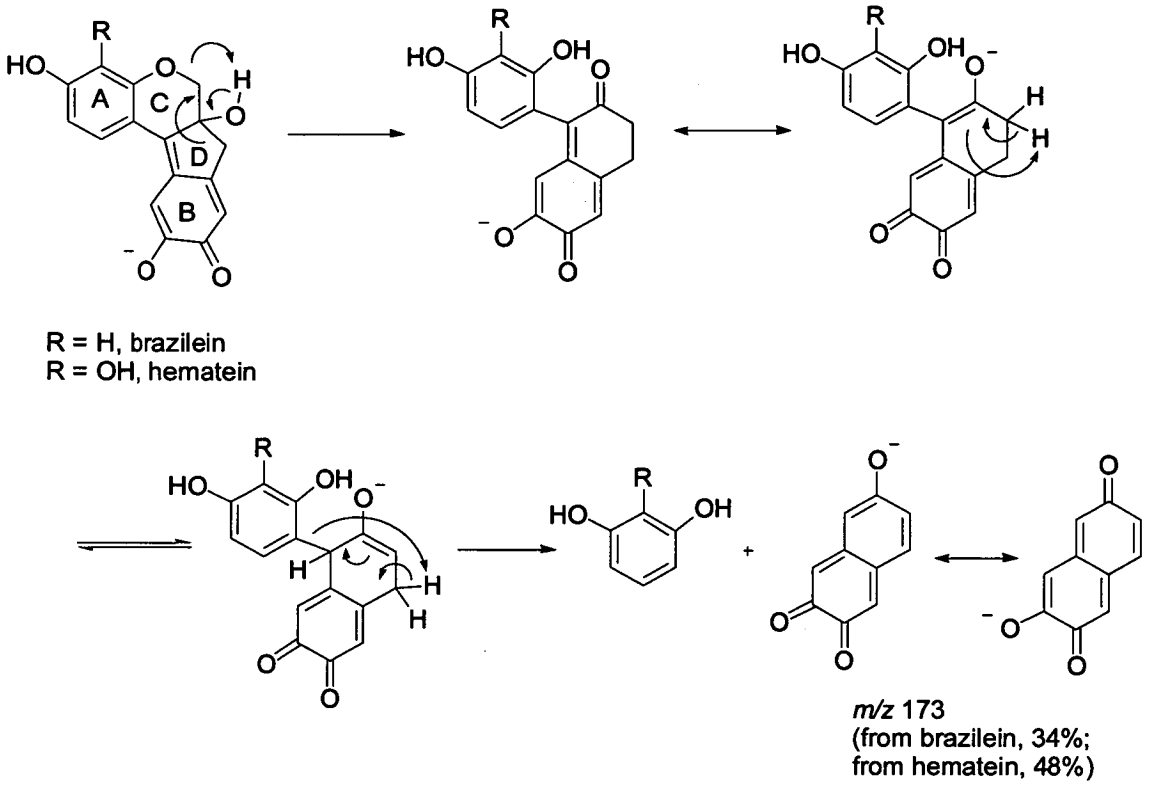

Scheme 3.4: Possible CID fragmentation of the oxidised neoflavonoid/homoisoflavonoid species brazilein and hematein

Again, the mechanism is supported by the results from the MeOD deuterium labelling experiments, which, in the case of brazilein show relatively little evidence of deuterium incorporation in the fragment ion. The scrambling which occurs, and which is more prevalent in the spectrum of hematein, may be explained by equilibration of hydroxyl groups and the anion centre in the intermediates. Thus, the CID mass spectra of the oxidised brazilein and hematein components provide information on the substituents of rings B, D and the methylene group of ring C, while the mass of the neutral fragment lost gives information on the substituent pattern of ring A.

The ion trap mass spectrometric behaviour of two important neoflavonoid/ homoisoflavonoid components have thus been rationalised. Partial structural information of the ring systems has also been successfully elucidated, with the

reduced and oxidised forms providing complementary data regarding the position of substituents.[43] Furthermore, this information may allow the discrimination of closely related natural sources, where minor components found in dyed yarn extracts are frequently isomers or structural analogues of the principal dyeing component. However, the behaviour of the components under the acid hydrolysis conditions must first be investigated before an effective method for biological dye source identification can be established.

3.2.2.2 Hematein marker compound

Although PDA HPLC is a convenient method to identify many historical dyes, in practice, the PDA HPLC traces obtained from the extracts of textile samples dyed with redwood or logwood appear to show 'marker compounds' for the respective components. These markers are chromatographically and spectroscopically different from the main dyeing constituents. To relate the compounds obtained when using the standard hydrochloric acid extraction method to the presence of the main neoflavonoid/homoisoflavonoid dyeing components from the redwood and logwood dyes, they must be structurally characterised.

The marker component found in the acid hydrolysed extracts of logwood dyed samples is related to the main hematein component. This can be confirmed by comparing the PDA HPLC results of a hematein reference solution with the results from the injection of a solution of the same hematein reference after undergoing the hydrochloric acid extraction protocol (Figure 3.19).

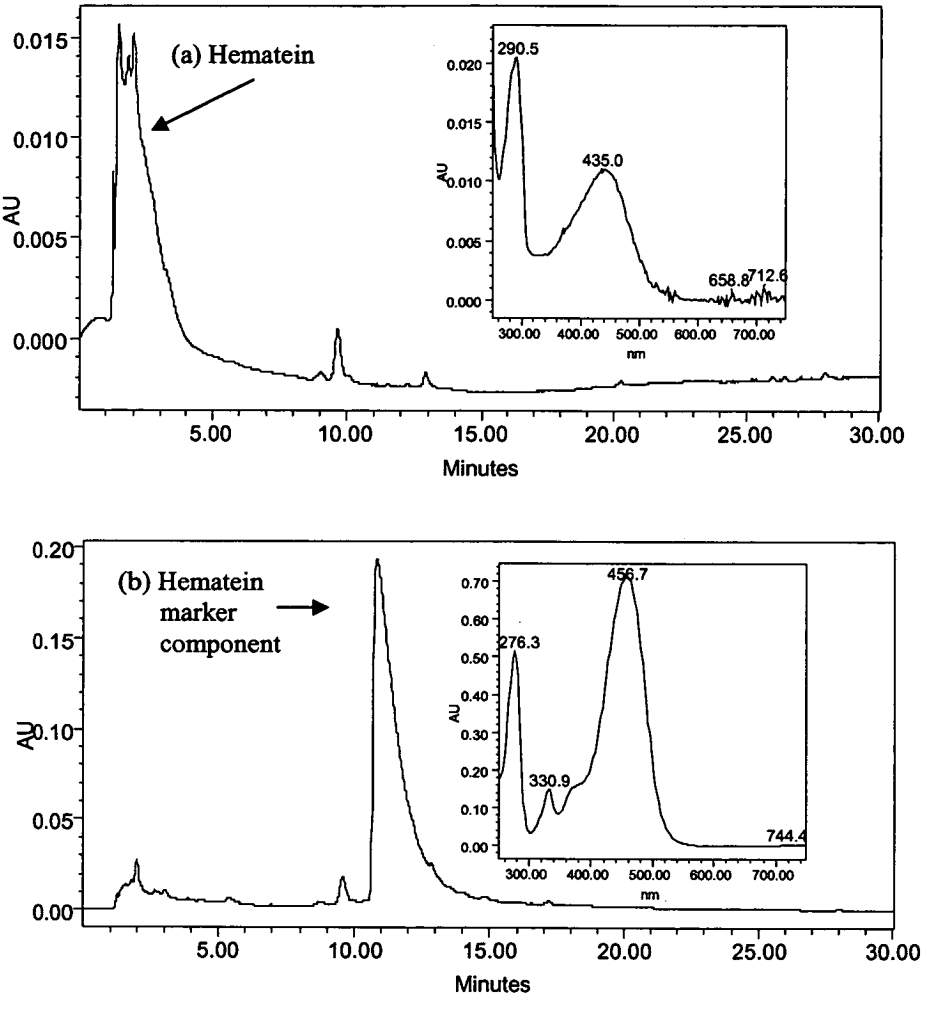

Figure 3.19: The chromatograms (monitored at 254 nm) and UV-Vis spectra of hematein and the hematein 'marker compound'

Hematein does not chromatograph well when analysed using the standard PDA HPLC method, eluting between *ca.* 1 and 4 min (λ_{max} = 290.5 and 435.0). However, after treatment using the standard hydrolysis extraction procedure with hydrochloric acid, a new compound is observed, eluting at *ca.* 11 min (λ_{max} = 276.3, 330.9 and 456.7). This peak has been used as a 'marker' for the presence of hematein, and thus logwood, when observed in the acid hydrolysed extracts of dyed yarns. This marker component is not observed when the hydrochloric acid in the extraction procedure is replaced with acetic acid (Chapter 6).

The mass spectrometry studies using methanolic solutions of the reduced neoflavonoid/homoisoflavonoid components indicated that the oxidised component was also present. When hematoxylin (the reduced form) was used in the dye bath preparation in place of hematein (the oxidised form), the acid hydrolysed yarn extract contained both hematoxylin and the hematein 'marker compound' (Figure 3.20), confirming the presence of hematein.

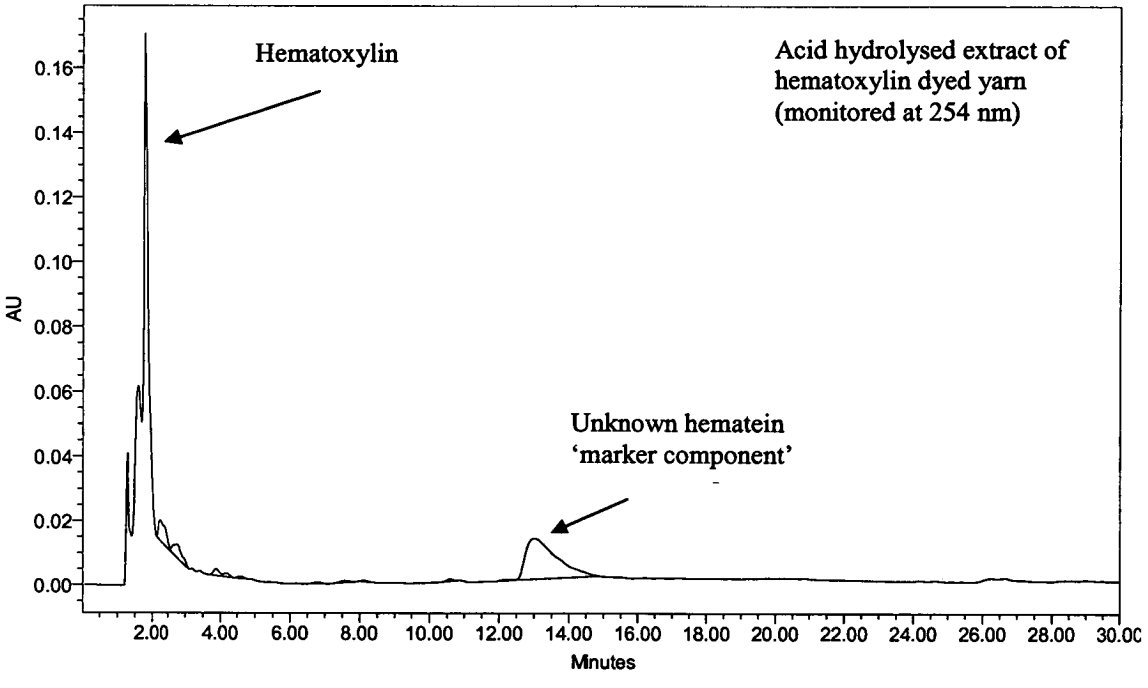

Figure 3.20: The chromatogram (monitored at 254 nm) of the acid hydrolysed extracts of hematoxylin dyed yarn

To investigate this hematein 'marker compound', the standard acid hydrolysis procedure was performed on a preparative scale, using hematein as a starting material (Chapter 6). The unknown 'marker compound' was obtained as a brick red powder, and a methanolic solution of this was directly injected into the mass spectrometer. A deprotonated molecular ion of *m/z* 281 was observed, corresponding to the loss of water from hematein. The *m/z* 281 component had a very unstable fragmentation pattern upon CID analysis, so further structural data could not be directly obtained. However, the proposed mechanism of hematein fragmentation under identical CID conditions involves the tertiary alcohol at the 6a position

(Scheme 3.4). As this no longer appears to be a breakdown pathway, it is likely that an elimination reaction has occurred at the tertiary alcohol. Acid catalysed elimination reactions from tertiary alcohols are particularly common, and in dilute HCl, the absence of reactive nucleophiles ensures that substitution reactions do not compete.

In an effort to elucidate the structure of this unknown compound, a series of NMR experiments was performed. A proton NMR spectrum of hematein was first obtained for reference and agreed with previously published data (Figure 3.21).[44] The solubility of the unknown compound in d_6-DMSO was poor, however, this was improved with the addition of a small amount of d_4-methanol.

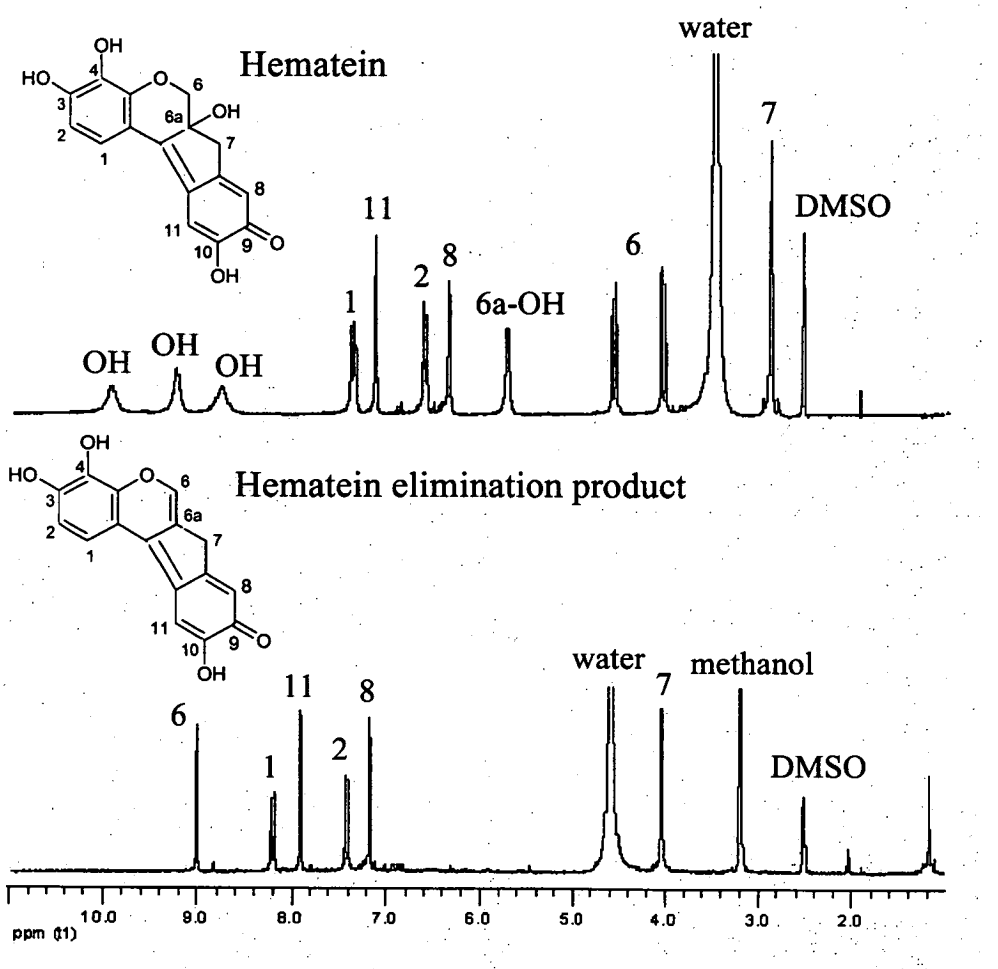

Figure 3.21: The ^{1}H NMR spectra of hematein (in d_6-DMSO) and the hematein elimination product (in d_6-DMSO/d_4-MeOH)

The ^{1}H NMR spectrum of the unknown 'marker compound' (Figure 3.21) clearly shows a new two-proton singlet at 4.04 ppm and a further one-proton singlet at 8.97 ppm. The two pairs of doublets due to the H-6 and H-7 protons (the latter almost degenerate) in the hematein spectrum were no longer observed. All chemical shifts and coupling constants are shown in Table 3.10. The absence of the pair of doublets due to the CH_2 group at the 6-position confirms the initial suggestion of an elimination reaction involving the tertiary alcohol (6a) to produce either the $\Delta^{6,6a}$ or $\Delta^{6a,7}$ isomer (Figure 3.22). The structure was confirmed as the $\Delta^{6,6a}$ isomer by the use of 2D NMR techniques as described below.

Hematein and structures of the two possible 'marker compounds'

(a) Hematein

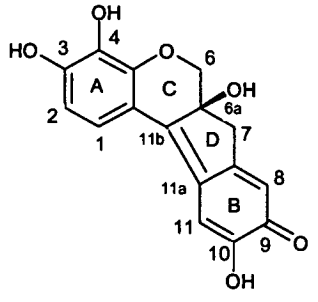

(b) $\Delta^{6,6a}$ elimination product

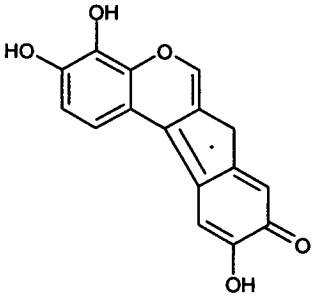

(c) $\Delta^{6a,7}$ elimination product

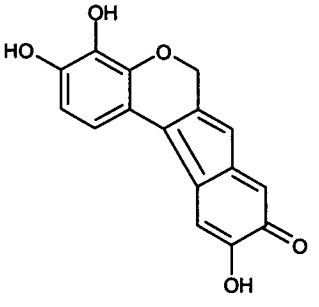

Figure 3.22: The structures of (a) hematein, and the two possible elimination products (b) ^{6,6a} isomer and (c) ^{6a,7} isomer

A NOESY (Nuclear Overhauser Effect Spectroscopy) experiment correlates protons which are close to one another in space. In the $\Delta^{6,6a}$ isomer, the CH_2 signal originating from the H-7 protons should correlate both with the signal due to H-6 and that due to H-8. In contrast, the CH_2 group in the alternative $\Delta^{6a,7}$ isomer would show only one correlation, with the signal from the H-7 proton. The 2D NOESY spectrum shown in Figure 3.23 clearly indicates that the CH_2 singlet at 4.04 ppm correlates both to the signal at 7.16 ppm (H-8) and to the new singlet at 8.97 ppm (H-6) providing strong evidence for the formation of the $\Delta^{6,6a}$ isomer. This technique also allows the signal from H-1 and H-2 to be distinguished, since only H-1 is in close spatial proximity to H-11. Interpretation of the unknown compound as the $\Delta^{6,6a}$ isomer was also supported by a COSY (Correlation Spectroscopy) experiment, which

correlates protons which are typically separated by up to 4 bonds within the molecule. Again, the signal from H-7 correlates with both H-6 and H-8.

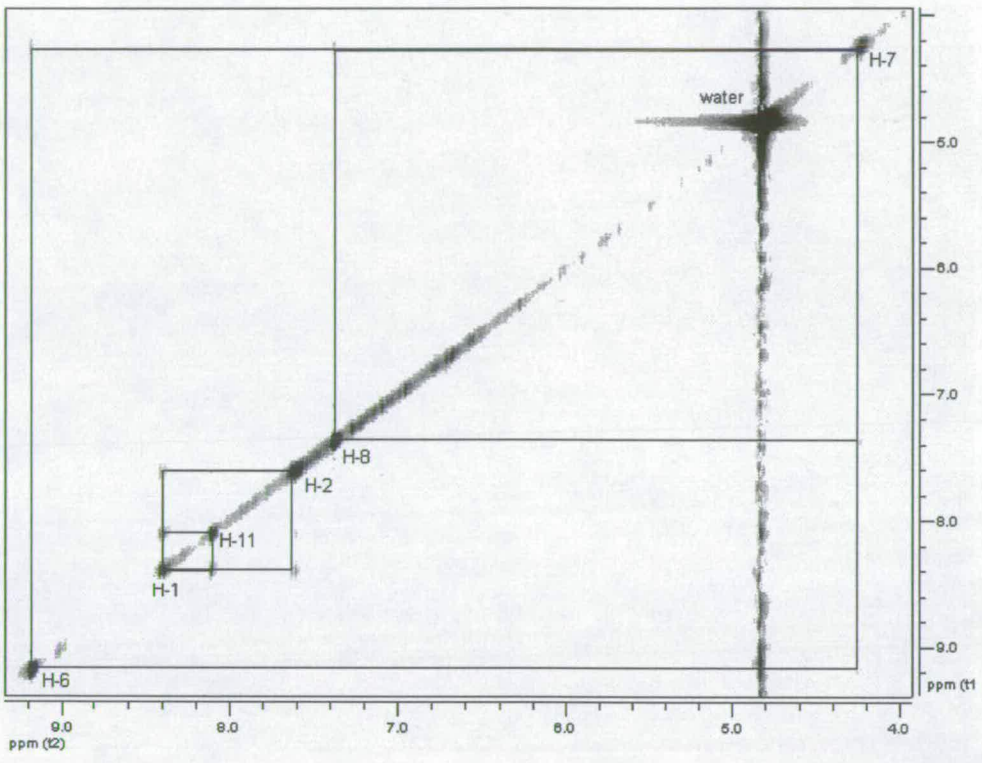

Figure 3.23: The 2D NMR NOESY spectrum of the hematein elimination product (d_6-DMSO/d_4-MeOH)

An HSQC (Heteronuclear Single Quantum Coherence) experiment correlates proton signals with the resonances due to the carbon atoms to which they are attached (Figure 3.24 and Table 3.10). Using this technique, the CH_2 signal at 4.04 ppm (assigned to H-7) was shown to correlate with a carbon whose chemical shift is 31.6 ppm, consistent with the shift expected for a benzylic CH_2 remote from a heteroatom. This further supports the formation of the $\Delta^{6,6a}$ isomer over the $\Delta^{6a,7}$ isomer. In addition, the singlet at 8.97 ppm was shown to correlate with a carbon chemical shift of just over 151.9 ppm, suggesting that it is next to a heteroatom (in this case, oxygen). The quality of the proton spectra obtained at the beginning and end of the experiments (*ca.* 18 h) indicated that the elimination product of hematein is unstable in solution for a prolonged length of time.

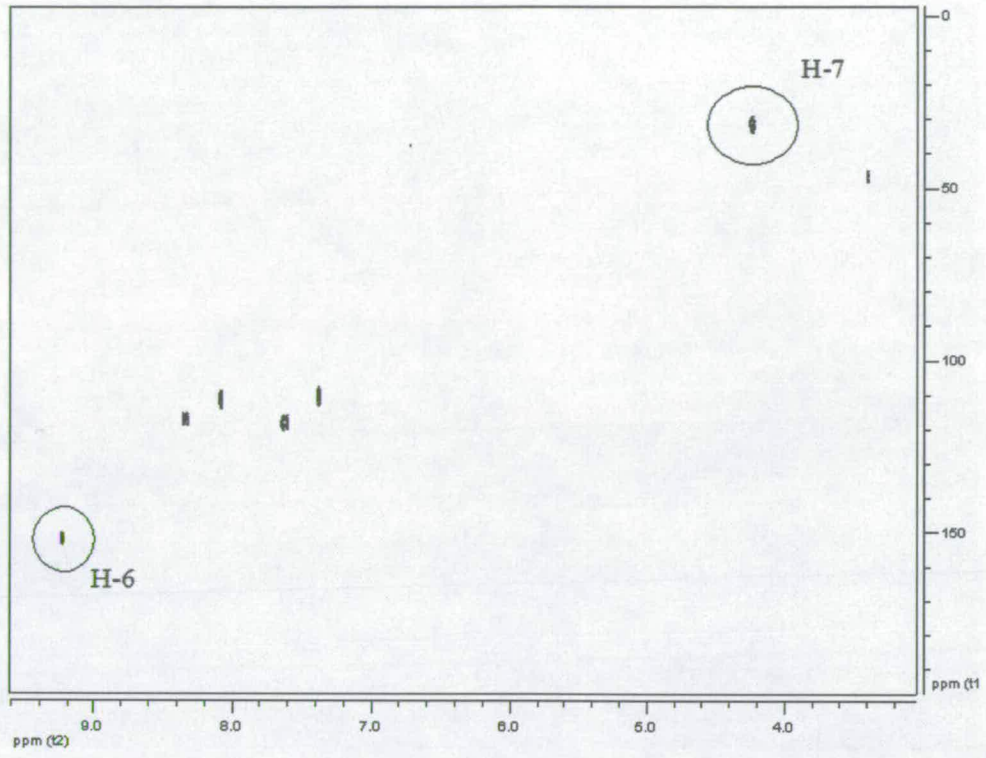

Figure 3.24: The 2D NMR HSQC spectrum of the hematein elimination product (d_6-DMSO/d_4-MeOH)

Table 3.10: ^{1}H and ^{13}C NMR chemical shifts (/ ppm) and coupling constants (J / Hz) for the hematein elimination product in a d_6-DMSO/d_4- MeOH mix, performed on a Bruker ARX 250 MHz spectrometer

H/C - assignment	^{1}H Chemical shift (δ / ppm)	Coupling constant (J / Hz)	^{13}C Chemical shift (δ / ppm)
6	8.97	s	151.9
1	8.18	d, 9.2	117.0
11	7.88	s	111.4
2	7.40	d, 9.2	118.1
8	7.16	s	110.5
7	4.04	s	31.6

The 'marker compound' observed for hematein is thus a hitherto unreported species, structurally related to hematein; 3,4,10-trihydroxy-*7H*-indeno[2,1-*c*]chromen-9-one.[45] It is formed by the acid catalysed elimination of the tertiary alcohol in hematein during the hydrochloric acid extraction protocol. Thus, the observation of this peak in the chromatogram of a sample prepared using the standard hydrolysis

procedure can now be directly related to the presence of hematein, the main colouring component of logwood.

Relating this 'marker' peak to hematein and thus logwood has proved to be important in the interpretation of the dye analysis results of several historical yarns sampled during the MODHT project (Chapter 5). For example, a black wool sample (BXL 2/27) from the reverse side of a tapestry woven in Brussels around 1520 (Figure 3.25) was analysed by PDA HPLC after undergoing the standard hydrochloric extraction method.

Figure 3.25: A black wool sample (BXL 2/27) taken from the reverse of *Christ before Pilate* (Brussels, ca. 1520), as part of the Monitoring of Damage in Historic Tapestries (MODHT) project © MODHT partners

The hematein elimination product was observed, together with ellagic acid, quercetin and maclurin (Figure 3.26) suggesting that the yarn was dyed using a combination of logwood, tannin and old fustic dye sources. However, due to the date of manufacture of this tapestry, the presence of the peak characteristic for logwood suggested that this particular sample was an early restoration thread.[45]

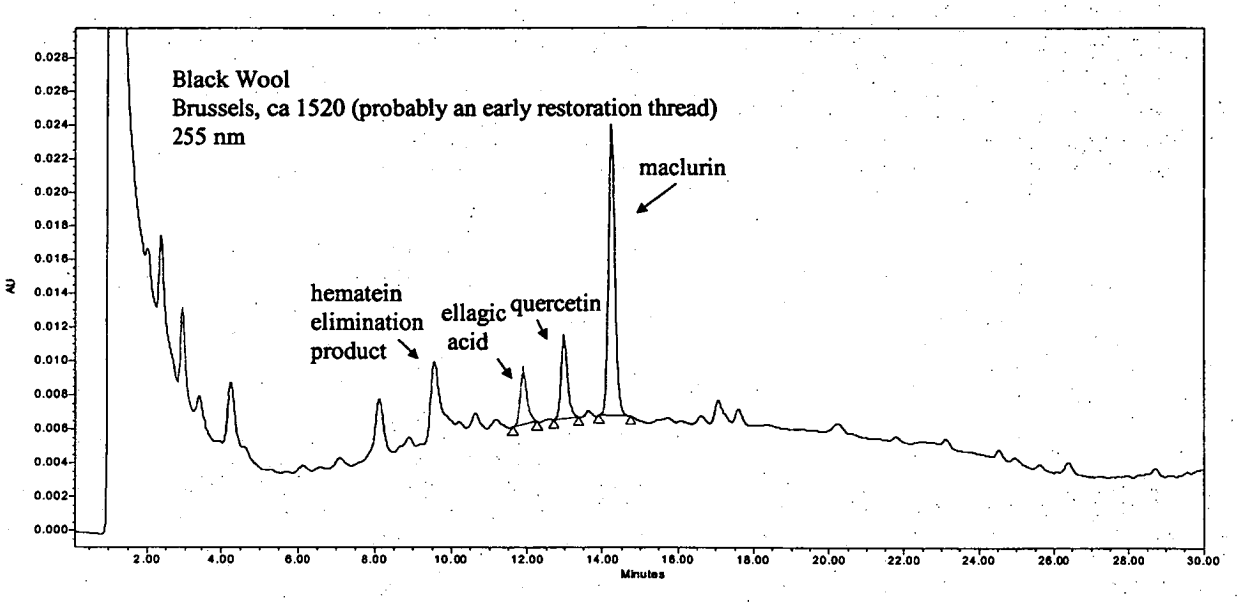

Figure 3.26: The HPLC chromatogram (monitored at 255 nm) of the acid hydrolysed extract of the historical sample, showing the hematein elimination product, ellagic acid, quercetin and maclurin

3.2.2.3 Brazilein marker compounds

The main colouring component found in brazilwood extracts, brazilein, was also investigated. However, similar characterisation studies to those performed on hematein were hampered by the lack of availability of a suitably pure brazilein reference material. Instead, experiments were performed using an authentic sample of *Caesalpinia sappan* L. obtained from Kew gardens, a reference sample of brazilin (the reduced form, probably isolated from a natural source) and 'brazilwood powder', used for the dyeing of the brazilwood reference yarns for the MODHT project. Three silk yarns were dyed using aqueous solutions of each brazilein source (Chapter 6). The yarns were acid hydrolysed and the reconstituted extracts analysed using the standard PDA HPLC method (Figure 3.27).

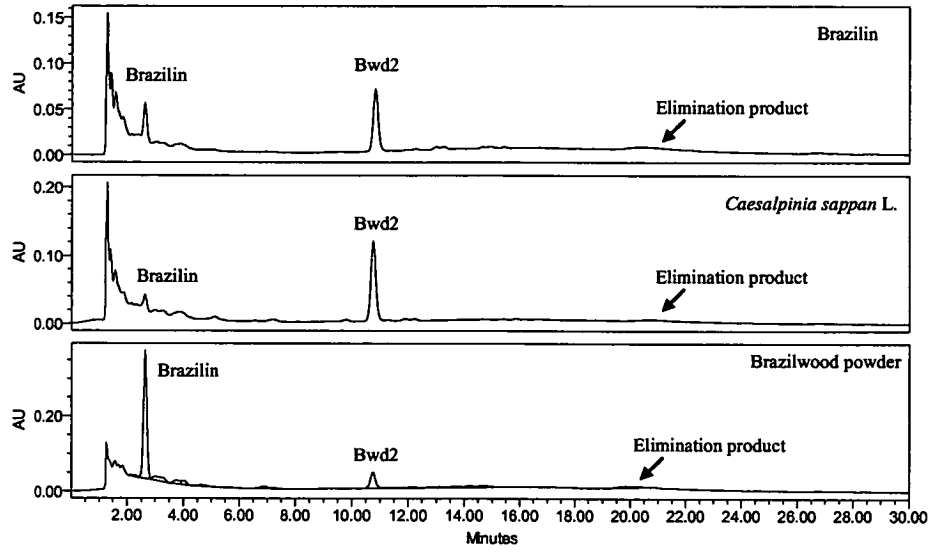

Figure 3.27: The PDA HPLC chromatograms (monitored at 254 nm) of the acid hydrolysed extracts from yarn dyed with brazilin, *Caesalpinia sappan* L., and 'brazilwood powder'

Two characteristic components, brazilin (retention time and UV-Vis spectrum matched those of the reference) and an unknown component, labelled Bwd2, were observed in the acid hydrolysed yarn extracts in each case. Furthermore, a component with a UV-Vis spectrum analogous to the spectrum obtained from the hematein dyed yarn extracts (Section 3.2.2.2), was also observed in each case (Figure 3.28).

This 'brazilein elimination product' did not chromatograph well, eluting in the above examples as a small, badly tailing peak at *ca.* 20 min. However, this retention time was found to be highly variable in subsequent experiments, suggesting that the component is not stable in the chromatographic system. As with its hematein counterpart, the proposed brazilein elimination product was not present in the unhydrolysed dye bath and was no longer observed when the hydrochloric acid in the extraction procedure was replaced with acetic acid (Chapter 6).

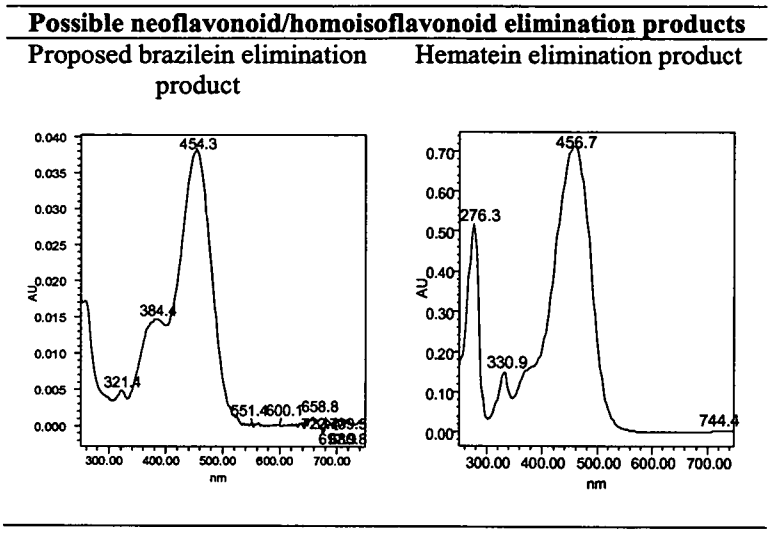

Figure 3.28: The UV-Vis spectra of the proposed brazilein elimination product, from the acid hydrolysed extracts of a yarn dyed with 'brazilwood powder' and of the hematein elimination product, from the acid hydrolysed extracts of a yarn dyed with pure hematein

HPLC ESI MS analysis of the extracts was attempted, although considerable difficulties were experienced in the interpretation of the data, possibly due to the slightly different chromatographic conditions necessary for hyphenation (Chapter 6). A peak with *m/z* 265, [brazilein-H-18]$^-$, corresponding to the proposed elimination product, was obtained, suggesting that brazilein undergoes the same reaction as hematein during acid hydrolysis. However sufficient quantities of either brazilein or the proposed elimination product could not be obtained for unambiguous structural confirmation by NMR spectroscopy.

The unknown component, labelled Bwd2 and eluting at *ca.* 10.8 min, had previously been reported in the acid hydrolysed extracts of a *Caesalpinia sappan* L. dye bath, together with the proposed brazilein elimination product, although neither component had been structurally characterised.[39] Unfortunately, the difficulties experienced in the HPLC ESI MS analysis of the extracts, possibly due to the slightly different chromatographic conditions necessary for hyphenation (Chapter 6) meant that a mass for the unknown Bwd2 component was not obtained using the chosen conditions.

Significantly, the Bwd2 component was also present in the unhydrolysed dye baths and continued to be observed when the hydrochloric acid in the extraction procedure was replaced with acetic acid (Chapter 6). This is in stark contrast to the respective elimination products of hematein and brazilein, neither of which were observed in the respective dye baths or acetic acid extracts.

The Bwd2 peak was observed in the extracts from some historical samples (Figure 3.29 and Chapter 5), and despite not being structurally characterised, was used as a tentative marker for the use of brazilwood or a related natural source.

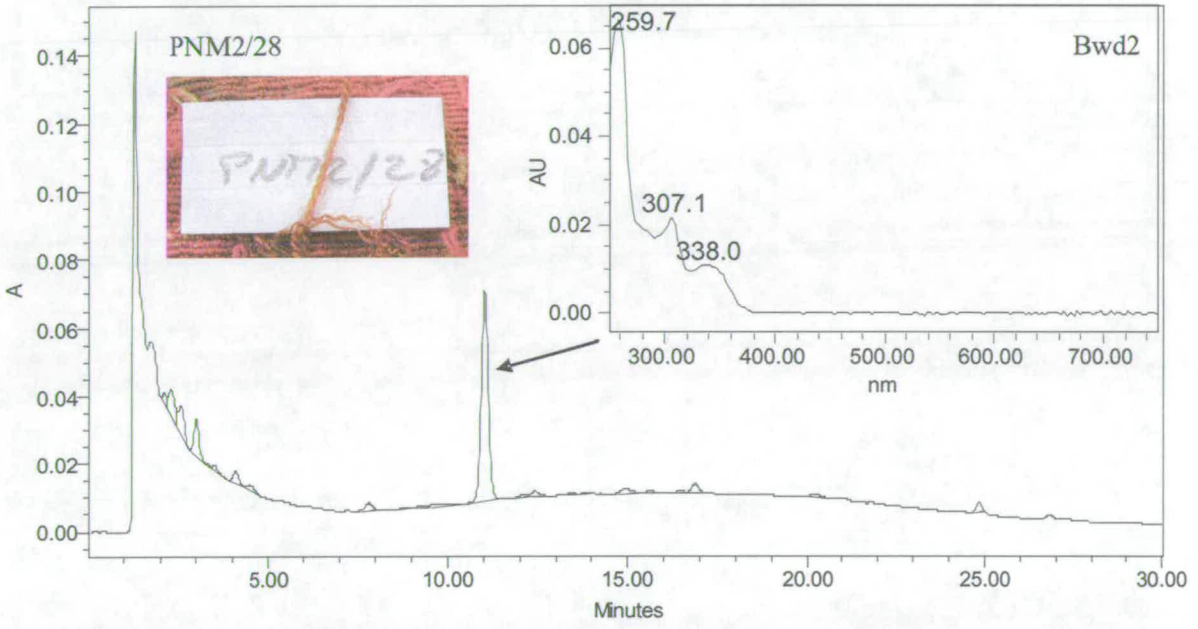

Figure 3.29: The PDA HPLC chromatogram (monitored at 254 nm) of an extract from an historical sample (PNM 2/28) containing the unknown Bwd2 component

However, as the unknown Bwd2 component is not formed as a result of the acid hydrolysis procedure and was observed in the reference dyebath solutions, the possibility remains that this component is not directly related to brazilein, but rather another brazilwood component which is mordanted onto the yarn and which survives the acid treatment of the extraction protocol. Thus, unlike the hematein elimination product, the unknown Bwd2 component may not necessarily be an exclusive 'marker component' for the neoflavonoids/homoisoflavonoids. It does, however, appear to

be a marker for redwoods. Interestingly, the light fastness of this marker is much better than the colouring component in redwood, brazilein, resulting in the ability to identify the use of redwood, even in a completely faded sample (Chapter 4).

3.2.3 Conclusion

Analysis of the reduced and oxidised neoflavonoid/homoisoflavonoid components using negative ion ESI MS^n enabled the identification of new, structure dependent, mass spectrometric breakdown pathways. The mechanisms were supported by deuterium labelling experiments and the results were shown to be useful for the structural determination of previously unidentified components.

Hematein, the principal dye component from logwood (*Haematoxylon campechianum* L.), was shown to undergo an elimination reaction during the acid hydrolysis extraction procedure. The structure of this product, observed in the PDA HPLC analysis of hematein dyed yarn extracts, was characterised using NMR techniques. A similar component, derived from brazilein, was also observed in brazilwood (*Caesalpinia sappan* L.) dyed yarn extracts. A second characteristic component was observed in both the unhydrolysed brazilwood dye bath and the extracts from dyed yarns. Although used for the identification of brazilwood dyed yarns, the component has not been structurally characterised.

3.3 References

[1] Ferreira, E.S.B.; Quye, A.; McNab, H.; Hulme, A.N.; Wouters, J.; Boon, J.J., *'The analytical characterisation of flavonoid photodegradation products: a novel approach to identifying natural yellow dyes in ancient textiles'*, Preprints to the ICOM Committee for Conservation, 12th Triennial meeting, **1999**, 1, 221-227

[2] Ferreira, E.S.B.; Quye, A.; McNab, H.; Hulme, A.N.; Wouters, J.; Boon, J.J., *'Development of analytical techniques for the study of natural yellow dyes in historic textiles'*, Dyes Hist Arch, **2001**, 16/17, 179-186

[3] Ferreira, E.S.B.; Quye, A.; Hulme A.N.; McNab, H., *'LC-Ion Trap MS and PDA-HPLC – Complementary Techniques in the Analysis of Flavonoid Dyes in Historical Textiles: The Case Study of an 18th Century Herald's Tabard'*, Dyes Hist Arch, **2003**, 19, 13-18

[4] Hofenk de Graaff, J.H., *'The Colourful Past'*, **2004**, Abegg-Stiftung and Archetype Publications Ltd., 1st edition, 147-149

[5] Wouters, J., *'High Performance Liquid Chromatography of Anthraquinones: Analysis of Plant and Insect Extracts and Dyed Textiles'*, Stud Conserv, **1985**, 30, 119-128

[6] Wouters, J.; Verhecken, A., *'The Scale Insect Dyes (*Homoptera: Coccoidea*). Species Recognition by HPLC and Diode-Array Analysis of the Dyestuffs'*, Annals Soc Ent Fr (N.S.), **1989**, 25, 4, 393-410

[7] Wouters, J.; Verhecken, A., *'The Coccid Insect Dyes: HPLC and computerized Diode Array Analysis of Dyed Yarns'*, Stud Conserv, **1989**, 34, 189-200

[8] González, M.; Méndez, J.; Carnero, A.; Lobo, M.G.; Afonso, A., *'Optimizing Conditions for the Extraction of Pigments in Cochineals (*Dactylopius coccus *Costa) using Response Surface Methodology'*, J Agr Food Chem, **2002**, 50, 6969-6974

[9] Derksen, G.C.H.; Niederländer, H.A.G.; van Beek, T.A., *'Analysis of anthraquinones in* Rubia tinctorium *L. by Liquid Chromatography Coupled with Diode-Array UV and mass spectrometric detection'*, J Chromatogr A, **2002**, 978, 119-127

[10] Mosi, A.A.; Reimer, K.J.; Eigendorf, G.K., *'Analysis of polyaromatic quinines in a complex environmental matrix using gas chromatography ion trap tandem mass spectrometry'*, Talanta, **1997**, 44, 985-1001

[11] Wouters, J.; Verhecken, A., *'The Chemical Nature of flavokermesic acid'*, Tetrahedron Lett, **1987**, 28, 11, 1199-1202

[12] Cuyckens, F; Claeys, M., *'Mass Spectrometry in the structural analysis of flavonoids'*, J Mass Spectrom, **2004**, 39, 1-15

[13] March, R.E.; Miao, X.; Metcalfe, C. D.; Stobiecki, M.; Marczak, L., *'A fragmentation study of an isoflavone glycoside, genistein-7-O-glucoside, using electrospray quadrupole time-of-flight mass spectrometry at high mass resolution'*, Int J Mass Spectrom, **2004**, 232, 171-183

[14] Stobiecki, M., *'Application of mass spectrometry for identification and structural studies of flavonoid glycosides'*, Phytochemistry, **2000**, 54, 237-256

[15] Yoshida, Z.; Takabayashi, F., *'Electronic Spectra of Mono-Substituted Anthraquinones and Solvent Effects'*, Tetrahedron, **1968**, 24, 913-943

[16] Sharma, A.; Kumar P.; Zaidi, Z.H., *'Effect of hydroxy substituents on the electronic absorption spectrum of 9,10-anthraquinone'*, Asian J Phys, **1998**, 7, 1, 162-164

[17] Fain, V.Y.; Zaitsev, B.E.; Ryabov, M.A., *'A Quantum-Chemical study of Prototropic Tautomerism in 1-Hydroxy-9,10-anthraquinones'*, Russ J Gen Chem, **2003**, 73, 4, 621-626

[18] Labhart, H. von, *'Zur quantitativen Beschreibung des Einflusses von Substituenten auf das Absorptionsspektrm ebener Molekeln. Anwendung auf Anthrachinon'*, Helv Chim Acta, **1957**, 152, 1410-1420

[19] Morgan, E.D., *'Biosynthesis in insects'*, **2004**, The Royal Society of Chemistry, 1st edition

[20] Staunton, J.; Weissman, K.J.; *'Polyketide biosynthesis: a millennium review'*, Nat Prod Rep, **2001**, 18, 380-416

[21] Lambert, J.B.; Shurvell, H.F.; Lightner, D.A.; Cooks, R.G., *'Organic Structural Spectroscopy'*, **1998**, Prentice-Hall, Inc., 8-152

[22] Reddy, V.L.N.; Ravikanth, V.; Lakshmi, V.V.N.S.J.; Murty, U.S.; Venkateswarlu, Y., *'Inhibitory activity of homoisoflavonoids from* Caesalpinia sappan *against* Beauveria bassiana*'*, Fitoterapia, **2003**, 600-602

[23] Camarda, L.; Merlini, L.; Nasini, G., *'Dragon's blood from* Dracaena draco*, structure of novel homoisoflavonoids'*, Heterocycles, **1983**, 20, 1, 39-43

[24] Bettinger, Ch.; Zimmermann, H.W., *'New investigations on haematoxylin, hematein, and hematein-aluminium complexes I'*, Histochemistry, **1991**, 95, 279-288

[25] Kim, D. S.; Baek, N.-I.; Oh, S. R.; Jung, K. Y.; Lee, I. S.; Lee H.-K., *'NMR Assignment of Brazilein'*, Phytochemistry, **1997**, 46, 177-178

[26] Namikoshi, M.; Nakata, H.; Yamada, H.; Nagai, M.; Saitoh, T., *'Homoisoflavonoids and Related Compounds II'*, Chem Pharm Bull, **1987**, 35, 7, 2761-2773

[27] de Oliveira, L.F.C.; Edwards, H.G.M.; Velozo, E.S.; Nesbitt, M., *'Vibrational spectroscopic study of brazilin and brazilein, the main constituents of brazilwood from Brazil'*, Vibr Spectrosc, **2002**, 243-249

[28] Puchtler, H.; Meloan, S.N.; Waldrop, F.S., *'Application of current chemical concepts to metal-hematein and -brazilein stains'*, Histochemistry, **1986**, 85, 353-364

[29] Arshid, F.M.; Desal, J.N.; Duff, D.J.; Giles, C.H.; Jain, S.K.; MacNeal, I.R., *'A Study of Certain Natural Dyes I'*, J Soc Dyers Colour, **1954**, 70, 392-401

[30] Arshid, F.M.; Connelly, R.F.; Desal, J.N., Fulton, R.G.; Giles, C.H.; Kefalas, J.C., *'A Study of Certain Natural Dyes II'*, J Soc Dyers Colour, **1954**, 70, 402-412

[31] Shirai, K.; Matsuoka, M., *'Structure and Properties of Hematein Derivatives'*, Dyes Pigments, **1996**, 32, 3, 159-169

[32] Lalor, G.C., *'Studies on Haematoxylin and Haematein, the colouring principles of logwood III'*, J Soc Dyers Colour, **1962**, 78, 549-551

[33] Lalor, G.C.; Martin, S.L., *'Studies on Haematoxylin and Haematein, the colouring principles of logwood I'*, J Soc Dyers Colour, **1959**, 75, 11, 513-517

[34] Lalor, G.C.; Martin, S.L., *'Studies on Haematoxylin and Haematein, the colouring principles of logwood II'*, J Soc Dyers Colour, **1959**, 75, 11, 517-521

[35] Fuke, C.; Yamahara, J.; Shimokawa, T.; Kinjo, J-E.; Tomimatsu, T.; Nohara, T., *'Two aromatic compounds related to Brazilin from* Caesalpinia sappan*'*, Phytochemistry, **1985**, 24, 10, 2403-2405

[36] Namikoshi, M.; Nakata, H.; Yamada, H.; Nagai, M.; Saitoh, T., *Homoisoflavonoids and related compounds. II. Isolation and absolute configurations of 3,4-dihydroxylated homoisoflavans and brazilins from* Caesalpinia sappan *L.'*, Chem Pharm Bull, **1987**, 35, 7, 2761-2773

[37] Namikoshi, M.; Saitoh, T., *'Homoisoflavonoids and related compounds. IV. Absolute configurations of homoisoflavonoids from* Caesalpinia sappan *L.'*, Chem Pjarm Bull, **1987**, 35, 9, 3597-3602

[38] Namikoshi, M.; Nakata, H.; Saitoh, T., *'Homoisoflavonoids from* Caesalpinia sappan*'*, Phytochemistry, **1987**, 26, 6, 1831-1833

[39] Nowik, W., *'The Possibility of Differentiation and Identification of Red and Blue 'Soluble' Dyewoods'*, Dyes Hist Arch, **2001**, 16/17, 129-144

[40] Ferreira, E.S.B., *'New Approaches Towards the identification of yellow dyes in ancient textiles'*, PhD Thesis, **2002**, The University of Edinburgh

[41] Fabre, N.; Rustan, I.; de Hoffmann, E.; Quetin-Leclercq, J., *'Determination of Flavone, Flavonol, and Flavanone Aglycones by Negative Ion Liquid Chromatography Electrospray Ion Mass Spectrometry'*, J Am Soc Mass Spectr, **2001**, 12, 707-715

[42] Ferreira, E.S.B.; Hulme, A.N.; McNab, H.; Quye, A., *'LC-Ion Trap MS and PDA-HPLC – Complementary Techniques in the Analysis of Different Components of Flavonoid Dyes: The Example of Persian Berries (*Rhamnus Sp.*)'*, Dyes Hist Arch, **2003**, 19, 19-23

[43] Hulme, A.N.; McNab, H.; Peggie, D.A.; Quye, A., *'Negative Ion Electrospray Mass Spectrometry of neoflavonoids'*, Phytochemistry, **2005**, 66, 2766-2770

[44] Bassoli, A.; Borgonovo, G.; Merlini, L.; Scaglioni, L., *'On the structure of haematein'*, Gazz Chim Ital, **1996**, 126, 761-763

[45] Hulme, A.N.; McNab, H.; Peggie, D.A.; Quye, A.; Berghe, I.V.; Wouters, J., *'Analytical Characterization of the main component found in logwood-dyed textile samples after extraction with hydrochloric acid'*, Preprints to the ICOM Committee for Conservation, 14th Triennial meeting, The Hague, **2005**, 2, 783-788

Chapter 4

4 ACCELERATED LIGHT AGEING

An investigation into the accelerated light ageing of dyed reference yarns is presented. The flavonoid compositions of the acid hydrolysed extracts from freshly dyed yarns were compared with the extracts obtained from yarns subjected to prolonged exposure to light. Thus, the photo-degradation of the characteristic components from yarns dyed with different biological sources was explored and the formation of any photo-degradation products investigated. These studies have improved the interpretation of the data from historical samples (Chapter 5).

4.1 Introduction

Photo-degradation reactions have the potential to alter the distinctive components identified in the acid hydrolysed extracts of dyed yarns, such as those characterised in Chapters 2 and 3. Thus, the unequivocal determination of the biological source used to dye an historical sample can become problematic. In a recent study, the sensitivity of different flavonoid dye components was assessed and some flavonoid photo-degradation products identified by means of accelerated ageing studies.[1] The present work utilises both PDA HPLC and LC ESI MS techniques to examine the accelerated ageing of several dye sources important within the context of the MODHT project.

The overall structural integrity of an historical textile artefact, such as a tapestry, will depend on the current condition of all the materials used in its construction. As the historic tapestries examined in this project were constructed for display, the greatest single factor likely to have contributed to the weakening of the woven structures is prolonged exposure to light. Exposure to appreciable amounts of light will have occurred throughout their use, whether as wall decorations or as carpets, blankets and patches for the roof; some of the more novel ways in which the tapestries have been used during their lifetimes (Chapter 5). If put on display, the exposure of the tapestries to light would have continued, although good practice now dictates that light levels for the exhibition of sensitive objects, such as dyed textiles, should be

kept to a minimum. If placed into storage, the amount of light reaching the tapestries would have been considerably reduced.

The type and significance of the damage caused by light can be altered by environmental factors such as the irradiation wavelength, temperature or relative humidity, and the absorbance properties of the sample *i.e.* whether the substrate is wool or silk, how it has been prepared or the dye-mordant combination. The majority of accelerated ageing studies concentrate on obtaining information that can be used to determine the 'ideal' display conditions (environmental factors) for artefacts containing natural dyes.[5] However, in the present study, selected reference yarns have been aged in an effort to assess the information that can be obtained from their acid hydrolysed extracts.

The identification of characteristic components in the extracts, along with their relative amounts, are frequently used to identify the biological species most likely to have been used to dye the samples.[2,3,4] Therefore, significant differences between the extracts from aged and unaged yarns may have implications in dye source recognition. It is already known, for example, that photo-degradation reactions can alter the characteristic components observed in dye sources containing flavonol components (Section 4.5).[1]

Thus, it is hoped that the ageing studies presented herein will improve the interpretation of the dye analysis data from historical sample extracts. Furthermore, the ability to collate the historical yarns from the MODHT sampling campaigns into groups of samples dyed with the same biological source (and which are therefore likely to have been prepared in at least a similar manner) may allow more information regarding the overall condition of the tapestries to be obtained *i.e.* the structural integrities of the tapestries may be better evaluated by comparing the amino acid analysis and tensile strength measurements of similarly dyed samples.

A full discussion of accelerated ageing methods can be found elsewhere,[1,5] however, it should be noted that the investigations into the photo-degradation of the dye

components utilized a different accelerated light ageing regime than the MODHT studies into the photo-degradation of the yarns. The latter study used an xenon arc climate chamber (Chapter 1) to induce fibre damage, while the former used a fluorescent light chamber to model dye photo-degradation under conditions already demonstrated to provide meaningful models for museum-displayed historical dyed textiles.[1] Accelerated ageing is based on the reciprocity principle; photochemical change is proportional to the net exposure, given by the product of the intensity of illuminance and exposure time. The dye degradation regime therefore used a smaller intensity of illuminance compared with the yarn studies, but the samples were exposed for a larger amount of time.

The luminous flux per square metre (lux) is the standard measure employed by museums to quantify the intensity of illuminance. The lumen is the photometric equivalent of the watt, taking into consideration the response of the human eye to radiation of different wavelengths. This unit of measurement is utilized because it can give a good indication of how well a visitor will be able to view objects on display, in addition to providing some information on the amount of photometric energy to which the objects will be exposed. Evidently, the lux measurement is not a 'true' expression of the total amount of photometric energy absorbed by the object, however, the comparison of lux measurements can be useful when examining the results from different accelerated ageing experiments conducted under identical light sources.

According to the reciprocity principle, the damage caused by 100 lux of illuminance for 1 h is comparable to the damage produced by 1 lux of intensity for 100 h. It has been demonstrated that the reciprocity principle is applicable when comparing identical light sources of different intensities, and when the relative humidity and temperatures are also identical.[6] However, as the conditions to which the tapestries have been exposed during their lifetime are not known, the results from accelerated ageing can only be viewed as a means of producing a model from which to predict and compare with real, long-term, ageing effects.[7]

The accelerated light ageing equipment consisted of a box containing 12 fluorescent light bulbs to simulate daylight (for spectral distribution, see Chapter 6). The average intensity of illuminance, measured at the centre of the box throughout the ageing experiments, was calculated to be 8,600 lux. The recommended museum light level for sensitive objects, such as dyed textiles, is usually *ca.* 50 lux.[8] Dyed textile yarns may also be damaged by exposure to UV light, however, UV levels are not adequately accounted for by lux measurement, as the human eye has only a weak response to shorter wavelengths. Therefore, the total amount of UV (mW m^{-2}) was also measured. The average value, measured at the centre of the accelerated ageing box during the experiments, was calculated at 1340 mW m^{-2}. The amount of UV in museum galleries is usually kept to a minimum (*ca.* 20 mW m^{-2} or less).

No temperature or relative humidity (RH) control was available in the accelerated ageing box, so these remained at ambient levels and were monitored together with the intensity of illuminance and UV. Individual yarn samples were threaded across acid free card and placed simultaneously in the ageing box. These were then removed after set periods of time and kept in the dark until analysis. Full details of all the accelerated ageing experiments, including sampling times and environmental conditions, can be found in Chapter 6. The photo-degradation of the characteristic components from the dyed MODHT reference yarns were then explored by comparing the relative ratios from their acid hydrolysed extracts with the relative ratios from the extracts of unaged equivalents.

The dye sources chosen for investigation were those most commonly employed in the dyeing of textile yarns for high quality items, such as tapestries, in Europe from 15^{th}-18^{th} century (Chapter 5). The biological sources most commonly used for colouring yarns yellow, including weld (*Reseda luteola* L.), dyer's greenweed (*Genista tinctoria* L.), sawwort (*Serratula tinctoria* L.) and young fustic (*Cotinus coggygria* Scop.), were investigated. Some of the biological sources used to colour yarns red were also investigated, including cochineal (*Dactylopius coccus* Costa.) and brazilwood (*Caesalpinia sappan* L.).

4.2 Yarn degradation

Two yarn degradation peaks are observed in the acid hydrolysed extracts from undyed alum mordanted wool samples, aged in the accelerated ageing box (Figure 4.1). Their retention time and UV-Vis spectra match with those of 4-hydroxybenzoic acid (R_t = 3.1 min, $_{max}$ = 255.0 nm) and its methyl ester (R_t = 7.9 min, $_{max}$ = 256.2).

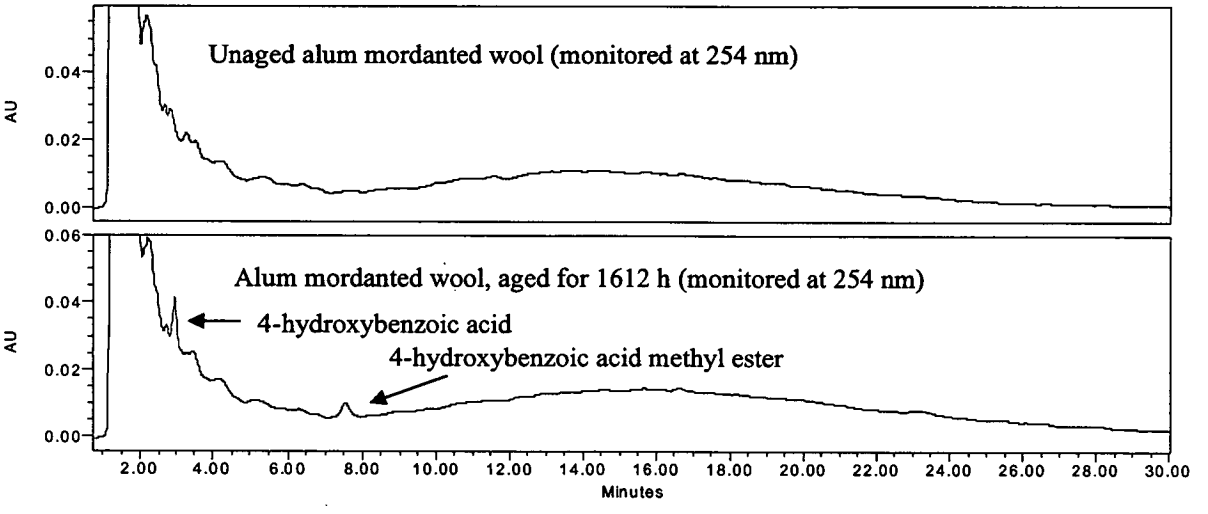

Figure 4.1: The acid hydrolysed extracts (monitored at 254 nm) of unaged (top) and aged (bottom) wool yarn

The same degradation products are found in the acid hydrolysed extracts from alum mordanted silk samples which have undergone prolonged exposure to light in the accelerated ageing box (Figure 4.2).

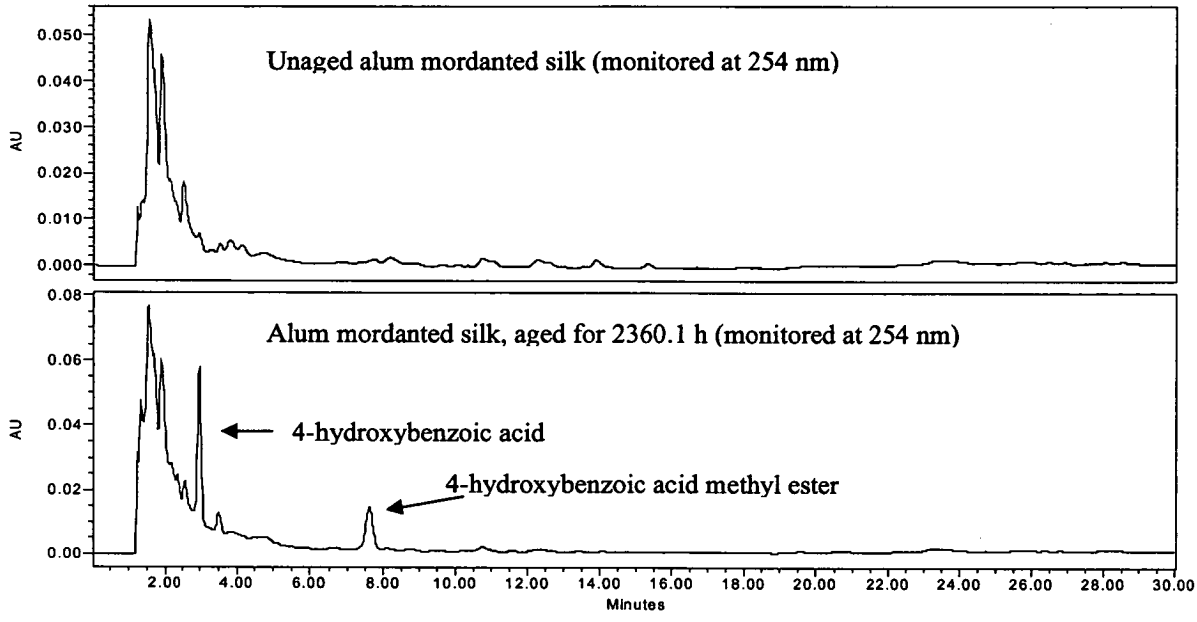

Figure 4.2: The acid hydrolysed extracts (monitored at 254 nm), of unaged (top) and aged (bottom) silk yarn

Furthermore, the two components are also observed in the extracts from dyed reference samples which have undergone prolonged exposure to light in the accelerated ageing box and in many of the extracts from historical yarns. This suggests that the accelerated ageing experiments are successfully modelling the photo-oxidative damage occurring on the historical yarns through 'natural' ageing.

It has previously been shown that both components are observed upon the photo-degradation and subsequent acid hydrolysis of mordanted yarns,[1] and that 4-hydroxybenzoic acid methyl ester is formed from 4-hydroxybenzoic acid under the acidic conditions present during the extraction procedure (Scheme 4.1).

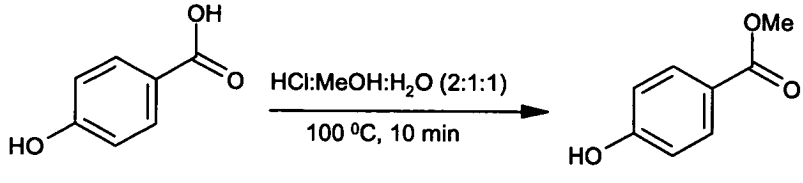

Scheme 4.1: Esterification of 4-hydroxybenzoic acid to its methyl ester in the acidic conditions present during dye extraction

Despite numerous studies on the photo-induced changes that occur in proteinaceous fibres such as silk and wool, the degradation mechanisms have not been completely clarified.[9,10,11,12] However, the proteins found in both silk and wool contain a high proportion of the amino acid residue, tyrosine (Figure 4.3).[13]

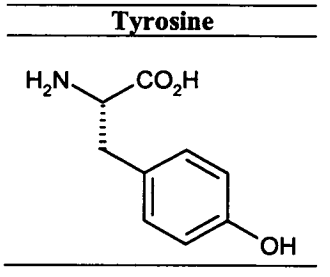

Figure 4.3: Tyrosine, an important amino acid residue in both wool and silk

This residue contains an aromatic side-chain, and consequently has UV absorbing properties. Furthermore, a large reduction in the tyrosine content of aged yarn samples is observed in the amino acid analysis of aged silk when compared with the equivalent unaged yarn extracts.[12] This reduction in tyrosine content has also been observed in the amino acid analysis from aged wool and silk reference yarns produced as part of the MODHT project (Chapter 1).[14] It is therefore suggested that the yarn degradation products observed in the acid hydrolysed extracts may be derived from the photo-oxidative breakdown of tyrosine in the wool or silk polymer.

4.3 Weld (*Reseda luteola* L.)

The investigation of the characteristic flavonoid components in the acid hydrolysed extracts from weld reference samples revealed that neither the substrate, nor additional steps in the dyeing process, significantly altered their relative ratios (Chapter 2). However, variations in the photo-degradation rates of these characteristic components have the potential to alter the flavonoid ratio in extracts from aged yarns. This may result in significant differences between chromatograms from reference and historical extracts, even when dyed with the same dye source.

To explore the relative photo-degradation of the three characteristic flavonoid components observed in the acid hydrolysed extracts of weld (Figure 4.4), an

accelerated light ageing experiment was conducted on a weld dyed reference yarn (Y/W1).

Flavonoid components from weld (*Reseda luteola* L.)

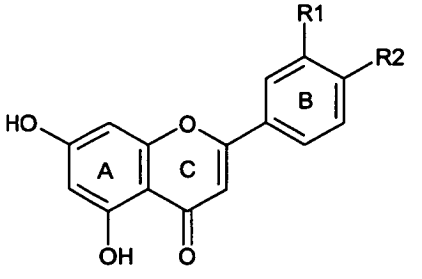

Luteolin: R1 = R2 = OH
Apigenin: R1 = H, R2 = OH
Chrysoeriol: R1 = OMe, R2 = OH

Figure 4.4: The main flavonoid constituents in the acid hydrolysed extract from a weld dyed yarn

The final sample was removed from the light box after 4571 h. This level of exposure equates to *ca.* 200 years at 'ideal' museum lighting conditions for sensitive objects, such as dyed textiles (50 lux for 10 h per day), although with a substantially higher UV content.

The total amount of light exposure experienced by the tapestries from the MODHT project during their (*ca.* 500 year) lifetime is likely to be in excess of this value. However, the historical yarns were almost exclusively sampled from the reverse of the objects (Chapter 5). Consequently, these yarns will have had less exposure to light than the yarns from the front. Some tapestries were also backed with a loose cotton lining, providing further protection from damage. Indeed, a distinct colour difference was usually observed between the (faded) front and (relatively brighter) back of the tapestries and was particularly noticeable with areas of pink or yellow colour.

The three distinctive components of weld were observed in the acid hydrolysed extract from the final sample from the accelerated ageing study (Y/W1_t_{final}), subjected to 4571 h of exposure in the light box (Chapter 6). However, the peak areas (monitored at 254 nm) were significantly less than those observed in the acid

hydrolysed extract from the initial, unaged sample (Y/W1_t_0) and the relative ratios of the components had altered (Table 4.1).

Table 4.1: Relative peak areas (monitored at 254 nm) of the main flavonoid components in the acid hydrolysed extracts of alum mordanted wool dyed with weld

Sample	Relative peak area (monitored at 254 nm) / %		
	Luteolin	**Apigenin**	**Chrysoeriol**
Weld on wool (Y/W1_t_0)	94	4	2
Weld on wool (Y/W1_t_{final})	86	11	3

The use of acid hydrolysis to extract the dye components from the yarn converts any flavonoid-*O*-glycosides present into their parent aglycones. For example, the presence of several luteolin-*O*-glycosides, including luteolin-7-glucoside, luteolin-3'-glucoside and luteolin-3',7-diglucoside, have been observed in weld plant extracts (Figure 4.5).[15]

Luteolin glucosides

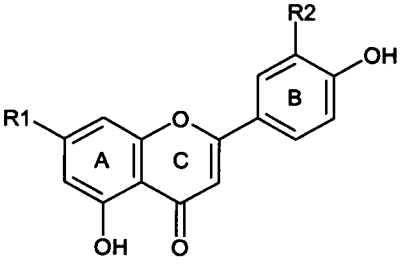

Luteolin-7-glucoside	R1 = O-glucose, R2 = OH
Luteolin-3'-glucoside	R1 = OH, R2 = O-glucose
Luteolin-3'7-diglucoside	R1 = R2 = O-glucose

Figure 4.5: Some of the O-glycosides known to be present in weld

However, only luteolin is observed in the acid hydrolysed extracts from weld dyed yarns. Thus, the above result is due to the combined effect produced by the photo-degradation of the parent aglycone and any *O*-glycosides present on the yarn, and not necessarily to the degradation of the specific aglycone components alone.

The data in Table 4.1 therefore suggest that the photo-degradation of any luteolin and chrysoeriol components mordanted onto the fibre occurs at a faster rate than apigenin. Thus, upon prolonged exposure to light, the percentage of apigenin in the acid hydrolysed extracts increases relative to luteolin and chrysoeriol. The slightly higher susceptibility of the luteolin derivatives to photo-degradation compared with apigenin may be due to the additional hydroxyl functionality in the B-ring. Solution studies have shown that the chemical reactivity of the flavonoids is largely controlled by the structure of ring C, but a small influence is attributed to the number and position of OH substituents on rings A and B.[16]

The relative differences in the overall degradation rates of the three components (and any glycosidic 'precursors') can be shown graphically by plotting the percentage area obtained from the extracts (monitored at 254 nm) against the length of time each yarn sample was exposed in the light box (Figure 4.6).

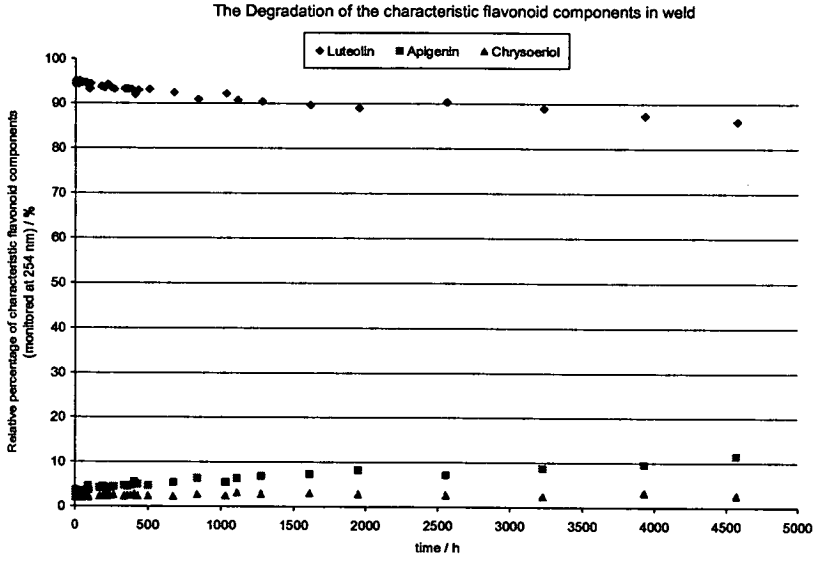

Figure 4.6: The relative degradation of the main flavonoid components observed in the acid hydrolysed extracts of aged weld

The lower portion of the graph has been expanded in Figure 4.7 to allow the increasing relative percentage of apigenin to be more clearly observed.

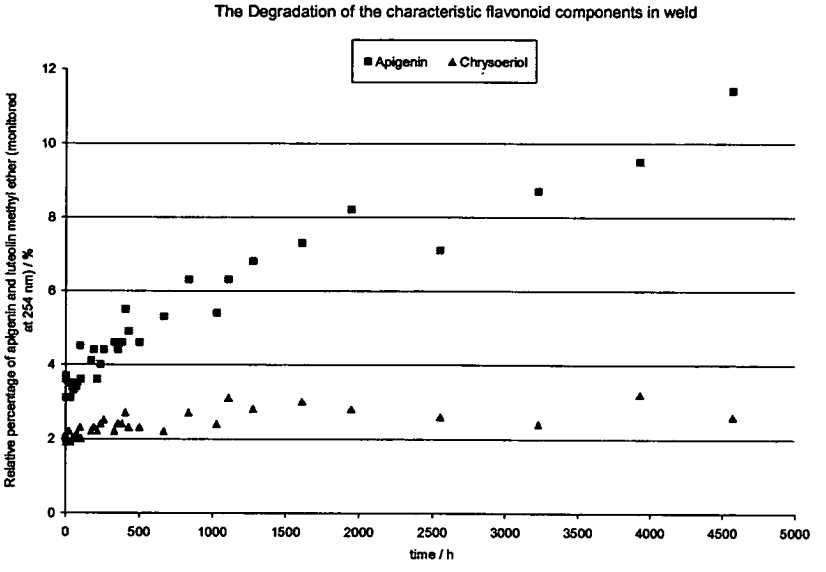

Figure 4.7: The relative degradation of apigenin and chrysoeriol, observed in the acid hydrolysed extracts of aged weld

This trend is also apparent in green wool yarns, dyed using weld and woad, where the relative amount of apigenin in the acid hydrolysed extracts also increases upon prolonged exposure to light (Table 4.2). The three distinctive components of weld were observed in the acid hydrolysed extracts of the final samples from the accelerated ageing study (G/W1_t_{final} and G/W2_t_{final}), both subjected to 4056 h of exposure in the light box (Chapter 6). However, the peak areas (monitored at 254 nm) were significantly less than those observed in the acid hydrolysed extracts from the initial, unaged samples (G/W1_t_0 and G/W2_t_0) and the relative ratios of the components had altered.

Table 4.2: Relative peak areas (monitored at 254 nm) of the main flavonoid components in the acid hydrolysed extracts of alum mordanted wool dyed with weld and overdyed (G/W1) or underdyed (G/W2) with woad

Sample	Relative peak area (monitored at 254 nm) / %		
	Luteolin	Apigenin	Chrysoeriol
Weld / woad on wool ($G/W1\_t_0$)	97	2	1
Weld / woad on wool ($G/W1\_t_{final}$)	93	5	2
Woad / weld on wool ($G/W2\_t_0$)	94	4	2
Woad / weld on wool ($G/W2\_t_{final}$)	89	8	3

The additional indigo component is present on the yarn in the form of an insoluble pigment, aggregated between yarn fibres. In both the weld overdyed with woad (G/W1) and woad overdyed with weld (G/W2) samples, the apigenin was once again the component least affected upon exposure of the yarn to light (Figure 4.8 and Figure 4.9). The presence of the indigoid pigment has therefore not altered the relative photo-degradation characteristics of the three components.

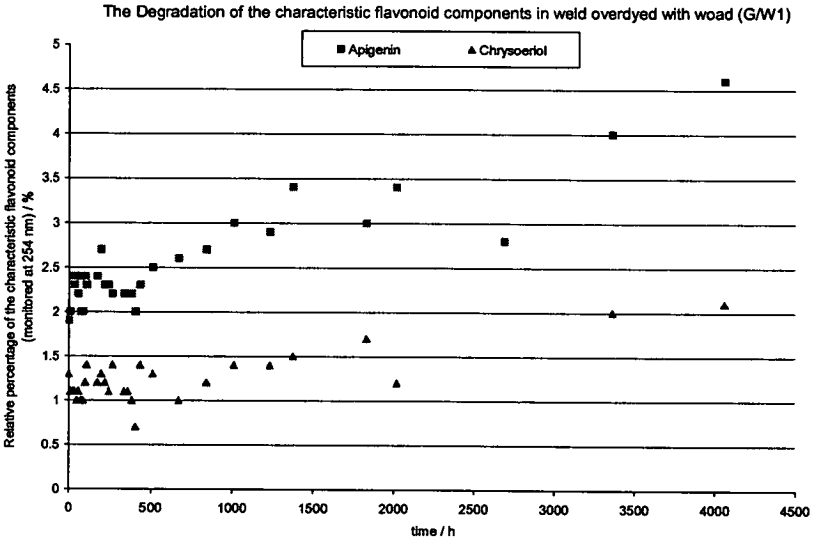

Figure 4.8: The relative percentages of the minor components apigenin, and chrysoeriol in the extracts from aged yarn dyed with weld and over-dyed with woad (G/W1)

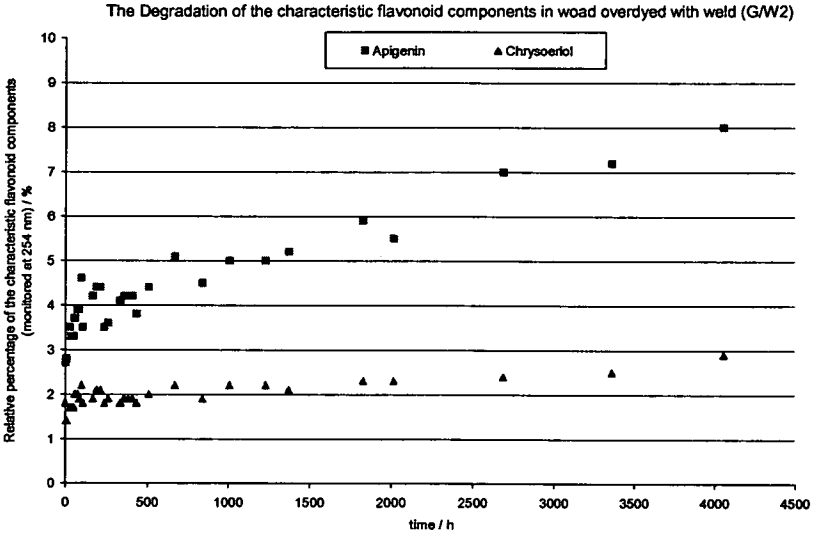

Figure 4.9: The relative percentages of the minor components apigenin and chrysoeriol in the extracts from aged yarn dyed with woad and over-dyed with weld (G/W2)

Thus, the ratio of characteristic flavonoids in the acid hydrolysed extracts from a freshly dyed reference sample of weld differs from the flavonoid ratios in the extract from a photo-degraded yarn sample. Furthermore, the magnitude of this difference is determined by the total amount of light to which the yarn has been exposed.

The ratio of the flavonoid components observed in extracts from samples that have undergone accelerated ageing compare favourably with the flavonoid ratios in many of the extracts from historical yarns sampled as part of the MODHT project (Chapter 5), despite the fact that the 'initial' flavonoid ratios in these historical samples were unknown.

The luteolin: apigenin: chrysoeriol ratio observed in the extracts from the unaged yarn (Y/W1, t_0) was 94:4:2, while the ratio of the three main components in the extract from the most photo-degraded yarn sample in the weld accelerated ageing study (Y/W1, t_{final}) was 86:11:3. The ratio obtained from the extracts of the aged reference yarns closely reflects the average values obtained from the historical sample extracts identified as having been dyed with a weld source, where the mean luteolin: apigenin: chrysoeriol ratio was found to be 85:10:5 (Chapter 5). This

suggests that the accelerated ageing experiments are successfully modelling the 'natural' ageing of the dye components from historical samples. However, the ratios in the historical samples have an extremely large range (98:2:0 to 33:34:33), making it impossible to draw conclusions regarding the light exposure of each sample, particularly because it is not known if this is caused by recipes, ageing or natural variations in botanical source.

A degradation product (R_t = 7.3, $_{max}$ = 252.6, 314.2) was also observed in the extracts from weld dyed samples which had undergone prolonged exposure to light in the accelerated ageing box (Figure 4.10). This unknown degradation product was observed in the extracts of aged weld yarn before the yarn degradation peaks, discussed above, became visible (Figure 4.10, middle) and continued to be present as the yarn degradation peaks became visible (Figure 4.10, bottom). However, the unknown degradation peak was not present in the extracts from the unaged, dyed yarn (Figure 4.10, top), thus must be derived from one of the dye components.

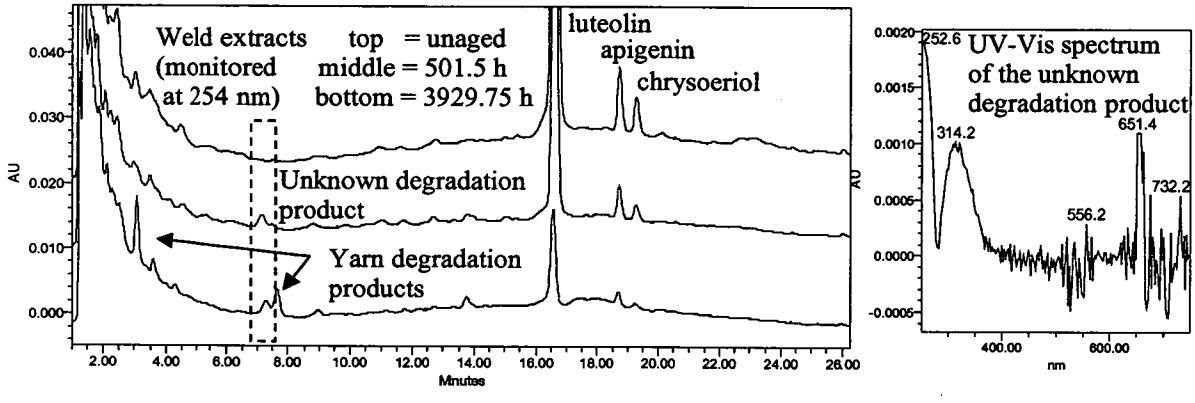

Figure 4.10: The unknown degradation product can be observed in the extracts of aged weld yarns. (Top) the unaged yarn extract, with no degradation products; (Middle) the unknown degradation product is now present although the yarn degradation peaks are not (Bottom) the unknown degradation peak is present, together with the yarn degradation peaks. The UV-Vis spectrum of the unknown degradation product is shown on the right

Due to the small amount of this unknown component present in the extracts, difficulties were encountered during further investigations, since it was present at a level close to the detection limit. Thus it was not possible to obtain any further information regarding its identity, however, it was observed in some of the extracts

from historical yarns believed to have been dyed with weld, for example, BRU 3/9 (Figure 4.11).

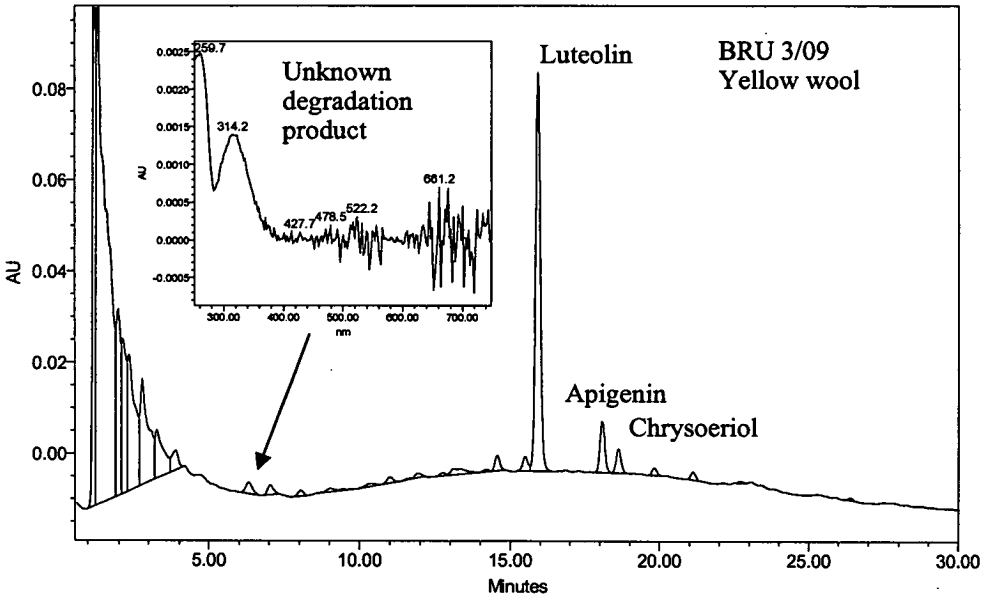

Figure 4.11: The unknown degradation product observed in the accelerated ageing yarns is also present in some extracts from historical yarns, for example, BRU 3/09, a yellow wool yarn from a tapestry woven in *ca.* 1630

The accelerated ageing of weld reference yarns indicated that the relative amounts of the three characteristic flavonoid components observed in the acid hydrolysed extracts (luteolin, apigenin and chrysoeriol) are altered by photo-degradation reactions. In addition, although one photo-degradation product was observed in the acid hydrolysed extracts, it could not be characterised. This information has allowed a greater confidence in the assignment of weld as the most probable biological dye source in a number of historical yarn samples (Chapter 5).

4.4 Dyer's greenweed (*Genista tinctoria* L.)

In contrast to weld dyed yarns, the ratio of the main flavonoid aglycones identified in the acid hydrolysed extracts from unaged reference yarns dyed with dyer's greenweed (Figure 4.12) varied considerably (Chapter 2).

Flavonoid components from dyer's greenweed (*Genista tinctoria* L.)

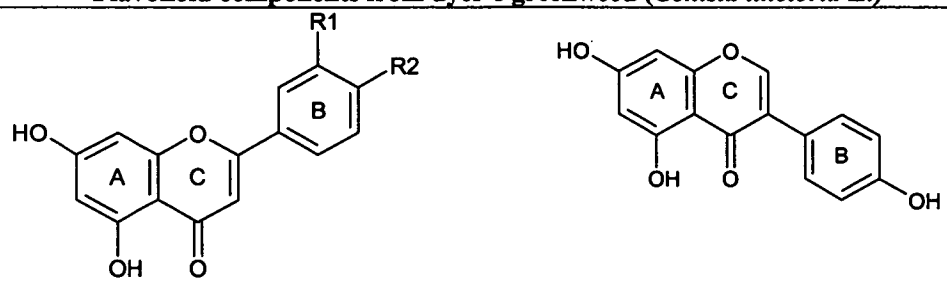

Luteolin: R1 = R2 = OH
Apigenin: R1 = H, R2 = OH

Genistein

Figure 4.12: The flavonoid components observed in the acid hydrolysed extract from yarn dyed with dyer's greenweed

Although a comprehensive study of the relative amounts of genistein and luteolin in the extracts from reference yarns was hampered by the partial co-elution of the two peaks in the chromatographic method (Chapter 2), the relative amounts of genistein and luteolin were found to be dependent on the different dyeing procedures, (Appendix 7.2, Y/S3a-e).

However, the three distinctive components of dyer's greenweed (genistein, luteolin and apigenin) were observed in all the acid hydrolysed extracts from the final samples of the accelerated ageing study (Y/S3a-e_t_{final}), subjected to 4850 h of exposure in the light box (Chapter 6). The peak areas (monitored at 254 nm) were significantly less than those observed in the acid hydrolysed extracts from the initial, unaged samples (Y/S3a-e_t_0) but the relative percentage of both genistein and apigenin increased with respect to luteolin in all the samples (Table 4.3). Although genistein and luteolin co-eluted in the chromatographic method, analysis of the 'peak purity' data confirmed that differences in the ratios were not due to instrumental variation. No significant flavonoid degradation products were observed in any of the extracts.

Table 4.3: Relative peak areas (monitored at 254 nm) of the main flavonoid components in the acid hydrolysed extracts of alum mordanted silk dyed with dyer's greenweed. Y/S3a-d = alum mordanted silk dyed with dyer's greenweed using different recipes and Y/S3e = silk dyed with dyer's greenweed with no mordant (Appendix 7.2)

Sample	**Relative peak area (monitored at 254 nm) / %**		
Dyer's greenweed on silk	**Genistein**	**Luteolin**	**Apigenin**
Y/S3a_t_0	46	47	7
Y/S3a_t_{final}	51	41	8
Y/S3b_t_0	26	69	5
Y/S3b_t_{final}	34	58	8
Y/S3c_t_0	30	63	6
Y/S3c_t_{final}	44	45	11
Y/S3d_t_0	18	78	4
Y/S3d_t_{final}	34	58	8
Y/S3e_t_0	46	45	8
Y/S3e_t_{final}	60	29	12

Although genistein does not contribute directly to the yellow colour of yarn dyed with dyer's greenweed, its presence in the extracts of the yarn allows this dye source to be easily distinguished from other alternatives, such as weld. Thus, when genistein is found in the extracts from an historical yarn sample, it is used as the main 'marker component' to identify the probable use of this biological species. Fortuitously, the degradation of this important compound appears to proceed at a relatively slower rate than the other main flavonoid component found in dyer's greenweed, the flavone, luteolin.

The relatively slow photo-degradation rate of the isoflavonoid, genistein, may be due to the fact that the B-ring is attached at the 3-position of the C-ring, rather than the 2-position as with the flavonoids (for example, luteolin and apigenin). In addition, the number and positions of the hydroxyl group substitutions on the B-ring have been shown to influence the rate of photo-degradation reactions.[16,17,18]

Due to the partial co-elution of genistein and luteolin in the chromatographic method, further investigation into the relative degradation rates of the two aglycones in these samples was difficult. Thus, an alum mordanted wool yarn 'dyed' with pure genistein was aged under accelerated conditions. The results were then compared

with the degradation of luteolin in weld (Y/W1) and have been plotted in Figure 4.13, where the area of each component, per mg of yarn (monitored at 254 nm) has been expressed as a percentage of the area obtained in the unaged sample extract.

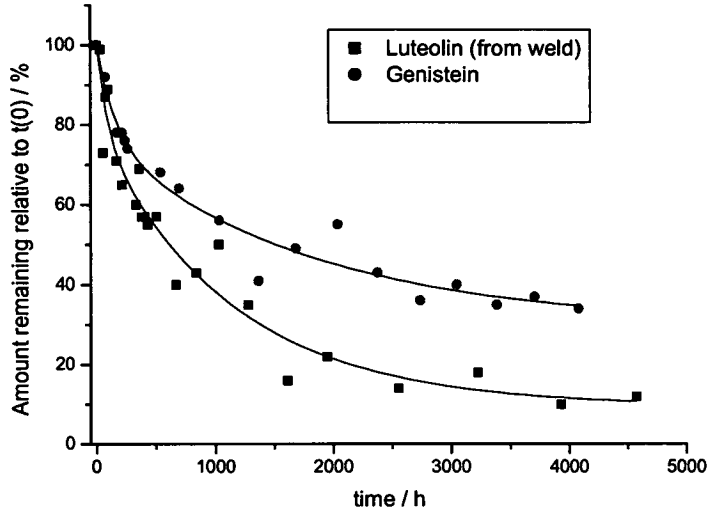

Figure 4.13: The photo-degradation rate of genistein and luteolin

The degradation rate of both components can be fitted to a double exponential model, predicted by previous work.[1] The reason for this is best explained, at least to a first approximation, by the two different degradation rates associated with the dye on the surface of the yarn and the dye in the bulk of the yarn. After 4000 h of exposure in the light box, the amount of luteolin observed in the extract (per mg of yarn) had fallen to *ca.* 10% of that observed in the original, unaged, extract. In contrast, the amount of genistein observed in the extract after 4000 h of ageing had only fallen to *ca.* 35% of that observed in the original, unaged, extract, thus confirming the observation that genistein (on an alum mordanted wool substrate) degrades at a slower rate than luteolin.

Although the relative amount of genistein observed in the acid hydrolysed extracts of dyed yarns is highly dependent on the original dyeing procedure (Chapter 2), the accelerated ageing results suggest that it would be a good 'marker' for the use of dyer's greenweed, and in 49 of the 59 historical sample extracts from yarns believed

to have been dyed with a dyer's greenweed source, genistein was the major component, despite not contributing directly to the yellow colour of the dyed yarn (Chapter 5).

4.5 Sawwort (*Serratula tinctoria* L.)

The PDA HPLC and HPLC ESI MS studies on the acid hydrolysed extracts of yarn dyed with the *Serratula* species, sawwort (*Serratula tinctoria* L.) and *Serratula coronata* L. provided important information on the identity of their characteristic flavonoid components (Chapter 2). The flavonols quercetin, 3-*O*-methylquercetin and kaempferol, and the flavones luteolin and apigenin were observed in the acid hydrolysed extracts of the samples (Figure 4.14).

Flavonoid components from sawwort (*Serratula tinctoria* L.) and *Serratula coronata* L.

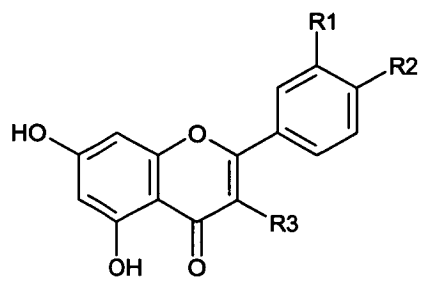

Quercetin:	R1 = R2 = R3 = OH
3-*O*-methylquercetin:	R1 = R2 = OH, R3 = OMe
Kaempferol:	R1 = H, R2 = R3 = OH
Luteolin:	R1 = R2 = OH, R3 = H
Apigenin:	R1 = R3 = H, R2 = OH

Figure 4.14: The main flavonoid constituents observed in the acid hydrolysed extract from a yarn dyed with sawwort

An accelerated ageing study of sawwort, dyed onto alum mordanted wool, was initiated to model the behaviour of sawwort dyed yarn over prolonged exposure to light. Most of the characteristic components were observed in the acid hydrolysed extract from the final sample of the accelerated ageing study (SWW_t_{final}), subjected to 4571 h of exposure in the light box (Chapter 6). However, the peak areas (monitored at 254 nm) were significantly less than those observed in the acid hydrolysed extract from the initial, unaged sample (SWW_t_0) and the relative ratios of the components had altered (Table 4.4). In addition, the relative amount of luteolin and 3-*O*-methylquercetin had to be calculated together, as they co-eluted in the PDA HPLC method.

Table 4.4: Relative peak areas (monitored at 254 nm) of the main flavonoid components in the acid hydrolysed extracts of alum mordanted wool dyed with sawwort

Sample	Relative peak area (monitored at 254 nm) / %			
Sawwort on wool	Luteolin + 3-*O*-Methylquercetin	Apigenin	Quercetin	Kaempferol
SWW_t_0	78	6	14	2
SWW_t_{final}	78 (luteolin only)	17	4	1

The difference in the relative ratios of the flavonoids present in the extracts of sawwort dyed yarn before and after ageing can be explained by the preferential degradation of the flavonols (quercetin and kaempferol) compared with the flavones (luteolin and apigenin) upon prolonged exposure to light. Previous accelerated ageing studies have shown that due to the hydroxyl group at the 3-position, the flavonols are particularly light sensitive.[1] In addition, solution studies have shown that the 3-OH group is a prerequisite for the formation of the depside.[18] In the acidic conditions encountered during the extraction of the dye from the yarn, the depside hydrolyses to give the corresponding hydroxybenzoic acids (Scheme 4.2).

Although the 2,4,6-trihydroxybenzoic acid produced from the A-ring is not observed in the acid hydrolysed extracts due to a decarboxylation reaction, leading to the formation of a mixture of components,[1] the hydroxybenzoic acid formed from the B-ring is often observed in the extracts from aged yarns dyed with flavonol containing sources. Furthermore, the hydroxybenzoic acid methyl ester is also formed in the acidic conditions present during the extraction procedure *via* an identical reaction undergone by the 4-hydroxybenzoic acid yarn degradation product (Scheme 4.1).

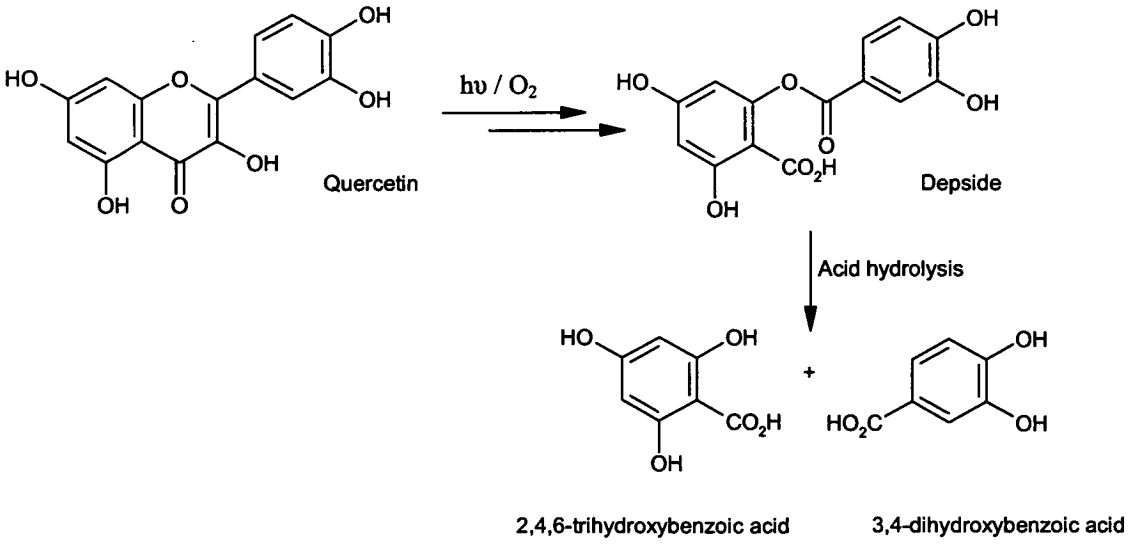

Scheme 4.2: The solution photo-oxidation of quercetin to the depside, followed by the formation of 2,4,6-trihydroxybenzoic acid and 3,4-dihydroxybenzoic acid during acid hydrolysis

The photo-degradation products of flavonols can therefore be characteristic of the original compound, sometimes allowing the dye source to be identified indirectly. However, in cases where flavonols are the minor constituents of a dye source, as in sawwort, these degradation products are often below the detection limits. Thus, the small amount of quercetin present on the unaged yarn probably accounts for the absence of 3,4-dihydroxybenzoic acid and its methyl ester in the aged yarn extracts.

The expected photo-degradation products from the flavonol, kaempferol, are 4-hydroxybenzoic acid and its methyl ester. Although these components were observed in the PDA HPLC analysis of extracts from aged yarn samples, they also appear in the aged, alum mordanted blank wool sample and are produced upon photo-degradation and acid hydrolysis of the aged wool or silk yarns (Section 4.2).

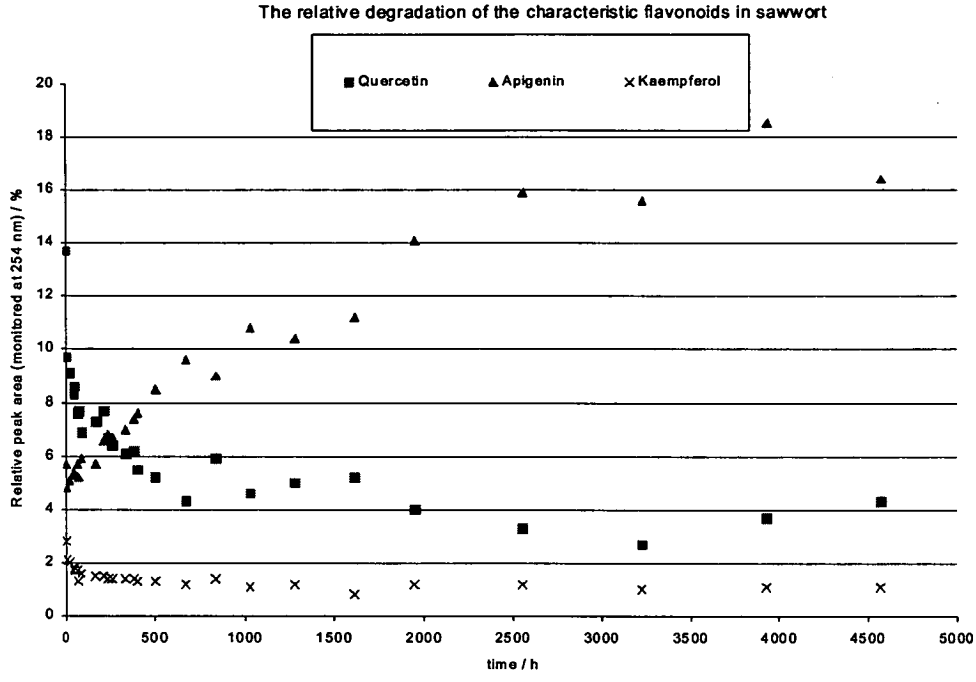

Figure 4.15: The relative degradation of some of the characteristic components in sawwort; quercetin, apigenin and kaempferol

The photo-degradation of the minor flavonol components in sawwort (quercetin and kaempferol) proceed at a faster rate than the flavone components such as luteolin. Consequently, there is a significant change in the flavonoid 'profile' observed in the extracts from aged yarns compared with a freshly dyed yarn after prolonged exposure to light (Figure 4.15), highlighting the problem associated with the use of flavonol components as biological source 'markers' in historical extracts.

A minor amount of 3-*O*-methyquercetin co-eluting with luteolin was identified by HPLC ESI MS analysis of the unaged yarn extract (Chapter 2). However, similar analysis of the acid hydrolysed extract from the final sample in the accelerated ageing study, exposed for 4571 h in the light box, found no evidence for the presence of 3-*O*-methylquercetin. The rate at which 3-*O*-methylquercetin photo-degrades would be expected to be less than quercetin, its light sensitive 3-hydroxy analogue, due to the presence of the methoxy group at the 3-position.[16] Thus, it is likely that only a relatively small amount of 3-*O*-methylquercetin was initially present.

The photo-degradation rate of the combined luteolin and 3-*O*-methylquercetin in the sawwort extracts was compared with the photo-degradation rate of luteolin in the weld extracts by examining the luteolin/apigenin ratio in both sets of samples (Figure 4.16).

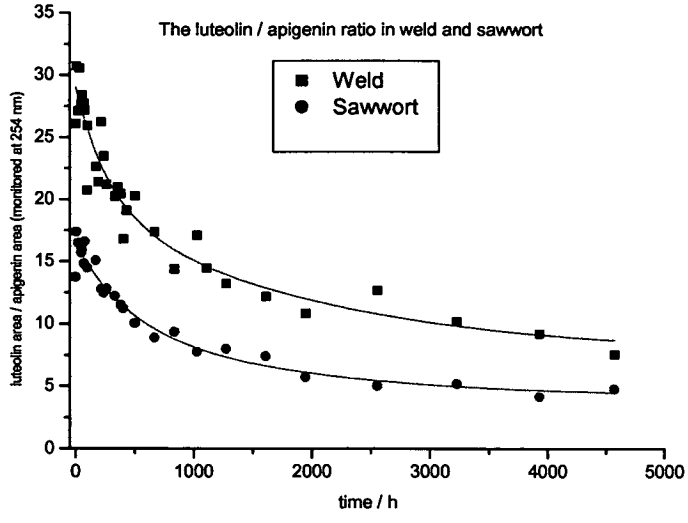

Figure 4.16: The luteolin / apigenin ratio of sawwort and weld

The degradation rates are similar, suggesting minimal perturbation in the rate of luteolin degradation by the 3-*O*-methylquercetin component, again indicating that only a small amount of 3-*O*-methylquercetin was present in the sawwort extracts. However, more comprehensive studies, should be undertaken to assess the suitability of 3-*O*-methylquercetin as a biological species 'marker' component for sawwort on historical yarns.

Although sawwort is mentioned in historical dye manuals as an alternative dye source to weld,[19] published evidence from the analysis of historical textiles for its use does not exist. Furthermore, no evidence was found for the use of sawwort in any of the historical yarn extracts sampled as part of the MODHT project (Chapter 5). These accelerated ageing results may go some way towards explaining why

analytical evidence for the use of sawwort in historical samples is difficult to obtain, despite the distinctive profile of the extracts from freshly dyed sawwort yarns.

The acid hydrolysed extracts from severely photo-degraded yarns dyed with sawwort may only contain luteolin and apigenin due to the poor light fastness of the flavonol components. The ratio of these components (monitored at 254 nm) from the aged sawwort sample would also be similar to those expected from an aged weld extract. The flavonoid profile for sawwort can therefore be mistaken for weld if the PDA HPLC results are interpreted solely on the detection of luteolin and apigenin. Thus, the detection of at least a trace amount of chrysoeriol with luteolin and apigenin is very important for the assignment of weld as the dye source rather than sawwort.

Furthermore, if an historical sample was dyed with sawwort in combination with another source such as weld or dyer's greenweed, it is likely that the use of sawwort would remain undetected, since both luteolin and apigenin are also found in the acid hydrolysed extracts of the other sources. The development of 'softer' extraction methods may make it possible to observe components not currently detected using acid hydrolysis,[20] such as characteristic glycosides, which might then allow aged sawwort to be easily distinguished from sources such as weld.

4.6 Young fustic (*Cotinus coggygria* Scop.)

The main colouring components from young fustic have been identified as the aurone, sulfuretin, and the flavonol, fisetin (Figure 4.17). The identity of several minor components was also conjectured (Chapter 2), although the relatively small amounts of these compounds observed in the acid hydrolysed extracts probably preclude their usefulness as species identifiers when analysing historical yarns.

Components from young fustic (*Cotinus coggygria* Scop.)

Fisetin

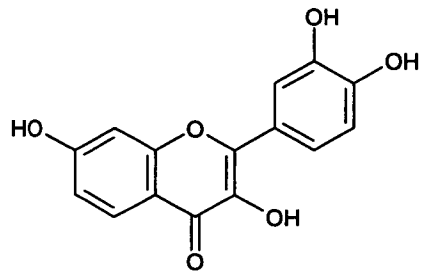

Sulfuretin

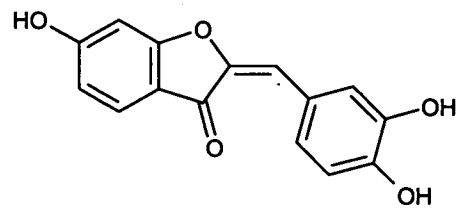

Figure 4.17: The major constituents observed in the acid hydrolysed extract of yarn dyed with young fustic

The acid hydrolysed extracts from the reference samples dyed for the MODHT project (Y/S3a and Y/S3b) contained only a very small amount of the two main colouring components, fisetin and sulfuretin. Ellagic acid was also observed in the acid hydrolysed extracts, most probably from tannins present in the wood used in the dyebath. The presence of ellagic acid may also help in identifying young fustic as a possible dye source, although only when identified along with other characteristic components.

Although fisetin (a flavonol) is known to be highly light fugitive,[1,21] the photo-degradation characteristics of sulfuretin (an aurone) were unknown. Thus, an accelerated ageing study of young fustic dyed onto alum mordanted silk (Y/S3b) was initiated. The peak area of sulfuretin (monitored at 254 nm), expressed as a percentage of the peak area obtained in the unaged sample extract (per mg of yarn), has been plotted against the time (h) that each yarn sample was exposed in the accelerated ageing chamber (Figure 4.18).

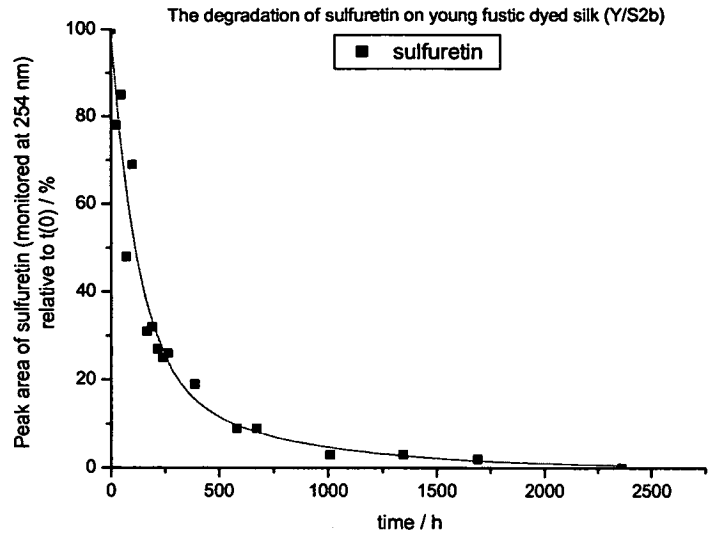

Figure 4.18: The degradation of sulfuretin in young fustic, expressed as a percentage of the amount of sulfuretin in the extracts compared with the extracts from the unaged yarn (per mg of yarn)

The yarn was not very strongly dyed and after only 2000 h of exposure in the light box, almost no sulfuretin was present in the acid hydrolysed extracts and no significant degradation products were observed. The aurone, sulfuretin is therefore not likely to be a suitable marker in the identification of a young fustic source from a faded historical yarn. However, as this was a very light coloured yarn, containing small amounts of sulfuretin (and fisetin), the extracts from a young fustic dyed yarn produced at the National Museums of Scotland (Chapter 6) were examined. These contained a significantly larger amount of the main colouring components, so a yarn sample was aged in the accelerated ageing box for 1342.5 h to investigate the formation of any significant degradation products.

The two distinctive components of young fustic, fisetin and sulfuretin, were both observed in the acid hydrolysed extracts from the yarn after exposure in the light box. The peak areas (monitored at 254 nm) were, however, less than those observed in the acid hydrolysed extract from the initial, unaged sample. Furthermore, as a consequence of the photo-degradation of fisetin, the acid hydrolysed extracts contained 3,4-dihydroxybenzoic acid and its methyl ester (Figure 4.19).

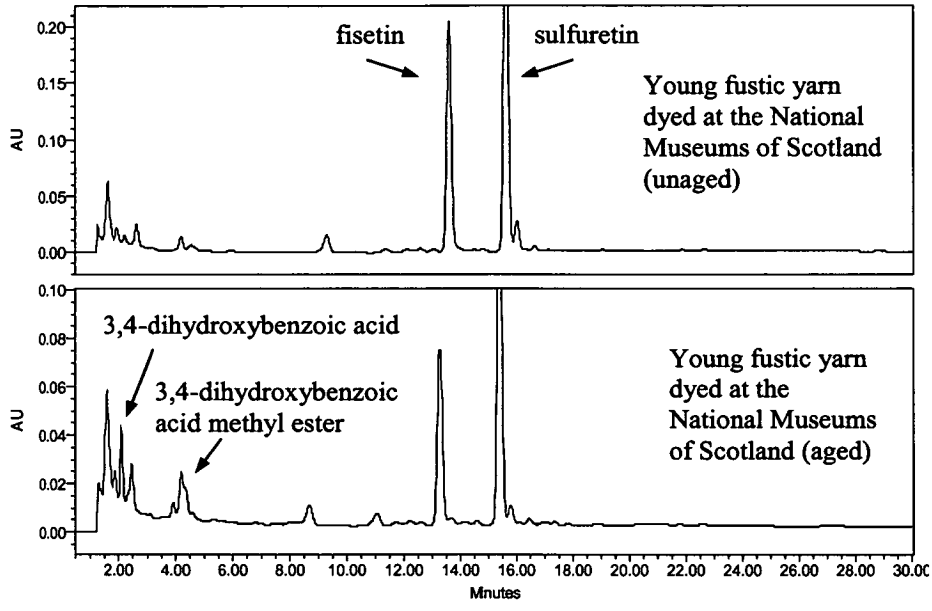

Figure 4.19: The chromatograms (monitored at 254 nm) from the acid hydrolysed extracts of an unaged yarn sample dyed with young fustic (top) and the extracts from a yarn which has undergone accelerated ageing in the light box for 1342.5 h

These components were formed by an identical pathway to that of the quercetin photo-degradation products, outlined in Section 4.5 (Scheme 4.2). Thus, the acid hydrolysed extracts from photo-degraded yarns dyed with young fustic may contain characteristic degradation products, indicative of the source.

4.7 Cochineal (*Dactylopius coccus* Costa)

The characteristic components observed in the acid hydrolysed extracts from yarn dyed with cochineal are all structurally related anthraquinones (Chapter 3). The dcIV and dcVII components were found to be isomers of carminic acid, most probably differing only in the stereochemistry of the sugar moiety. Furthermore, on the basis of experimental results from mass spectrometry and UV-Vis analysis, the anthraquinone core of carminic acid differed from that of the dcII component by the presence of an additional phenolic group (Figure 4.20). The aglycones of both structures, flavokermesic acid and kermesic acid, were also observed in the acid hydrolysed extracts.

Components from cochineal (*Dactylopius coccus* Costa)

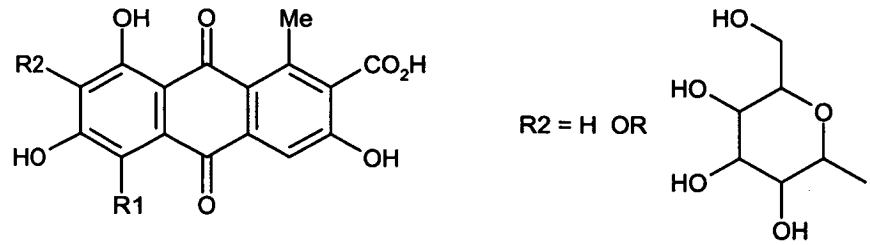

Carminic acid:	R1 = OH, R2 = hexose (glucose)
dcII:	R1 = H, R2 = hexose
dcIV:	R1 = OH, R2 = hexose
dcVII:	R1 = OH, R2 = hexose
Kermesic acid:	R1 = OH, R2 = H
Flavokermesic acid:	R1 = R2 = H

Figure 4.20: The characteristic constituents observed in the acid hydrolysed extracts of cochineal dyed yarns

The identification of the particular coccid species used for dyeing can sometimes be achieved by examining the type and relative ratio of the components observed in the acid hydrolysed extracts.[22,23] For example, the extracts from yarn dyed with Polish cochineal (*Porphyrophora polonica* L.) contain a smaller percentage of dcII and carminic acid compared with extracts from Mexican cochineal (*Dactylopius coccus* Costa), but a larger percentage of the aglycones flavokermesic acid and kermesic acid.[24]

If the characteristic ratios obtained from the acid hydrolysed extracts were to change significantly upon prolonged exposure of the dyed yarn to light, species identification could become problematic, if not impossible. Although there is some published data on the ageing of carminic acid in solution and on painted layers,[25] there have been no investigations into the effects of photo-degradation on the relative ratios of the characteristic components from dyed yarns. An accelerated ageing experiment was therefore conducted on alum mordanted wool dyed with Mexican cochineal (*Dactylopius coccus* Costa) in order to model the relative degradation of the components upon prolonged exposure to light (Table 4.5).

Table 4.5: The characteristic components observed in the acid hydrolysed extracts of alum mordanted wool dyed with cochineal (R/W5). Yarn samples were placed into the accelerated ageing box then removed and analysed at The Royal Institute for Cultural Heritage (KIK)[14]

Time / h	Relative peak area (monitored at 255 nm) / %					
	dcII	Carminic acid	dcIV	dcVII	Flavokermesic acid	Kermesic acid
0	4	91	2	2	1	0
50	3	91	2	2	1	1
95.25	3	90	2	2	2	1
265.33	3	91	2	2	2	1
698.42	5	89	2	3	1	0
3706.75	5	88	2	3	1	1

The relative ratios of the components from the aged yarns remain very similar to the ratios in the extracts from a freshly dyed yarn. The similarity in the photo-degradation rates of the main components in cochineal is most probably due to their close structural relationship. The anthraquinone cores of carminic acid, dcIV, dcVII and kermesic acid are identical, with the core of dcII and flavokermesic acid differing from the other components only in the absence of a phenolic group (R1 = H). Furthermore, the data suggests that there is no significant difference in the photo-stability of the glycosidic components (carminic acid, dcII, dcIV and dcVII) compared with the aglycone components (flavokermesic acid and kermesic acid), thus, the presence of the sugar moiety does not significantly alter the photo-degradation mechanism.

The anthraquinone core is responsible for the relative stability of these characteristic components when compared with other natural colourants, such as the yellow flavonoids, for example. This marked difference in degradation rates between the two classes of compounds (flavonoids and anthraquinones) is also apparent on the historical tapestries themselves, where areas of yellow dyed yarn have almost completely lost their colour, in contrast to the red dyed areas which often remained richly coloured. Furthermore, no significant photo-degradation products were observed in the extracts of cochineal dyed yarn aged in the accelerated ageing box. A longer study, or one using harsher ageing conditions, would therefore be recommended to investigate the apparent similarity of the relative degradation rates for the characteristic cochineal components over prolonged periods.

The interpretation of data from historical yarn samples is therefore unlikely to be complicated by the preferential degradation of some of the characteristic components, so the identification of a particular species on an historical yarn remains theoretically possible. The accelerated ageing study and the characterisation of the minor components (Chapter 3) have therefore allowed the ageing characteristics of dyed yarns to be better understood, improving the confidence of assigning Mexican cochineal as the most probable biological dye source in historical yarn samples (Chapter 5).

4.8 Brazilwood (*Caesalpinia sappan* L.)

The PDA HPLC analysis of the acid hydrolysed extracts from historical yarns often yields the unaltered dye source components, allowing the direct identification of the biological species in many cases. However, in some instances, such as with the neoflavonoids/homoisoflavonoids, the extraction process can alter the principal dyeing components (Figure 4.21), leaving 'marker compounds' which can then be related to the dye source. Careful studies must be undertaken to ensure that the observed components can be directly linked to the use of certain biological dye sources (Chapter 3).

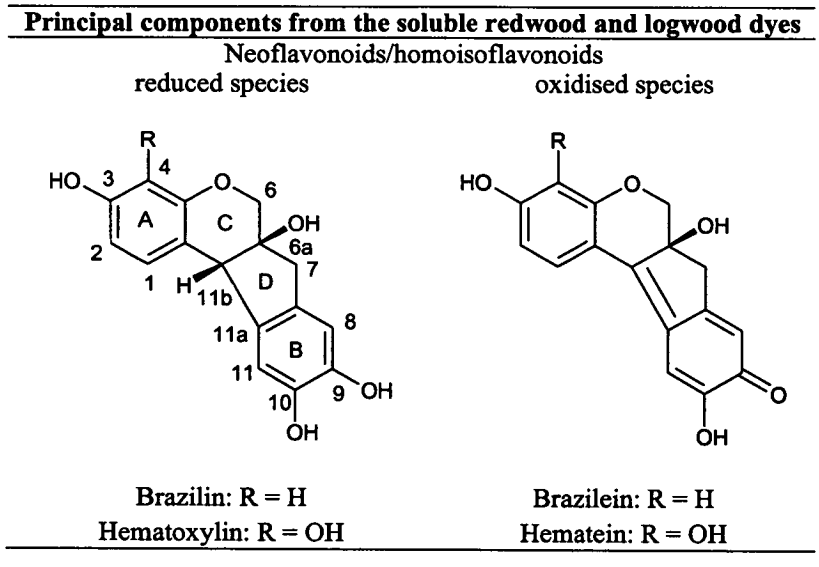

Figure 4.21: Neoflavonoid/homoisoflavonoid derivatives such brazilin and hematoxylin (reduced) and brazilein and hematein (oxidised)

Although the structure of the brazilwood 'marker component' was not elucidated, nor its exact relationship to the principal dyeing component ascertained (Chapter 3), a yarn dyed with brazilwood powder was aged in the accelerated ageing box and the photo-degradation of the 'marker component' and brazilin monitored over 4232.42 h (Figure 4.22). The photo-degradation of brazilein was not monitored due to its sensitivity to the extraction conditions. For the same reason, no accelerated ageing studies were performed on hematein dyed yarns.

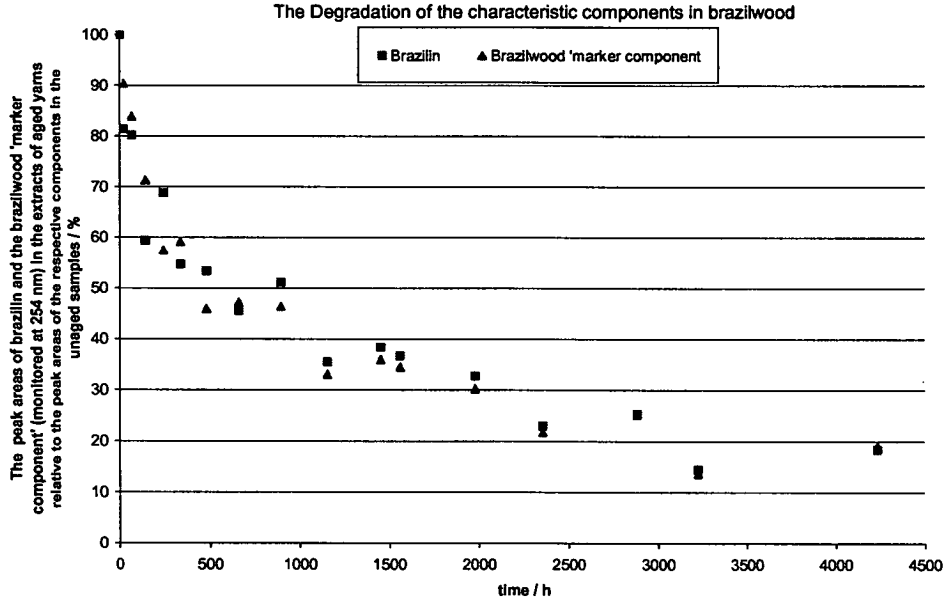

Figure 4.22: The degradation of brazilin and the brazilwood 'marker component' expressed as a percentage of the amount of the respective components from extracts of the unaged yarn (per mg of yarn)

The photo-degradation rates of the two components were identical and *ca.* 20% of both components remained after 4232.42 h exposure in the light box compared with the amounts in the extract from an unaged yarn. Furthermore, no significant degradation peaks were visible in the aged extracts. Thus, the brazilwood 'marker component' is likely to be observed in the extracts of yarns which have undergone prolonged exposure to light, and which may appear almost colourless.

4.9 Summary

Reference yarns dyed with different natural dye sources were aged by prolonged exposure to light and the characteristic components from the acid hydrolysed extracts compared with those from the unaged equivalents. The identification of biological sources such as weld and dyer's greenweed from the aged yarns presented fewer problems than the identification of sources such as sawwort and young fustic. The difficulties encountered in dye source identification from the aged yarns dyed with sawwort and young fustic were due to the relatively faster photo-degradation rates of the distinguishing components.

In contrast, the close structural similarities between the characteristic components observed in the extracts of Mexican cochineal dyed yarns resulted in similar photo-degradation rates for the components on the dyed yarns. Thus, the dye source is easily identified from the extracts of an aged yarn. The results from the photo-degradation of the brazilwood 'marker component' suggest that it may also be observed in the extracts from yarns which have undergone prolonged exposure to light.

These studies have allowed the accurate identification of the dye sources used in many of the yarns sampled from the selected historical tapestries (Chapter 5). Information on the dye sources may also prove to be necessary for an effective assessment of the damage to historic tapestries (see below).

4.10 The Monitoring of Damage to Historic Tapestries

The studies into the degradation phenomena of the distinct wool and silk components were conducted on the MODHT reference dyed yarns and woven models. The analysis of both the unaged and aged reference yarns using different physical and chemical techniques (Chapter 1) found that the dye sources and dyeing procedures significantly influenced the results.[26,27,28,29]

The tensile strength measurements from the majority of the unaged dyed wool samples were fairly similar, with a minimum percentage elongation of 19.48% for

the weld dyed yarn overdyed with woad (G/W1), and a maximum value of 32.10% elongation for the woad dyed yarn (Bl/W1).[26] The weld dyed yarn (Y/W1) also had a relatively low percentage elongation of 21.5%, suggesting that dyeing with weld weakened the yarns relatively more than dyeing with the other natural sources.

Weld dyeing was carried out by first boiling the yarn with an alum mordant (pH 4) for 2 h and then boiling with weld and potassium carbonate (pH 10.2) for 1 h (Appendix 7.2). The strongest yarn, dyed with woad (Bl/W1), was dyed according to medieval practice in a woad vat by bacterial reduction at 45-50 °C and with pH 8.2-8.5 *i.e.* the dyeing conditions for the weld dyed yarn were significantly harsher than those for the woad dyed yarn, causing a relatively greater amount of damage to the yarn and thus a greater reduction in its tensile strength. In addition, dyeing with iron sulfate, which utilized similarly harsh conditions, also had a deleterious effect on the tensile strength of the yarns. Interestingly, when woad was overdyed onto a weld dyed yarn (G/W2), the yarn was not significantly weaker than the other reference samples, indicating that the indigo dyeing process increased the mechanical properties of the yarn.

However, after accelerated ageing, the same trends were not maintained, thus the factors responsible for the weakening of the yarns during the dyeing process are not the same as those imparting vulnerability to increased degradation during light ageing.[26] These results highlight the importance of ageing studies using reference yarns. The reference samples showing a particularly large increase in degradation after accelerated ageing included the red yarns dyed with brazilwood and those dyed with madder. The tensile strength of the black dyed yarns containing iron sulfate were also greatly affected upon ageing. Significantly, brazilwood is a particularly light fugitive dye while madder is less so, thus, the colour remaining on an historical tapestry may not necessarily be immediately indicative of its structural integrity.

In general, less degradation due to the processing conditions were found in the silk models compared with the analogous wool samples.[26] This is in contrast to the degradation caused by accelerated ageing, which was generally higher in the silk

samples compared with wool *i.e.* the silk yarns were less effected by the dyeing and mordanting processes than by photo-degradation reactions during ageing. The silk sample dyed with woad showed the most favourable mechanical properties, like its wool counterpart,[26] and although there was even less variation amongst the silk yarns dyed with different sources compared with the wool yarns, brazilwood and madder again demonstrated inferior mechanical properties both before and after accelerated ageing.[26]

The tensile strength results from the reference samples were then correlated with the results from calibrated amino acid analysis,[14] and size exclusion chromatography (silk samples only).[26] This was necessary as the small sample size and limited number of samples meant that tensile strength measurements could not be performed on the samples from the historic tapestries.

The calibrated amino acid analysis of both wool and silk historical yarns was successfully employed to measure the extent of oxidative degradation. Interestingly, all the samples were in a more advanced state of degradation than originally suspected.[14] This was surprising given the fact that the majority of the samples had been taken from the reverse of the textile, which would not have been exposed to light when on display. This suggests that factors other than light exposure may also be important in the degradation of historical yarns.

The historical silk yarns analysed by SEC also had consistently low average molecular weight distributions when compared with reference yarns subjected to accelerated ageing conditions.[26] In addition, a large variation in the molecular weight distribution of yarns within the same tapestry was observed.[26] This may be due to the use of different dye sources, although no firm correlations could be obtained.

4.11 Conclusion

The analysis of the reference and historical yarns highlight that both the dyeing process and natural or accelerated ageing, produce damage in the yarns that will ultimately affect the structural integrity of the tapestries themselves. As the dyeing

method is dependent on the natural source used, accurate identification of the original dye source may prove to be an important factor when assessing damage to historic tapestry structures.

4.12 References

[1] Ferreira, E.S.B, *'New Approaches towards the identification of yellow dyes in ancient textiles'*, PhD Thesis, **2002**, The University of Edinburgh

[2] Ferreira, E.S.B.; Quye, A.; Hulme, A.N.; McNab, H., *'LC-Ion Trap MS and PDA-HPLC – Complementary Techniques in the Analysis of Flavonoid Dyes in Historical Textiles: The Case Study of an 18th Century Herald's Tabard'*, Dyes Hist Arch, **2003**, 19, 13-18

[3] Petroviciu I.; Wouters, J., *'Analysis of Natural Dyes from Romanian 19th- and 20th-Century Ethnographical Textiles by DAD-HPLC'*, Dyes Hist Arch, **2002**, 18, 57-62

[4] Trojanowicz, M.; Orska-Gawryś, J.; Surowiec, I.; Szostek, B.; Urbaniak-Walczak, K.; Kehl, J.; Wrobel, M, *'Chromatographic Investigation of Dyes Extracted from Coptic Textiles from the National Museum in Warsaw'*, Stud Conserv, **2004**, 49, 115-130

[5] Feller, R.L., *'Accelerated Aging: Photochemical and Thermal Aspects'*, **1994**, The J. Paul Getty Trust, 1st edition

[6] Saunders, D.; Kirby, J., *'Light induced damage: Investigating the reciprocity principle'*, Preprints to the ICOM Committee for Conservation 11th triennial meeting, **1996**, 1, 87-90

[7] Saunders, D.; Kirby, J., *'A Comparison of Light-Accelerated Ageing Regimes in Some Galleries and Museums'*, Conservator, **2001**, 25, 95-104

[8] Ashley-Smith, J.; Derbyshire, A.; Pretzel, B.; *'The continuing development of a practical lighting policy for works of art on paper and other object types at the Victoria and Albert Museum'*, Preprints to the ICOM Committee for Conservation 13th triennial meeting, **2002**, 1, 3-8

[9] Criado, S.; Marioli, J.M.; Allegretti, P.E.; Furlong, J.; Nieto, F.J.R.; Martire, D.O., Garcia, N.A., *'Oxidation of di- and tripeptides of tyrosine and valine mediated by singlet molecular oxygen, phosphate radicals and sulphate radicals'*, J Photoch Photobio B, **2001**, 65, 74-84

[10] Endo, K.; Seya, K.; Hikino, H., *'Photo-oxidation of L-Tyrosine, an efficient 1,4-Chirality Transfer Reaction'*, J Chem Soc Chem Commun, **1988**, 934-935

[11] Earland, C.; Stell, J.G.P., *'The reaction of silk fibroin with oxidizing agents'*, Biochim Biophys Acta, **1957**, 23, 97-102

[12] Baltova S.; Vassileva, V., *'Photochemical behaviour of natural silk – II. Mechanism of fibroin photodestruction'*, Polym Degrad Stabil, **1998**, 60, 61-65

[13] Lewin, M.; Pearce, E.M. (eds.), *'Handbook of Fiber Chemistry'*, **1998**, International Fiber Science and Technology series / 15, Marcel Dekker Inc., 2nd edition

[14] Lamens, K.; Vanden Berghe, I.; Wouters, J., *Unpublished data*, **2005**, The Royal Institute for Cultural Heritage (KIK), Belgium

[15] Cristea, D.; Bareau, I.; Vilarem, G., *'Identification and quantitative HPLC analysis of the main flavonoids present in weld (*Reseda luteola *L.)'*, Dyes Pigments, **2003**, 57, 267-272

[16] Tournaire, C.; Croux, S.; Maurette, M-T.; Beck, I.; Hocqquaux, M.; Braun, A., *'Antioxidant activity of flavonoids: efficiency of singlet oxygen quenching'*, J Photoch Photobio B, **1993**, 19, 195-215

[17] Smith, G.J.; Thomsen, S.J.; Markham, K.R.; Andary, C.; Cardon, D., *'The photostabilities of naturally occurring 5-hydroxyflavones, flavonols, their glycosides and their aluminium complexes'*, J Photoch Photobio A, **2000**, 136, 87-91

[18] Matsuura, T.; Matsushima, H.; Nakashima, R., *'Photosensitized oxygenation of 3-hydroxyflavones as a nonenzymatic model for quercetinase'*, Tetrahedron, **1979**, 26, 436-443

[19] Bancroft, E., *'Experimental Refearches concerning the philosophy of permanent colours'*, **1794**, Vol. 1, London, 410-415

[20] Laursen, R.A.; Zhang, X., *'Development of mild extraction methods for the analysis of natural dyes in textiles of historical interest using LC-diode array detector-MS'*, Anal Chem, **2005**, 77, 2022-2025

[21] Poteau, X.; Saroja, G.; Spies, C.; Brown, R.G., *'The photophysics of some 3-hydroxyflavone derivatives in the presence of protons, alkali metal and alkaline earth cations'*, J Photoch Photobio A, **2004**, 162, 431-439

[22] Wouters, J., *'High Performance Liquid Chromatography of Anthraquinones: Analysis of plant and insect extracts and dyed textiles'*, Stud Conserv, **1985**, 30, 119-128

[23] Hofenk de Graaff, J.H., *'The Colourful Past: Origins, Chemistry and Identification of Natural Dyestuffs'*, **2004**, Abegg-Stiftung and Archetype Publications Ltd., 1st edition, 52-91

[24] Wouters J.; Verhecken A., *'The Coccid insect dyes: HPLC and computerized diode-array analysis of dyed yarns'*, Stud Conserv, 34, **1989**, 189-200

[25] Favaro, G.; Miliani, C.; Romani, A.; Vagnini, M., *'Role of protolytic interactions in photo-aging processes of carminic acid and carminic lake in solution and painted layers'*, J Chem Soc Perkin Trans 2, **2002**, 192-197

[26] Hallet, K.; Howell, D., *'Size exclusion chromatography of silk – inferring the tensile strength and assessing the condition of historic tapestries'*, Preprints to the ICOM Committee for Conservation, 14th Triennial meeting, The Hague, **2005**, 2, 911-919

[27] Hallet, K.; Howell, D., *'Size exclusion chromatography as a tool for monitoring silk degradation in historic tapestries'*, Postprints to the AHRB Research Centre for Textile Conservation and Textile Studies 1st Annual Conference, **2005**, 143-150

[28] Hacke, A-M., PhD Thesis, **2006**, The University of Manchester

[29] Odlyha, M.; Wang, Q.; Foster, G.M.; de Groot, J.; Horton, M.; Bozec, L., *'Thermal analysis of model and historic tapestries'*, J Therm Anal Calorim, **2005**, 82, 3, 627-636

Chapter 5

5 DYE ANALYSIS OF HISTORICAL YARN SAMPLES

The different biological species employed to dye the yarns in a selection of high status tapestries, woven from the 15th to the 17th century and now housed in collections across Europe, were investigated. The results from the dye analysis, conducted by PDA HPLC on the acid hydrolysed yarn extracts, are presented. The emphasis has been placed on the interpretation of the results from the yellow and green yarns, analysed as part of this thesis. In addition, the significant results from the red coloured yarns, analysed by the Royal Institute for Cultural Heritage, Belgium (KIK) have been summarised.

5.1 The historic tapestries

Historic tapestries in varying degrees of preservation were selected and sampled from sites in both northern and southern European locations (Table 5.1). Many of the tapestries were of high monetary and cultural value and housed within Royal collections, so a relatively large amount of documentary evidence existed regarding their histories. The selection took several variables into consideration, including their current state of preservation, the amount and nature of previous conservation treatments, and both their past and current display or storage conditions.

Table 5.1: The historic tapestries, sampled from sites in both northern and southern European locations with varying degrees of past conservation

Code	Current location	Title	Place (and date) of manufacture	Conservation / restoration history
TOU 1	Tournai	Story of St Piatus and Eleutherius	Arras 1402	Restored around 1850
BXL 3	Brussels	The Legend of Herkenbald	Brussels 1513	1975 (traces of older restorations also found)
HRP 1	London	The Triumph of Time Over Fame	Brussels *ca.* 1515	1919 (W. Morris Comp.) - most silk weft is restored
HRP 3	London	The Triumph of Death over Chastity	Brussels *ca.* 1515	Damaged by fire in the 1880's, but received little or no repair work
BXL 1	Brussels	Justitia disarmed by Misericordia	Brussels 1519-1524	Traces of old restoration work evident
BXL 4	Brussels	Man and the Seven Sins	Brussels 1519-1524	Traces of old restoration work evident
BXL 2	Brussels	Christ before Pilate	Brussels *ca.* 1520	Good condition with only minor restoration work
BRU 1	Bruges	Verdure with coat of arms	Bruges *ca.* 1530	1959 (De Wit) and 1987 (KIK)
HRP 2	London	Tobias and Raphael taking leave of Tobit	Brussels *ca.* 1544-46	Repaired and relined in 1714, conservation work at Hampton Court (1990)
PNM 1	Madrid	The Fall of Icarus	Brussels *ca.* 1545	No known previous conservation work
PNM 2	Madrid	Perseus liberates Andromeda	Brussels *ca.* 1545	Previous conservation treatment (details not known)
PNM 5	Madrid	The Sacrifice of Polyxena	Brussels *ca.* 1545	No known previous conservation work
PNM 7	Madrid	Raphael presented by Tobias to his father	Brussels *ca.* 1550	No known previous conservation work
PNM 8	Madrid	Atalanta wounds the wild boar from Calydon	Bruges *ca.* 1620	No known previous conservation work
BRU 3	Bruges	Miracles of Holy Mary of the Potterie	Bruges *ca.* 1630	Probably restored pre-1910, then 1925 (Chaudoir) & 1987 (KIK)
BRU 2	Bruges	Mary's dedication in the temple	Bruges 1639	1987 (KIK)
PNM 9	Madrid	Vine Arbour Galleries	Antwerp *ca.* 1660	No known previous conservation work

The following three sections describe the tapestries selected from each of the sampling locations; Spain (Section 5.1.1), Belgium (Section 5.1.2) and the United Kingdom (Section 5.1.3) respectively, and are largely based on curatorial reports that were compiled specifically for the MODHT project.[1,2,3] These comprehensive reports detailed the title of the sampled tapestries, together with the series to which they belonged, their date of manufacture and any additional information, where known, regarding the designer or weaver. Also included were descriptions of the iconography and the display and conservation histories of the artefacts. This

information has been summarised here to enable the varying histories and states of preservation of the tapestries to be compared and contrasted with one another. Following this, the results obtained from the dye analysis of 487 historical yarns, sampled from the reverse of the artefacts, are examined. Further details of the sampling protocol can be found in Chapter 6.

5.1.1 Spanish collection

The tapestries from the Spanish Royal collection, housed in Madrid, have spent time in storage, but have also been used at various times for permanent exhibition and ceremonial occasions at the Royal Court. Indeed, the tapestries from this collection are unique within the present study, as to this day they remain an integral part of the working life at the Royal Court. For example, tapestries were used to decorate the Palace for a recent Royal wedding (Figure 5.1).

Figure 5.1: The tapestries used to decorate the Royal Palace, Madrid for a recent Royal wedding, on view to the public after the event © Dr Concha Carretero Herrero, Patrimonio Nacional, Palacio Real, Madrid

Six tapestries from the Spanish Royal collection (PNM 1, 2, 5, 7-9) were sampled, with their place and date of manufacture covering much of the period of interest (Table 5.2).

Table 5.2: A summary of the place and date of manufacture of the selected tapestries from Spain

PNM 1	PNM 2	PNM 5	PNM 7	PNM 8	PNM 9
Brussels				Bruges	Antwerp
ca. 1545			*ca.* 1550	*ca.* 1620	*ca.* 1660

Additionally, the selection represented tapestries from the Spanish Royal collection with differing but typical display histories, especially over the last fifty years *i.e.* some had been used in ceremonies of court, some had been on permanent exhibition, while others had remained in storage and never been exhibited.[1]

5.1.1.1 PNM 1, 2 and 5

'The Tales of Ovid' series (Brussels, *ca.* 1545) was manufactured by Wilhelm Pannemaker (a monogram appears on all the tapestries), with cartoons attributed to Jan Cornelisz Vereyen and Pierre Coeck van Aelst. Gold and silver metal threads are present in these three tapestries, in contrast to the remaining Spanish tapestries sampled during this study (PNM 7-9), where no metal threads were utilised.[1]

The tapestries represent scenes from Ovid's Metamorphosis, with the first tapestry to be sampled, 'The Fall of Icarus' (PNM 1), depicting the story of the boy who flew too close to the sun. The second tapestry, 'Perseus liberating Andromeda' (PNM 2) represents the story of Perseus, who falls in love with Andromeda and rescues her from imprisonment, while 'The Sacrifice of Polyxena' (PNM 5) illustrates the story of Agamemnon, who sacrifices Polyxena to appease the ghost of Achilles. Two further tapestries belonging to this series, 'The Abduction of Gannymede' (PNM 3) and 'Apollo's flaying of Marsyas' (PNM 4) were not sampled due to time constraints.

The display history of these tapestries is typical for all the tapestries sampled from the Spanish Royal collection, however, only 'Perseus liberating Andromeda' (PNM 2) is known to have received past conservation work.[1]

5.1.1.2 PNM 7

'Raphael presented by Tobias to his father' (PNM 7) from the biblical series 'The Story of Tobias' (Brussels, *ca.* 1550) is attributed to Baltasar van Vlierden with cartoons by Bernard van Orley.[1] The tapestry illustrates a scene from the Old Testament with the guardian angel, Rapheal, who has been sent to cure Tobit of his blindness so that he might see God's light again.

The display history of this tapestry is again typical for those from the Spanish Royal collection. However, it has a counterpart in the Hampton Court Palace collection, 'Tobias and Raphael taking leave of Tobit' (HRP 2) which was sampled during the United Kingdom sampling campaign. This allowed a unique comparison of tapestries from a parallel series housed in different European locations.

5.1.1.3 PNM 8 and 9

The two remaining tapestries represent 17th century tapestry makers and were chosen because they originated from two important centres of production in the Low Countries; Bruges and Antwerp.

The Bruges trademark appears in the edging of 'Atalanta wounds the wild boar from Calydon' (PNM 8). The imagery for this tapestry again comes from Ovid's Metamorphosis, with the story of Atalanta, the girl warrior who wounds the wild boar let loose by the goddess Diana.

The monogram of Jacob Wauters, one of the most important 17th century Antwerpian manufacturers, appears in the 'Vine Arbour Galleries' (PNM 9) tapestry, despite having lost a large part of its textile and lower edging during the 19th century.[1]

5.1.2 Belgian collection

The sampling campaign in Belgium took place in three separate locations. One tapestry was sampled in Tournai, three in Bruges and four in Brussels. Together, their place and dates of manufacture cover much of the period of interest (Table 5.3).

Table 5.3: A summary of the place and date of manufacture of the selected tapestries from Belgium

BXL 1	BXL 2	BXL 3	BXL 4	TOU 1	BRU 1	BRU 2	BRU 3
Brussels				Arras	Bruges		
ca. 1520		1513	*ca.* 1520	1402	*ca.* 1530	1639	*ca.* 1630

None of the tapestries have city or weavers' marks, as many were woven in Brussels before weavers' marks became compulsory in 1528. However, associated documentation has, in many cases, provided information regarding both the designer and weaver.

5.1.2.1 TOU 1

'The Story of St Piatus and Eleutherius' (Arras, 1402) are two tapestries currently displayed in the cathedral of Tournai, Belgium. They were ordered by a cleric of the Cathedral of Tournai, Toussaint Prier, woven by Pierrot Ferre of Arras and delivered in December 1402. The tapestries illustrate the legendary history of the first apostles of Christendom in Tournai and its vicinity.[2]

Originally there were two large tapestries with nine scenes each, but only fourteen of the scenes have survived. The tapestries were used to decorate the pews at special occasions until the beginning of the 17th century. By the beginning of the 19th century they were being used as carpets and as patches on the roof. Around 1850, the four largest remaining fragments were washed and restored and since 1873 have been on display in the Chapel of the Holy Spirit. They were washed again in 1999 by the Royal Manufacturer De Wit, Malines.[2]

5.1.2.2 BXL 1 and 4

'Justitia disarmed by Misericordia' (BXL 1) and 'Man and the seven sins' (BXL 4) belong to the set of four tapestries known as 'Virtues and Vices' (Brussels, 1519-24) originally bought by the cathedral of Palencia (Spain) and hung in 1524. The remaining two tapestries in the series are 'The Peace' and 'The Prodigal Son'. The battle between virtues and vices in man evicted from paradise after the fall is one of the main themes in medieval religious iconography.[2]

The tapestries were purchased by the Royal Museum of Art and History, Brussels, in 1964. Another complete, but less detailed edition of 'Justitia disarmed by Misericordia' and a broader right part of 'Man and the Seven Sins' are preserved at Hampton Court Palace, London, but were not sampled during this project. Traces of old restorations have been found on all of these tapestries.

5.1.2.3 BXL 2

'Christ before Pilate', (Brussels, *ca.* 1520) was part of a set of four 'Passion' tapestries, of which two are in the Spanish Royal collection and one is in the Rijksmuseum, Amsterdam. The tapestry contains gold and silver metal threads and represents the final phase of the trial of Jesus. In the upper zone, four more scenes from the Passion are represented, with the two outer scenes inspired by a work of Albert Durer, 'The Great Passion' (1511).[2]

The piece bought by the Royal Museum of Art and History, Brussels in 1962 came from the Ildebrando Bossi collection in Genua. The tapestry is in good condition, with only minor restorations.

5.1.2.4 BXL 3

'The legend of Herkenbald', (Brussels, 1513) is a unique piece, not woven in a set and now owned by the Royal Museum of Art and History, Brussels. The tapestry was ordered for the church of St Peter in Leuven by the Confrerie of the Saint Sacrament and was designed by Jan Van Roome and woven in Brussels by Leon. The theme for this tapestry was taken from the 'Dialogus miraculorum', by the Cistercian monk Caesarius of Heisterback (1219-1223) and is the legend of the righteous judge Erkenbaldus de Burdan or Herkenbald.[2]

The tapestry was displayed in the chapel in 1513, although it is not known if this was on a permanent basis or for special occasions only. It was sold to the Royal Museum of Art and History, Brussels, in 1862 and conservation treatment was performed at

the Royal Institute for Cultural Heritage, Belgium (KIK) in 1975, where traces of older restorations were found.

5.1.2.5 BRU 1

'Verdure with the coat of arms of the Brugse Vrije' (Bruges, *ca.* 1530) consists of several fragments, housed in the Municipal Museum, Bruges. The aldermans of the Bruges Vrije ordered 15 tapestries for the wall and benches. In 1528-29 Antoon Segon delivered the first ones, which remained in the room until the middle of the 17th Century. Millefleurs tapestries were once very popular and sometimes, as here, weapons were also represented within them.[2]

In 1878 the Archaeological Association of Bruges bought two fragments, while other sources from 1884 mention a few fragments found in the cellar. In 1959, De Wit restored the fragments and conservation treatment was performed at the Royal Institute for Cultural Heritage, Belgium (KIK) in 1987.

5.1.2.6 BRU 2

'The Life of the Virgin' series (Bruges, 1639) from the Church of the Cloister of the Potterie, was probably ordered in 1639 (woven date in the border) as the church was rebuilt in this period. It consists of two tapestries, 'Mary's Dedication in the Temple' (BRU 2) and 'The Annunciation'. Mary's dedication in the temple is not included in the canonic gospels, but in apocryphal texts that were issued from the middle ages onwards. The title of the tapestry was woven in Dutch into the bottom border. In the second tapestry, the angel Gabriel visits Mary at Nazareth and the words of greeting were woven into the lower border.[2]

The tapestries are mentioned in written sources from 1666 and it appears that they were only hung on special occasions. Previous conservation work was performed by the Royal Institute for Cultural Heritage, Belgium (KIK) in 1987.

5.1.2.7 BRU 3

One tapestry of the three belonging to the 'Miracles of Holy Mary of the Potterie' series (Bruges, *ca.* 1630) was also sampled. The tapestries are believed to have been ordered for the Church of the Cloister of the Potterie and each one depicts six scenes, representing miracles that were bestowed on pilgrims and ill people.[2]

The tapestries were used as blankets in the French Revolution and are therefore inevitably in a poor state. They most probably received some sort of restoration, after which they were hung in the corridor of the cloister (1910). Two restorations are known, the first in 1925 by the firm Chaudoir in Brussels and again in 1987 by the Royal Institute for Cultural Heritage, Belgium (KIK).

5.1.3 United Kingdom collection

Only three tapestries were sampled in the United Kingdom, all belonging to the Royal collection and currently housed at Hampton Court Palace. All originated from Brussels and were woven between 1515 and 1546 (Table 5.4).

Table 5.4: A summary of the place and date of manufacture of the selected tapestries from the United Kingdom

HRP 1	HRP 2	HRP 3
	Brussels	
ca. 1515	*ca.*1544-46	*ca.* 1515

The selected tapestries have always been part of the Royal collection, either on permanent display or in storage at Hampton Court Palace.

5.1.3.1 HRP 1 and 3

'The triumph of Petrarch' series (Brussels, *ca.* 1515), originally comprised six scenes, but the pieces sampled were 'The Triumph of Time over Fame' (HRP 1) and 'The Triumph of Death over Chastity' (HRP 3). The set is based on the cycle of allegorical poems 'I Trionfi', written by Petrarch between 1352 and 1374.[3] The original six scenes represented the successive triumphs of love, chastity, death, fame, time and religion. The subject had become popular in Netherlandish tapestry design around 1500, but this series must have been conceived in *ca.* 1507, as a duplicate

panel of 'The Triumph of Chastity' in the Victoria and Albert Museum, London, has a date of 1507 woven into the design.[3]

The pieces have most probably been on permanent or semi-permanent display at Hampton Court Palace since 1522. 'The Triumph of Time over Fame' (HRP 1) had much restoration carried out in 1919 by the William Morris Company weavers and most of the silk weft is restoration. 'The Triumph of Death over Chastity' (HRP 3) was possibly damaged by fire in the 1880's but received little or no further major repair work. It was removed from display in December 1988 during a re-decoration and was not put back on display.

5.1.3.2 HRP 2

'Tobias and Raphael taking leave of Tobit' (HRP 2) is the only survivor from the eight piece 'Story of Tobias' series (Brussels, *ca.* 1544-46), purchased by Henry VIII, most probably from Erasmus Schetz. This tapestry contains gold and silver metal threads, unlike the tapestry sampled from the Spanish Royal collection illustrating another scene from this Old Testament story, 'Raphael presented by Tobias to his father' (PNM 7), which contained no metal threads.

The set remained in the royal collection into the 17th Century, hung intermittently for major events at Hampton Court Palace, Westminster Abbey, Whitehall Palace and Windsor Castle. It continued to be recorded among the Hampton Court goods until the early 18th century, when it was cleaned and repaired prior to five pieces being permanently installed at St. James's Palace. In 1714, a single panel, probably the piece now at Hampton Court Palace, was repaired and relined and put on permanent display in various locations at the Palace. From 1902 it has been in storage at Windsor Castle and from 1990 has been undergoing conservation work at Hampton Court Palace. A duplicate set, purchased by Mary of Hungary, survives in part in the Spanish Royal collection, although several pieces have lost their borders.[3]

5.2 Historical yarn samples

The preparation and chromatographic analysis of the historical yarns were conducted in exactly the same manner as the studies on the reference samples (Chapter 6). The combined results of the dye analysis undertaken in Edinburgh and by the Belgian partner laboratory, the Royal Institute for Cultural Heritage (KIK) shows weld and dyer's greenweed to be the most widely employed yellow dye sources in the historic yarns sampled during the MODHT project (Section 5.3.1). The accelerated ageing experiments on yarns dyed with these biological sources (Chapter 4) indicated that the characteristic flavonoid components in both were relatively light-fast and that none of the flavonoid components produced significant, identifiable, photo-degradation products.

However, some general differences were observed between the results from the historical samples believed to have been dyed with weld or dyer's greenweed and the respective reference samples that had been subjected to accelerated ageing. These differences are examined in Section 5.2.1 and Section 5.2.2 respectively, before an overall consideration of the dye source information obtained from the historic tapestries is presented in Section 5.3

5.2.1 Weld

The identification of weld on historical samples was achieved by the qualitative and quantitative analysis of the three characteristic components; luteolin, apigenin and chrysoeriol, in the acid hydrolysed yarn extracts (Figure 5.2).

Flavonoid components from weld (*Reseda luteola* L.)

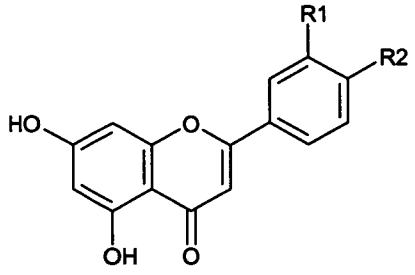

Luteolin: R1 = R2 = OH
Apigenin: R1 = H, R2 = OH
Chrysoeriol: R1 = OMe, R2 = OH

Figure 5.2: The main flavonoid constituents in the acid hydrolysed extract from weld dyed yarn

The relative percentages of these components were calculated at a detection wavelength of 254 nm and the results tabulated in order of descending percentage of luteolin (Chapter 6). The mean luteolin: apigenin: chrysoeriol ratio observed in the extracts from the historical yarns was 85:10:5, closely reflecting the results obtained from the accelerated ageing studies. In the extract from the most photo-degraded yarn sample in the weld accelerated ageing study (Y/W1, t_{final}), the ratio of the characteristic components was 86:11:3, compared with a ratio of 94:4:2 from the extracts of an unaged weld dyed yarn (Y/W1, t_0) (Chapter 4).

These results suggest that the dye components from half of the historical samples were less photo-degraded than those from the accelerated ageing experiments, while half were considerably more degraded. This is perhaps somewhat surprising, as the historical yarns were sampled from the reverse of the tapestries, and were therefore not expected to have been exposed to large amounts of light. Consideration should therefore be given to other possible reasons for unusual or unexpected ratios of dye components in the acid hydrolysed extracts, for example, differences in the initial relative abundances due to growth season or region (Chapter 2).

However, the historical yarn fibres were also found to be considerably more degraded than the samples subjected to accelerated light ageing (Chapter 1 and Chapter 4). For example, the studies on the polymer degradation of silk yarns using Size Exclusion Chromatography (SEC) consistently found a low average molecular

weight distribution in historic samples when compared with modern silk subjected to accelerated ageing (Chapter 4).[4] This indicated that all the historical yarn fibres, sampled from the reverse of the tapestries, were in a severely degraded state and suggested that light may not be the sole factor with respect to silk fibre damage. It is therefore feasible that additional degradation mechanisms may also operate on the dye components.

A typical chromatogram (monitored at 254 nm) of extracts from historical wool yarns appearing to have been dyed with weld is shown in Figure 5.3. This example is a yellow wool yarn, sampled from a 16th Century tapestry manufactured in Brussels and now part of the Spanish Royal collection (PNM 7/12). The three characteristic weld peaks are clearly observed in the PDA HPLC trace; luteolin (84%), apigenin (11%) and chrysoeriol (6%). In addition, three unidentified peaks, labelled W1-3, are observed.

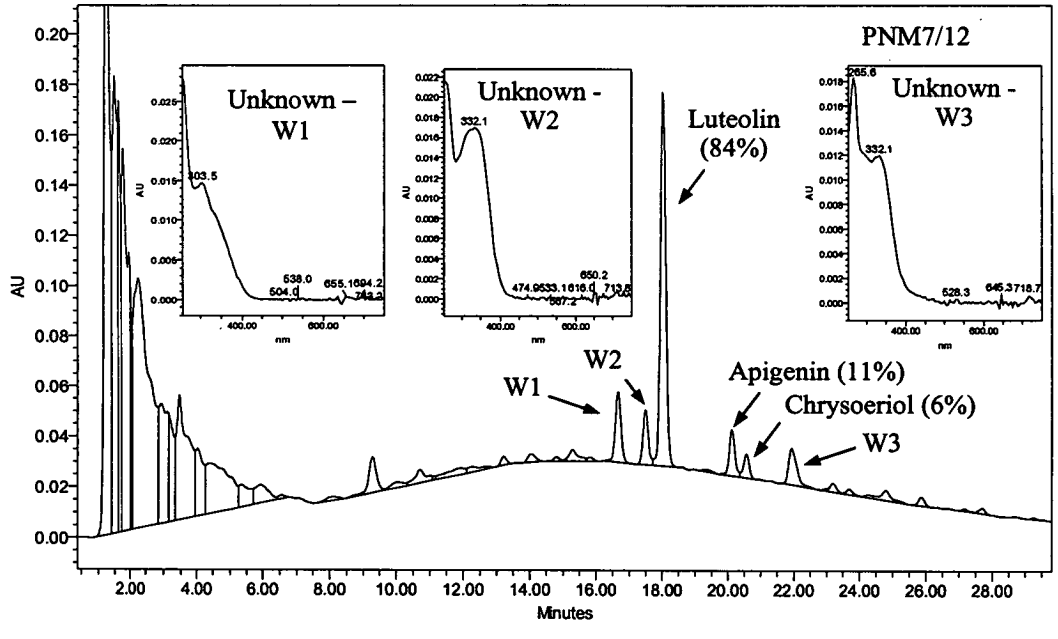

Figure 5.3: A typical chromatogram (monitored at 254 nm) of the extracts from an historical wool yarn, believed to have been dyed with weld (PNM 7/12)

The UV-Vis spectra of W1, W2 and W3 (inset of Figure 5.3) are all similar, with 'ill-defined' λ_{max} values between 300 and 335 nm, although their retention times differ considerably. Analysis of the PNM 7/12 sample extract by HPLC ESI MS^n, with data collection between 100 and 1000 Da, was therefore undertaken in an effort to obtain more information regarding the identity of the chemical components in the extracts (Figure 5.4).

The three known components, apigenin (*m/z* 269), luteolin (*m/z* 285), and chrysoeriol (*m/z* 299) were clearly identified in the mass range chromatograms (Figure 5.4b-d respectively) and their identity confirmed by MS^n fragmentation. The largest peak observed in the base peak chromatogram, with a retention time of 13.9 min (Figure 5.4a) had an *m/z* value of 344, but did not appear to absorb at the detection wavelength of 254 nm and could not be identified. No further information was gained regarding the identities of W1-3, possibly due to the small sample size, together with the difficulty in tuning the mass spectrometer for the detection of unknown compounds.

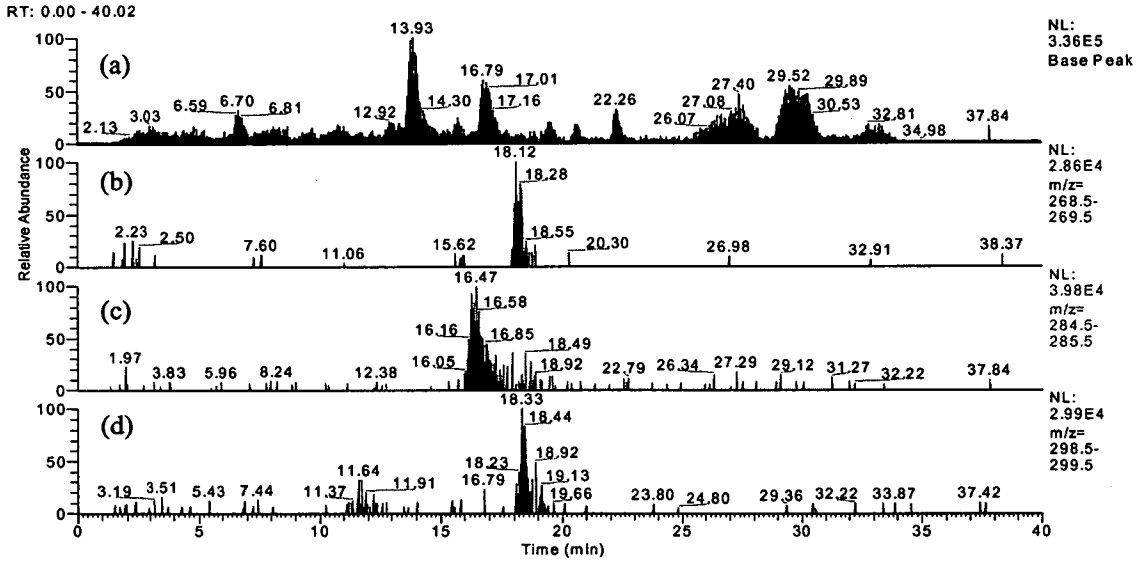

Figure 5.4: The HPLC ESI MS analysis of the historical wool sample, PNM 7/12. (a) Base peak chromatogram, (b) 268.5-269.5 mass range chromatogram, (c) 284.5-285.5 mass range chromatogram, (d) 298.5-299.5 mass range chromatogram

The unknown peaks were observed in the majority of the historical sample extracts assigned as weld, whether they were dyed onto a wool or a silk substrate. For example, the chromatogram and UV-Vis spectra for PNM 8/3, a yellow silk sample from a 17th Century tapestry manufactured in Bruges and now part of the Spanish Royal collection, were similar to those from PNM 7/12 (Figure 5.5).

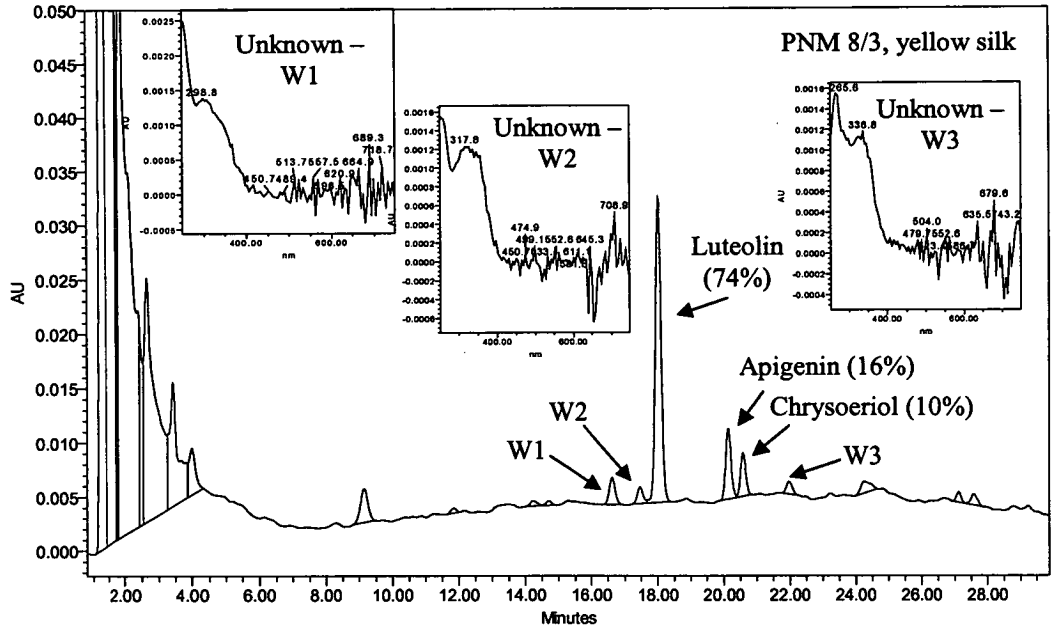

Figure 5.5: A typical chromatogram (monitored at 254 nm) of the extracts from an historical silk yarn, believed to have been dyed with weld (PNM 8/3)

Furthermore, a few of the historical extracts, such as BRU 3/9, from a tapestry woven in Bruges around 1630, contained the unknown W1-3 components together with the unknown degradation peak observed during the accelerated ageing of weld dyed yarn (Section 4.1.1) (Figure 5.6).

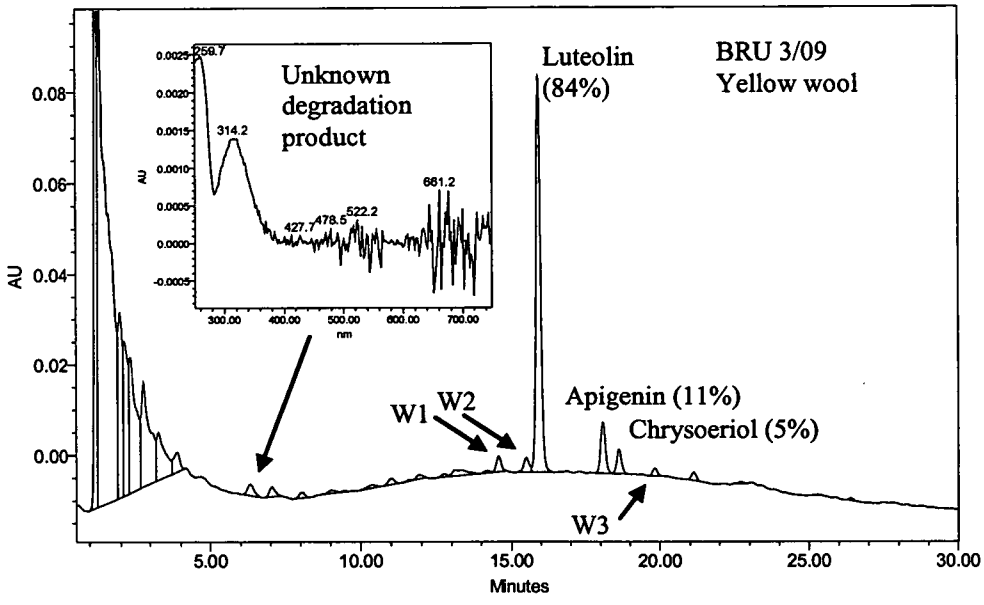

Figure 5.6: The chromatogram of the BRU 3/9 yarn extract (monitored at 254 nm)

Thus, both the source and identity of the unknown components W1, W2 and W3 remain to be established. Similar peaks were also observed in the extracts of historical yarns believed to have been dyed with dyer's greenweed, which also contains luteolin as the main colouring component (Section 5.2.2). However, as the yarns appear to be considerably more degraded than the reference samples subjected to accelerated ageing, it is also possible that the unknown W1-3 components may be from the breakdown of the natural wool or silk polymer, rather than from the degradation of individual dye components.

5.2.2 Dyer's greenweed

The identification of dyer's greenweed on historical samples was achieved by the qualitative analysis of three characteristic components observed in the acid hydrolysed yarn extracts; genistein, luteolin and apigenin (Figure 5.7).

Flavonoid components from dyer's greenweed (*Genista tinctoria* L.)

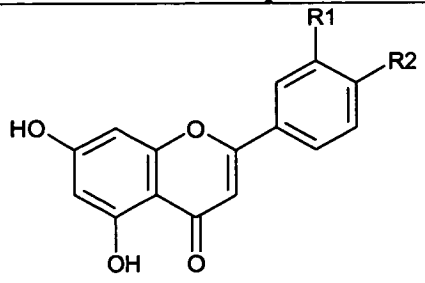

Luteolin: R1 = R2 = OH
Apigenin: R1 = H, R2 = OH

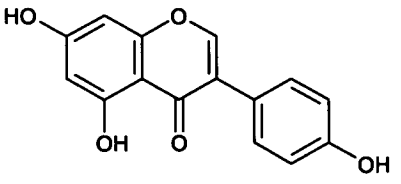

Genistein

Figure 5.7: The flavonoid components observed in the acid hydrolysed extract from yarn dyed with dyer's greenweed

Although accurate quantitative analysis of the three components was hindered by the close elution of genistein and luteolin, the relative percentages of the three components in the historical samples could be calculated at a detection wavelength of 254 nm. These have been tabulated in the order of descending luteolin percentage (Chapter 6).

A typical chromatogram (monitored at 254 nm) of the extracts from historical yarns appearing to have been dyed with dyer's greenweed is shown (PNM 5/34, Figure 5.8).

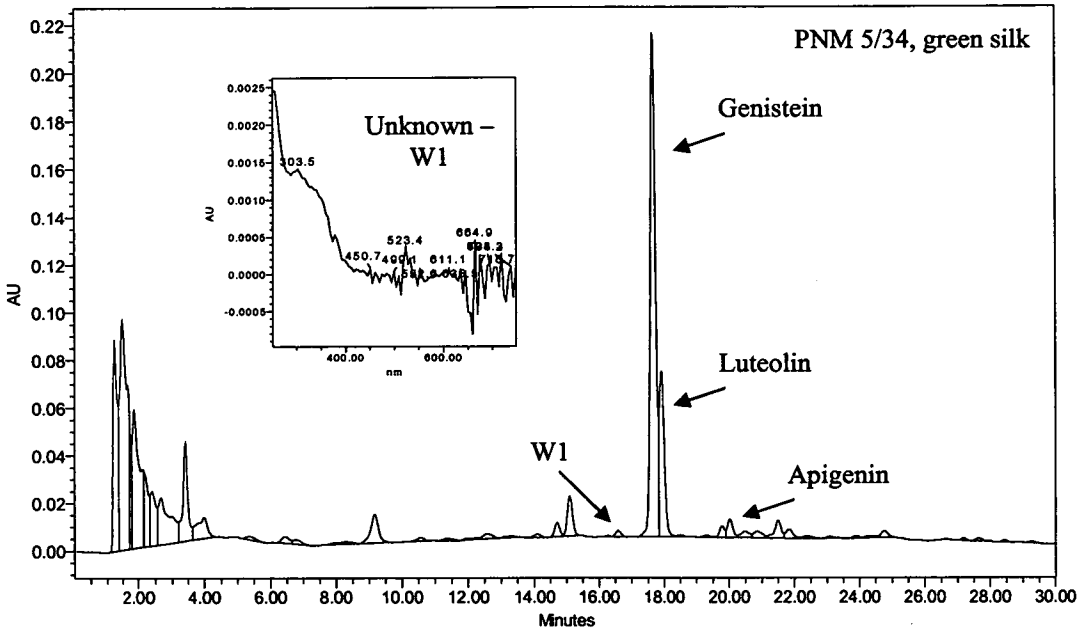

Figure 5.8: A typical chromatogram (monitored at 254 nm) of the extracts from an historical silk yarn, believed to have been dyed with dyer's greenweed (PNM 5/34) with the UV-Vis spectrum of the unknown W1 component (inset)

This extract was from a green silk yarn, sampled from a 16th century Belgian tapestry in the Spanish Royal collection. A peak with a retention time and UV-Vis spectrum identical to the W1 peak seen in extracts from aged weld dyed yarns, is observed. However, the presence of the unknown W2 peak is difficult to verify as genistein elutes at the same retention time, while the detection of the W3 peak is problematic due to the presence of small amounts of several unknown components in this area.

The component that distinguishes the use of dyer's greenweed from other dye alternatives, including weld, is the non-colouring component, genistein. The historical yarns assigned as dyer's greenweed generally had a greater amount of genistein relative to luteolin (monitored at 254 nm) in the acid hydrolysed extracts (Chapter 6). Interestingly, studies with unaged reference yarns found that the amount of genistein decreased relative to luteolin with successive dyeings to produce more intensely coloured yellow yarns (Chapter 2). However, accelerated ageing studies indicated that the degradation of genistein proceeded at a relatively slower rate than that of luteolin, the other main flavonoid component found in yarn extracts

dyed with dyer's greenweed (Chapter 4). Thus, the relative amount of genistein would be expected to increase with respect to luteolin upon prolonged exposure of the dyed yarn to light, possibly accounting for the results observed in the historical sample extracts.

A few of the sample extracts from yarns apparently dyed with dyer's greenweed also contained additional components, for example, BXL 1/1, obtained from a tapestry woven in Brussels in the early 1520's (Figure 5.9).

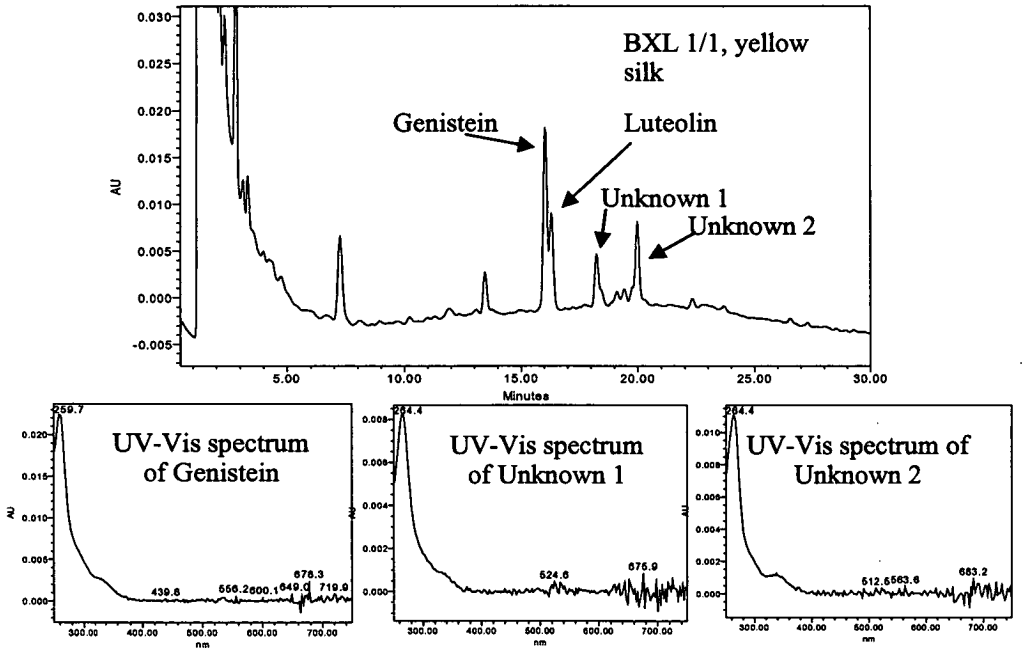

Figure 5.9: The chromatogram (monitored at 254 nm) of the extracts from an historical silk yarn, apparently dyed with dyer's greenweed (BXL 1/1), but with two additional components possessing similar UV-Vis spectra to genistein

The characteristic genistein and luteolin peaks are both observed, but apigenin is partially co-eluting with another peak, 'Unknown 1'. A second peak, 'Unknown 2', with a similar UV-Vis spectrum to the first, is observed eluting slightly later. The spectra of these two unknown components are similar to that of genistein, with λ_{max} values around 260 nm. It is not known whether they are genistein photo-degradation products, or related compounds present in the dye source, but if the unknown components have not been formed by the photo-degradation of genistein, it is

conceivable that they may indicate the presence of another dye source. Historical yarn extracts containing peaks with similar spectra, although eluting at different retention times, are discussed in Section 5.3.2. However, pending further investigation, the use of dyer's greenweed has been assumed in the small number of extracts like the one above.

5.3 Yellow dyes identified in MODHT historical samples

To investigate the natural dye sources employed in the creation of the high status tapestries described in Section 5.1, 487 yarns were analysed by PDA HPLC. Approximately half of these yarns (245) were described as 'yellow or green' upon visual inspection, and were thus analysed in Edinburgh. The remainder were analysed by an MODHT partner laboratory in Brussels. The total number of yarns sampled from each tapestry and the number analysed in Edinburgh are summarised in Table 5.5 below.

Table 5.5: The total number of yarns sampled from each tapestry (excluding metal threads) and the number analysed in Edinburgh

Code	Current location	Place (and date) of manufacture	Total number of yarn samples	Number analysed in Edinburgh
TOU 1	Tournai	Arras (<1500)	32	18
BXL 1	Brussels	Brussels (1500-1550)	16	8
BXL 2	Brussels		21	10
BXL 3	Brussels		18	4
BXL 4	Brussels		18	8
HRP 1	London		47	34
HRP 2	London		66	41
HRP 3	London		50	20
PNM 1	Madrid		27	15
PNM 2	Madrid		20	11
PNM 5	Madrid		26	10
PNM 7	Madrid		23	10
BRU 1	Bruges	Bruges (1500-1550)	19	8
BRU 2	Bruges	Bruges (1600-1650)	31	12
BRU 3	Bruges		28	13
PNM 8	Madrid		19	7
PNM 9	Madrid	Antwerp (1650-1700)	26	16
		TOTALS	**487**	**245**

5.3.1 Weld and dyer's greenweed

The combined dye analysis results from both laboratories show weld and dyer's greenweed (dgw) to be the two most widely employed yellow flavonoid dye sources for the tapestries analysed, being present in a total of 179 samples. The majority of the analysed extracts were from wool yarns (115/179) and a 'tapestry by tapestry' breakdown of the results from these samples is shown (Table 5.6).

Table 5.6: The frequency with which weld and dyer's greenweed (dgw) were employed to dye wool yarns from the historic tapestries analysed for the MODHT project. The extracts from samples described as yellow contained no evidence of other dye sources, while those described as green/orange contained additional blue or red components

Code	Place (and date) of manufacture	Wool yarns			
		yellow		green/orange	
		weld	dgw	weld	dgw
TOU 1	Arras (<1500)	3	0	4	0
BXL 1	Brussels (1500-1550)	0	0	3	0
BXL 2		1	0	0	0
BXL 3		0	3	0	12
BXL 4		1	0	1	2
HRP 1		7	0	12	1
HRP 2		1	0	9	5
HRP 3		0	0	1	0
PNM 1		1	0	2	0
PNM 2		1	1	2	0
PNM 5		3	0	3	0
PNM 7		3	0	2	3
BRU 1	Bruges (1500-1550)	1	0	5	0
BRU 2	Bruges (1600-1650)	2	0	7	0
BRU 3		3	0	5	0
PNM 8		0	0	2	0
PNM 9	Antwerp (1650-1700)	1	0	2	0
TOTALS		**28**	**4**	**60**	**23**

Samples described as 'green' contained the blue indigo component in addition to either weld or dyer's greenweed, while samples described as 'orange' contained red components, usually from either madder, cochineal or brazilwood sources (Section 5.4).

Although the number of wool yarns sampled in each tapestry was sometimes limited, a general trend for the use of weld as the dye source, in preference to dyer's greenweed, is observed. This is apparent in all tapestries, with the exception of BXL 3, where no weld dyed yarns were found, and BXL 4 where the overall incidence of weld and dyer's greenweed was equal.

Weld was the most frequently observed biological source in the yellow samples, where neither blue or red colouring components were observed in the extracts (28/32) *i.e.* the first and second columns of Table 5.6. Furthermore, three of the four

samples found to have been dyed with dyer's greenweed were from the same tapestry, BXL 3, 'The Legend of Herkenbald', manufactured in Brussels in 1513 as a unique commission for a church. It is interesting that this tapestry had a distinctive set of dye analysis results, as unlike many of the others, it was not woven as part of a larger set.

The fourth dyer's greenweed sample was from PNM 2, 'Perseus liberates Andromeda', a tapestry woven in Brussels around 1545. This is the only tapestry sampled from the Spanish Royal collection known to have received past conservation treatment, although the details of this work are unknown. While every effort was made to sample original yarns, this may have been an early restoration yarn. Any repairs made to the tapestry before the introduction of synthetic dyes in the 1850's would have necessitated the need for yarns dyed with natural dye sources, while even repairs made in the early part of the 20th century sometimes utilised yarns dyed with natural sources.

To investigate the possibility that the wool yarns dyed with dyer's greenweed were actually early restoration threads, data from other techniques, such as amino acid analysis, were examined for these samples. Assuming the PNM 2 sample, or any of the other wool yarns dyed with dyer's greenweed, were indeed restoration threads, they would be considerably younger than the original yarns. Thus, the extent of oxidative degradation would be expected to be less than for the original, older yarns. Examination of the available data showed no such anomalous results, therefore no scientific evidence exists to suggest that any of the wool yarns dyed with dyer's greenweed were restoration threads. This highlights some of the difficulties encountered when considering data from historical objects.

Weld was also the most frequently observed biological source in samples where the components from blue or red colouring components were also observed in the extracts (60/83) *i.e.* the third and fourth columns of Table 5.6. Furthermore, over half of the samples found to have been dyed with dyer's greenweed (12/23) were

yarns from the BXL 3 tapestry, where no weld dyed yarns were detected. The remaining eleven wool yarns dyed with dyer's greenweed originated from four different tapestries; BXL 4 (2 samples), HRP 1 (1 sample), HRP 2 (5 samples) and PNM 7 (3 samples). The greater number of green/orange wool yarns dyed with dyer's greenweed compared with the number in the yellow yarn category, together with the lack of evidence suggesting they were early restoration threads, indicates that dyer's greenweed may have occasionally been employed in the dyeing of wool, especially when producing colours involving the use of two or more dye sources of different colours, for example, a yellow and a blue source to produce a green coloured yarn. This is termed over-dyeing or combination dyeing.

Interestingly, examination of the data from the silk yarns indicates an opposing general trend for weld and dyer's greenweed, with dyer's greenweed appearing to be favoured over weld. However, there are considerably fewer silk samples than wool with which to base the conclusions (Table 5.7).

Table 5.7: The frequency with which weld and dyer's greenweed (dgw) were observed in the extracts from silk yarns sampled from the historic tapestries analysed for the MODHT project. The extracts from samples described as yellow contained no evidence for other dye sources, while those described as green/orange contained an additional blue or red component

Code	Place (and date) of manufacture	Silk yarns			
		yellow		green/orange	
		weld	dgw	weld	dgw
TOU 1	Arras (<1500)	--	--	--	--
BXL 1	Brussels (1500-1550)	0	1	0	1
BXL 2		1	0	0	0
BXL 3		--	--	--	--
BXL 4		0	1	0	1
HRP 1		0	0	0	1
HRP 2		1	2	2	8
HRP 3		0	2	0	5
PNM 1		0	3	1	5
PNM 2		2	2	0	2
PNM 5		0	3	1	2
PNM 7		0	2	0	2
BRU 1	Bruges (1500-1550)	0	0	0	2
BRU 2	Bruges (1600-1650)	--	--	--	--
BRU 3		1	0	0	0
PNM 8		5	0	0	0
PNM 9	Antwerp (1650-1700)	--	--	--	--
TOTALS		**10**	**16**	**4**	**29**

This trend appears to be most evident in the combination dyed yarns, where only four of the thirty-three samples analysed were dyed with weld. For the yellow yarns, a slightly larger number were dyed with dyer's greenweed than with weld (16/26), although the numbers were more comparable in this case. The most significant departure from this trend was within PNM 8, a Bruges tapestry woven around 1620 and part of the Spanish Royal collection. None of the silk samples (or the two wool yarns sampled from this tapestry) had been dyed with dyer's greenweed, thus the results from this tapestry accounted for half of the yellow weld dyed silk samples (5/10).

Despite the relatively small number of silk yarns sampled from the tapestries, the analysis of the data suggests that the biological species most frequently chosen to dye silk yarns, especially those for combination dyeing, was dyer's greenweed. However, the relatively high incidence of weld indicates that more silk yarns from

tapestries manufactured in the period of interest should be analysed before any conclusions can be reached. Additionally, documentary sources from that period could provide written historical evidence to support these empirical observations.

5.3.2 The remaining yellow samples

Although the majority of flavonoid containing extracts were characteristic of either weld or dyer's greenweed, there were some exceptions. Many of these samples are considered to be early restoration yarns, for example, five extracts from different tapestries contained the characteristic components for the natural yellow dye source, old fustic (*Chlorophora tinctoria* L.).[9] The dyestuff contains morin, maclurin and kaempferol (Figure 5.10) and is therefore easily distinguished from other common alternatives.

Flavonoid components from old fustic (*Chlorophora tinctoria* L.)

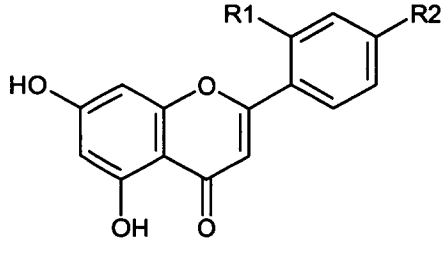

Morin: R1 = R2 = OH
Kaempferol: R1 = H, R2 = OH

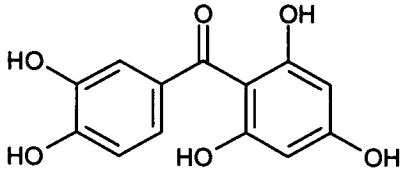

Maclurin

Figure 5.10: The main colouring components of old fustic, morin, kaempferol and maclurin

It was the only source used to dye one sample (HRP 2/30), while it was observed together with additional sources in four other samples; with logwood (BXL 2/12 and BXL 2/27), madder (BXL 2/38) and weld (HRP 2/30). After the discovery of South America, old fustic arrived in Europe at the beginning of the 16th Century, and its use as a dye source dates from around this time.[8] Due to the early construction date of the BXL 2 tapestry, woven in Brussels around 1520, the old fustic dyed yarns are most likely to be early restoration threads. Furthermore, the use of logwood as a dye

source, found on two of the samples, was also unknown in Europe before the beginning of the 16th century.[8]

The characteristic components of young fustic (*Cotinus coggyria* Scop.), fisetin and sulfuretin (Figure 5.11) were found in the extracts from one yarn sampled from HRP 2, a tapestry woven in Brussels around 1545.

Components from young fustic (*Cotinus coggygria* Scop.)

Fisetin

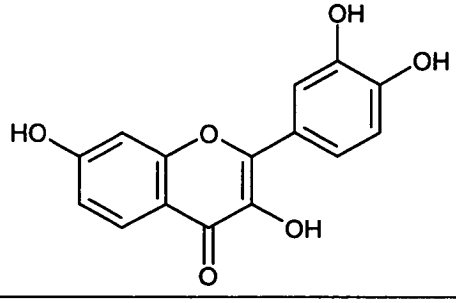

Sulfuretin

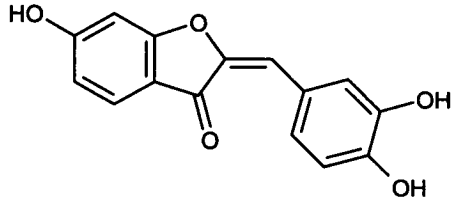

Figure 5.11: The major constituents observed in the acid hydrolysed extract of yarn dyed with young fustic

Although this natural yellow dye source has been used since antiquity, its light-fugitive nature was well known, and many municipal dye regulations banned its use for good quality textiles.[8] The presence of yarns dyed with young fustic in the main weave of a high status tapestry would therefore be highly unusual, but, the tapestry was repaired and relined in 1714, so this may also be an early restoration thread. Young fustic was, however, routinely used to dye the silk cores of the metal threads (Section 5.3.3).

An interesting collection of unknown peaks, together with the flavonoids characteristic of dyer's greenweed, were observed in the extracts from several yarns sampled from the BXL 1 tapestry, woven in Brussels between 1519 and 1524 and in yarn extracts from BXL 4, also woven in Brussels between 1519 and 1524 (Figure 5.12).

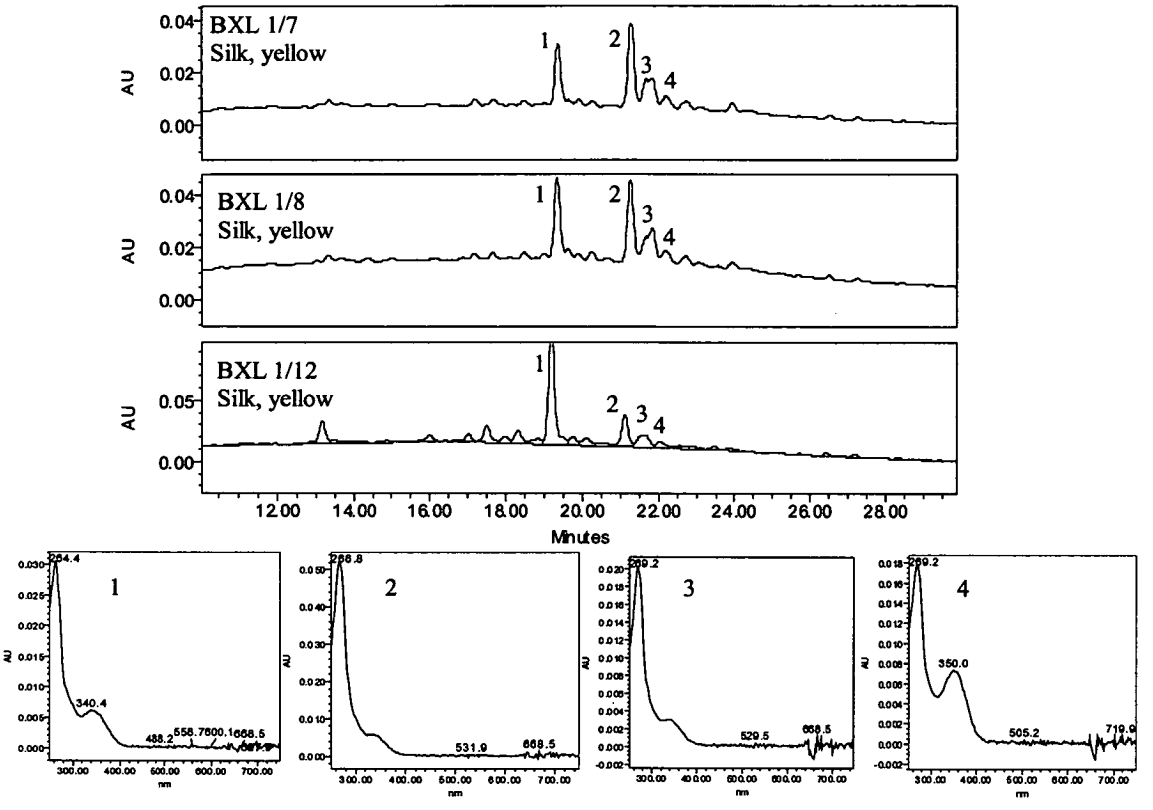

Figure 5.12: The HPLC chromatograms (monitored at 254 nm) of the extracts of BXL 1/7 (top), BXL 1/8 (middle) and BXL 1/12 (bottom) and the UV-Vis spectra of the four unknown components (1-4)

Components 1-3 are essentially uncoloured, suggesting that they may be the degradation products of a synthetic dye, following acid hydrolysis extraction. Although the UV-Vis spectra are similar to the unknown components observed in some of the extracts from historical samples apparently dyed with dyer's greenweed (Section 5.2.2), their retention times are not the same. Further investigative work is therefore required before these samples can be categorized as yarns dyed with a synthetic dye or a novel natural source.

A number of samples were found to have been dyed with modern synthetic dyestuffs, including yarns sampled from TOU 1, woven in Arras in 1402 (Figure 5.13).

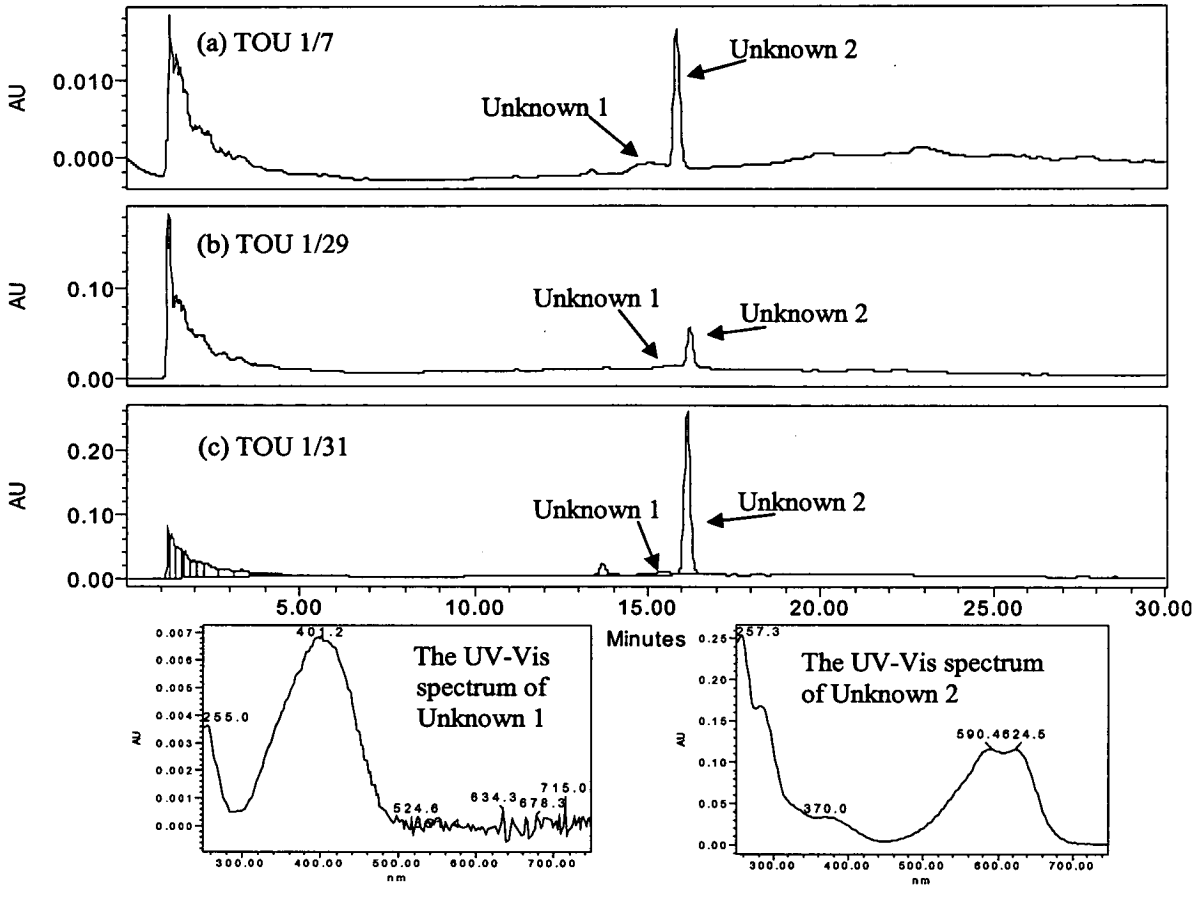

Figure 5.13: The HPLC chromatograms (monitored at 254 nm) of the extracts from (a) TOU 1/7, (b) TOU 1/29 and (c) TOU 1/31 together with the UV-Vis spectra of the two unknown components

Finally, in addition to the samples described above, a number of extracts were found to contain only luteolin. This suggests that a natural flavonoid dye source was used, however, the biological species is impossible to identify with this information alone because many dye sources contain luteolin as the major colouring component, for example, weld and sawwort.

5.3.3 Metal thread cores

Decorative metals have been incorporated into textiles for thousands of years. The earliest metal threads were thin strips of gold, cut from a beaten metal foil and directly woven or embroidered into textiles. Later, these strips were wound around a fibrous core to introduce more flexibility to the thread and make it more versatile (Figure 5.14).[5] The metallic elements of the threads have been the subject of

extensive study by other MODHT project partners,[5,6] and the biological source of the dye used to colour the core yarn is also of interest.

Figure 5.14: A gilt metal thread, wound around a silk core (PNM 5/26) © MODHT partners

The metal threads sampled during the MODHT project appear over large areas of five of the tapestries (HRP 2, BXL 2, PNM 1, PNM 2 and PNM 5), especially areas depicting clothing. In each case, their fibrous cores were made of silk. The cores would not usually have been visible, except through small gaps between the twists of the outer metal 'sheaths'. To ensure the aesthetic quality of the tapestry, the core yarns were often dyed according to the colour of the metal wrapping, *i.e.* yellow or reddish for gold or gilt threads, pale yellow or undyed white silk for silver threads.[5] Indeed, upon visual inspection of the historical core samples protected from exposure to light, this frequently seemed to be the case, with the silk cores appearing white or light yellow for the silver metal threads and darker shades of yellow for the gilt metal threads.

The yellow dye source presumed most likely to have been used to colour the silk cores is the woody shrub, young fustic (*Cotinus coggyria Scop.*).[7] When used as a mordant dye, this produces orange-yellow to strong red-brown coloured yarns, ideal for generating core threads with colours closely matching those of the metal. Although young fustic was often considered a dye of poor quality, only used for the

dyeing of cheaper textile product, because it was not particularly light fast,[8] it may have been used for the metal cores as they are protected from light.

The PDA HPLC and HPLC ESI MS studies performed on the acid hydrolysed extracts of young fustic dyed yarns in Chapter 2, identified the main colouring components to be the flavonol, fisetin and the aurone, sulfuretin. In addition, ellagic acid was often observed, most probably from tannins present in the dye wood. The presence of ellagic acid, together with fisetin and sulfuretin is therefore highly characteristic for the use of a young fustic dye source.

The flavonols in young fustic were already known to be highly light fugitive,[9] and as a consequence of photo-degradation and subsequent acid hydrolysis, dye extracts of aged yarns containing fisetin produce two marker components; 3,4-dihydroxybenzoic acid and its methyl ester (Scheme 5.1). Although accelerated ageing studies conducted in Chapter 4 (Section 4.1.4) also found the aurone, sulfuretin to be highly fugitive, no significant degradation products could be characterised.

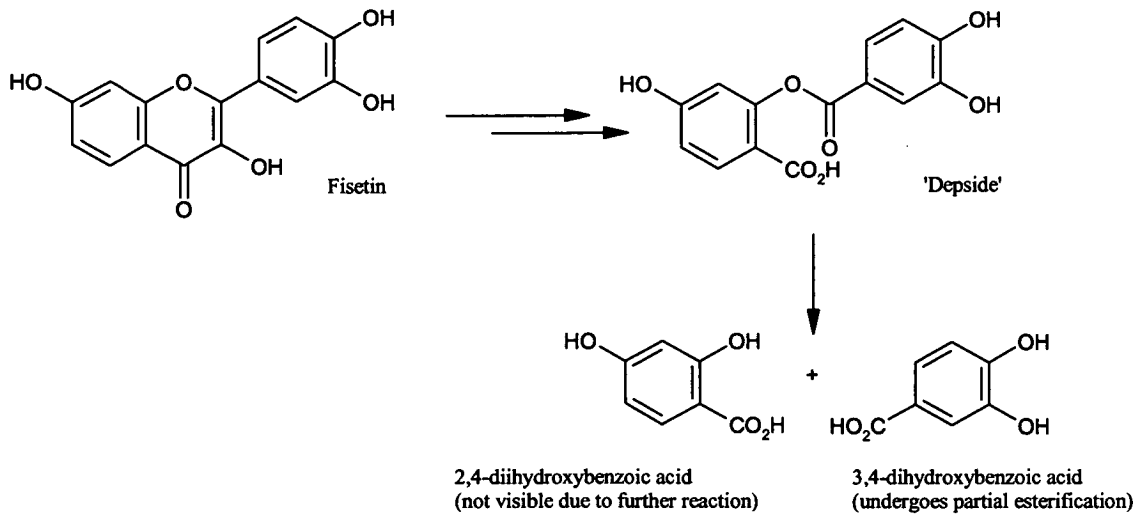

Scheme 5.1: The solution photo-oxidation of fisetin to the depside, followed by the formation of 2,4-dihydroxybenzoic acid and 3,4-dihydroxybenzoic acid during the acid hydrolysis procedure (adapted from reference 9)

The results from the chromatographic analysis of the acid hydrolysed extracts of twelve metal thread cores from four of the tapestries containing metal threads (BXL 2, PNM 1, PNM 2 and PNM 5) confirmed the use of young fustic. However, it appears to have been used in combination with other biological sources (Table 5.8).

Table 5.8: Possible dye sources used to colour metal thread cores. The sources in brackets have been assigned using only one molecular component when several are usually required

MODHT sample code	Dye sources	Metal thread category
PNM 2/06	Young fustic + weld + brazilwood	Gilt, small diameter
PNM 1/38	Young fustic + brazilwood	Gilt, medium diameter
PNM 2/19		Gilt, corrosion
PNM 5/26		Gilt, medium diameter
PNM 1/06	Young fustic + brazilwood + (weld)	Gilt, corrosion
PNM 2/18	Dyer's greenweed only	Silver
BXL 2/19	Unknown, but probably	Gilt, medium diameter
PNM 5/05	(weld) + (young fustic)	Triple wrapped
PNM 5/09		Silver
PNM 1/01	Unknown	Silver
BXL 2/14	Synthetic	--
BXL 2/15		--

The PDA HPLC results from the acid hydrolysed extract of sample PNM 2/06 suggest that the yarn was dyed with young fustic in combination with weld and brazilwood (Figure 5.15). The characteristic components for young fustic; fisetin, sulfuretin and ellagic acid are observed, as are the three characteristic components of weld; luteolin, apigenin and chrysoeriol, together with the unknown brazilwood marker component. However, it must also be remembered that the identity of the brazilwood marker component remains unknown, thus its specificity as evidence for the use of brazilwood is not assured. This dye combination may have produced a dark yellow to orange coloured yarn, enabling it to be closely matched with the colour of the gilt metal used in the construction of the metal thread.

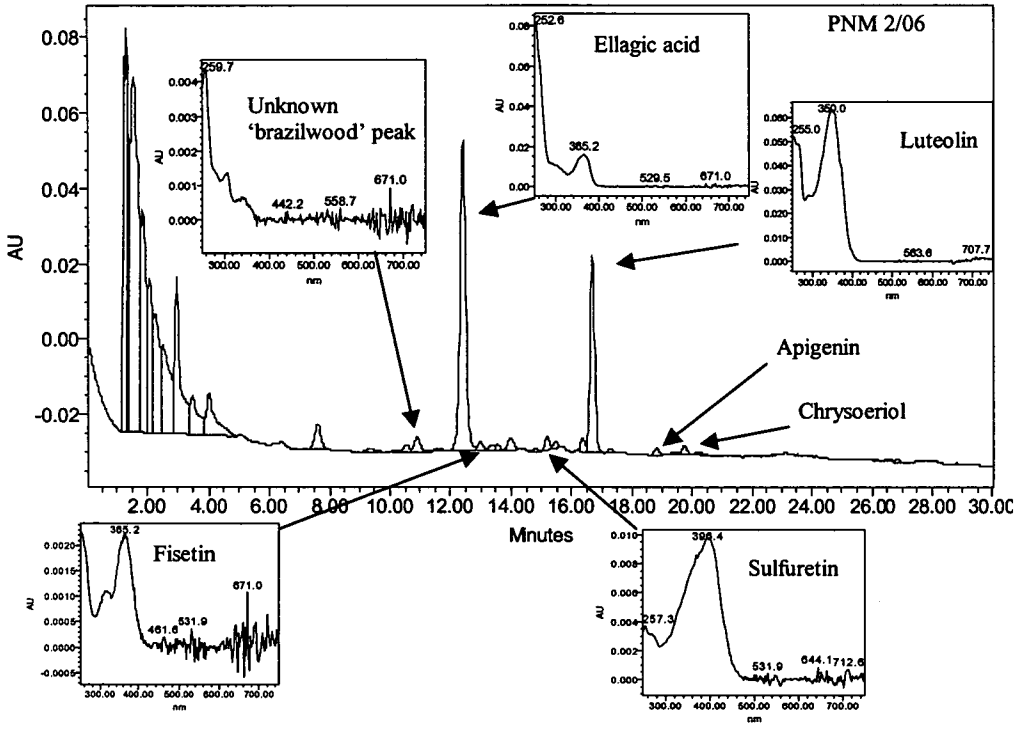

Figure 5.15: The PDA HPLC chromatogram (monitored at 254 nm) of the acid hydrolysed extracts from the PNM 2/06 sample. The unknown brazilwood marker component is observed, as are the characteristic components for young fustic (ellagic acid together with small amounts of fisetin and sulfuretin) and the three characteristic components of weld (luteolin, apigenin and chrysoeriol)

A further four extracts similar to the one above contain only the components characteristic for young fustic together with the marker component for brazilwood (PNM 1/38, PNM 2/19, PNM 5/26 and PNM 1/06). The extract of one of these

samples (PNM 1/06) also contains luteolin, suggesting that a small amount of another flavonoid dye source, possibly weld, may have been used. It is highly conceivable that the combination of brazilwood (red) with young fustic (yellow) would have produced an orange colour closely matching that of the gilt metal used in the construction of these metal threads.

The result from the silk core of PNM 2/18 is unusual, as its extract contained a small amount of both genistein and luteolin, suggesting the use of a dyer's greenweed source. The metal thread was constructed using silver and, upon visual inspection of the core yarn before acid hydrolysis, it appeared to be colourless. The reference dyeing experiments conducted with dyer's greenweed (Section 2.1.2.2) suggested that a single dyeing with this biological source could produce a light yellow coloured yarn.

The PDA HPLC results from three samples (BXL 2/19, PNM 5/05 and PNM 5/09) were difficult to interpret since their respective acid hydrolysed extracts contained only ellagic acid and luteolin. Although conclusive dye source assignments are impossible with this information alone, by comparing the results with those from the previous samples, it can be hypothesised that natural yellow dye sources such as weld and young fustic were used to colour the silk cores. The metal thread of sample PNM 5/09 was constructed using silver, and upon visual inspection the silk core appeared to be colourless. The presence of ellagic acid in the extract may suggest the use of a faded young fustic source, although the expected fisetin photo-degradation products were not observed. The ellagic acid may therefore be present due to the use of tannins to 'weight' the silk. Alternatively, a very pale coloured yarn could have been produced with a small amount of dye. Any degradation products formed by the breakdown of the characteristic components might then be below the limit of detection, or perhaps also photo-degrade.

The metal thread of sample PNM 1/01 was also constructed using silver with an apparently colourless silk core. However, the acid hydrolysed extract contained a

trace amount of luteolin, along with relatively large yarn degradation peaks (matching with 4-hydroxybenzoic acid and its methyl ester). This suggests that the silk core may have originally been lightly dyed with a natural yellow source and that prolonged exposure to light has degraded minor components that would have been characteristic of the specific source.

Finally, the PDA HPLC results from two samples (BXL 2/14 and BXL 2/15) suggested that they were modern restoration threads (Figure 5.16).

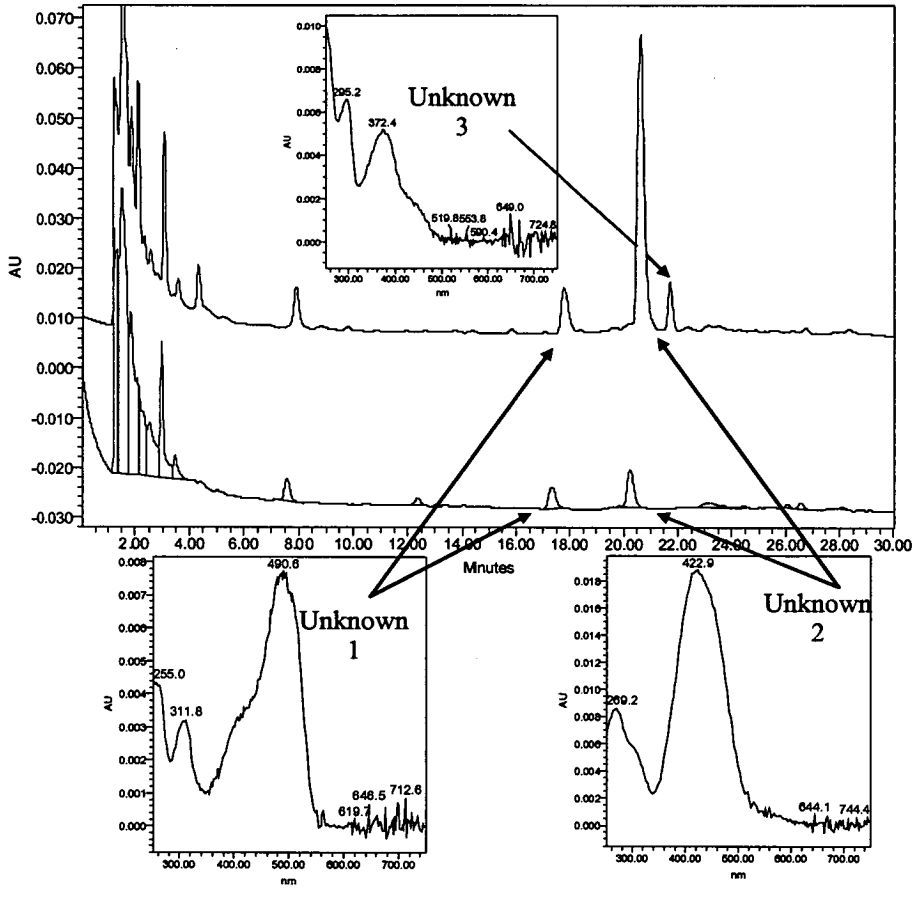

Figure 5.16: The PDA HPLC chromatograms (monitored at 254 nm) of the extracts from BXL 2/14 (top) and BXL 2/15 (bottom) together with the UV-Vis spectra of the main components (inset).

During acid hydrolysis, the BXL 2/14 extract became bright purple, while the BXL 2/15 extract became a bright red colour. This is a highly unusual observation for natural mordant dyes. Furthermore, the respective PDA HPLC results of both

samples contained unknown colouring components, suggesting that the samples are restoration threads, with the silk cores coloured using synthetic dyes.

A summary of the chemical components observed in the acid hydrolysed extracts of the twelve metal thread cores is shown (Table 5.9).

Table 5.9: Chemical components observed in the acid hydrolysed extracts from the metal thread cores

Code	Samples	Young fustic	Weld	Dyer's greenweed	Brazilwood
BXL 2	14 *				
	15 *				
	19	ellagic acid	luteolin		
PNM 1	01		luteolin		
	06	ellagic acid, sulfuretin, fisetin	luteolin		unknown peak
	38	ellagic acid, sulfuretin, fisetin			unknown peak
PNM 2	06	ellagic acid, sulfuretin, fisetin (& its degradation products)	luteolin, apigenin & chrysoeriol		unknown peak
	18			genistein & luteolin	
	19	ellagic acid, sulfuretin			unknown peak
PNM 5	05	ellagic acid	luteolin		
	09	ellagic acid	luteolin		
	26	ellagic acid, sulfuretin, fisetin degradation products			unknown peak

NB: * = Probably a restoration thread

The chromatographic investigation into the biological species used to dye the metal thread silk cores from four of the tapestries sampled within the MODHT project (BXL 2, PNM 1, PNM 2 and PNM 5) has confirmed the use of young fustic. In addition, it has provided information regarding the use of combinations of biological sources, probably utilized to colour match the core yarns with the outer metal.

5.4 Summary of red dyes identified in MODHT historical samples

Although the responsibility for the analysis of the red samples was with another of the MODHT project partners (Royal Institute for Cultural Heritage, Belgium), a short summary of the results have been included here.

The most widely used red dye source was found to be madder (*Rubia tinctorum* L.), used either alone or in combination with additional red sources such as brazilwood, or with other colouring components such as the yellow flavonoids or the blue indigoids. No connection between dye sources and yarn type *i.e.* wool or silk was found. The small number of red yarns dyed using brazilwood were often found with an additional red source such as madder, possibly due to the fugitive nature of the brazilwood dye source, or with other colouring components.

Several yarns dyed with Mexican cochineal (*Dactylopius coccus* Costa) were observed on five of the sampled tapestries (Table 5.10).

Table 5.10: The number of Mexican cochineal dyed yarns found on each of the tapestries

Sample code	Place (and date) of manufacture	Number of yarns dyed with Mexican Cochineal
BXL 2	Brussels (*ca.* 1520)	2
HRP 2	Brussels (*ca.* 1544-46)	3
PNM 2	Brussels (*ca.* 1545)	1
PNM 5	Brussels (*ca.* 1545)	1
BRU 2	Bruges (1639)	8

Mexican cochineal was imported into Europe for the first time in 1518, shortly after the discovery of Mexico.[8] Due to the early construction date of the BXL 2 tapestry, these two samples are likely to be early restoration yarns. However, the yarns from the remaining four tapestries, which were all manufactured slightly later, may indeed represent original dyed samples.

A small number of other dye sources were also occasionally observed including henna and lichen.

5.5 Conclusion

Research into the characteristic components found in the extracts of dyed yarns (Chapters 2 and 3) has allowed the identification of the biological species utilized in the colouring of historical yarns from a selection of high quality tapestries selected from several significant European collections. Many of the observations could be rationalised on the basis of the accelerated ageing experiments conducted on reference dyed yarns (Chapter 4).

Throughout the period of interest (*ca.* 300 years) and in tapestries manufactured in different weaving centres, the most widely used natural yellow dye sources were consistently found to be weld and dyer's greenweed. These empirical observations have helped to inform the art historical community by adding essential material evidence to existing documentary evidence regarding the historical use of natural dye sources.

Furthermore, the dye source information has proved invaluable for the analysis of data obtained from other chemical and physical experiments conducted on the samples within the Monitoring of Damage to Historic Tapestries (MODHT) project (Chapter 1). For example, the process for dyeing yarns with weld appears to cause increased fibre degradation, while the reference samples showing a particularly large increase in degradation after accelerated ageing included the red yarns dyed with brazilwood and those dyed with madder. The identification of the biological species used to dye the historical yarns has therefore contributed to the assessment and monitoring of the structural integrity of these culturally significant items.

5.6 References

[1] Carretero, C.H., *'Colección real espanola, Patrimonio Nacional'*, Report prepared for the Monitoring of Damage in Historic Tapestries (MODHT) project, **2002**

[2] de Meuter, I., *'Colección nacional belga, Musées Royaux d'Art et d'Histoire'*, Report prepared for the Monitoring of Damage in Historic Tapestries (MODHT) project, **2003**

[3] Campbell, T., *'Royal Collection. Hampton Court Palace'*, Report prepared for the Monitoring of Damage in Historic Tapestries (MODHT) project, **2003**

[4] Hallet, K.; Howell, D.; *'Size exclusion chromatography as a tool for monitoring silk degradation in historic tapestries'*, Postprints to the AHRB Research Centre for Textile Conservation and Textile Studies 1st Annual Conference, **2005**, 143-150

[5] Hacke, A.M.; Carr, C.M.; Brown, A., *'Characterisation of metal threads in Renaissance tapestries'*, Postprints to the AHRB Research Centre for Textile Conservation and Textile Studies 1st Annual Conference, **2005**, 71-78

[6] Hacke, A.M.; Carr, C.M.; Brown, A.; Howell, D., *'Investigation into the nature of metal threads in a renaissance tapestry and the cleaning of tarnished silver by UV/Ozone (UVO) treatment'*, J Mater Sci, **2003**, 38, 3307-3314

[7] Vanden Berghe, I., *Personal communication*, **2005**, The Royal Institute for Cultural Heritage (KIK), Belgium

[8] Hofenk de Graff, J., *'The colourful past: Origins, chemistry and identification of natural dyestuffs'*, **2004**, Abegg-Stiftung and Archetype Publications Ltd., 1st edition

[9] Ferreira, E.S.B, *'New Approaches towards the identification of yellow dyes in ancient textiles'*, PhD Thesis, **2002**, The University of Edinburgh

Chapter 6

6 EXPERIMENTAL

6.1 Preparation of dyed yarn references

As part of the Monitoring of Damage to Historic Tapestries (MODHT) project, a series of historically accurate reference samples were dyed by Anne-Marei Hacke, The University of Manchester (Appendix 7.1), using biological sources likely to have been used during the period of interest. Authentic plant material was sourced and the recipes followed historical procedures as closely as possible. For further details of these samples, including information on how the recipes were derived and the actual dyeing conditions, see Appendix 7.2. When these samples have been referred to in the text, their unique identifier *i.e.* Y/W1 for the yellow weld dyed wool yarn, has been specified.

The majority of experiments were conducted using these MODHT dyed reference yarns, however, it was necessary to prepare additional samples for further investigative work. Sawwort, young fustic, brazilwood and logwood yarns were all dyed at the National Museums of Scotland, together with yarns dyed with pure chemical components, such as genistein, sulfuretin and 3-*O*-methylquercetin. The mordanting and dyeing procedures for these samples are therefore described below.

All samples were dyed onto either scoured (de-greased) English sheep wool (3-ply, 158 Tex) or degummed Italian spun *Bombyx mori* silk (2-ply, 66 Tex), which compared favourably with the historical yarns sampled from the tapestries.

6.1.1 Sawwort (*Serratula tinctoria* L.) and a related species (*Serratula coronata* L.) on alum mordanted wool

Sawwort harvested from two different geographical locations, together with a related species, *Serratula coronata* L. from a third location were obtained (Chapter 2). The alum mordanted wool for the dyeing of these samples was prepared as follows. The pre-scoured wool (1.2 g) was boiled in deionised water (100 ml) containing alum

(0.05 g) for 2 h before being wrung out and left to dry. The wool was then cut into five equal lengths, three for the dyeing of the sawwort samples, one for the dyeing of hematein (Section 6.1.5.1) and one for the dyeing of brazilwood (Section 6.1.5.3).

The first sawwort sample was harvested from the garden of Dominique Cardon in the Lanquedoc-Roussillon region of France (Location 1). The dried leaves, stems and flowers of the sawwort (0.54 g) were ground and added to boiling deionised water (30 ml) containing potassium carbonate (0.02 g). The mordanted wool was wetted under deionised water before being immersed in the hot dyebath and boiled for 1 h. The yarn was left for a further 2 h as the bath cooled, then wrung and rinsed with cold, deionised water and left to dry. The second sawwort sample, harvested from Mount Aigoual, France (Location 2) by D. Cardon and the related *Serratula coronata* L. sample, also harvested by D. Cardon but from Mount Dzungarian, Kazakhstan, were prepared in an identical manner to the first.

The sawwort dyed yarn used for the accelerated ageing study was prepared from sawwort obtained from the Association de Garance, Lauris, France. The mordanting procedure used pre-scoured wool (1.8 g), which was boiled in deionised water (90 ml) containing alum (0.03 g) for 2 h before being wrung out and left to dry. The dried leaves and stems of the sawwort (0.22 g) were ground and added to boiling deionised water (25 ml) containing potassium carbonate (0.03 g). Some of the mordanted wool (0.43 g, dry weight) was wetted under deionised water before being immersed in the dye bath, which was then boiled gently for 1 h. The yarn was removed, wrung and rinsed with cold water and left to dry.

6.1.2 Luteolin and genistein on alum mordanted wool

To study the photo-degradation of the main components of dyer's greenweed, accelerated ageing studies were performed on yarn dyed with genistein (Chapter 4). A pre-scoured wool yarn (1.4 g) was mordanted by boiling in deionised water (70 ml) containing alum (0.03 g) for 2 h. It was then removed, wrung and left to dry. To dye the yarn, the genistein (8.8 mg) was added to boiling deionised water (70 ml)

containing potassium carbonate (0.03 g). The mordanted wool was cut in half and one portion was wetted under deionised water before being immersed in the dye bath and boiled for 1 h. The yarn was then removed, rinsed with deionised water and left to dry.

6.1.3 Young fustic (*Cotinus coggygria* Scop.) on alum mordanted silk

An authentic source of young fustic (*Cotinus coggygria* Scop.) was supplied by the Association de Garance, Lauris, France. Two samples were provided; a 'fresh' batch, consisting of dried heartwood harvested within the last year, and an 'old' batch, consisting of dried heartwood harvested more than one year previously.

The wood from each batch was separately de-barked, chipped and rasped, and used to dye the MODHT yarns Y/S2a ('old') and Y/S2b ('fresh') (Appendix 7.2). However, the dyeing conditions for these samples produced very light coloured yarns. Furthermore, the acid hydrolysed extracts from the yarns contained only a small amount of the main colouring components, and were therefore not suitable for characterisation studies or accelerated ageing experiments. Thus, an additional dyeing was performed with the 'fresh' young fustic chips at the National Museums of Scotland. This yarn remained in the dyebath for 19 h, considerably longer than the 30 min that the MODHT yarn samples were immersed in the dyebath.

The 'fresh' young fustic chips (0.21 g) were immersed in deionised water (40 ml) and heated until boiling. The bath was then boiled gently for 1 h before the heat was removed and the bath allowed to cool for a further 1 h. The pre-wetted silk (Y/S2 mordanted, 0.02 g dry weight) was then immersed and left overnight (19 h). The yarn was removed, rinsed with deionised water and allowed to dry.

6.1.4 Sulfuretin and 3-*O*-Methylquercetin

Further examination into the photo-degradation of some of the components from young fustic and sawwort required yarns dyed with sulfuretin and 3-*O*-

methylquercetin (Chapter 4). The following samples were thus prepared for the accelerated ageing studies on the respective components.

6.1.4.1 Sulfuretin on alum mordanted silk (based on Y/S2)

Alum (98 mg) was dissolved in warm water (20 ml, 48 °C). Pre-wetted silk (211 mg, dry weight) was then mordanted by immersing the yarn for 2 h while the bath was allowed to cool. The yarn was then removed, rinsed and allowed to dry. Alum (22 mg) and sulfuretin (1.8 mg) were added to warm water (15 ml, 40 °C) and the pre-wetted, mordanted silk was immersed in the bath for 2 h before removal. The yarn was then rinsed with deionised water and left to dry.

6.1.4.2 3-*O*-Methylquercetin on alum mordanted silk (based on Y/S1)

Alum (89 mg) was dissolved in warm water (20 ml, 50 °C). Pre-wetted silk (237 mg, dry weight) was then mordanted by immersing the yarn in the bath, which was allowed to cool. The yarn was left soaking overnight (22 h) before being removed, rinsed and allowed to dry. The pre-wetted silk was then immersed in warm water (15 ml, 40 °C), to which had been added 3-*O*-methylquercetin (1.0 mg). The bath was held at approximately this temperature for 2 h. The yarn was then removed, rinsed with deionised water and left to dry.

6.1.4.3 3-*O*-Methylquercetin on alum mordanted wool (based on Y/W1)

Alum (42 mg) was dissolved in boiling water (40 ml). Pre-scoured wool (500 mg, dry weight) was then mordanted by immersing the yarn in the bath and gently boiled for 2 h. The yarn was then removed, rinsed with deionised water and left to dry. The pre-wetted wool was then immersed in boiling water (15 ml), to which had been added 3-*O*-methylquercetin (0.6 mg) and potassium carbonate (27 mg). The heat was then removed and the bath left for 1 h. The yarn was removed, rinsed with deionised water and left to dry. It was then dyed a second time by adding the pre-wetted wool to a bath of warm water (15 ml, 40 °C) containing 3-*O*-methylquercetin (0.7 mg) and potassium carbonate (12 mg). The bath was held at approximately this temperature for 2 h before the yarn was removed, rinsed with deionised water and left to dry.

6.1.5 Neoflavonoids/Homoisoflavonoids

The characterisation studies conducted on the neoflavonoid/homoisoflavonoid components (Chapter 3) required the use of several dyed yarns, described below.

6.1.5.1 Hematein on alum mordanted wool

Hematein (0.1 g) and potassium carbonate (0.02 g) were added to boiling water (20 ml) and left for 1 h. Small amounts of water were added periodically to ensure the volume of dye liquor remained approximately constant. One of the pre-wetted alum mordanted wool samples from Section 6.1.1 (0.18 g, dry weight) was immersed in the boiling bath for 1.5 h with constant stirring and periodic refills. The bath was removed from the heat and left to stand for a further 1 h before the yarn was removed, rinsed and left to dry. Both dye bath and yarn extracts were utilised in characterisation studies.

Characterisation studies were also performed using the extracts from the following dyed yarn. Hematein (20 mg) was added to boiling water (30 ml) then pre-wetted alum mordanted wool (mordanted for R/W3, 33.1 mg, dry weight) was immersed and the bath boiled gently for 2 h before being removed, rinsed and left to dry.

6.1.5.2 Hematoxylin on alum mordanted silk

Hematoxylin (44 mg) was added to warm water, to which was added the pre-wetted, alum mordanted silk (mordanted for R/S2, 36 mg dry weight). The yarn immediately became purple, although the dye bath solution remained a turbid yellow solution. The yarn was immersed for 2 h before being removed, rinsed and left to dry. Both dye bath and yarn extracts were utilised in characterisation studies.

A second yarn, dyed in the following manner, was also utilised. Hematoxylin (65.3 mg) was added to boiling water (20 ml) then pre-wetted, alum mordanted silk (mordanted for R/S1, 20.7 mg, dry weight) was immersed and the bath boiled gently for 1 h. The yarn was removed, rinsed and allowed to dry.

6.1.5.3 Brazilwood powder on alum mordanted wool

For the accelerated ageing of brazilwood dyed yarn (Chapter 4), the following sample was prepared. Brazilwood powder (0.1 g) and potassium carbonate (0.02 g) were added to boiling water (20 ml) and left for 1 h. To begin, the bath was an orange-red colour, but it gradually became dark red. Small amounts of water were added periodically to ensure the amount of dye liquor remained approximately constant. One of the pre-wetted, alum mordanted wool samples from Section 6.1.1 (0.25 g, dry weight) was immersed in the boiling bath for 2 h with constant stirring and periodic refills. The bath was removed from the heat and left to stand for a further 1 h before the yarn was removed, rinsed and left to dry.

6.1.5.4 Brazilwood powder on alum mordanted silk

Studies were also performed using a silk yarn, dyed in a similar manner. Brazilwood powder (0.65 g) was added to boiling water (20 ml) then pre-wetted, alum mordanted silk (mordanted for R/S1, 21.8 mg, dry weight) was immersed and the bath boiled gently for 1 h. The yarn was then removed, rinsed and left to dry.

6.1.5.5 Brazilin on alum mordanted silk

Brazilin (52.7 mg) was added to boiling water (20 ml) then pre-wetted, alum mordanted silk (mordanted for R/S1, 22.7 mg, dry weight) was immersed and the bath boiled gently for 1 h. The yarn was then removed, rinsed and left to dry.

6.1.5.6 Brazilwood reference (*Caesalpinia Sappan* L.) on alum mordanted silk

Some heartwood chips from the *Caesalpinia Sappan* L. reference (0.44 g) were added to boiling water (20 ml) then pre-wetted, alum mordanted silk (mordanted for R/S1, 23.0 mg, dry weight) was immersed and the bath boiled gently for 1 h. The yarn was then removed, rinsed and left to dry.

6.2 Dye extraction

The dye components from both the reference yarns and the historical yarns were extracted using an identical acid hydrolysis procedure (Section 6.2.1), while the

neoflavonoid/homoisoflavonoid characterisation studies also utilised a modified extraction method (Section 6.2.2).

6.2.1 System 1 (for reference and historical samples)

The hydrochloric acid extraction protocol, originally developed for the routine analysis of the dye components from reference and historical samples, was as follows. The dyed yarn or solid reference material (typically 0.1 – 5 mg) was placed in a 2 ml glass test tube, to which was added a 2:1:1 (v/v/v) mixture of 37% hydrochloric acid: methanol: water (400 µl). The tube was then placed in a water bath at 100 °C and heated for precisely 10 min. After rapid cooling under cold water, the extract was filtered using a 5 µm Analytichem polypropylene frit under positive pressure. The test tube was rinsed with methanol (200 µl) and the combined filtrates dried by rotary vacuum evaporation over a water bath at 40 °C. The dry residue was then reconstituted with methanol (25 µl) and water (25 µl).

6.2.2 System 2 (acetic acid extraction protocol)

The 'standard' extraction protocol, developed to study the dye components from reference and historical yarn samples (Section 6.2.1) was modified by replacing the hydrochloric acid in the extraction mixture with acetic acid. The impact on the formation of the neoflavonoid/homoisoflavonoid 'marker' components was then assessed (Section 6.5.6).

6.3 Chromatographic methods

To characterise the components in the acid hydrolysed extracts of both reference and historical samples, a PDA HPLC method developed for the routine analysis of acid hydrolysed extracts was utilised (Section 6.3.1). This enabled the retention time (R_t) and UV-Vis spectral information of each component in the extracts to be compared against an 'in-house' library of standards. The investigation of the unknown components on cochineal dyed yarn required this method to be slightly modified (Section 6.3.2 and Section 6.3.3).

6.3.1 System 1 (for reference and historical samples)

The chromatographic method for the analysis of reference and historical samples used a Phenomenex Sphereclone ODS2, 5 μm particle size, 150 × 4.6 mm (length × internal diameter), reverse phase column, with a guard column containing the same stationary phase. This was enclosed in a heat-controlled chamber and maintained at 25±1 °C. Sample extracts were injected *via* a Rheodyne injector with a 20 μl sample loop. A Waters 600 gradient pump and a Waters 2996 PDA detector were controlled by Waters Empower software, which also collected and manipulated the data.

The total run time was 35 min at a flow rate of 1.2 ml min^{-1}. A tertiary solvent system was used; A = 20% (v/v) MeOH (aq.), B = MeOH, C = 5% (v/v) ortho-phosphoric acid (aq.). The elution programme was isocratic for 3 min (67A: 23B: 10C) then a linear gradient from 3 min to 29 min (0A: 90B: 10C) before initial conditions recovery over 1 min and equilibration over 5 min. Solvents were sparged using a vacuum in-line degasser and chromatographed peaks were monitored at 254 nm although the PDA detector measured all spectral information between 250 and 750 nm. The bandwidth (resolution) was 2.4 nm, and response time set to 1 s. This information has been summarised in Table 6.1 below.

Table 6.1: The chromatographic conditions for the analysis of reference and historical samples

Column		Phenomenex Sphereclone ODS2, 5 μm particle size, 150 × 4.6 mm					
Run time		35 min					
Solvent System			A 20% MeOH	B MeOH	C 5% phosphoric acid	Injection volume	20 μl
Gradient / min	Isocratic	0-3	67%	23%	10%	Temperature	25±1 °C
	Linear	3-29	0%	90%	10%		
	Linear	29-30	67%	23%	10%	Flow rate	1.2 ml min^{-1}
	Isocratic	30-35	67%	23%	10%		

6.3.2 System 2 (for cochineal)

The 'standard' chromatographic method, developed for the routine analysis of acid hydrolysed extracts (Section 6.3.1) was modified by replacing the ortho-phosphoric

acid with formic acid and adjusting the gradient. Thus, a Phenomenex Sphereclone ODS2, 5 μm particle size, 150 × 4.6 mm (length × internal diameter), reverse phase column, with a guard column containing the same stationary phase, was enclosed in a heat-controlled chamber and maintained at 25±1 °C. Sample extracts were injected *via* a Rheodyne injector with a 20 μl sample loop. A Waters 600 gradient pump and a Waters 2996 PDA detector were controlled by Waters Empower software, which also collected and manipulated the data.

The total run time was 40 min at a flow rate of 1.2 ml min^{-1}. A tertiary solvent system was used; A = H_2O, B = MeOH, C = 5% (v/v) formic acid (aq.). The elution programme was isocratic for 2 min (67A: 23B: 10C) then a linear gradient from 2 min to 30 min (0A: 90B: 10C) before initial conditions recovery over 2 min and equilibration over 8 min. Solvents were sparged using a vacuum in-line degasser and chromatographed peaks were monitored at 254 nm, 275 nm and 430 nm, although the PDA detector measured all spectral information between 250 and 750 nm. The bandwidth (resolution) was 2.4 nm, and response time set to 1 s.

6.3.3 System 3 (for 'large scale' cochineal)

The chromatographic method for the separation of the characteristic components in cochineal extracts for NMR analysis used a reverse phase Phenomenex Luna C18(2) 10 μm particle size, 60 × 21.20 mm (length × internal diameter) column at ambient temperature. Sample extracts were injected *via* a Rheodyne injector with a 200 μl sample loop. A Waters 600 gradient pump and a Waters 2996 PDA detector were controlled by Waters Empower software, which also collected and manipulated the data.

The total run time was 35 min at a flow rate of 8.0 ml min^{-1}. A tertiary solvent system was used; A = 20% (v/v) MeOH (aq.), B = MeOH, C = 5% (v/v) formic acid (aq.). The elution programme was isocratic for 3 min (67A: 23B: 10C) then a linear gradient from 3 min to 29 min (0A: 90B: 10C) before initial conditions recovery over 1 min and equilibration over 5 min. Solvents were sparged using a vacuum in-line

degasser and chromatographed peaks were monitored at 254 nm, 275 nm and 430 nm, although the PDA detector measured all spectral information between 250 and 750 nm. The bandwidth (resolution) was 2.4 nm, and response time set to 1 s. This information has been summarised in Table 6.2 below.

Table 6.2: The chromatographic conditions for the separation of the characteristic components in cochineal extracts

Column		Phenomenex Luna C18(2) 10 μm particle size, 60 × 21.20 mm					
Run time		35 min					
Solvent System			A 20% MeOH	B MeOH	C 5% formic acid	Injection volume	200 μl
Gradient / min	Isocratic	0-3	67%	23%	10%	Temperature	Ambient
	Linear	3-29	0%	90%	10%		
	Linear	29-30	67%	23%	10%	Flow rate	8 ml min^{-1}
	Isocratic	30-35	67%	23%	10%		

6.4 Mass spectrometry conditions

Chromatographic analysis with photo diode array detection was not always sufficient to identify the unknown components from natural dye sources or their dyed yarn extracts. However, investigative work using Electrospray Ionisation (Ion Trap) Mass Spectrometry (ESI MS^n) was sometimes able to provide additional information. The operating parameters for the ion source and the chromatographic methods utilised for the ESI MS^n experiments are outlined below.

6.4.1 Direct injection

A Finnigan Thermoquest LCQ™ ESI quadrupole ion trap mass spectrometer, operating in the negative ion mode, was used. The sample solutions, of methanol or deuteriated methanol (MeOD) as appropriate, were directly injected into the source *via* a syringe pump delivering 8 μl min^{-1}. Peaks were selected for CID with a band-width of 1.0 atomic mass units (a.m.u.) and the operating parameters were dependent on the experiment (Sections 6.4.1.1 to 6.4.1.4). Data were collected and processed by the LCQ Navigator™ software.

6.4.1.1 System 1 (for the direct injection of flavonoids)

The analysis of solutions containing flavonoid components required the following operating parameters for the electrospray ionisation source; The capillary temperature was 200 °C, the source voltage 4.50 kV, the sheath gas (N_2) flow rate 80 AU (Arbitrary Units), the auxiliary gas (N_2) flow rate 10 AU (Arbitrary Units) and the capillary voltage -5.00 V. Additional parameters included; a tube lens offset of 60.00 V, an octapole 1 offset of 2.75 V, an octapole 2 offset of 6.00 V, and an inter-octapole lens voltage of 20.00 V.

For studies on a specific component, the detector could be tuned on its deprotonated molecular ion peak. The parameters were then automatically adjusted to provide a signal maximum for this component. The relative collision energy required for the MS^n experiments was usually around 20-25%.

6.4.1.2 System 2 (for the direct injection of neoflavonoids/homoisoflavonoids)

The analysis of solutions containing neoflavonoid/homoisoflavonoid components required the following operating parameters for the electrospray ionisation source; the capillary temperature was 175 °C, the source voltage 3.50 kV, the sheath gas (N_2) flow rate 69 AU (Arbitrary Units), the auxiliary gas (N_2) flow rate 2 AU (Arbitrary Units) and the capillary voltage -5.00 V. The MS^n breakdown studies involved tuning the detector on the particular deprotonated molecular ion peak of interest. The parameters were then automatically adjusted to provide a signal maximum for this component. The relative collision energy required for the MS^n experiments was usually around 25-30%.

6.4.1.3 System 3 (for the direct injection of sulfuretin)

The operating parameters of the electrospray ionisation source for the analysis of flavonoid solutions (Section 6.4.1.1) were adjusted slightly for the breakdown study of the aurone, sulfuretin. The capillary temperature was 200 °C, the source voltage 4.55 kV, the sheath gas (N_2) flow rate 80 AU (Arbitrary Units), the auxiliary gas (N_2) flow rate 10 AU (Arbitrary Units) and the capillary voltage -5.05 V. Once again,

additional parameters were tuned using the deprotonated molecular ion peak. The relative collision energy required for the MS^n experiments was usually around 20-25%.

6.4.1.4 System 4 (for the direct injection of cochineal extracts)

The operating parameters of the electrospray ionisation source for the analysis of flavonoid solutions (Section 6.4.1.1) provided initial conditions. A methanolic solution of carminic acid was then injected and the parameters 'tuned' using the deprotonated molecular ion peak. The tuning of the source was performed at the beginning of each study involving cochineal extracts, thus ensuring that the parameters were automatically adjusted to provide a signal maximum for the components of interest. The relative collision energy required for the MS^n experiments was usually around 20-25%.

6.4.2 HPLC ESI (ion trap) MS

Samples were analysed by means of a high performance liquid chromatography instrument connected in series to a single wavelength, tuneable UV-visible detector and an electrospray ionisation ion trap mass spectrometer, operating in negative ion mode. The liquid chromatograph (HPLC) was a Finnigan Mat Spectra™ system, composed of an AS3000 autosampler, a P4000 pump and a V2000 detector. The sample (20 µl) was injected *via* the autosampler, with the column and gradient system dependent on the particular study (Sections 6.4.2.1 to 6.4.2.4).

The mass analysis was performed using a Thermoquest Finningan LCQ™ mass spectrometer, operating in negative ion mode and controlled by LCQ Navigator™ software. The parameters for the electrospray ionisation source were also dictated by the nature of the experiments (Sections 6.4.2.1 to 6.4.2.4).

6.4.2.1 System 1 (for the HPLC ESI MS of the flavonoids)

A reverse phase Prodigy (Phenomenex) ODS3, 5 µm particle size column, 150 mm × 2.0 mm (length × internal diameter) column, with a guard column containing the same stationary phase, was used at ambient temperature. The total run time was 35

min at a flow rate of 0.35 ml min^{-1}, although a flow splitter was utilized to reduce the eluent flow into the mass spectrometer by approximately two thirds.

A binary solvent system of; A = H_2O, B = MeOH was used, while the elution programme was isocratic for 2 min (70A: 30B) then a linear gradient to 30 min (10A: 90B) before initial conditions recovery over 2 min and isocratic for 3 min. A further 5 min equilibration was introduced between injections. Solvents were sparged using a vacuum in-line degasser and chromatographed peaks were monitored at 254 nm. This information has been summarised in Table 6.3 below. The operating parameters for the electrospray ionisation source were the same as those for direct injection of the flavonoids (Section 6.4.1.1).

Table 6.3: The chromatographic conditions for the HPLC ESI MS of the flavonoids

Column		Prodigy (Phenomenex) ODS3, 5 µm particle size column, 150 mm × 2.0 mm				
Run time		40 min				
Solvent System			A H_2O	B MeOH	Injection volume	200 µl
Gradient / min	Isocratic	0-2	70%	30%	Temperature	Ambient
	Linear	2-30	10%	90%		
	Linear	30-32	70%	30%	Flow rate	0.35 ml min^{-1} (and flow splitter)
	Isocratic	32-40	67%	23%		

6.4.2.2 System 2 (for the HPLC ESI MS of young fustic)

The HPLC system for the analysis of young fustic extracts was the same as for the flavonoids analysis (Section 6.4.2.1), while the operating parameters from the direct injection of sulfuretin (Section 6.4.1.3) were utilised for the electrospray ionisation source.

6.4.2.3 System 3 (for the HPLC ESI MS of cochineal)

The cochineal method developed for the PDA HPLC (Section 6.3.2) was utilised to ensure results obtained from each instrument were directly comparable. Thus, a Phenomenex Sphereclone ODS2, 5 µm particle size, 150 × 4.6 mm (length × internal diameter), reverse phase column, with a guard column containing the same stationary phase, was used at ambient temperature. Sample extracts (20 µl) were injected *via* the

autosampler. The total run time was 40 min at a flow rate of 1.2 ml min^{-1}, although a flow splitter was used to reduce the flow into the mass spectrometer to *ca.* 0.30 ml min^{-1}.

An identical tertiary solvent system of; A = H_2O, B = MeOH, C = 5% (v/v) formic acid (aq.) was also used. The elution programme was isocratic for 2 min (67A: 23B: 10C) then a linear gradient from 2 min to 30 min (0A: 90B: 10C) before initial conditions recovery over 2 min and equilibration over 8 min. Solvents were sparged using a vacuum in-line degasser and chromatographed peaks were monitored at 430 nm. The operating parameters for the electrospray ionisation source were arrived at in the same way as those for the direct injection of the cochineal extracts (Section 6.4.1.4).

6.4.2.4 System 4 (for the HPLC ESI MS of the neoflavonoids/ homoisoflavonoids)

The chromatographic system for the analysis of the neoflavonoids/ homoisoflavonoids and their elimination products utilized a large bore column and a flow splitter. Thus, a Phenomenex Sphereclone ODS2, 5 μm particle size, 150 × 4.6 mm (length × internal diameter), reverse phase column, with a guard column containing the same stationary phase, was used at ambient temperature. Sample extracts (20 μl) were injected *via* the autosampler. The total run time was 35 min at a flow rate of 1.2 ml min^{-1}, although a flow splitter was used to reduce the flow into the mass spectrometer to *ca.* 0.30 ml min^{-1}.

A binary solvent system of; A = H_2O, B = MeOH was used. The elution programme was isocratic for 2 min (70A: 30B) then a linear gradient to 30 min (10A: 90B) before initial conditions recovery over 2 min and isocratic for 3 min. Solvents were sparged using a vacuum in-line degasser and chromatographed peaks were monitored at 254 nm.

The operating parameters for the electrospray ionisation source were as follows; the capillary temperature was 180 °C, the source voltage 5.00 kV, the sheath gas (N_2) flow rate 80 AU (Arbitrary Units), the auxiliary gas (N_2) flow rate 2 AU (Arbitrary Units) and the capillary voltage -17.00 V. Additional parameters included; a tube lens offset of -45.00 V, an octapole 1 offset of 2.50 V, an octapole 2 offset of 6.50 V, and an inter-octapole lens voltage of 18.00 V.

6.5 PDA HPLC

6.5.1 Weld (*Reseda luteola* L.)

The luteolin methyl ether 'spiking experiments' with chrysoeriol and diosmetin (Chapter 2) were based on the standard hydrochloric acid extraction protocol (Section 6.2.1). However, the dry residues from the extracted weld dyed wool yarns were reconstituted with 1:1 (v/v) MeOH:H_2O solutions of chrysoeriol (50 µl, *ca.* 10 µg ml^{-1}) or diosmetin (50 µl, *ca.* 10 µg ml^{-1}) respectively.

The relative ratios of the characteristic components observed in the extracts from the weld dyed reference yarns were examined (Chapter 2). Thus, the peak areas of each component, per mg of yarn (monitored at 254 nm) have been tabulated below (Table 6.4 and Table 6.5).

Table 6.4: The peak areas per mg of yarn (monitored at 254 nm) of the main flavonoid components in the acid hydrolysed extracts from all the weld dyed wool yarns

	Peak area (monitored at 254 nm) per mg of yarn / AU		
	Luteolin	**Apigenin**	**Chrysoeriol**
Y/W1: weld on wool			
Sample 1	2154297	80242	49048
Sample 2	1956093	73796	41894
Sample 3	1941891	71558	42086
Sample 4	2064535	79272	44924
MEAN	2029204	76217	44488
±95% confidence	±158765 (7.8%)	±6695 (8.8%)	±5316 (11.9%)
G/W1: weld overdyed with woad			
Sample 1	967101	18023	19117
Sample 2	1111780	21515	15161
Sample 3	1133863	23882	16119
Sample 4	1095309	23469	17896
MEAN	1077013	21722	17073
±95% confidence	±119275 (11.1%)	±4254 (19.6%)	± 2820 (16.5%)
G/W2: woad overdyed with weld			
Sample 1	1107745	33039	20057
Sample 2	1120698	33604	20862
Sample 3	1013948	35581	20744
Sample 4	1047359	36182	21098
MEAN	1072438	34602	20690
±95% confidence	±80225 (7.5%)	±2412 (7.0%)	±711 (3.4%)

Table 6.5: The peak areas per mg of yarn (monitored at 254 nm) of the main flavonoid components in the acid hydrolysed extracts from all the weld dyed silk yarns

	Peak area (monitored at 254 nm) per mg of yarn / AU		
	Luteolin	**Apigenin**	**Chrysoeriol**
Y/S1a: weld on silk			
Sample 1	7731055	390971	273779
Sample 2	4860735	218813	153708
Sample 3	7258647	335994	248512
Sample 4	6306137	285209	207012
MEAN	6539144	307747	220753
±95% confidence	±2014787 (30.8%)	±116719 (37.9%)	±83526 (37.8%)
Y/S1b: weld on silk			
Sample 1	4925875	290136	195769
Sample 2	5777661	311045	220307
Sample 3	5046331	267061	194428
Sample 4	4599617	241529	172145
MEAN	5087371	277443	195662
±95% confidence	±791448 (15.6%)	±47629 (17.2%)	±31316 (16.0%)
G/S1: weld overdyed with woad (boil mordant)			
Sample 1	7344882	361843	258453
Sample 2	8437173	381738	266833
Sample 3	5489283	228458	182449
Sample 4	5966248	286672	200620
MEAN ± 95%	6809397	314678	227089
confidence interval	±2132874 (31.3%)	±112291 (35.7%)	±66608 (29.3%)
G/S2: weld overdyed with woad			
Sample 1	4486630	233530	160345
Sample 2	3817903	181390	125520
Sample 3	4769353	234299	179146
Sample 4	4417901	206496	145343
MEAN ± 95%	4372947	213929	152589
confidence interval	±636593 (14.6%)	±40184 (18.8%)	±36177 (23.7%)
G/S3: woad overdyed with weld (boil mordant)			
Sample 1	9964094	455239	300127
Sample 2	7536586	401116	279302
Sample 3	7599878	438153	304140
Sample 4	9610386	397394	282956
MEAN ± 95%	8677736	422976	291631
confidence interval	±2051910 (23.6%)	±45040 (10.6%)	±19616 (6.7%)
G/S4: woad overdyed with weld			
Sample 1	6741710	471620	299145
Sample 2	4304803	299664	191891
Sample 3	5099186	313340	216587
Sample 4	5773067	362358	251438
MEAN ± 95%	5479692	361746	239765
confidence interval	±1644413 (30.0%)	±124177 (34.3%)	±74018 (30.9%)

6.5.2 Dyer's greenweed (*Genista tinctoria* L.)

The relative ratios of the characteristic components observed in the extracts from the dyer's greenweed dyed reference yarns were also examined (Chapter 2). Thus, the peak areas of each component, per mg of yarn (monitored at 254 nm) have been tabulated below (Table 6.6 and Table 6.7). The mean and 95% confidence intervals have not be given in this case due to the partial co-elution of genistein and luteolin, the two main components.

Table 6.6: The peak areas, per mg of yarn (monitored at 254 nm) of the main flavonoid components in the acid hydrolysed extracts from alum mordanted wool dyed with dyer's greenweed

Dyer's greenweed on wool (Y/W2)	Peak area (monitored at 254 nm) per mg of yarn / AU		
	Genistein	Luteolin	Apigenin
Sample 1	1798278	1495408	322867
Sample 2	1549990	1267174	274202
Sample 3	1716416	1354113	311018
Sample 4	1498117	1201393	262088

Table 6.7: The peak areas, per mg of yarn (monitored at 254 nm) of the main flavonoid components in the acid hydrolysed extracts from alum mordanted silk dyed with dyer's greenweed

Dyer's greenweed on silk	Peak area (monitored at 254 nm) per mg of yarn / AU		
	Genistein	Luteolin	Apigenin
Y/S3a Sample 1	3600384	3942742	680127
Y/S3a Sample 2	3407053	3829676	746897
Y/S3b Sample 1	1767102	4473553	468824
Y/S3b Sample 2	2155086	6375183	433671
Y/S3c Sample 1	553926	1325605	122986
Y/S3c Sample 2	987076	2937844	330339
Y/S3d Sample 1	464371	3860508	186713
Y/S3d Sample 2	735208	7239014	416613
Y/S3e Sample 1	511279	445686	99256
Y/S3e Sample 2	614717	534454	111730

6.5.3 Sawwort (*Serratula tinctoria* L.) and related species (*Serratula coronata* L.)

Detailed spectral information for the components observed in the acid hydrolysed extracts from the NMS dyed sawwort yarns have been tabulated below (Table 6.8 –

Table 6.10). In addition, where the retention time (R_t) and UV-Vis spectral information of a component has matched with the details from a component in the 'in-house' library of standards, this has also been indicated.

Table 6.8: The retention times (R_t), relative percentage peak area (monitored at 254 nm) and UV-Vis spectra of the components in the acid hydrolysed extracts from the yarn dyed with sawwort from location 1

UV-Visible spectra from the extracts of yarn dyed with sawwort from location 1		
R_t 14.9 min (1.2%)	R_t 15.5 min (7.9%) Quercetin	R_t 16.6 min (75.2%) Luteolin (Not spectrally pure)
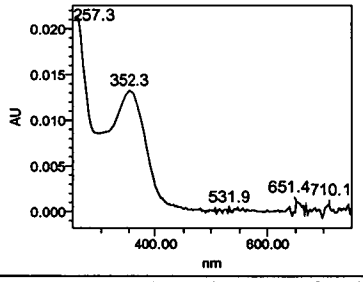	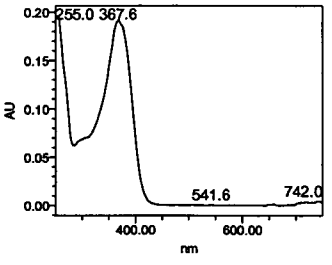	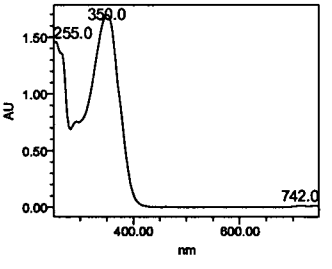
R_t 18.1 min (2.9%) Kaempferol	R_t 18.8 min (12.7%) Apigenin	
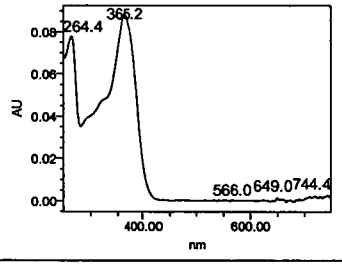	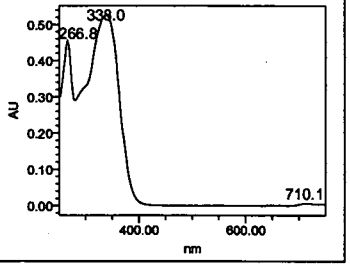	

Table 6.9: The retention times (R_t), relative percentage peak area (monitored at 254 nm) and UV-Vis spectra of the components in the acid hydrolysed extracts from the yarn dyed with sawwort from location 2

UV-Visible spectra from the extracts of yarn dyed with sawwort from location 2		
R_t 8.7 min (0.8%) 3,4-Dihydroxycinnamic acid methyl ester 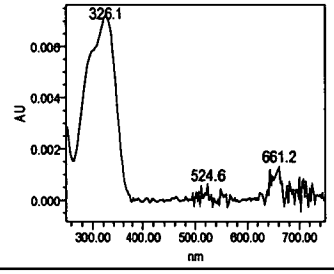	R_t 9.4 min (1.4%) 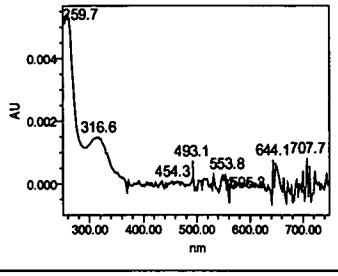	R_t 10.2 min (1.8%) 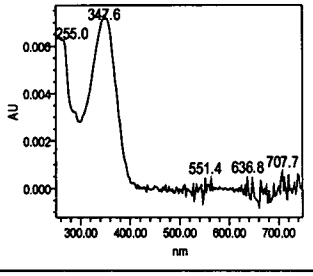
R_t 14.2 min (1.0%) 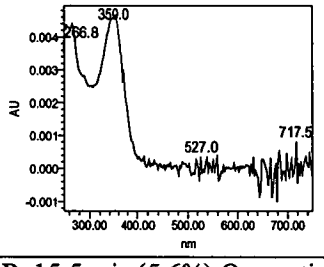	R_t 14.7 min (0.8%) 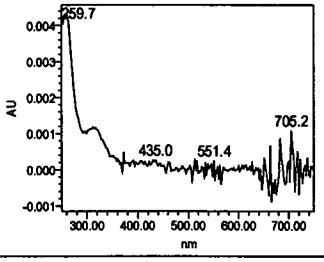	R_t 14.9 min (0.8%) 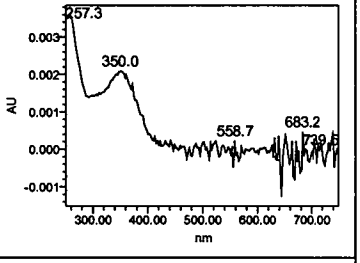
R_t 15.5 min (5.6%) Quercetin 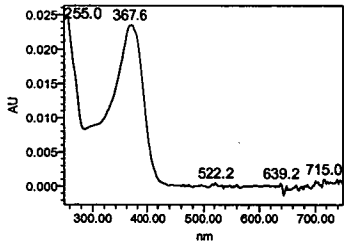	R_t 16.7 min (82.9%) Luteolin (not spectrally pure) 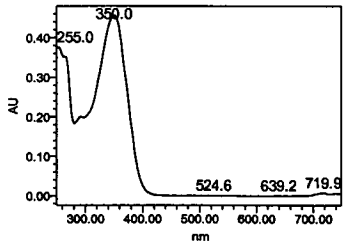	R_t 18.1 min (0.3%) Kaempferol 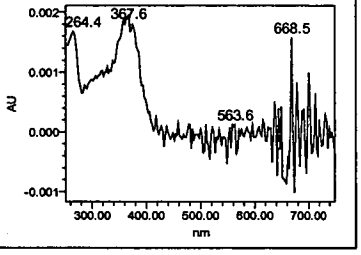
R_t 18.8 min (4.4%) Apigenin 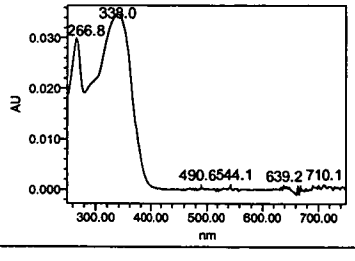	R_t 19.4 min (0.2%) 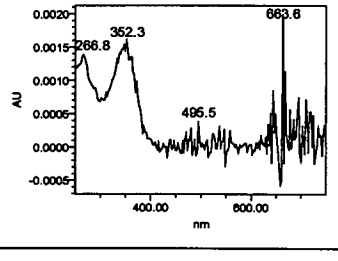	

Table 6.10: The retention times (R_t), relative percentage peak area (monitored at 254 nm) and UV-Vis spectra of the components in the acid hydrolysed extracts from the yarn dyed with *Serratula coronata* L.

UV-Visible spectra from the extracts of yarn dyed with the related *Serratila coronata* L. species		
R_t 14.9 min (0.9%)	R_t 15.5 min (12.7%) Quercetin	R_t 16.6 min (74.3%) 3-*O*-Methylquercetin (not spectrally pure)
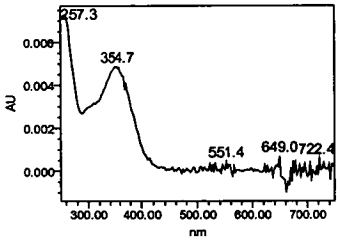	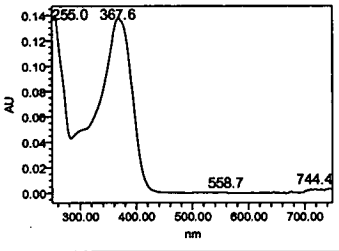	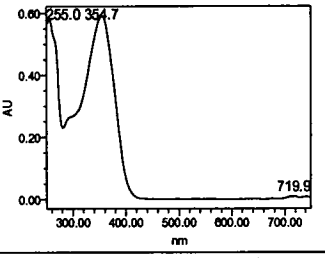
R_t 18.1 min (4.1%) Kaempferol	R_t 18.8 min (7.6%) Apigenin	R_t 19.5 min (0.6%)
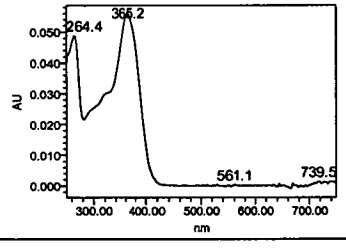	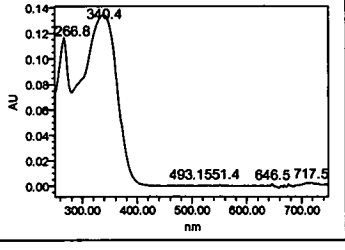	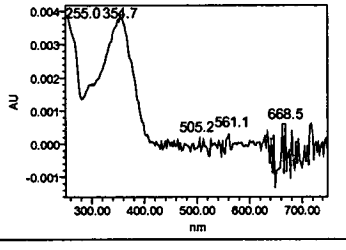

6.5.4 Young fustic (*Cotinus coggygria* Scop.)

Detailed spectral information for all the components observed in the acid hydrolysed extracts from the NMS dyed young fustic yarn have been tabulated below (Table 6.11). In addition, where the retention time (R_t) and UV-Vis spectral information of a component has matched with the details from a component in the 'in-house' library of standards, this has also been indicated.

Table 6.11: The retention times (R_t), relative percentage peak areas (monitored at 254 nm) and UV-Vis spectra of the components in the acid hydrolysed extracts from the NMS dyed young fustic yarn

UV-Visible spectra of the components observed in the extracts from yarn dyed with young fustic		
R_t 2.6 min (2.3%)	R_t 4.2 min (1.7%)	R_t 4.5 min (1.0%) Dihydrofisetin
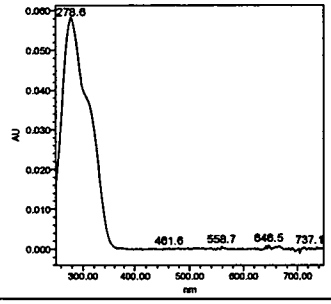	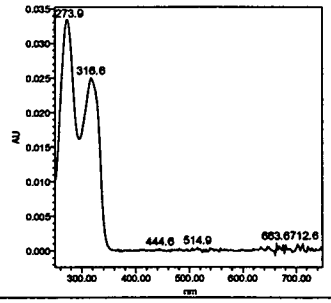	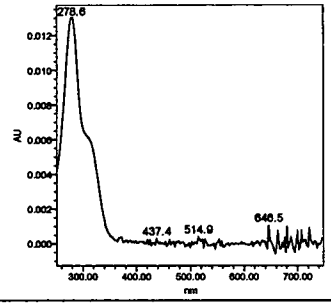
R_t 5.9 min (0.4%)	R_t 9.3 min (3.2%) Unknown 1	R_t 13.6 min (31.7%) Fisetin
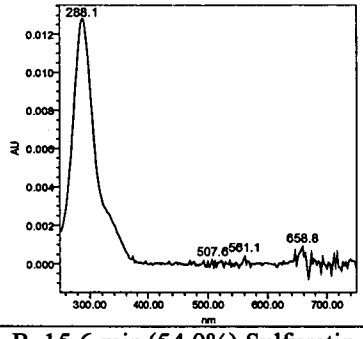	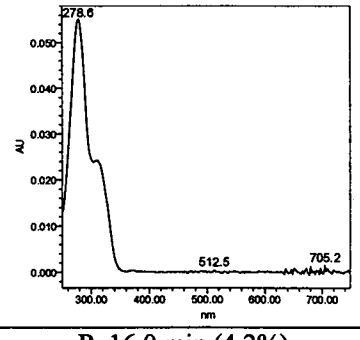	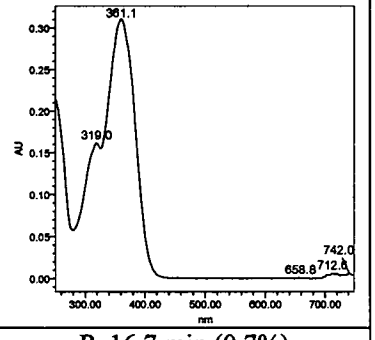
R_t 15.6 min (54.9%) Sulfuretin	R_t 16.0 min (4.2%) Unknown 2	R_t 16.7 min (0.7%)
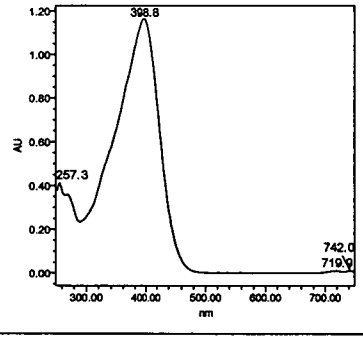	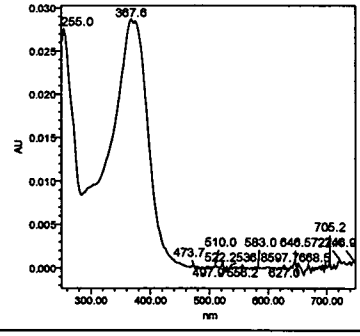	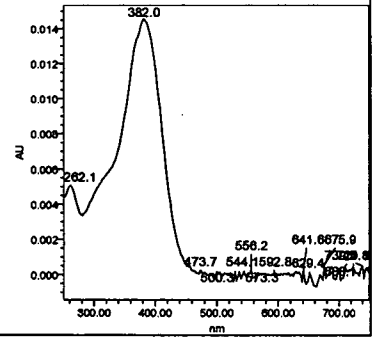

6.5.5 Cochineal (*Dactylopius coccus* Costa)

The relative ratios of the characteristic components observed in the extracts from the cochineal dyed reference yarns were examined (Chapter 3). Thus, the areas of each

component, per mg of yarn (monitored at 430 nm and 275 nm), have been tabulated below (Table 6.12).

Table 6.12: Retention times (R_t) and peak areas (monitored at both 430 nm and 275 nm) of the main anthraquinone components of the acid hydrolysed extracts of cochineal (*Dactylopius coccus* Costa) dyed wool (R/W5)

Peak	R_t	Peak area at 430 nm / AU	Peak area at 275 nm / AU
dcII	13.6	29689	150618
Carminic acid	14.1	621693	5544438
dc IV	18.1	10059	84743
dc VII	20.0	13118	133823
Flavokermesic acid	22.0	13651	46134

Detailed spectral information for the components can be found in Chapter 3.

6.5.6 Hematein and Brazilwood

In addition to this elimination product, a number of minor components were also observed during chromatographic analysis of acid extracts. Two samples of a hematein dyed yarn (from Section 6.1.5.1) were thus extracted using the hydrochloric acid extraction procedure (Section 6.2.1) and the acetic acid extraction protocol (Section 6.2.2) respectively. The results from the 'standard' chromatographic analysis of the respective extracts (Section 6.3.1) were compared and have been tabulated below (Table 6.13). Significantly, the main hydrochloric acid elimination product characterised in Chapter 3 (3,4,10-trihydroxy-*7H*-indeno[2,1-*c*]chromen-9-one), is absent in the re-constituted extract from the acetic acid protocol.

Table 6.13: The retention times (R_t), relative percentage peak areas (monitored at 254 nm) and UV-Vis spectra of the components obtained from a hematein dyed yarn upon chromatographic analysis of the hydrochloric acid extract

UV-Visible spectra of the components observed in the hydrochloric acid extracts from yarn dyed with hematein		
R_t 2.1 min (2.9%)	R_t 5.0 min (1.9%)	R_t 7.4 min (81.7%) (Hematein elimination product)
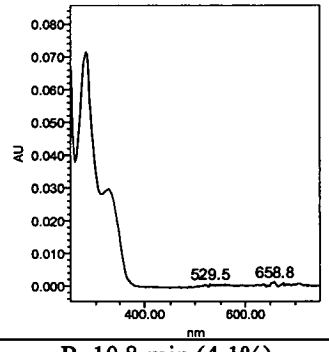	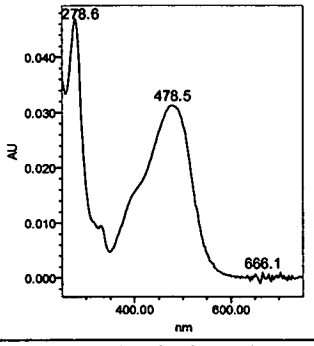	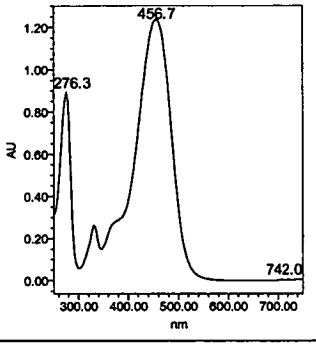
R_t 10.8 min (4.1%)	R_t 13.0 min (2.7%)	R_t 14.0 min (2.4%)
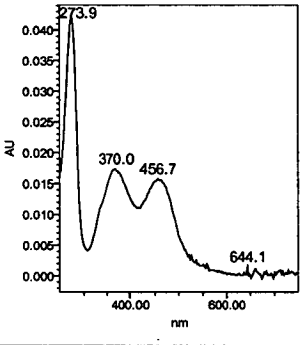	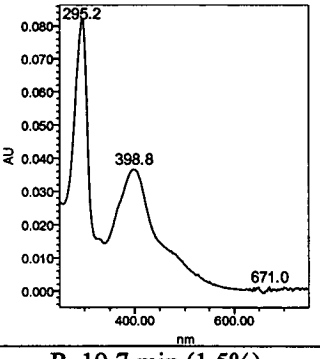	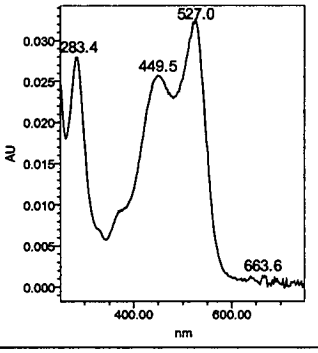
R_t 15.6 min (2.8%)	R_t 19.7 min (1.5%)	
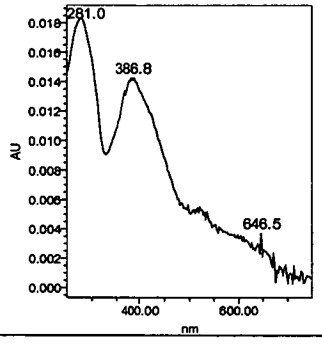	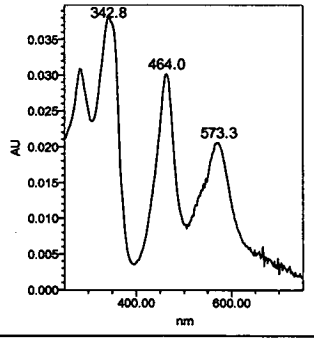	

Table 6.14: The retention times (R_t), relative percentage peak areas (monitored at 254 nm) and UV-Vis spectra of the components obtained from a hematein dyed yarn upon chromatographic analysis of the acetic acid extract

UV-Visible spectra of the components observed in the acetic acid extracts from yarn dyed with hematein		
R_t 1.9 min (13.3%)	R_t 2.9 min (19.8%)	R_t 6.4 min (27.5%)
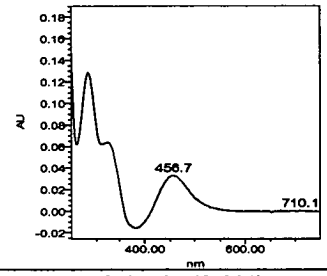	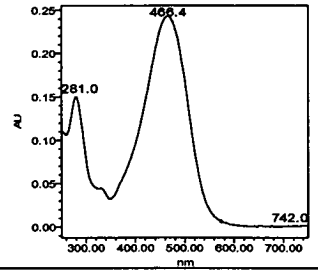	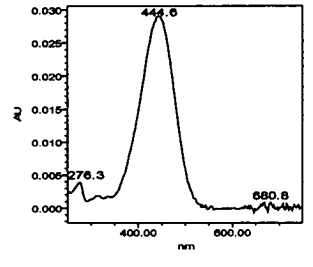
R_t 8.6 min (2.3%)	R_t 9.5 min (6.2%)	R_t 12.0 min (5.6%)
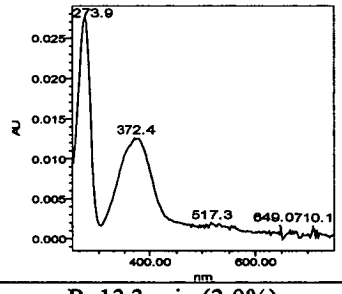	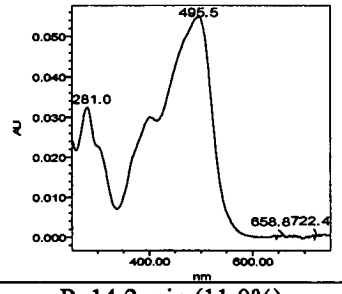	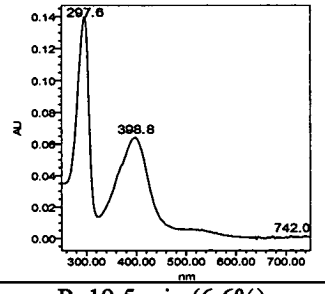
R_t 13.3 min (3.9%)	R_t 14.2 min (11.0%)	R_t 19.5 min (6.6%)
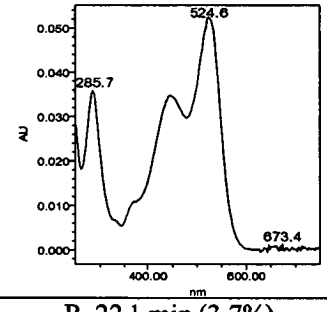	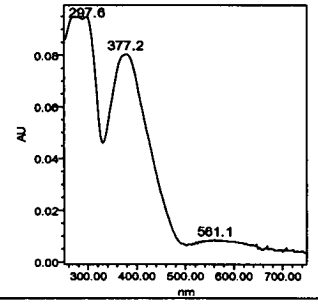	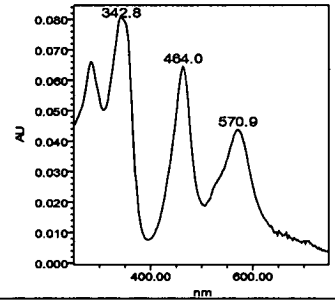
R_t 22.1 min (3.7%)		
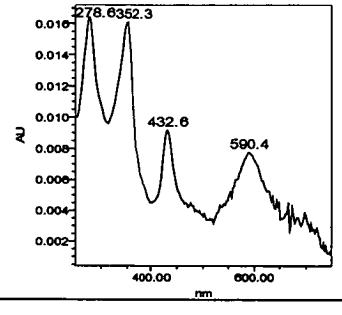		

The analogous component to the hematein elimination product, formed during the hydrochloric acid extraction of brazilein from yarn dyed with brazilwood powder (Section 6.1.5.3), has not yet been fully characterised. However, a component with a similar UV-Vis spectrum is observed in the chromatogram from the hydrochloric acid extracts, but is not present in the acetic acid extracts (Table 6.15). Both samples were run using the 'standard' chromatographic method (Section 6.3.1).

Table 6.15: The retention times (R_t), relative percentage peak areas (monitored at 254 nm) and UV-Vis spectra of the components obtained from chromatographic analysis of the hydrochloric acid extract of a yarn dyed with brazilwood powder

UV-Visible spectra of the components observed in the hydrochloric acid extracts from yarn dyed with brazilwood powder		
R_t 2.8 min (68.8%)	R_t 7.8 min (3.3%)	R_t 10.3 min (9.8%) (possibly the analogous elimination product to hematein)
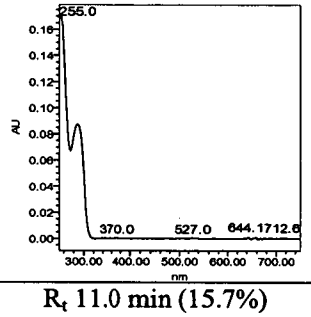	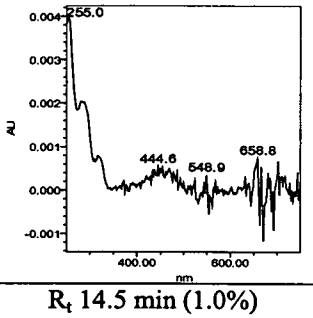	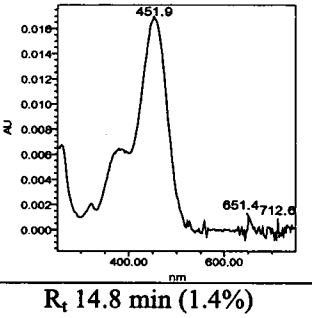
R_t 11.0 min (15.7%)	R_t 14.5 min (1.0%)	R_t 14.8 min (1.4%)
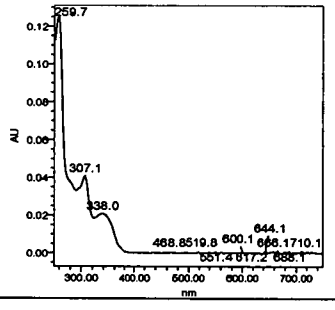	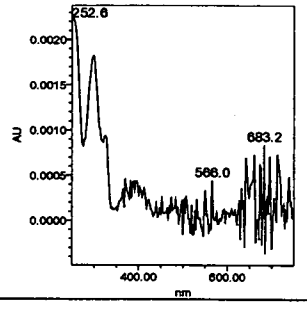	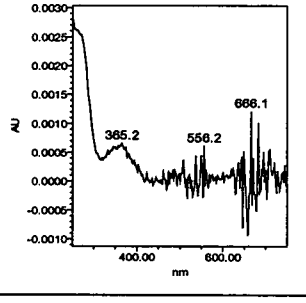

Table 6.16: The retention times (R_t), relative percentage peak areas (monitored at 254 nm) and UV-Vis spectra of the components obtained from chromatographic analysis of the acetic acid extract of a yarn dyed with brazilwood powder

UV-Visible spectra of the components observed in the acetic acid extracts from yarn dyed with brazilwood powder		
R_t 2.54 min (64.8%)	R_t 2.9 min (10.4%)	R_t 2.9 min (3.7%)
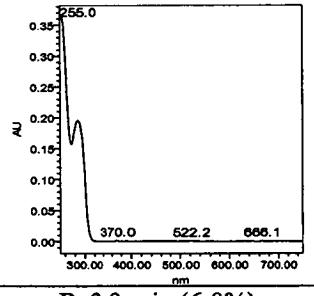	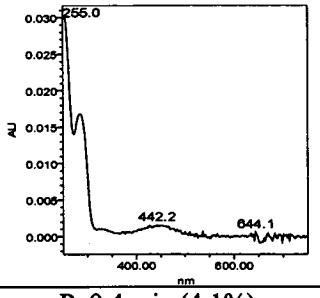	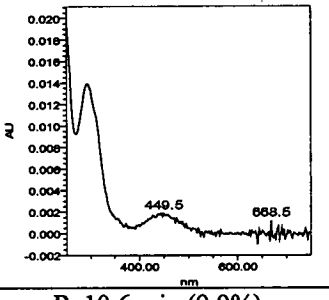
R_t 3.9 min (6.8%)	R_t 9.4 min (4.1%)	R_t 10.6 min (9.9%)
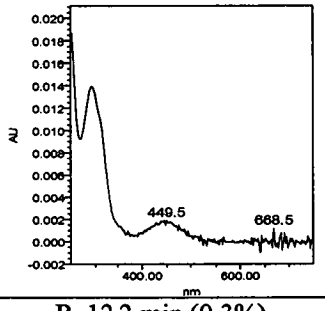	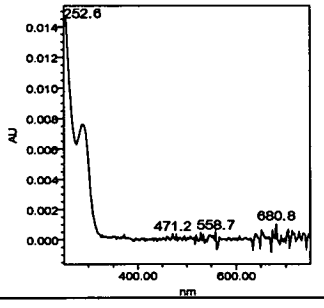	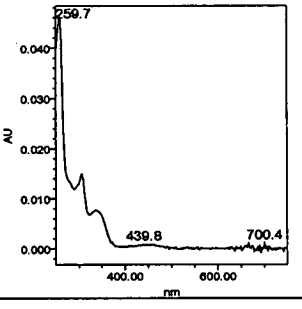
R_t 12.2 min (0.3%)		
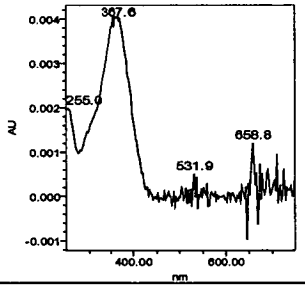		

6.6 Structural characterisation of diosmetin and chrysoeriol

The structures of the two flavonoid isomers, diosmetin (4'-methoxy-5,7,3'-trihydroxyflavone) and chrysoeriol (3'-methoxy-5,7,4'-trihydroxyflavone) (Figure 6.1) were confirmed by the NMR analysis of d_6-acetone solutions of the purchased reference materials. The ^1H chemical shifts relative to tetramethylsilane (δ / ppm) and coupling constants (J / Hz) for the two components, obtained on a Bruker DPX

360 MHz instrument operated by Fiona McMillan, have been tabulated below (Table 6.17).

Table 6.17: ^{1}H and NMR chemical shifts (/ ppm) and coupling constants (J / Hz) for the luteolin methyl ether reference components diosmetin and chrysoeriol in d_6-acetone, performed on a Bruker DPX 360 MHz spectrometer

Chrysoeriol		Diosmetin	
^{1}H Chemical shift (δ / ppm)	**Coupling constant (J / Hz)**	**^{1}H Chemical shift (δ / ppm)**	**Coupling constant (J / Hz)**
7.66 (CH)	m	7.62 (CH) 7.60	d,d 2.3 and 8.5
7.64 (CH)	d, 2.2	7.54 (CH)	d, 2.3
7.05 (CH)	d, 8.3	7.17 (CH)	d, 8.5
6.75 (CH)	s	6.69 (CH)	s
6.60 (CH)	d, 2.1	6.60 (CH)	d, 2.1
6.30 (CH)	d, 2.1	6.30 (CH)	d, 2.1
4.04 (CH_3)	s	3.99 (CH_3)	s

A 2-D Nuclear Overhauser Effect Spectroscopy (NOESY) spectrum was also obtained on the Bruker DPX 360 MHz instrument, operated by Fiona McMillan. The CH proton adjacent to the CH_3 singlet in diosmetin has a large coupling constant due to ortho-coupling with the neighbouring CH. A correlation between the signal from the CH_3 singlet and this CH signal was observed in the NOESY spectrum, confirming the structure of diosmetin. The signal from the CH proton adjacent to the CH_3 singlet in chrysoeriol has only a small coupling constant due to meta-coupling. This signal correlates with the CH_3 singlet in the NOESY spectrum, confirming the structure of chrysoeriol. The significant NOESY correlations have been shown in Figure 6.1

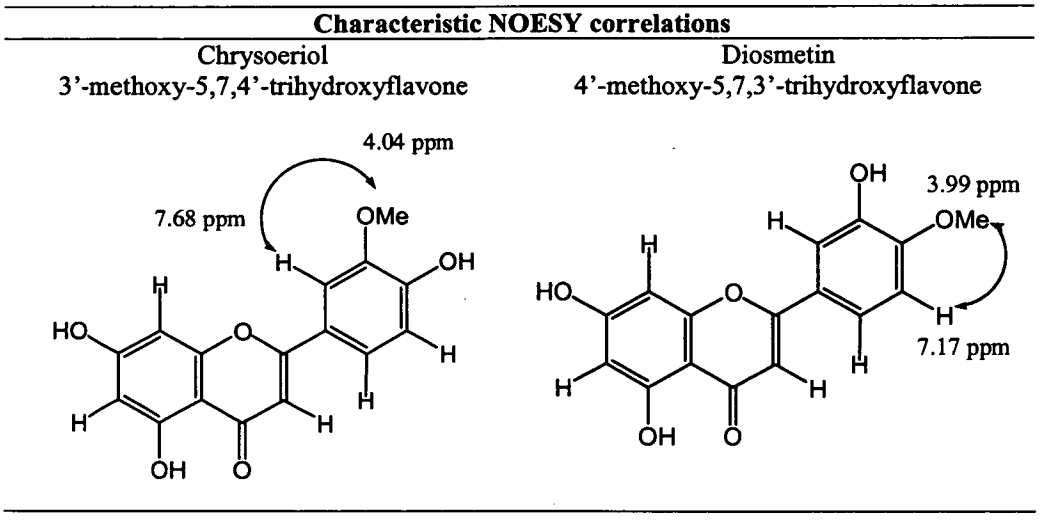

Figure 6.1: Significant NOESY correlations, allowing the two luteolin methyl ether isomers to be distinguished

6.7 Structural characterisation of minor components in cochineal (*Dactylopius coccus* Costa) extracts

Preparation of sufficient amounts of cochineal extract for NMR analysis required raw, ground cochineal (0.21 g) to be added to a test tube containing a 2:1:1 (v/v/v) solvent mixture of 37% hydrochloric acid: methanol: water (20 ml). The tube was then placed in a water bath at 100 °C and heated for precisely 10 min. After rapid cooling under cold water, the extract was filtered using a 5 μm Analytichem polypropylene frit under positive pressure. The solution was dried by rotary vacuum evaporation over a water bath at 40 °C and the dry residue reconstituted with methanol (3 ml) and water (3 ml). The reconstituted solution was then chromatographed on a semi-preparative scale (Section 6.3.3). Three separate fractions, corresponding approximately with dcIV, dcVII and flavokermesic acid, were collected. The respective fractions from nine injections were then combined and evaporated to dryness.

The ^{1}H chemical shifts relative to tetramethylsilane (δ / ppm) and coupling constants (J / Hz) for the β-D-glucopyranose of carminic acid in d^2-water were obtained and assigned using a 1-D proton spectrum and Correlation Spectroscopy (COSY),

Heteronuclear Single Quantum Coherence (HSQC) and Total Correlation Spectroscopy (TOCSY) techniques (Table 6.18). Only the coupling constants for H-1 (CH, anomeric) and H-6 (CH_2) were obtained due to overlapping signals.

Table 6.18: ^{1}H and NMR chemical shifts (/ ppm) and coupling constants (J / Hz) for the -D-glucopyranose sugar component of carminic acid, performed in d_2-water on a Bruker AVA600 spectrometer

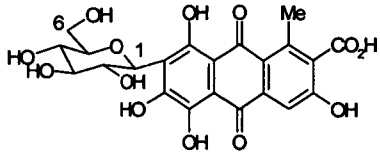

H assignment	^{1}H Chemical shift (δ / ppm)	Coupling constant (J / Hz)
1 (anomeric)	5.0	d, 9.90
2	4.3	m
3	3.5	m
4	3.5	m
5	3.4	m
6(1)	3.9	d,d, 2.38 and 12.20
6(2)	3.8	d,d, 5.59 and 12.20

To obtain structural information on the dcIV and dcVII constituents, isomeric with carminic acid (the proposed 'Sugar 1' and 'Sugar 2' components), the ^{1}H chemical shifts relative to tetramethylsilane (δ / ppm) and coupling constants (J / Hz) for the two sugars were obtained from fraction 2 in d_2-water, acquired on a Bruker AVA600 spectrometer operated by Juraj Bella. (Table 6.19 and Table 6.20 respectively). Assignments were made on the basis of information from proton, COSY and TOCSY experiments.

Table 6.19: ^{1}H and NMR chemical shifts (/ ppm) and coupling constants (J / Hz) for 'Sugar 1' in fraction 2, performed in d_2-water on a Bruker AVA600 spectrometer

H assignment	^{1}H Chemical shift (δ / ppm)	Coupling constant (J / Hz)
1 (anomeric)	5.8	d, 3.30
2	4.6	m
3	4.4	m
4	4.5	d,d, 3.49 and 8.44
5	4.1	m
6(1)	3.9	d,d, 3.12 and 11.37
6(2)	3.8	d,d, 5.41 and 11.37

Table 6.20: ^{1}H and NMR chemical shifts (/ ppm) and coupling constants (J / Hz) for 'Sugar 2' in fraction 2, performed in d_2-water on a Bruker AVA600 spectrometer

H assignment	^{1}H Chemical shift (δ / ppm)	Coupling constant (J / Hz)
1 (anomeric)	5.4	d, 2.93
2	4.3	m
3	4.3	m
4	4.1	d,d, 2.48 and 7.70
5	4.1	m
6(1)	3.8	d,d, 3.58 and 11.74
6(2)	3.7	d,d, 5.69 and 11.74

The 1-D proton spectrum of this fraction appeared to contain two anomeric proton signals in addition to the anomeric proton signal from carminic acid, which matched with the anomeric signal from the carminic acid reference. This was confirmed by a 2-D TOCSY experiment, which found three sugar spin systems, one matching with carminic acid and the two remaining systems likely to be due to the dcIV and dcVII components (Chapter 3). Despite additional information regarding coupling constants within the spin-systems, obtained *via* 1-D TOCSY experiments on fraction 2, the identity of the two sugars could not be conclusively elucidated.

6.8 Structural characterisation of hematein and its elimination product

For the preparation of the hematein elimination product, hematein (82 mg) was added to a 2:1:1 (v/v/v) hot solvent mixture of 37% hydrochloric acid: methanol: water (400 ml) and heated to reflux for 10 min. After rapid cooling under cold water, the solution was dried by rotary vacuum evaporation over a water bath at 40 °C. The solid was recovered as a 'brick red' powder (70.8 mg, 91.8% yield). The mass spectrum (FAB, NOBA conditions) of the 'large scale' sample showed a molecular ion $[M+H]^+$ at 283 (Found: $[M+H]^+$ 283.0600. $C_{16}H_{11}O_5$ requires 283.0607).

To obtain structural information on this hematein elimination product, the ^{1}H chemical shifts relative to tetramethylsilane (δ / ppm) and coupling constants (J / Hz) for hematein (Table 6.21) and the ^{1}H and ^{13}C chemical shifts relative to

tetramethylsilane (δ / ppm) and coupling constants (*J* / Hz) for the hematein elimination product (Table 6.22) were obtained on a Bruker ARX 250 MHz instrument. The hematein was dissolved in d_4-methanol for NMR analysis, while the elimination product was dissolved in a d_4-methanol / d_6-dimethylsulfoxide solvent mix.

Table 6.21: ^{1}H chemical shifts (/ ppm) and coupling constants (*J* / Hz) for hematein in d_6-dimethylsulfoxide, performed on a Bruker ARX 250 MHz spectrometer

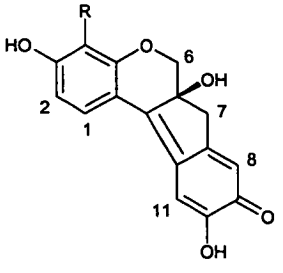

H assignment	^{1}H Chemical shift (δ / ppm)	Coupling constant (*J* / Hz)
1 (CH)	7.30	d, 8.7
11 (CH)	7.09	s
2 (CH)	6.54	d, 8.8
8 (CH)	6.32	s
6 (CH_2)	4.53	d, 11.7
	4.00	d, 11.7
7 (CH_2)	2.85 (almost degenerate; 2.93, 2.77)	

Table 6.22: ^{1}H and ^{13}C NMR chemical shifts (/ ppm) and coupling constants (*J* / Hz) for the hematein elimination product in a d_6-dimethylsulfoxide / d_4-methanol mix, performed on a Bruker ARX 250 MHz spectrometer

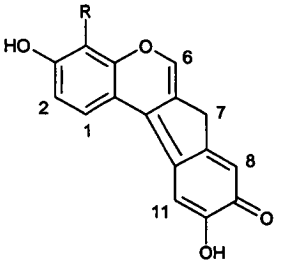

H/C assignment	^{1}H Chemical shift (δ / ppm)	Coupling constant (*J* / Hz)	^{13}C Chemical shift (δ / ppm)
6 (CH)	8.97	s	151.9
1 (CH)	8.18	d, 9.2	117.0
11 (CH)	7.88	s	111.4
2 (CH)	7.40	d, 9.2	118.1
8 (CH)	7.16	s	110.5
7 (CH_2)	4.04	s	31.6

The 2-D NOESY, COSY and HSQC studies were performed on a Bruker DPX 360 MHz instrument, operated by Stuart Wharton. An examination of the data obtained from the above experiments, confirming the identity of the hematein elimination compound as 3,4,10-trihydroxy-*7H*-indeno[2,1-*c*]chromen-9-one, can be found in Chapter 3.

6.9 Mordant identification

In an effort to address some of the problems associated with mordant identification, the use of Inductively Coupled Plasma (ICP) techniques was investigated. The plasma, an electrically neutral gas made up of positive ions and free electrons, has a sufficiently high energy to atomize, ionize and excite virtually all elements in the periodic table. Thus, a solution can be introduced into the plasma for elemental chemical analysis. The elemental ions can be detected in a variety of ways, but the most versatile techniques are Optical Emission Spectroscopy (OES) and Mass Spectrometry (MS).

Detection of the mordant with optical emission spectroscopy relies on the observation of unique spectral lines emitted by each element when an excited valence electron returns to a lower energy orbital. Although there are some spectral lines that are common between different elements, each element has at least one or more spectral lines that are unique. Furthermore, the high temperature (>3000 K) produced in the plasma is ideal for complete atomisation, reducing the interference from molecular species and more highly populated excited states and enabling a high degree of sensitivity (aluminium can confidently be identified in the parts per million range). Detection of the mordant by mass spectrometry is also possible by introducing the ions formed in the plasma into a quadrupole mass spectrometer. Detection limits with this technique are routinely in the parts-per-billion (ppb) to parts-per-trillion (ppt) range.

6.9.1 ICP OES

The instrument used was a Thermo Jarrel Ash IRIS ICP OES. The operating parameters were as follows; the R.F. Power was 1350 W, the auxiliary flow was 0.5 l min^{-1}, the nebuliser flow was 26.06 psi, the pump rate was 100 rpm and the purge time was 90 s.

6.9.1.1 Standard preparation

The aluminium solutions were prepared by diluting an aluminium stock (1000 parts per million) with deionised water to produce four standard solutions (0.1 ppm, 0.5 ppm, 1 ppm and 2 ppm) with which to calibrate the instrument (Table 6.23).

Table 6.23: The instrument calibration details for the aluminium standards

Aluminium standards (monitored at 309.2 nm)		
Standard	**Found**	
Blank	0	Slope = 19.2370
1 ppm	0.99502	Y-intercept = 4.3371
0.1 ppm	0.094739	$R^2 = 0.9999365$
0.5 ppm	0.49546	
2.0 ppm	2.0148	

6.9.1.2 Sample preparation

The sample preparation followed the dye extraction protocol for historical and reference yarns (Section 6.2.1). Accurately measured aliquots of each reconstituted acid hydrolysed extract (20 µl) were then diluted with deionised water (3 ml). The diluted extracts of the selected samples (Table 6.24) were analysed in triplicate and the mean concentration of aluminium in each solution (per mg of yarn) calculated (see below).

Table 6.24: The ICP OES results from the selected reference samples

Sample	Description	Mass of yarn / mg	Results per mg yarn		
			Al (mean) / ppm	Al (mean) / mM	% RSD of three replicate injections
R/W3 mordant	Wool yarn mordanted with alum	2.6	0.3781	2.1	0.8
R/W3	Above yarn dyed with brazilwood	2.4	0.2887	1.6	3.2
Y/S1,3 mordant	Silk yarn mordanted with alum	0.8	0.4873	2.8	2.8
Y/S1a	Above yarn dyed with weld	1.3	0.3605	2.0	0.4
Blank 1	Reagent blanks	--	0.0479	--	30.3
Blank 2	(containing no yarn)	--	0.0292	--	29.9

To calculate the mean aluminium concentration in each sample, the density of each solution is assumed to be 1, thus;

$$1 \text{ ppm} \equiv 1 \text{ mg l}^{-1}$$

Therefore;

$$\text{Al content of extracted solution per mg yarn} = \frac{\text{Instrument reading (mg l}^{-1}) \times \text{Dilution factor}}{\text{Mass of yarn (mg)}}$$

For example, sample R/W3 was found to contain 0.69288 ppm of aluminium. The dilution factor was (3.02/0.02) and the mass of yarn was 2.4 mg, giving an aluminium content of 1.91 mg l^{-1} per mg of yarn, or 1.6 mM.

6.9.2 ICP MS

The samples were analysed using a VG Elemental PlasmaQuad 3 ICP MS instrument, operated by Lorna Eades.

6.9.2.1 Standard preparation

Standards were gravimetrically prepared by diluting an aluminium stock (1000 parts per million) with deionised water to produce six standard solutions with nominal values of 1000 ppb, 500 ppb, 300 ppb, 10 ppb, 50 ppb and 10 ppb. The calibration information has been tabulated for both the initial study (Table 6.25) and the second study (Table 6.26).

Table 6.25: The instrument calibration details for the aluminium standards in the first ICP MS experiment

Experiment 1: Initial ICP MS study			
Nominal ^{27}Al concentration / ppb	**Actual ^{27}Al concentration, by weight / ppb**	**Calibration information**	
1000	1034.7		
500	513.4181	Intercept counts	47723.92
300	310.4196	Intercept concentration	1.24
100	103.5032	Sensitivity	38639.89
50	51.7950	Correlation Coefficient	0.9997
10	10.3497		

Table 6.26: The instrument calibration details for the aluminium standards in the second ICP MS experiment

Experiment 2: Study of reference and historical yarns			
Nominal ^{27}Al concentration / ppb	**Actual ^{27}Al concentration, by weight / ppb**	**Calibration information**	
1000	1034.7		
500	513.4	Intercept counts	111208.26
300	310.4	Intercept concentration	12.25
100	103.5	Sensitivity	9076.61
50	51.8	Correlation Coefficient	0.9993
10	10.3		

The semi quantitative multi-element ICP MS scan for both experiments used a general 10 ppm standard solution, consisting of the following ions; ^{27}Al, ^{52}Cr, ^{53}(ClO), ^{55}Mn, ^{56}Fe, ^{65}Cu, ^{66}Zn, ^{115}In, ^{118}Sn, ^{121}Sb, ^{125}Te, ^{137}Ba, ^{208}Pb. Individual element signals were then adjusted accordingly.

6.9.2.2 Sample preparation

The initial sample preparation followed the dye extraction protocol for historical and reference yarns (Section 6.2.1). An aliquot from each reconstituted acid hydrolysed extract (*ca.* 10 µl) was then gravimetrically prepared by diluting with deionised water (*ca.* 5 ml). Five replicate injections of each of the diluted extracts of the selected samples (Table 6.27) were made and the mean concentration of aluminium in each solution (per mg of yarn) calculated as before (Section 6.9.1.2).

Table 6.27: The fully quantitative ICP MS results from the selected reference and historical samples

Code	Mass of yarn / mg	Mass of sample aliquot / g	Mass of sample after dilution / g	Mean results (from five replicate injections) per mg yarn		
				$^{27}Al^{+}$ (mean) / ppb	$^{27}Al^{+}$ (mean) / mM	% RSD
			Experiment 1			
Y/S3e	1.1	0.00946	5.02255	9	0.2	3.3
Y/S2 mordant	1.1	0.01876	5.02765	167	3.5	1.5
Y/S2a	0.9	0.00992	5.02389	78	1.4	3.5
Y/S1,3 mordant	1.0	0.00967	5.00507	116	2.2	2.0
Y/S3b	0.8	0.00999	5.01735	32	0.6	2.3
R/W4,5 mordant	1.9	0.00978	5.01489	41	0.8	1.5
Y/W1	2.6	0.00900	5.02727	52	1.1	2.3
Blank	--	0.00866	5.01300	18	--	8.7
Blank (frozen)	--	0.00997	5.01880	4	--	7.1
			Experiment 2			
BXL 3/13	0.5	0.01458	5.01692	204	2.6	3.2
TOU 1/11	0.8	0.01509	4.97279	148	1.8	5.2
BXL 3/09	0.4	0.01278	4.98472	64	1.0	2.7
BRU 2/29	1.9	0.01685	5.01746	99	1.1	1.7
PNM 2/09	0.3	0.01886	5.01471	535	5.3	6.6
PNM 8/12	1.3	0.01449	4.99361	138	1.8	2.7
BRU 1c/16	0.8	0.01224	5.01028	137	2.1	4.2
PNM 1/32	0.8	0.02021	5.01448	101	0.9	4.7
Y/W2	2.1	0.01913	5.00277	49	0.5	5.8
Y/W1	2.7	0.01905	5.01559	134	1.3	3.9
G/W1	2.2	0.01823	5.00896	131	1.3	4.3
Y/S3a	1.4	0.01903	5.01865	246	2.4	5.1
Y/S1a	0.9	0.01896	5.02052	216	2.1	5.1
G/S4	0.8	0.01864	5.02209	154	1.5	2.2
Blank (frozen)	--	0.01714	5.01111	7	--	2.8
Blank1	--	0.01852	5.03054	23	--	25.1
Blank2	--	0.01844	5.02063	18	--	3.5

The semi-quantitative ICP MS results from the selected reference and historical samples have also been tabulated (Table 6.28).

Table 6.28: The semi-quantitative ICP MS results from the selected reference and historical samples

	Mean results (from five replicate injections) / ppb					
Sample	**$^{24}Mg^+$**	**$^{27}Al^+$**	**$^{52}Cr^+$**	**$^{56}Fe^+$**	**$^{65}Cu^+$**	**$^{206}Pb^+$**
BXL 3/13	32	136	6	147	11	41
Y/W2	28	33	2	28	1	1
TOU 1/11	21	99	9	124	6	18
Y/W1	19	89	1	20	1	1
BXL 3/09	17	43	7	135	4	31
No equiv. ref.	--	--	--	--	--	--
BRU 2/29	31	66	3	81	6	8
G/W1	18	87	2	37	3	2
PNM 2/09	132	358	106	1121	20	5
Y/S3a	231	165	3	54	4	1
PNM 8/12	31	92	9	270	3	6
Y/S1a	17	144	4	65	5	1
BRU 1c/16	21	98	3	95	10	10
No equiv. ref.	--	--	--	--	--	--
PNM 1/32	52	67	9	210	11	6
G/S4	83	103	6	122	12	34

6.9.3 Scanning Electron Microscopy (SEM)

The samples were analysed using a CamScan MX 2500 SEM with an attached Noran Vantage EDX system, operated by Jim Tate. Bundles of fibres from the selected historical samples were mounted on standard, spectroscopically pure, 'sticky' carbon SEM stubs. Each sample was then viewed in controlled pressure (Envac) mode at 20 Pa and at either 15 or 20 keV before elemental analysis, performed using the attached energy dispersive X-ray spectrometer.

6.10 Accelerated light ageing

The ageing experiments were performed in an accelerated ageing box, designed and manufactured by Complete Lighting Systems, St Albans, Great Britain. This consisted of 12 × 20 W fluorescent tubes, each with a spectral distribution as shown in Figure 6.2.

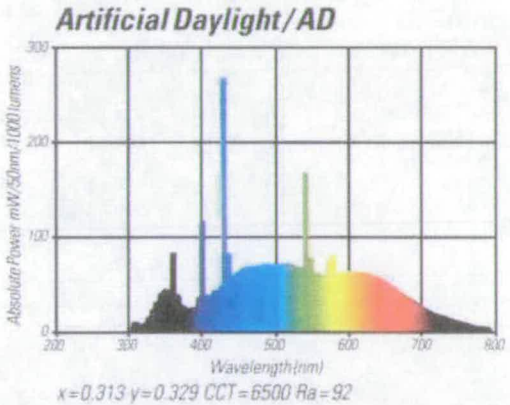

Figure 6.2: The spectral distribution of the Artificial Daylight (AD) fluorescent tubes used in the accelerated ageing box

No temperature or relative humidity (RH) control was available in the box, so these remained at ambient levels and were monitored hourly, together with the intensity of illuminance and UV levels. These were monitored with an Elsec IRLOG environmental Logger and the data periodically downloaded to computer. Seven separate studies were conducted, designated A-G.

One ageing experiment was performed in a similar accelerated ageing box at the Scientific Department of the National Gallery, London (Study 1, Section 6.10.2.1). This study has been distinguished from those performed in the other accelerated ageing box by the designation of a numerical rather than an alphabetic character. This box was also designed and manufactured by Complete Lighting Systems, St Albans, Great Britain and contained 12 × 20 W fluorescent tubes with an identical spectral distribution to that shown in Figure 6.2. Again, no temperature or relative humidity (RH) control was available, so these remained at ambient levels. Although

no monitoring equipment was present during this study, the illuminance was measured at the beginning of the experiment and found to be comparable to the values obtained during the ageing studies using the alternative box (Studies A–G).

6.10.1 Sample preparation

One Sample holder was produced for each time point in a particular ageing study. They were created from acid-free, conservation quality card and consisted of a rectangular 'frame' *ca.* 5 cm in width (from outside edge to outside edge) and holes pierced down each side. The number of different samples to be aged in each study determined the length of the holders. The width of the middle of the frame *i.e.* from inside edge to inside edge, was *ca.* 3 cm and the individual yarns were threaded across this gap, using the holes pierced down either side. This avoided the need for any adhesives that might have interfered with the ageing of the yarns.

The sample cards for each study were then placed into the accelerated ageing box, together with a 'dark' control, covered by a large square of acid-free card. The sampling regime varied for each study, but generally, a large number of sample cards were removed at the beginning of the experiment, *e.g.* one per day for the first week. The rate of removal was then gradually diminishing *e.g.* to around one sample card per month. The sample cards were then kept in the dark, wrapped in acid-free tissue, until analysis of the yarns.

6.10.2 Accelerated ageing studies

6.10.2.1 Study 1 (National Gallery, London)

The first ageing study, conducted in the accelerated ageing box at the National Gallery, London, was performed on two yellow dyed yarn samples; sawwort on alum mordanted wool (Section 6.1.1) and weld on alum mordanted wool (Y/W1). Each sample card also contained an undyed alum mordanted wool 'blank'. The sampling regime is indicated in Table 6.29 below.

Table 6.29: The cumulative exposure time of each sample card from Study 1

Time point	Cumulative time / h : min	Time point	Cumulative time / h : min
t_0	0	t_{16}	357:45
t_1	5	t_{17}	382:25
t_2	22:30	t_{18}	405:30
t_3	29:45	t_{19}	429:30
t_4	46:30	t_{20}	501:30
t_5	51:50	t_{21}	669:30
t_6	70:30	t_{22}	837:50
t_7	75:30	t_{23}	1029:55
t_8	94:45	t_{24}	1109:55
t_9	99:30	t_{25}	1277:55
t_{10}	171:15	t_{26}	1612
t_{11}	190:55	t_{27}	1948:05
t_{12}	214:40	t_{28}	2555
t_{13}	237:25	t_{29}	3227
t_{14}	261:45	t_{30}	3929:45
t_{15}	333:45	t_{31} + control	4571

6.10.2.2 Study A

The following yarn samples were aged during Study A; the blue woad dyed yarn (Bl/W1) and the two green yarns dyed with both weld and woad (G/W1 and G/W2). In addition, the MODHT reference brazilwood dyed yarns, both with and without lye (R/W3a and R/W3b) were also included, as was an alum mordanted wool 'blank'. Selected cards (control, t_0, t_1, t_2, t_{14}, t_{15}, t_{29}, t_{30}) also contained weld dyed silk yarns (Y/S1) and an alum (boil) mordanted silk 'blank'. The sampling regime and environmental conditions have been indicated below (Table 6.30).

Table 6.30: The cumulative exposure time of each sample card from Study A, together with the average results from the environmental monitoring over the periods indicated

Time point	Cumulative time (nominal) / h	Cumulative time (actual) / h : min	Week	Average values over the period indicated			
				Light / lux	UV / mW m^{-2}	T / °C	RH / %
t_0	0	0					
t_1	9	8:20					
t_2	24	24:25					
t_3	33	33:25					
t_4	48	48:40	1	10704	1797	22.6	33.3
t_5	57	56:30					
t_6	72	72:50					
t_7	81	82:35					
t_8	96	96:45					
t_9	105	105:20					
t_{10}	168	168:35					
t_{11}	192	191:50					
t_{12}	216	215:20	2	Not recorded			
t_{13}	240	240:15					
t_{14}	264	264:45					
t_{15}	336	336:25					
t_{16}	360	360:05					
t_{17}	384	384:05	3	10611	1808	24.4	21.9
t_{18}	408	408:20					
t_{19}	432	434:10					
t_{20}	504	509:40	4	10375	1786	23.6	22.1
t_{21}	672	672:10	5	10190	1754	22.9	30.8
t_{22}	840	840:30	6	10076	1734	22.7	30.1
t_{23}	1008	1008:45	7	10003	1712	22.4	36.3
t_{24}	1224	1230:15	8	10019	1706	21.9	36.5
t_{25}	1368	1373:15	9	10044	1702	22.1	39.0
t_{26}	1824	1828:45	11	9868	1676	21.7	41.7
t_{27}	2016	2016:35	13	10069	1635	21.9	43.0
t_{28}	2688	2688:15	17	10152	1655	24.5	45.2
t_{29}	3360	3359:50	21	9666	1579	23.3	53.3
t_{30} + control	4056	4056:20	25	9222	1500	22.4	55.4

6.10.2.3 Study B

The following dyed yarns were aged in Study B; the four red madder dyed yarns (R/W1a, R/W1b, R/W2a and R/W2b) and three of the black samples (B/W2, B/W3 and B/W4). An alum mordanted 'blank' wool yarn was also aged. The sampling regime and environmental conditions have been indicated below (Table 6.31).

Table 6.31: The cumulative exposure time of each sample card from Study B, together with the average results from the environmental monitoring over the periods indicated

Time point	Cumulative time (nominal) / h	Cumulative time (actual) / h : min	Week	Average values over the period indicated			
				Light / lux	UV / mW m^{-2}	T / °C	RH / %
t_0	0	0	1	--	--	--	--
t_1	504	509:15	3	10018	1703	22.0	38.1
t_2	1008	1007:20	6	9909	1653	21.7	42.8
t_3	1512	1511:55	9	10154	1656	24.2	45.4
t_4	2184	2183:30	13	9870	1611	24.1	51.1
t_5	2856	2854:20	17	9233	1506	22.2	54.4
t_6	3528	3536	21	9347	1498	23.6	65.4
t_7	4392	4395:35	26	8946	1421	22.6	62.7
t_8 + control	4896	4899:15	29	8553	1358	21.5	59.7

6.10.2.4 Study C

The following yarn samples were aged during Study C; the two cochineal dyed yarns on wool (R/W4 and R/W5) together with cochineal dyed onto silk (R/S3) and two of the madder dyed silk yarns (R/S2a and R/S2d). The single dyed component sample of genistein dyed wool was also aged during this experiment in addition to a blank R/W4&5 alum mordanted wool yarn. The sampling regime and environmental conditions have been indicated below (Table 6.32).

Table 6.32: The cumulative exposure time of each sample card from Study C, together with the average results from the environmental monitoring over the periods indicated

Time point	Cumulative time (nominal) / h	Cumulative time (actual) / h : min	Week	Average values over the period indicated			
				Light / lux	UV / mW m^{-2}	T / °C	RH / %
t_0	0	0					
t_1	24	24					
t_2	48	50	1	8516	1286	22.3	55.0
t_3	72	74:30					
t_4	96	95:15					
t_5	168	173:15					
t_6	192	191:40					
t_7	216	216:20	2	8476	1283	22.6	55.0
t_8	240	239:30					
t_9	264	265:20					
t_{10}	336	346:25	3	8531	1294	23.3	43.3
t_{11}	528	536:45	4	8352	1271	22.5	50.6
t_{12}	696	698:25	5	8270	1261	22.3	53.0
t_{13}	1032	1032	7	8331	1264	23.0	52.9
t_{14}	1368	1367:50	9	8296	1256	23.5	48.6
t_{15}	1680	1683:05	11	8228	1242	23.3	51.0
t_{16}	2040	2039:50	13	8264	1246	23.2	46.1
t_{17}	2376	2376	15	8137	1226	23.2	46.1
t_{18}	2688	2736:35	17	7851	1175	21.7	66.2
t_{19}	3024	3048:30	19	7857	1180	22.0	57.6
t_{20}	3360	3384:30	21	7847	1398	22.3	56.0
t_{21}	3696	3706:45	23	7809	1143	21.6	62.7
t_{22} + control	4080	4079:45	25	7811	1144	22.0	54.1

6.10.2.5 Study D

The following yarn samples were aged; the five silk yarns dyed with dyer's greenweed (Y/S3a-e) together with the two young fustic yarns (Y/S1a and Y/S1b) and a blank, alum mordanted silk yarn. The sampling regime and environmental conditions have been indicated below (Table 6.33).

Table 6.33: Cumulative exposure time of each sample card from Study D, together with the average results from the environmental monitoring over the periods indicated

Time point	Cumulative time (nominal) / h	Cumulative time (actual) / h : min	Week	Average values over the period indicated			
				Light / lux	UV / mW m^{-2}	T / °C	RH / %
t_0	0	0					
t_1	24	23					
t_2	48	47:35	1	10169	1639	22.2	42.4
t_3	72	71					
t_4	96	100:05					
t_5	168	167:15					
t_6	192	190:55					
t_7	216	215:30	2	10004	1629	22.1	42.5
t_8	240	239:40					
t_9	264	262:20					
t_{10}	336	388:15	3	9963	1630	23.2	49.4
t_{11}	504	581:20	4	10307	1678	25.3	46.4
t_{12}	672	671:55	5	10216	1665	25.2	41.4
t_{13}	1008	1008:05	7	10144	1652	25.4	48.2
t_{14}	1344	1343:30	9	9595	1569	22.8	54.0
t_{15}	1680	1689:50	11	9314	1521	22.3	54.3
t_{16}	2016	2014:50	13	9148	1489	22.1	54.6
t_{17}	2352	2360:05	15	9347	1509	23.4	60.8
t_{18}	2688	2698	17	9348	1487	23.9	70.2
t_{19}	3362	3361:30	21	8980	1426	22.7	63.1
t_{20}	3842	3844:25	24	8642	1373	21.6	61.2
t_{21}	4178	4176:50	26	8441	1340	21.5	58.5
t_{22} + control	4850	4849:55	30	8448	1325	22.1	58.4

6.10.2.6 Study E

Two exploratory accelerated ageing experiments were conducted on the NMS dyed young fustic yarn (Section 6.1.3). Samples were removed from the light box where indicated (Table 6.34).

Table 6.34: The cumulative exposure time of each sample card from Study E, together with the average results from the environmental monitoring over the periods indicated

Time point	Cumulative time (nominal) / h	Cumulative time (actual) / h : min	Week	Average values over the period indicated			
				Light / lux	UV / mW m^{-2}	T / °C	RH / %
			Experiment 1				
t_0	0	0	0	--	--	--	--
t_1	336	334:45	1	9600	1363	21.5	61.4
t_2	1344	1342:30	8	9341	1330	21.9	58.4
			Experiment 2				
t_0	0	0	0	--	--	--	--
t_1	5376	5384:40	32	7611	1108	22.7	75.4

6.10.2.7 Study F

The accelerated ageing of brazilwood dyed wool yarn (Section 6.1.5.3) was the subject of this study. Two sampling cards were used, each containing eight yarns which were removed sequentially at the time intervals indicated below (Table 6.35).

Table 6.35: The cumulative exposure time of each sample from Study F, together with the average results from the environmental monitoring over the periods indicated

Time point	Cumulative time (nominal) / h	Cumulative time (actual) / h : min	Week	Average values over the period indicated			
				Light / lux	UV / mW m^{-2}	T / °C	RH / %
t_0	0	0					
t_1	24	23:05	1	7977	1195	22.9	53.9
t_2	72	71:35					
t_3	144	143:45	2	7850	1175	22.4	56.6
t_4	240	239:55					
t_5	336	335:50	3	7745	1161	21.8	56.4
t_6	480	479:25	4	7894	1155	21.9	64.6
t_7	648	658:10	5	7741	1134	21.4	61.2
t_8	888	890:45	6	Not recorded			
t_9	1152	1151:40	8	7760	1138	22.1	62.8
t_{10}	1440	1450:40	9	7693	1125	22.2	73.0
t_{11}	1560	1559:45	10	7656	1116	22.0	71.6
t_{12}	1968	1977:50	12	7903	1138	23.8	79.9
t_{13}	2352	2354	15	7953	1143	24.6	79.2
t_{14}	2880	2880:35	18	Not recorded			
t_{15}	3216	3223:10	20	7629	1099	23.5	83.9
t_{16} + control	4224	4232:25	26	7422	1070	22.9	81.7

6.10.2.8 Study G

The sulfuretin dyed silk yarn and the 3-*O*-methylquercetin dyed wool and silk yarns (Section 6.1.4) were aged in this final accelerated ageing study. The sampling regime and environmental conditions have been indicated below (Table 6.36).

Table 6.36: The cumulative exposure time of each sample card from Study G, together with the average results from the environmental monitoring over the periods indicated

Time point	Cumulative time (nominal) / h	Cumulative time (actual) / h : min	Week	Average values over the period indicated			
				Light / lux	UV / mW m^{-2}	T / °C	RH / %
t_0	0	0					
t_1	24	23:05	1	8022	1171	22.4	62.1
t_2	72	76:25					
t_3	144	143:30	2	7801	1143	21.6	68.6
t_4	192	191:30					
t_5	312	322:15	3	7741	1135	21.5	56.3
t_6	408	413:05					
t_7	552	554:50	4	Not recorded			
t_8	696	695:20	5	Not recorded			
t_9	1008	1012:20	7	7686	1127	22.0	72.1
t_{10}	1224	1223:50	8	7701	1122	22.3	71.6
t_{11}	1632	1639:55	10	7903	1138	23.8	79.9
t_{12}	2016	2018:10	13	7953	1143	24.6	79.2
t_{13}	2544	2544:40	16	Not recorded			
t_{14}	2880	2887:15	18	7629	1099	23.5	83.9
t_{15}	3888	3896:25	24	7422	1070	22.9	81.7
t_{16} + control	4728	4736:45	29	7204	1045	22.2	84.3

6.10.3 Degradation profiles

6.10.3.1 Weld (*Reseda luteola* L.)

The degradation profiles of the main components observed in the acid hydrolysed extracts of weld dyed yarn have been tabulated (Table 6.37).

Table 6.37: The degradation profiles of the main components in the acid hydrolysed extracts of weld dyed yarn

Time / h	Mass of yarn / mg	Peak area (monitored at 254 nm) / AU			Relative peak area / %		
		Luteolin	Apigenin	Chrysoeriol	Luteolin	Apigenin	Chrysoeriol
control	2.9	2043947	79575	42443	94.4	3.7	2.0
0	1.1	5422500	207821	119526	94.3	3.6	2.1
5	1.6	3102380	100973	62928	95.0	3.1	1.9
22.5	1.5	3052165	112536	70947	94.3	3.5	2.2
29.75	1.2	2216713	72545	45260	95.0	3.1	1.9
46.5	1.3	2524118	91453	53685	94.6	3.4	2.0
51.75	1.3	1763094	62117	36938	94.7	3.3	2.0
70.5	1.0	2130290	76839	47323	94.5	3.4	2.1
75.5	1.1	1797882	66222	39127	94.5	3.5	2.1
94.75	1.1	1834455	88492	44853	93.2	4.5	2.3
99.5	2.3	2467964	95089	52178	94.4	3.6	2.0
171.25	0.7	925196	40854	21418	93.7	4.1	2.2
190.92	1.0	858602	40120	20730	93.4	4.4	2.3
214.67	1.3	1587821	60543	36778	94.2	3.6	2.2
237.42	0.8	1713733	72959	44102	93.6	4.0	2.4
261.75	0.7	1220259	57609	33273	93.1	4.4	2.5
333.75	0.9	1006441	49737	24070	93.2	4.6	2.2
357.75	1.1	1428551	68004	36129	93.2	4.4	2.4
382.42	1.3	1383103	67643	35324	93.1	4.6	2.4
405.5	1.0	1059040	63045	30755	91.9	5.5	2.7
429.5	3.0	3061878	160106	75670	92.9	4.9	2.3
501.5	0.9	960194	47394	23931	93.1	4.6	2.3
669.5	0.9	679204	39128	16354	92.4	5.3	2.2
837.83	0.9	729194	50723	22026	90.9	6.3	2.7
1029.92	0.8	747794	43793	19383	92.2	5.4	2.4
1109.92	3.2	1241935	85896	41814	90.7	6.3	3.1
1277.92	0.9	592655	44814	18317	90.4	6.8	2.8
1612	3.5	1016900	83340	34510	89.6	7.3	3.0
1948.08	0.8	334007	30801	10633	89.0	8.2	2.8
2555	0.8	206405	16296	5930	90.3	7.1	2.6
3227	0.8	263760	25908	7078	88.9	8.7	2.4
3929.75	0.9	163589	17750	6069	87.3	9.5	3.2
4571	1.2	258905	34313	7729	86.0	11.4	2.6

The degradation profile of the three components; luteolin, apigenin and chrysoeriol, can also be shown as fading curves (Figure 6.3-Figure 6.5 respectively), but only tabulated data has been presented in subsequent sections.

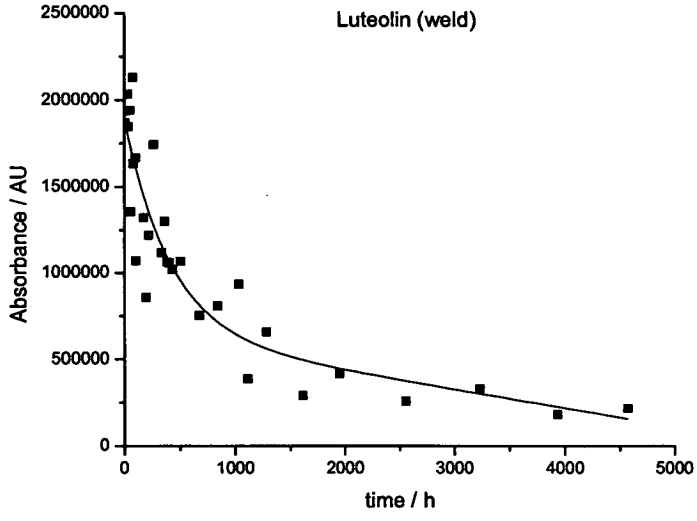

Figure 6.3: Degradation profile of luteolin from acid hydrolysed extracts of aged weld

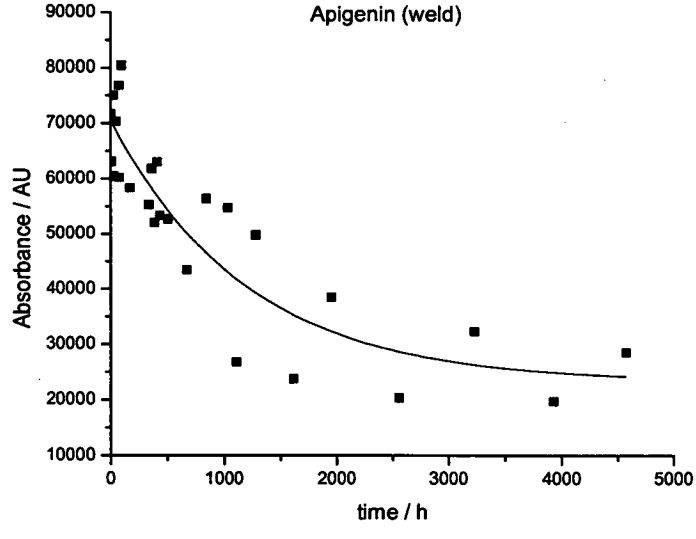

Figure 6.4: Degradation profile of apigenin from acid hydrolysed extracts of aged weld

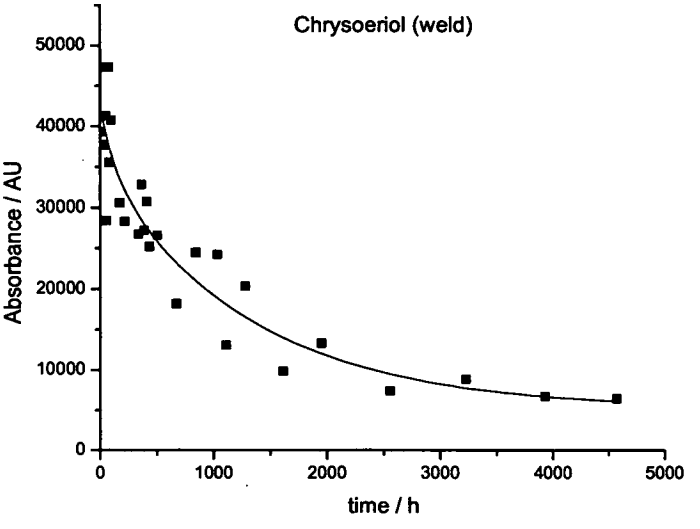

Figure 6.5: Degradation profile of chrysoeriol from acid hydrolysed extracts of aged weld

The formation of an unknown degradation product was also observed in the acid hydrolysed extracts of aged weld dyed yarns (Table 6.38).

Table 6.38: The formation of the unknown degradation product, observed in the acid hydrolysed extracts of aged weld dyed yarn, monitored at 254 nm

Unknown degradation product (monitored at 254 nm)					
Time / h	**Area / AU**	**Relative peak area / %**	**Time**	**Area / AU**	**Relative peak area / %**
control	0	0	357.75	30522	2.0
0	0	0	382.42	27095	1.8
5	0	0	405.5	26164	2.2
22.5	0	0	429.5	0	0
29.75	0	0	501.5	22251	2.1
46.5	0	0	669.5	28564	3.7
51.75	0	0	837.83	34671	4.1
70.5	0	0	1029.92	38380	4.5
75.5	0	0	1109.92	99266	7.1
94.75	7006	0.4	1277.92	47426	6.7
99.5	0	0	1612	85243	7.4
171.25	7082	0.7	1948.08	36487	8.7
190.92	9677	1.0	2555	25013	9.6
214.67	9733	0.6	3227	35501	10.4
237.42	14243	0.8	3929.75	28460	13.0
261.75	25172	1.9	4571	52291	15.2
333.75	17761	1.6			

The degradation profiles of the main components in the acid hydrolysed extracts of the green yarns dyed using weld have also been tabulated (Table 6.39 and Table 6.40).

Table 6.39: The degradation profiles of the main components in the acid hydrolysed extracts of yarn dyed with woad then weld (G/W1)

Time / h	Mass of yarn / mg	Peak area (monitored at 254 nm) / AU			Relative peak area / %		
		Luteolin	Apigenin	Chrysoeriol	Luteolin	Apigenin	Chrysoeriol
control	1.6	1572642	35618	22603	96.4	2.2	1.4
0	1.0	1371331	27006	18863	96.8	1.9	1.3
8.33	1.7	1598375	33568	18034	96.9	2.0	1.1
24.42	1.3	1038341	25642	12003	96.5	2.4	1.1
33.25	1.6	1174090	27710	13105	96.6	2.3	1.1
48.67	1.9	1310900	33155	13941	96.5	2.4	1.0
56.5	1.7	1377790	31297	15319	96.7	2.2	1.1
72.83	1.9	1972956	40217	21150	97.0	2.0	1.0
82.58	1.5	1620214	32621	16719	97.0	2.0	1.0
96.75	1.9	1794724	44456	22689	96.4	2.4	1.2
105.33	1.0	1105091	26841	16616	96.2	2.3	1.4
168.58	1.7	1395614	34980	17859	96.4	2.4	1.2
191.83	1.7	1236840	34675	17100	96.0	2.7	1.3
215.33	1.9	1586760	38507	19576	96.5	2.3	1.2
240.25	1.6	1108698	25909	12939	96.6	2.3	1.1
264.75	1.2	1132605	25717	16140	96.4	2.2	1.4
336.42	1.5	1175373	26879	13291	96.7	2.2	1.1
360.08	1.4	1096832	24597	12064	96.8	2.2	1.1
384.08	1.3	921879	21009	9670	96.8	2.2	1.0
408.33	1.5	855639	17746	6465	97.2	2.0	0.7
434.17	1.0	770046	18210	11381	96.3	2.3	1.4
509.67	1.6	1066294	27863	14348	96.2	2.5	1.3
672.17	1.2	568998	15384	5861	96.4	2.6	1.0
840.5	1.4	799679	22640	10180	96.1	2.7	1.2
1008.75	1.8	855662	26822	12331	95.6	3.0	1.4
1230.25	2.1	759636	22722	11506	95.7	2.9	1.4
1373.25	2.0	645701	23405	10137	95.1	3.4	1.5
1828.75	1.1	321480	10089	5884	95.3	3.0	1.7
2016.58	1.3	480917	16922	6233	95.4	3.4	1.2
2688.25	1.4	239151	6872	0	97.2	2.8	0
3359.83	1.0	197558	8331	4197	94.0	4.0	2.0
4056.33	1.6	193562	9440	4341	93.4	4.6	2.1

Table 6.40: The degradation profiles of the main components in the acid hydrolysed extracts of yarn dyed with weld then woad (G/W2)

Time / h	Mass of yarn / mg	Peak area (monitored at 254 nm) / AU			Relative peak area / %		
		Luteolin	Apigenin	Chrysoeriol	Luteolin	Apigenin	Chrysoeriol
control	1.9	1634116	64696	32140	94.4	3.7	1.9
0	1.3	1829238	52435	34134	95.5	2.7	1.8
8.33	1.3	1090467	31733	15686	95.8	2.8	1.4
24.42	1.5	1121567	41281	20679	94.8	3.5	1.7
33.25	1.4	1443775	50739	26069	94.9	3.3	1.7
48.67	1.5	1323867	45464	24129	95.0	3.3	1.7
56.5	2.2	1945327	76505	41650	94.3	3.7	2.0
72.83	2.3	1916450	80299	40768	94.1	3.9	2.0
82.58	1.4	968541	39741	19264	94.3	3.9	1.9
96.75	1.7	1083764	53991	25347	93.2	4.6	2.2
105.33	0.8	839129	31001	15709	94.7	3.5	1.8
168.58	1.6	1020979	45471	20372	93.9	4.2	1.9
191.83	1.6	1075369	50941	24179	93.5	4.4	2.1
215.33	1.9	1243232	57926	27587	93.6	4.4	2.1
240.25	1.8	1450371	53858	27155	94.7	3.5	1.8
264.75	1.2	931549	35681	18455	94.5	3.6	1.9
336.42	1.8	1193983	51915	22979	94.1	4.1	1.8
360.08	1.9	981487	43386	19459	94.0	4.2	1.9
384.08	1.6	1041649	46664	21634	93.8	4.2	1.9
408.33	1.7	938178	41495	19029	93.9	4.2	1.9
434.17	1.0	873906	35359	16271	94.4	3.8	1.8
509.67	1.4	845749	39546	18116	93.6	4.4	2.0
672.17	1.7	793481	43615	19116	92.7	5.1	2.2
840.5	1.3	822034	39427	16664	93.6	4.5	1.9
1008.75	1.5	782747	42051	18221	92.9	5.0	2.2
1230.25	1.6	904814	48464	21940	92.8	5.0	2.2
1373.25	2.0	1098756	61511	24883	92.7	5.2	2.1
1828.75	1.5	626088	40508	15726	91.8	5.9	2.3
2016.58	1.5	805821	48002	20190	92.2	5.5	2.3
2688.25	1.8	490903	37886	13216	90.6	7.0	2.4
3359.83	1.6	482440	38355	13587	90.3	7.2	2.5
4056.33	1.6	463867	41395	15309	89.1	8.0	2.9

6.10.3.2 Dyer's greenweed (*Genista tinctoria* L.)

For the accelerated ageing study of the dyer's greenweed dyed silk yarns, only the initial and final results have been indicated (Table 6.41).

Table 6.41: The degradation profiles of the main components in the acid hydrolysed extracts of yarn dyed with dyer's greenweed

Sample		Time / h	Mass of yarn / mg	Peak area (monitored at 254 nm) / AU			Relative peak area / %		
				Genistein	Luteolin	Apigenin	Genistein	Luteolin	Apigenin
Y/S3a	t_0	0	0.7	3374893	3444738	500818	46	47	7
	t_{22}	4849.92	0.7	2481256	2008205	412696	51	41	8
Y/S3b	t_0	0	0.8	1116405	3028404	230314	26	69	5
	t_{22}	4849.92	0.6	482828	819886	111513	34	58	8
Y/S3c	t_0	0	0.6	742901	1555670	157203	30	63	6
	t_{22}	4849.92	0.7	549806	559139	135395	44	45	11
Y/S3d	t_0	0	0.7	1181855	4984707	225283	18	78	4
	t_{22}	4849.92	0.9	587223	993135	141200	34	58	8
Y/S3e	t_0	0	0.8	487756	461626	87054	47	45	8
	t_{22}	4849.92	0.7	332262	158281	64731	60	29	12

An alum mordanted wool yarn 'dyed' with pure genistein was aged under accelerated conditions and the results have been tabulated below (Table 6.42)

Table 6.42: The degradation profile of genistein in the acid hydrolysed extracts of yarn dyed with pure genistein

Time / h	Mass of yarn / mg	Genistein peak area (monitored at 254 nm) / AU	Peak area relative to t_0 peak area / %
0	0.7	1783230	100
74.50	1.1	2590435	92
173.25	0.8	1587913	78
216.33	1.1	2191611	78
239.50	0.6	1158221	76
265.33	0.8	1500987	74
536.75	0.9	1556929	68
698.42	1.0	1632225	64
1032.00	0.8	1143704	56
1367.83	1.2	1250605	41
1683.08	0.9	1132918	49
2039.83	0.7	989510	55
2376.00	1.1	1196189	43
2736.58	1.1	1004176	36
3048.50	1.0	1013251	40
3384.50	1.8	1627338	35
3706.75	1.4	1302916	37
4079.75	1.6	1403628	34

6.10.3.3 Sawwort (*Serratula tinctoria* L.)

The degradation profiles of the main components in the acid hydrolysed extracts of yarn dyed with sawwort have been tabulated (Table 6.43).

Table 6.43: The degradation profiles of the main components in the acid hydrolysed extracts of yarn dyed with sawwort

Time	Mass	Peak area (monitored at 254 nm) / AU				Relative peak area / %			
/ h	/ mg	Luteolin	Quercetin	Apigenin	Kaempferol	Luteolin	Quercetin	Apigenin	Kaempferol
0	1.2	750734	65673	53207	14570	84.9	7.4	6.0	1.6
0	2.6	1528439	269139	111334	55730	77.8	13.7	5.7	2.8
5	1.0	715270	82866	41217	17806	83.4	9.7	4.8	2.1
22.5	0.8	553114	60217	33538	13258	83.8	9.1	5.1	2.0
46.5	0.9	667724	65593	42567	13796	84.6	8.3	5.4	1.7
51.75	0.8	593912	60330	37397	12378	84.4	8.6	5.3	1.8
70.5	0.8	538962	48121	36373	10728	85.0	7.6	5.7	1.7
75.5	0.9	589576	52595	35552	8962	85.9	7.7	5.2	1.3
94.75	0.9	588648	47415	40644	11327	85.6	6.9	5.9	1.6
171.25	0.8	453442	38422	30118	7897	85.6	7.3	5.7	1.5
214.67	2.3	1019806	93053	79845	18227	84.2	7.7	6.6	1.5
237.42	2.0	944664	74074	75718	16089	85.1	6.7	6.8	1.4
261.75	1.4	748737	55819	58506	12617	85.5	6.4	6.7	1.4
333.75	1.1	488526	34578	39993	8149	85.5	6.1	7.0	1.4
382.42	1.3	608839	44459	52928	9965	85.0	6.2	7.4	1.4
405.5	1.6	705078	45250	62950	10338	85.6	5.5	7.6	1.3
501.5	1.4	531348	32824	52950	8111	85.0	5.2	8.5	1.3
669.5	1.0	296675	15087	33414	4202	84.9	4.3	9.6	1.2
837.5	2.2	723390	50616	77498	11930	83.8	5.9	9.0	1.4
1029.92	1.8	445669	24744	57603	5974	83.5	4.6	10.8	1.1
1277.92	1.5	413500	25025	51759	6112	83.3	5.0	10.4	1.2
1612	3.8	741409	46722	100209	7036	82.8	5.2	11.2	0.8
1948.08	1.5	289304	14462	50538	4257	80.7	4.0	14.1	1.2
2555	0.9	173458	7132	34663	2615	79.6	3.3	15.9	1.2
3227	1.3	171777	5812	33084	2070	80.7	2.7	15.6	1.0
3929.75	1.0	118706	5736	28685	1758	76.6	3.7	18.5	1.1
4571	0.9	131982	7311	27609	1910	78.2	4.3	16.4	1.1

The luteolin/apigenin ratio in the acid hydrolysed extracts of aged yarn dyed with weld has been compared with the same ratio from aged sawwort dyed yarns (Table 6.44). This data was derived from the respective peak areas, obtained from Table 6.37 and Table 6.43.

Table 6.44: A comparison of the luteolin/apigenin ratio in the acid hydrolysed extracts of aged yarn dyed with weld and sawwort respectively

Weld (monitored at 254 nm)		Sawwort (monitored at 254 nm)	
Time / h	**luteolin/apigenin ratio**	**Time / h**	**luteolin/apigenin ratio**
0	25.69	0	13.73
5	30.72	5	17.35
22.5	27.12	22.5	16.49
29.75	30.56	46.5	15.69
46.5	27.60	51.75	15.88
51.75	28.38	70.5	14.82
70.5	27.72	75.5	16.58
75.5	27.15	94.75	14.48
94.75	20.73	171.25	15.06
99.5	25.95	214.67	12.77
171.25	22.65	237.42	12.48
190.92	21.40	261.75	12.80
214.67	26.23	333.75	12.22
237.42	23.49	382.42	11.50
261.75	21.18	405.5	11.20
333.75	20.24	501.5	10.04
357.75	21.01	669.5	8.88
382.42	20.45	837.5	9.33
405.5	16.80	1029.92	7.74
429.5	19.12	1277.92	7.99
501.5	20.26	1612	7.40
669.5	17.36	1948.08	5.72
837.83	14.38	2555	5.00
1029.92	17.08	3227	5.19
1109.92	14.46	3929.75	4.14
1277.92	13.22	4571	4.78
1612	12.20		
1948.08	10.84		
2555	12.67		
3227	10.18		
3929.75	9.22		
4571	7.55		

6.10.3.4 Young fustic (*Cotinus coggygria* Scop.)

The degradation profile of sulfuretin, one of the main components in the acid hydrolysed extracts of silk yarn dyed with young fustic (Y/S2b), has been tabulated (Table 6.45).

Table 6.45: The degradation profile of sulfuretin, one of the main components in the acid hydrolysed extracts of silk yarn dyed with young fustic (Y/S2b)

Time / h	Mass / mg	Sulfuretin (monitored at 254 nm)	
		Area / AU	Peak area relative to t_0 peak area / %
0	0.7	194193	100
23	0.7	151294	78
47.58	0.6	141637	85
71	0.9	118681	48
100.08	0.7	134703	69
167.25	1.0	86987	31
190.92	0.7	61991	32
215.5	0.7	52442	27
239.67	0.8	54783	25
262.33	0.7	50294	26
388.25	0.9	47851	19
581.33	0.8	20518	9
671.92	0.9	22810	9
1008.08	0.9	7134	3
1343.58	0.9	6419	3
1689.92	0.7	4662	2
2014.83	0.8	0	0
2360.08	0.7	0	0

6.10.3.5 Brazilwood (*Caesalpinia sappan* L.)

The degradation profiles of the main components in the acid hydrolysed extracts of wool yarn dyed with brazilwood powder (Section 6.1.5.3) have been tabulated (Table 6.46).

Table 6.46: The degradation profiles of the main components in the acid hydrolysed extracts of wool yarn dyed with brazilwood powder

Time / h	Mass / mg	Peak area (monitored at 254 nm) / AU		Relative peak area / %		Peak area *cf.* t_0 peak area / %	
		Unknown 1	Unknown 2	Unknown 1	Unknown 2	Unknown 1	Unknown 2
control	1.6	1972968	329881	86	14	--	--
0	0.8	1727200	295975	85	15	100	100
23.08	1.3	2283454	434540	84	16	81	90
71.58	1.3	2249405	403578	85	15	80	84
143.75	1.8	2306015	474536	83	17	59	71
239.92	1.3	1929946	276312	87	13	69	57
335.83	1.7	2007759	371797	84	16	55	59
479.42	1.4	1611853	237784	87	13	53	46
658.17	1.5	1473906	262105	85	15	46	47
890.75	1.4	1544092	240214	87	13	51	46
1151.67	1.4	1071608	171125	86	14	35	33
1450.67	1.3	1075772	172779	86	14	38	36
1559.75	1.5	1187043	191125	86	14	37	34
1977.83	1.2	846226	134053	86	14	33	30
2354	1.9	941555	152751	86	14	23	22
2880.58	1.4	764485	130053	85	15	25	25
3223.17	1.1	342919	55382	86	14	14	14
4232.42	1.1	435747	77396	85	15	18	19

6.11 Sampling from the tapestries

Based on the requirements of the techniques to be used by each partner, it was decided that each historical yarn sampled should be *ca.* 35 mm (in whole or in parts) and each metal thread should be *ca.* 20 mm (again in whole or in parts). The tapestries were given unique codes and placed on a large, flat table for viewing and photographic documentation (Figure 6.6). The majority of yarns were sampled from the reverse of the tapestries where there were usually loose yarns resulting from the weaving process. Where a tapestry was badly damaged, it was sometimes possible to take a sample from the front without any impairment of aesthetic quality.

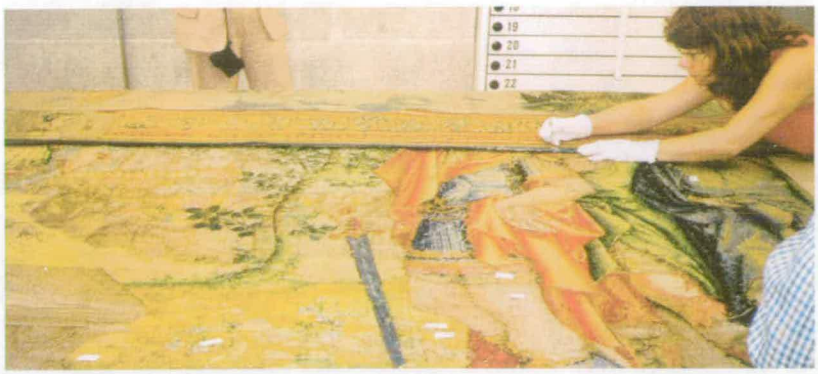

Figure 6.6: The removal of yarn samples from the reverse of a tapestry. The positions of the selected yarns were recorded and each sample given a unique code before being photographed then removed © MODHT partners

The selected yarns were each provided with a unique number, which together with the tapestry code, was recorded on a piece of paper and placed at the appropriate place on the tapestry (white rectangles in Figure 6.6). The following information was also recorded for each yarn; the yarn type *i.e.* wool, silk or metal thread, warp or weft, colour, and whether it was taken from the front or the back of the tapestry. For documentation purposes, a reference of the geographical location of the sample, using length and breadth measurements, was noted and two digital photographs taken, one large scale and one detail, before the yarn was finally removed using embroidery scissors.

6.11.1 Historical sample results

The sample preparation and chromatographic method of the historical yarns were identical to those used in the reference studies (Section 6.2.1 and Section 6.3.1 respectively). The dye analysis results showed weld and dyer's greenweed to be the most widely employed yellow dye sources (Chapter 5).

6.11.1.1 Historical weld samples

The identification of weld on historical samples was achieved by the qualitative and quantitative analysis of the three characteristic components; luteolin (L), apigenin (A) and chrysoeriol (C), in the acid hydrolysed yarn extracts. The relative percentages of these components were calculated at a detection wavelength of 254 nm using automatic integration software. The samples have been ordered with a

descending percentage of luteolin and only those analysed in Edinburgh have been included (Table 6.47).

Table 6.47: The relative percentages of luteolin (L), apigenin (A) and chrysoeriol (C) (monitored at 254 nm) in the acid hydrolysed extracts of historical samples believed to have been dyed using weld. The samples have been ordered with a descending percentage of luteolin and only those analysed in Edinburgh have been included

Sample	Sample mass	Yarn type	Yarn colour	%L	%A	%C
PNM 2/37	0.2	wool	green (appeared blue)	98	2	0
PNM 2/22	0.3	wool	green	95	4	2
HRP2/37	1.9	wool	green	94	3	2
TOU 1/18	0.2	wool	dark green	94	4	2
BXL 4/11	1.5	wool	green	93	3	4
HRP1/41	0.9	wool	green	93	7	0
HRP1/43	1	wool	dark green	93	3	4
HRP1/47	0.7	wool	yellow	93	7	0
HRP2/67	1.2	wool	blue	93	4	3
HRP2/75	1.6	wool	green	93	4	3
TOU 1/08	0.5	wool	green	93	4	2
TOU 1/12	0.5	wool	green	93	5	2
TOU 1/17	0.4	wool	dark green	93	5	2
BRU 1a/06	0.9	wool	yellow	92	5	3
BRU 1a/07	1.7	wool	green	92	4	4
BRU 2/02	2.6	wool	green	92	8	0
HRP1/28	1.1	wool	green (appeared yellow)	92	5	3
HRP1/33	2.2	wool	green (appeared yellow)	92	7	1
TOU 1/11	0.8	wool	ochre (appeared yellow)	92	6	3
TOU 1/16	0.2	wool	dark green	92	6	2
BRU 1a/09	2.5	wool	green	91	5	5
HRP1/7	1.8	wool	light green	91	6	3
HRP3/38	2.1	wool	green / patch	91	5	4
TOU 1/28	0.5	wool	ochre (appeared yellow)	91	6	4
BXL 4/15	1.4	wool	beige-brown / orange	90	10	0
HRP1/20	0.4	wool	yellow	90	10	0
HRP1/3	2	wool	green	90	6	4
HRP1/32	0.5	wool	green (appeared yellow)	90	6	5
HRP1/44	2.2	wool	green	90	6	5
BRU 3/18	2.3	wool	yellow	89	7	4
HRP1/42	0.6	wool	green	89	8	3
HRP1/45	1.4	wool	green	89	7	4
HRP2/38	1	wool	green	89	7	4
HRP2/63	1.3	wool	yellow	89	8	4

PNM 5/10	0.8	wool	green	89	7	4
HRP1/34	1.4	wool	green (appeared yellow)	88	8	5
BRU 2/29	1.9	wool	green	87	13	0
BRU 3/05	0.2	wool	green	87	9	4
HRP1/13	0.2	wool	green	87	9	4
HRP1/31	1.6	wool	green (appeared yellow)	87	9	4
HRP2/80	1	wool	yellow	87	8	5
PNM 8/05	1.4	wool	green	87	13	0
HRP1/14	1.2	wool	khaki (appeared yellow)	87	11	3
BRU 1a/04	1.2	wool	light green	86	10	4
HRP1/27	0.2	wool	green (appeared yellow)	86	14	0
PNM 1/29	1.1	wool	green	86	9	5
PNM 1/40	0.7	wool	green (appeared yellow)	86	10	4
PNM 5/14	0.5	wool	yellow	86	9	4
BRU 2/01	2.4	wool	green	85	10	5
HRP1/12	0.5	wool	green	85	9	6
HRP2/54	0.5	silk	yellow	85	9	6
PNM 5/12	0.9	wool	yellow	85	10	5
PNM 5/13	0.3	wool	yellow	85	9	6
BRU 3/09	1.2	wool	yellow	84	11	5
BRU 3/14	4.9	silk	beige (appeared yellow)	84	11	5
BXL 1/10	3.2	wool	ochre (appeared yellow)	84	9	7
HRP2/39	0.4	wool	green	84	12	4
PNM 2/30	0.6	wool	green (appeared yellow)	84	9	7
PNM 7/12	4	wool	yellow	84	11	6
BRU 1b/12	3.9	wool	yellow	83	5	11
HRP2/86	0.4	silk	green	83	9	8
PNM 1/32	0.8	silk	green (very brittle)	83	11	6
PNM 7/01	0.9	wool	yellow	83	12	6
PNM 7/02	0.7	wool	green	83	11	5
PNM 7/05	2	wool	yellow / green	83	11	6
PNM 9/19	0.3	weft	yellow	83	8	9
BRU 2/04	1.4	wool	green	82	10	7
BXL 1/11	1.5	wool	dark green	82	9	10
HRP2/69	2	wool	green	82	11	8
PNM 1/44	0.4	wool	green	82	14	4
PNM 5/19	1.3	silk	yellow	82	14	4
PNM 9/22	0.7		yellow / green	82	11	7
PNM 9/25	1.4		green	82	11	8
BRU 2/25	1.8	silk	green	81	11	7
BRU 3/09b	2.6	wool	yellow	81	14	5
HRP2/32	0.5	silk	green (appeared yellow)	81	10	9
BRU 2/26	2.5	wool	green	80	11	8
BRU 3/12	0.8	silk	yellow	80	12	8

HRP2/66	1.2	wool	blue	80	12	8
PNM 2/23	0.1	silk	yellow	80	15	5
PNM 7/04	1	wool	green (appeared blue)	80	10	10
BRU 2/21	1.4	wool	yellow	79	13	8
HRP1/46	2.5	wool	yellow	79	15	6
PNM 9/05	0.5		pale yellow	78	13	9
PNM 9/08	0.2		yellow	78	13	9
BRU 2/24	0.7	wool	yellow	75	17	8
PNM 2/24	0.7	wool	green	75	15	10
BRU 2/14	0.9	wool	brown (appeared yellow)	74	18	8
BRU 3/16	3.5	wool	green	74	16	10
BXL 2/40	0.3	silk	yellow	74	20	6
PNM 8/03	0.6	silk	yellow	74	16	10
PNM 8/12	1.3	silk	yellow	72	17	11
PNM 8/17	1.4	silk	yellow	72	19	9
BRU 3/08	1.8	wool	green	70	12	17
PNM 8/16	0.7	silk	yellow	69	20	11
PNM 8/09	1.4	silk	yellow	68	21	11
HRP2/77	1.7	wool	green	33	34	33

6.11.1.2 Historical dyer's greenweed samples

The identification of dyer's greenweed on historical samples was achieved by the qualitative analysis of three characteristic components observed in the acid hydrolysed yarn extracts; genistein (G), luteolin (L) and apigenin (A). Accurate quantitative analysis of the three components was hindered by the close elution of genistein and luteolin, however, the relative percentages of the three components were calculated as accurately as possible at a detection wavelength of 254 nm using automatic integration software. The samples have been ordered with a descending percentage of luteolin and only those analysed in Edinburgh have been included (Table 6.48).

Table 6.48: The relative percentages of luteolin (L), apigenin (A) and genistein (G) (monitored at 254 nm) in the acid hydrolysed extracts of historical samples believed to have been dyed using dyer's greenweed. The samples have been ordered with a descending percentage of luteolin and only those analysed in Edinburgh have been included

Sample	Sample mass	Yarn Type	Yarn colour	%L	%A	%G
HRP1/10	1.6	wool	blue	81	6	14
HRP1/14	1.2	wool	khaki (appeared yellow)	78	10	12
HRP2/28	2.1	silk	beige (appeared yellow)	77	8	15
HRP2/44	1.3	wool	green	76	5	19
HRP2/27	1	wool	green	67	3	31
PNM 7/21	2.2	wool	green	62	9	29
HRP2/71	0.3	silk	green (appeared yellow)	61	6	33
BXL 3/09	0.4	wool	green	56	9	35
HRP2/19	0.6	wool	blue-green	51	3	45
BRU 1c/16	0.8	silk	yellow	50	4	46
HRP2/20	1.3	wool	blue (appeared green)	47	2	51
PNM 5/31	0.5	Silk	beige (appeared colourless)	45	0	55
PNM 1/20	0.4	silk	green (appeared yellow)	42	10	48
HRP3/28	0.4	silk	yellow	36	1	63
BXL 3/15	0.7	wool	beige (appeared yellow)	34	8	57
BXL 1/01	0.9	silk	yellow	34	5	62
BXL 3/13	0.5	wool	yellow	33	3	64
HRP1/5	1.4	silk	green (appeared yellow)	31	5	64
BRU 1a/03	0.8	silk	yellow	29	1	71
HRP2/64	1	silk	yellow	29	2	69
HRP2/52	0.5	silk	yellow	28	16	56
PNM 7/17	1.6	silk	yellow	28	2	70
HRP2/45	1.2	silk	yellow	28	2	70
HRP2/22	1.3	silk	yellow	27	2	71
HRP2/41	0.8	wool	green	26	0	74
HRP2/51	1.1	silk	green	26	3	71
HRP2/59	2.6	silk	green	26	3	71
HRP3/32	0.2	silk	green (appeared yellow)	25	13	61
HRP2/49	0.8	silk	green	25	2	73
BXL 4/18	1.2	wool	light green	25	1	74
PNM 7/10	2	silk	green	25	3	72
BXL 3/04	1.1	wool	yellow	24	3	73
PNM 5/34	0.6	silk	green	24	3	73
BXL 1/02	2	silk	yellow	23	3	73
HRP2/43	1	silk	green	23	2	75
HRP3/49	0.1	silk	green/blue	22	0	78
HRP2/48	1.8	silk	pink (appeared yellow)	22	2	76
HRP3/33	0.9	silk	blue (appeared green)	21	3	76
PNM 7/18	0.2	silk	yellow	21	2	78

PNM 1/11	0.6	silk	yellow	20	2	79
PNM 5/35	0.1	silk	yellow	19	2	80
PNM 1/09	0.9	silk	green	19	2	80
PNM 1/14	0.5	silk	green (appeared yellow)	19	3	78
PNM 1/13	0.3	silk	green (appeared yellow)	19	2	79
PNM 2/10	0.5	silk	green (appeared yellow)	19	2	79
PNM 2/21	0.8	silk	green	18	2	79
HRP3/18	0.1	silk	yellow	17	0	83
HRP2/26	1.4	cotton	blue	17	1	83
PNM 1/12	0.1	silk	green (appeared yellow)	17	1	82
PNM 1/19	0.4	silk	green	17	1	82
PNM 5/28	0.5	silk	yellow	16	2	82
PNM 1/51	0.8	silk	yellow	16	0	84
PNM 5/36	0.6	silk	yellow	16	2	82
HRP3/46	1	silk	yellow	15	4	81
PNM 2/09	0.3	silk	Yellow	15	1	84
HRP3/35	0.2	silk	green (appeared yellow)	13	3	84
PNM 7/23	1	silk	grey (appeared uncoloured)	12	0	88
PNM 2/29	0.6	silk	green (appeared yellow)	9	1	90
PNM 1/48	1.4	silk	green / yellow	9	2	89

Appendix

7 APPENDIX

7.1 MODHT PARTNERS

Prof. Chris Carr (Project coordinator) and Anne-Marei Hacke
The University of Manchester, Textiles and Paper, School of Materials, PO Box 88, Sackville Street, Manchester. M60 1QD, UK.
emails: chris.carr@manchester.ac.uk and a.hacke@postgrad.manchester.ac.uk

Dr Marianne Odlyha
Birkbeck College, University of London, School of Biological & Chemical Sciences, Malet Street, London. WC1E 7HX, UK.
email: m.odlyha@bbk.ac.uk

David Howell (formerly project co-ordinator) and Kathryn Hallett
Historic Royal Palaces, Conservation and Collections Care, Hampton Court Palace, Surrey. KT8 9AU, UK.
email: kathryn.hallett@hrp.org.uk

Dr Jan Wouters, Ina Vanden Berghe, Vera Vereecken and Ingrid de Meûter
The Royal Institute for Cultural Heritage (KIK-IRPA), Jubelpark 1, B-1000 Brussels, Belgium.
emails: jan.wouters@kikirpa.be, ina.vandenberghe@kikirpa.be,
vera.vereecken@kikirpa.be, demeuter@kmkg-mrah.be

Dr Concha Carretero Herrero,
Patrimonio Nacional, Palacio Real, Madrid, Area de Conservación y Departamento de Restauración, 28071 Madrid, Spain.
email: concha.herrero@patrimonionacional.es

Dr Anita Quye,

National Museums of Scotland, Conservation and Analytical Research Department, Chambers Street, Edinburgh. EH1 1JF, UK.

email: a.quye@nms.ac.uk

Prof. Hamish McNab and Dr Alison Hulme,

School of Chemistry, University of Edinburgh, West Mains Road, Edinburgh. EH9 3JJ, UK.

email: Alison.hulme@ed.ac.uk, H.McNab@ed.ac.uk

7.2 MODHT DYE RECIPES

As part of the MODHT project, a series of historically accurate reference samples were dyed by Anne-Marei Hacke, The University of Manchester.[1] The majority of experiments were conducted using these MODHT dyed reference yarns,

The principal literature references used for the preparation of the dyed yarns was the Plictho of Gioanventura Rosetti,[2] and transcriptions of three texts; (a) Ms. 517, Wellcome Historical Medical Library, London, late 15th century, (b) Tbouck van Wondre, Brussels, 1513 and (c) Hs. 1317, University Library Ghent, first half of 16th century, written in Brabant language.[3] A number of other primary literature references were also consulted.[4,5,6,7,8]

Many problems were encountered in compiling the historical dye recipes, not only with respect to the translation, but also with the conversion of units of volume, mass and time. Old units were converted into modern ones in a pragmatic way, *e.g.* by associating a weight of 454 g to 16 ounces and 16 ounces to one pound in weight. Finally, in order to compare the old recipes, they were normalised *i.e.* the amounts of all ingredients were recalculated for the dyeing of 100 g of dry, scoured/de-gummed yarn. Based on the comparison of these 'adapted recipes', representative recipes were generated for each dye source to create the standards for the project. The essential ingredients and relative proportions from these 'adapted recipes' have been tabulated below (Table 7.1–Table 7.4).

Table 7.1: The ingredients from the 'adapted recipes' for dyeing silk yellow and black

	Yellow / S1	**Yellow / S2**	**Yellow / S3**	**Black / S1**
Essential dye	weld (200 g)	young fustic (100 g)	dyer's greenweed (700 g)	galls (100 g)
Other Ingredients	yarn (100 g) alum (37.5 g)	yarn (100 g) alum (56.25 g)	yarn (100 g) alum (37.5 g)	yarn (100 g) iron filings (137.5 g) vitriol (118.75 g) gum arabic (112.5 g)

Table 7.2: The ingredients from the 'adapted recipes' for dyeing silk red

	Red / S1	**Red / S2**	**Red / S3**
Essential dye	brazilwood (300 g)	madder (25 g) (or 200 g if 'non-flanders')	cochineal (25 g)
Other Ingredients	yarn (100 g)	yarn (100 g)	yarn (100 g)
	alum (25 g)	alum (25 g)	gum Arabic (19 g) galls (19 g) curcumin (1 root)

Table 7.3: The ingredients from the 'adapted recipes' for dyeing wool yellow and black

	Yellow / W1	**Black / W2**
Essential dye	weld (50 g)	galls (100 g)
Other	yarn (100 g)	yarn (100 g)
Ingredients	alum (15 g)	ferrous sulphate (150 g)
	wood ash	gum arabic (100 g)

Table 7.4: The ingredients from the 'adapted recipes' for dyeing wool red

	Red / W1	**Red / W2**	**Red / W3**	**Red / W4**	**Red / W5**
Essential dye	madder (60 g)	madder (60 g)	brazilwood (25 g)	cochineal (6.3 g)	cochineal (5.4 g)
Other Ingredients	yarn (100 g)	yarn (100 g)	yarn (100 g)	yarn (100 g)	yarn (100 g)
	alum (15 g)	alum (5 g)	alum (15 g)	starch paste (18.7 g)	senegal gum (7.9 g)
		galls (10 g)		curcuma (1.6 g)	tartaric acid (1.6 g)
				cinnabar (1.6 g)	curcumin (1.3 g)
				salt (3.2 g)	cinnabar (0.9 g)
					alum (0.2 g)
					salt (0.8 g)

Correct botanical species of each of the sources to be used for dyeing were then sourced and an initial test yarn was dyed for authentication by chemical analysis. The dye components were extracted from the yarns using an acid hydrolysis method then analysed by PDA HPLC following the routine protocol used by he National Museum of Scotland. Although analysis could have been conducted on the aqueous extracts of the raw plant material, the adopted procedure ensured that only the hydrolysed chemical compounds routinely used for dye source identification, rather than the many additional compounds in the raw extracts, were observed. Thus the identification process was simplified. The exception was turmeric, used with cochineal to dye silk red, which was analysed by PDA HPLC without dyeing onto

yarn, as the available literature information for its identification was based on the water-extract.[9] All species were found to be correct except young fustic (*Cotinus coggygra* Scop.), so another source was obtained and authenticated.

Alum, copper turnings, ferrous sulphate, gum arabic, iron filings, potassium carbonate and tartaric acid were all sourced from Fisher Chemicals, England, while the brazilwood, cochineal, madder, oak galls and weld were obtained from Verfmolen De Kat, Netherlands. George Weil Fibrecraft, England, supplied the dyer's greenweed, saunderswood and turmeric, while the woad (couched) was from John Edmonds, Reading University, England (in co-operation with SPINDIGO) and the young fustic from Association de Garance, Lauris, France. Finally, the Royal Botanic Gardens, Kew, England, provided *Caesalpinia sappan* and *Pterocarpus santilinus* reference material.

The wool and silk yarns for the reference dyeings were also selected to represent authentic original samples. The same 3-ply, 158 Tex English wool yarn was used for warp and weft, while the selected silk yarns were Italian spun 2-ply, 66 Tex. The yarns were mordanted and dyed in hanks (loose loops) in either an open or closed vat. The open vat had a volume of 90 l, steam heating and temperature controlled heating with an electric element and a hank rotating wince to provide constant agitation. The closed vat had a maximum volume of 200 l and a minimum working volume of 150 l, steam heating while a reverse flow liquor pump provided constant agitation. The recipes were followed as strictly as possible with the restrictions imposed by the equipment and parameters such as weight, liquor ratio, pH, temperature and time were controlled and recorded for later reference.

The dyed hanks were rewound onto cones and samples provided to all the partners. The remaining yarn was woven into single colour 'model tapestries' with undyed warp yarns and dyed weft yarns, representative of the woven structure from the historical tapestries. These were woven on a Northrop Single Shuttle loom, however, due to operational problems, the warp and weft yarns had to be reversed.

The following is a complete list of dyed reference yarns together with the data recorded during their preparation. The mordanting procedures for the silk yarns have been outlined in Section 7.2.2, while the dyeing procedures for the respective yarns, identified using the unique codes, have been described in Section 7.2.2.2. Similarly, the mordanting procedures for the wool yarns have been outlined in Section 7.2.3.1, while the dyeing procedures for the respective yarns have been described in Section 7.2.3.2.

7.2.1 Preparation of semelwater

Bran of wheat (2 kg) was added to water (45 l) and brought to the boil. The heat was turned off and more water (30 l) added before the bath was covered. This was stirred every h (7 times) during the first day. After 6 days, an aliquot (40 l, pH 4.87) was removed for the brazilwood, R/S1 recipe (Section 7.2.2.2.5). Hot water (40 l) was added, the bath stirred and left for another 24 h, before a second aliquot (70 l, pH 4.35) was removed for the madder, R/W1 recipe (Section 7.2.3.1.4).

7.2.2 Silk Yarns

7.2.2.1 Mordanting procedures

7.2.2.1.1 Boil mordant

Alum (437.5 g) was dissolved in boiling water (57 l) to produce a solution with pH 3.05. Ten silk hanks (1140 g) were immersed and the water held at boiling for 10 min before the silk was removed and left to cool. The bath was allowed to return to room temperature before the silk was re-immersed for 10 h.

7.2.2.1.2 Mordanting for weld and dyer's greenweed (Yellow / S1 and S3)

Alum (384.4 g) was dissolved in hot water (50 l, 38 °C) to produce a solution with pH 3.49 then nine silk hanks (1025 g) were immersed. They were left for 20 h, and three hanks rinsed and dried. These three silk hanks (346 g) were mordanted for a second time, as follows, to produce samples to be dyed with dyer's greenweed (Y/S3, Section 7.2.2.2.2). Alum (130 g) was dissolved in water (150 l, 22 °C) to produce a solution with pH 4.1. The silk hanks were immersed and left for 16 h

before being rinsed in cold water. The hanks remaining from the first mordanting were used for the dyeing of weld (Y/S1) samples (Section 7.2.2.2.1).

7.2.2.1.3 Mordanting for young fustic (Yellow / S2)

Alum (225 g) was dissolved in warm water (30 l, 43 °C), producing a solution with pH 2.90. Eleven hanks of silk (600 g) were immersed and left for 2 h (34 °C, pH 3.45).

7.2.2.1.4 Mordanting for brazilwood (Red / S1)

Alum (315 g) was dissolved in a small quantity of hot water then the bath was filled with cold water (150 l, 23 °C, pH 4.08). Ten silk hanks (1260 g) were immersed and left for 16 h. These were then rinsed until the waste water had a pH>6. Five hanks were dried for the preparation of brazilwood (R/S1) samples (Section 7.2.2.2.5).

A second mordanting was conducted by dissolving alum (315 g) in a small quantity of hot water and filling the bath with warm water (85 l, 33 °C, pH 3.51). Ten silk hanks, five from the first dyeing of brazilwood onto unmordanted yarn (Section 7.2.2.2.5), and five unmordanted yarns, were then immersed and left for 16 h. The vat was drained and the hanks wrung. Four hanks were removed and one of each rinsed, producing two samples dyed during the 'mordanting' process because of the presence of the brazilwood dyed yarns (R/S1a and R/S1b) and two mordant-dye-mordant samples (R/S1c and R/S1d).

7.2.2.1.5 Mordanting for madder (Red / S2a-c)

Alum (210.5 g) was dissolved in a small amount of boiling water and then the bath filled with water (50 l, 48 °C, pH 3.50). Eight silk hanks (842 g) were immersed and left for 20 h before being rinsed until the waste water had a pH>6. The bath was then drained before the removal and drying of two hanks.

7.2.2.1.6 Mordanting for cochineal (Red / S3)

Alum (267 g) was dissolved in boiling water (50 l) to which was added sodium chloride (66.75 g) and copper turnings (1 kg), producing a solution with pH 3.15.

The heat was removed and five silk hanks (534 g) immersed and left for 24 h while the bath cooled (22 °C, pH 3.97). The hanks were rinsed until the waste water had a pH> 6.

7.2.2.2 Dyeing Procedures

7.2.2.2.1 Weld (Yellow / S1a-b)

Weld (1130 g) was added to boiling water (50 l) and allowed to boil for 1.5 h (pH 6.05). Four pre-wetted boil mordanted hanks (from Section 7.2.2.1.1) were immersed (Y/S1a), while six hanks were transferred from the mordanting bath (Section 7.2.2.1.2) into the dye bath without wringing (Y/S1b). The yarns were boiled for 20 min before being rinsed with hot water.

7.2.2.2.2 Dyer's greenweed (Yellow / S3a-e)

Dyer's greenweed (4 kg) was added to water (150 l) and boiled for 1 h (pH 6.6) before five silk hanks were immersed. Three hanks from the mordanting bath (Section 7.2.2.1.2) were immersed (Y/S3a) while two boil mordanted hanks (Section 7.2.2.1.1) were also immersed. They were left at the boil for 30 min before being removed and left to dry without rinsing.

Dyer's greenweed (3 kg) and potassium carbonate (150 g) were added to water (150 l), which was heated to boiling and held at this temperature for 1 h (pH 8.1). All hanks from the first dyeing were then immersed for 10 min, at the boil. These were removed without rinsing, producing a boil mordanted and twice dyed sample (Y/S3b) and a mordanted and twice dyed sample (Y/S3c).

One pre-dyed (first and second), boil mordanted hank and one unmordanted hank were now immersed in the bath from the second dyeing. These were then dyed at the boil for 1.5 h and removed and left to dry, without rinsing. This produced a boil mordanted and three times dyed sample (Y/S3d) and an unmordanted sample dyed in only the third dye bath (Y/S3e).

7.2.2.2.3 Young fustic 'old' (Yellow / S2a)

An authentic source of young fustic (*Cotinus coggygria* Scop.) was supplied by the Association de Garance, Lauris, France. Two samples were provided; a 'fresh' batch, consisting of dried heartwood harvested within the last year, and an 'old' batch, consisting of dried heartwood harvested more than one year previously. The wood from each batch was separately de-barked, chipped and rasped, and used to dye the MODHT yarns.

The 'old' young fustic, consisting of dried heartwood harvested more than one year previously (250 g) was heated in water (15 l) until boiling, then left to cool for 1 h (53 °C, pH 5.9), before alum (47 g) was added and the bath allowed to cool further (40 °C, pH 3.3). An aliquot (10 l) was then strained into a clean vessel and the seven pre-mordanted silk hanks (250 g), six for metal threads and one extra, were immersed (pH 3.35) and left for 30 min while stirring. The hanks were removed then wrung and left to dry.

7.2.2.2.4 Young fustic 'fresh' (Yellow / S2b)

The 'fresh' young fustic, consisting of dried heartwood harvested within the last year (100 g) was added to water (5 l) which was heated until boiling before being left to cool for 1 h, (55 °C, pH 5.7). Alum (18.75 g) was then added and the bath left to cool further, (40 °C, pH 2.9) before an aliquot (4 l) was strained into a clean vessel and pre-mordanted silk (100 g) immersed, (pH 3.1). This was left for 30 min, with stirring, before the silk was removed, wrung and left to dry.

Both the young fustic dyeings produced very light coloured yarns. The acid hydrolysed extracts from the respective yarns produced only a small amount of dye components, thus, a further sample was dyed using the 'fresh' wood (Section 6.1.2).

7.2.2.2.5 Brazilwood (Red / S1a-e)

To water (50 l, pH 7.28, 45 °C), semelwater was added (40 l) producing a solution with pH 4.85. Brazilwood (1890 g) was then added and the solution slowly heated

over 6 h (80 °C). This was then strained to filter out the sludge and boiled for 1 h. An aliquot (45 l) was removed for the second dyeing, while water (5 l) was added to the remainder (50 l, 90 °C) producing a solution with pH 5.45. The mordanted pre-wetted silk (Section 7.2.2.1.4), was immersed for 20 min before draining and wringing. The second mordanting process (Section 7.2.2.1.4) produced four samples, R/S1a-d.

The saved dye liquor (10 l) was mixed with semelwater (10 l) producing a solution with pH 4.39. Water was then added (30 l) and the solution heated (90 °C, pH 4.95). The six silk hanks remaining from the second mordanting were then immersed for 15 min. There was no visible change in shade and the dye liquor was brownish. Potassium carbonate (150 g) was added, producing a solution with pH 10.15, then one additional boil mordanted, pre-wetted, silk hank (Section 7.2.2.1.1) was immersed and the solution allowed to stand for a further 15 min. Both the silk and the dye liquor became purple. This process produced three additional samples, a mordant-dye-mordant-dye-lye yarn (R/S1e), a second mordant-second dye-lye yarn (R/S1f) and a boil mordanted-second dye-lye yarn (R/S1g). All eleven hanks, with shades ranging from pink to purple, were wrung and rinsed.

7.2.2.2.6 Madder (Red / S2a-c)

Madder (157.5 g) was added to hot water (50 l), and eight pre-mordanted silk hanks (842 g) immersed (90 °C, pH 6.58). These were left for 20 min, (pH 5.90), before two hanks were removed, rinsed in cold water and dried (R/S2a and R/S2b). The first lye treatment proceeded by adding potassium carbonate (50 g) producing a solution with pH 9.0. The remaining hanks were added and left for a further 20 min. Two hanks were removed and dried (R/S2c). The second lye treatment involved the further addition of potassium carbonate (350 g) producing a solution with pH 10.80. The two remaining hanks were immersed and left for a further 20 min before being removed and dried (R/S2d).

7.2.2.2.7 Cochineal (Red / S3)

Gum arabic (101.5 g) was dissolved in warm water (35 l). Oak galls (101.5 g) were added, together with copper turnings (1 kg), cochineal (133.75 g) and turmeric (30 g). This was boiled for 2 h, then more water was added (50 l, 70 °C), producing a solution with pH 4.8. Five pre-mordanted silk hanks (534 g) were immersed for 10 min then removed. The liquor was brought to the boil and the silk re-immersed and boiled for 2 h. The hanks were then wrung and left to dry. Once dry, they were then rinsed.

7.2.2.2.8 Woad (Blue / S1)

All dyeings in the woad vat were performed by John Edmonds at Chiltern Open-air Museum conforming to medieval practice. Due to the volume of the vat (30 l) the dyeings were carried out in stages of three to five hanks at a time and 2 kg of couched woad was used in total. Reduction was achieved by bacterial action at 45-50 °C and at a pH of *ca.* 8.2-8.5. Wood ash and lime were used to maintain the alkalinity. Five silk hanks (Blue / S1) were prepared.

7.2.2.2.9 Woad (Green / S1a-b and S2a-b)

To produce green yarns, the over- and under-dyeing of yellow silk was performed. The blue over-dyeing was performed on two boil mordanted, weld dyed silk hanks (Y/S1a) and three mordanted, weld dyed silk hanks (Y/S1b), producing G/S1a and G/S1b respectively.

The yellow over-dyeing of the blue yarns was performed as follows. Water (50 l) was brought to the boil (pH 7.40) and weld (565 g) added. This was then boiled for 1.5 h (pH 5.94) before five hanks of pre-wetted silk were immersed. These consisted of two boil mordanted, woad dyed silk hanks and three mordanted, woad dyed hanks. The bath was boiled for 20 min (pH 6.14) before being allowed to cool for 4 h and the hanks rinsed and left to dry.

7.2.3 Wool yarns

7.2.3.1 Mordanting procedures

7.2.3.1.1 Alum mordanted wool (Alum / W)

Alum (150 g) was dissolved in water (50 l), producing a solution with pH 3.50, before four hanks of pre-wetted wool (670 g) were immersed and boiled for 1.5 h. The hanks were wrung, rinsed and dried.

7.2.3.1.2 Mordanting for weld (Yellow / W1)

Alum (22.5 g) was dissolved in boiling water (75 l), producing a solution with pH 4, before eight hanks of wool (1.5 kg) were immersed and boiled for 2 h before being wrung out.

7.2.3.1.3 Mordanting for dyer's greenweed (Yellow / W2)

To boiling water, (50 l, pH 7.2) was added alum (15 g), producing a solution with pH 3.23, and five hanks of wool (1 kg). These were immersed and boiled for 2 h (pH 6.0), before being wrung and left to dry.

7.2.3.1.4 Mordanting for madder (Red / W1)

To semelwater, (50 l, pH 4.35) was added alum (150 g), producing a solution with pH 3.17. Six wool hanks (1000 g) were immersed and the bath brought to the boil and held at this temperature for 2 h. The bath was then drained, but the hanks were not wrung.

7.2.3.1.5 Mordanting for madder (Red / W2)

The first mordanting was conducted as follows. Oak galls (70 g) were added to water (50 l) which was brought to the boil and left for 30 min before four wool hanks (700 g) were immersed and boiled for 2 h. The bath was then drained but the hanks were not wrung. Alum (35 g) was then dissolved in water (50 l) and brought to the boil for a second mordanting procedure. The wool was immersed and boiled for 2 h before the bath was drained and the hanks wrung.

7.2.3.1.6 Mordanting for brazilwood (Red / W3)

Alum (105 g) was dissolved in water (35 l) and four wool hanks (700 g) immersed and boiled for 1.5 h before being wrung.

7.2.3.1.7 Mordanting for cochineal (Red / W4 and W5)

Alum (106 g) was dissolved in boiling water (50 l) together with D-tartaric acid (69 g), sodium chloride (30.4 g) and sandalwood (30.4 g), producing a solution with pH 2.55. Eight wool hanks (1320 g) were immersed and boiled for 2 h, before the heat was turned off and the bath allowed to cool for 24 h. The hanks were removed, but not wrung.

7.2.3.1.8 Mordanting for oak galls (Black / W1 and Black / W2)

To hot water (50 l, 73 °C, pH 7.85), eight hanks of wool (1300 g) were immersed. Due to the commercial alkaline scour, this produced a bath with pH 8.69. The wool was removed, and oak galls (1300 g) added before the bath was brought to the boil, (pH 4.23). The wet wool was re-immersed and boiled for 2 h before draining, cooling down then being rinsed with hot water before being left to dry.

7.2.3.1.9 Mordanting for alder bark (Black / W3)

Alder bark (1800 g) was boiled in water (50 l), producing a solution with pH 5.70, before seven hanks of pre-wetted wool (1200 g) were immersed and boiled for a further 2 h. The bath was drained and the hanks wrung and left to dry.

7.2.3.1.10 Mordanting for oak galls (Black / W4)

Oak galls (1000 g) were added to boiling water (50 l), producing a solution with pH 4.30. Six hanks of pre-wetted wool (1000 g) were immersed and boiled for 2 h. The bath was drained and the hanks allowed to cool, rinsed with hot water then left to dry.

7.2.3.2 Dyeing procedures

7.2.3.2.1 Weld (Yellow / W1)

Weld (750 g) and potassium carbonate (75 g) were added to boiling water (75 l), producing a solution with pH 10.2. Eight hanks of the wet, pre-mordanted wool (1.5 kg, dry weight) were immersed and boiled for 1 h before the hanks were removed, wrung and rinsed with both cold and hot water.

7.2.3.2.2 Dyer's greenweed (Yellow / W2)

To boiling water (50 l, pH 7.4), was added potassium carbonate (75 g), producing a solution with pH 9.75. Dyer's greenweed (2.5 kg) was then added, producing a solution with pH 7.33. Five hanks of pre-mordanted, wetted wool (1 kg, dry weight) were immersed and boiled for 1 h (pH 7.05), before the hanks were removed, wrung and rinsed with cold water and left to dry.

7.2.3.2.3 Madder (Red / W1)

To semelwater (20 l, pH 4.35), water (30 l) was added then madder (600 g). The bath was stirred and heated (40 °C, pH 5). Six pre-mordanted wool hanks (1000 g) were immersed and the bath again heated (90 °C) and left for a further 3 h. The bath was then drained and the hanks rinsed before wringing. Three hanks were left to dry (R/W2a). A lye treatment was provided for the three remaining hanks. To water (50 l, 20 °C, pH 7.4), potassium carbonate (50 g) was added, producing a solution with pH 10.95. The three wool hanks were then immersed and left for 30 min before rinsing (R/W2b).

7.2.3.2.4 Madder (Red / W2)

Water (50 l) was heated (40 °C) and four pre-mordanted, wetted wool hanks (700 g, dry weight) immersed. The bath was heated further (90 °C) and held at this temperature for 3 h before the hanks were removed, wrung and rinsed. Two hanks were left to dry (R/W2a). A lye treatment was provided for the two remaining hanks, where potassium carbonate (35 g) was dissolved in a small quantity of hot water and the bath filled (50 l, 35 °C), producing a solution with pH 10.78. The remaining two

wool hanks were then immersed and left for 30 min before being rinsed with hot water (R/W2b).

7.2.3.2.5 Brazilwood (Red / W3)

Brazilwood (175 g) was added to boiling water (35 l) and left for 45 min. The bath was refilled with cold water (to make 35 l), and four hanks of pre-mordanted wool (700 g) immersed and boiled for 1.5 h. The hanks were then rinsed with hot water and two were left to dry (R/W3a). A lye treatment was provided for the two remaining hanks, where potassium carbonate (50 g) was dissolved in a small quantity of hot water and the bath filled (50 l, 35°C), producing a solution with pH 10.78. The remaining two wool hanks were immersed and left for 30 min before being rinsed with hot water (R/W3b).

7.2.3.2.6 Cochineal (Red / W4)

Starch (61.75 g) was mixed with water to make starch paste (123.5 g) which together with sodium chloride (21 g) was dissolved in boiling water (50 l). Cochineal (41.6 g) was then added together with turmeric (10.5 g), and four pre-mordanted wool hanks immersed (670 g) producing a solution with pH 4.2. This was then boiled for 1 h before the hanks were then rinsed in cold water.

7.2.3.2.7 Cochineal (Red / W5)

Gum arabic (53 g), alum (1.3 g), turmeric (8.7 g) and sodium chloride (5.4 g) were all dissolved in boiling water (50 l), before cochineal (36.2 g) was added and four pre-mordanted wool hanks (670 g) immersed and the bath boiled for 1 h. The hanks were then rinsed in cold water.

7.2.3.2.8 Oak galls (Black / W1)

Water (50 l, pH 7.40) was boiled and iron sulphate added (62.5 g) producing a solution with pH 4.5. Four hanks of pre-mordanted, wetted wool (650 g, dry weight) were immersed and the bath boiled for 30 min (pH 3.34). The bath was allowed to cool for 40 min, before one hank was removed (B/W1a). Three hanks were then boiled for 30 min and the bath allowed to cool for 40 min before another hank was

removed (B/W1b). The final two hanks were boiled for 30 min before the bath was allowed to cool for 40 min and removed (B/W1c). The pH of the bath remained unchanged during the second and third dyeings. All hanks were then rinsed together and left to dry.

7.2.3.2.9 Oak galls (Black / W2)

To boiling water (50 l, pH 7.40) was added iron sulphate (975 g), producing a solution with pH 4.1. Four hanks of pre-mordanted, wetted wool (650 g, dry weight) were immersed and boiled for 30 min. One hank was removed and rinsed (B/W2a), while the bath was allowed to cool for 40 min (pH 3.37). The remaining three hanks were then boiled for 30 min before one hank was removed (B/W2b) and rinsed. The pH of the bath remained unchanged and it was allowed to cool for a further 40 min. Finally, two hanks were boiled for 30 min then removed, rinsed and dried (B/W2c). The bath was then allowed to cool for 40 min (pH 3.39).

7.2.3.2.10 Alder bark (Black / W3)

To boiling water (50 l, pH 7.35) was added iron sulphate (250 g), producing a solution with pH 5. Four hanks of mordanted, pre-wetted wool (685 g, dry weight) were then immersed and boiled for 40 min (pH 4.40) before one hank was removed (B/W3a). The bath was allowed to cool for 30 min before the remaining three hanks were then re-immersed and boiled for 40 min (pH 4.20) and removed. The bath was allowed to cool for 30 min before the hanks were once again immersed and boiled for 40 min (pH 4.30). They were then removed and allowed to cool for 1 h (B/W3b). All hanks were then rinsed in cold water until the waste water was almost clear.

7.2.3.2.11 Oak galls (Black / W4)

To boiling water (50 l, pH 7.7) was added copper sulphate (109.4 g), producing a solution with pH 4.5 Iron sulphate (109.4 g) was then added, producing a solution with pH 3.77. Six hanks of pre-mordanted, wetted wool (1000 g, dry weight) were then immersed and boiled for 30 min. One hank was removed (BW/4a) and the bath allowed to cool for 40 min (pH 3.25). The remaining three hanks were boiled for a further 30 min before another one was removed (B/W4b). The bath was again

allowed to cool for 40 min before the remaining two hanks were boiled for 30 min and removed (B/W4b). The bath was then allowed to cool for 40 min. The pH of the bath remained unchanged during the second and third dyeings. All hanks were then rinsed together and left to dry.

7.2.3.2.12 Woad (Blue / W1)

As with the silk yarns, all dyeings in the woad vat were performed by John Edmonds at Chiltern Open-air Museum conforming to medieval practice. Due to the volume of the vat (30 l) the dyeings were carried out in stages of 3-5 hanks at a time and 2 kg of couched woad were used in total. Reduction was achieved by bacterial action at 45-50 °C and a pH of *ca.* 8.2-8.5. Wood ash and lime were used to maintain the alkalinity. Three wool hanks (Blue / W1) were prepared.

7.2.3.2.13 Woad (Green / W2)

To produce green yarns, the over- and under-dyeing of yellow wool was performed. The blue over-dyeing was performed on three weld dyed wool hanks (Y/W1), producing G/W1.

The yellow over-dyeing of the blue yarns was performed as follows. To boiling water (50 l, pH 7.50), was added alum (7.5 g) producing a solution with pH 3.60. Three hanks of pre-wetted, woad dyed wool (500 g, dry weight) were then immersed and boiled for 2 h (pH 6.02). The bath was drained before more water (50 l, pH 7.40) was brought to the boil and weld (250 g) added, producing a solution with pH 5.97. Potassium carbonate (25 g) was then added, producing a solution with pH 7.87. The pre-wetted wool was immersed, boiled for 1 h, rinsed in warm water then dried.

---

[1] Hacke, A-M, **2006**, PhD Thesis, The University of Manchester (submitted)

[2] Edelstein, S.M.; Borghetty, H.C., '*The Plictho of Gioanventura Rosetti. Instructions in the art of the dyers which teaches the dyeing of woolen cloths, linens, cottons, and silk by the great art as well as by*

the common', translation of the 1548 (first) edition, **1969**, *The M.I.T. Press*, Cambridge. MA., 131-152, 186-199

[3] Braekman, W.L. (ed), *'Middelnederlandse verfrecepten voor miniaturen en "allerhande substancien"'*, **1986**, Scripta 18

[4] De Nie, W.L.J., *'De ontwekkeling der Noord-Nederlandsche textielververij van de veertiende tot de achttiende eeuw'*, **1937**, Leiden, Fol. 64 xxxii-xxxv and 179-181

[5] Hofenk de Graaff, J.H., *'Geschiedenis van de textieltechniek'*, Lakennijverjeid – Sitsen – Zijde industrie, **1992**, Amsterdam

[6] Diehl, J.M.; de Graaf, A.J.; de Jonghe, D., *'Textiellexicon'*, **1991**, Amsterdam

[7] De Poerck, G., *'La draperie médiévale en Flandre et en Artois, technique et terminologie, I. La technique'*, **1951**, Brugge

[8] De Poerck, G., *'La draperie médiévale en Flandre et en Artois, technique et terminologie, III. Glossaire Flamand'*, **1951**, Brugge

[9] Hiserodt, R.; Hartman, T.G.; Ho, C-T, Rosen, R.T., *'Characterisation of powdered turmeric by liquid chromatography-mass spectrometry and gas chromatography-mass spectrometry'*, J Chromatogr A, **1996**, 740, 51-63

7.3 PUBLICATIONS

Hulme, A.N.; McNab, H.; Peggie, D.A.; Quye, A., *'Negative Ion Electrospray Mass Spectrometry of Neoflavonoids'*, Phytochemistry, **2005**, 66, 23, 2766-2770

Hulme, A.N.; McNab, H.; Peggie, D.A.; Quye, A.; Van den Berghe, I.; Wouters, J., *'The Analytical Characterisation of the Main Component Found in Logwood Dyed Textile Samples after Hydrochloric Acid Extraction'*, Preprints for the ICOM-CC 14th Triennial Meeting, The Hague, **2005**, Vol II, James and James, Earthscan, 783-788

Hulme, A.N.; McNab, H.; Peggie, D.A.; Quye, A., *'The application of liquid chromatography-mass spectrometry and accelerated light ageing for the analytical identification of yellow flavonoid dyes in historical tapestries'*, postprints for the Research Centre for Textile Conservation and Textile Studies 1st Annual Conference, Scientific Analysis of Ancient And Historic Textiles: Informing Preservation, Display and Interpretation, **2005**, Archetype Publications Ltd, 208-213

Accepted and in press;

Hulme, A.N.; McNab, H.; Peggie, D.A.; Quye, A., *'The Chemical Characterisation by PDA HPLC and HPLC ESI MS of aged and unaged fibre samples dyed with sawwort (Serratula tinctoria L.)'*, postprints for the Dyes in History and Archaeology 22nd annual meeting, Switzerland, **2003**

Available online at www.sciencedirect.com
SCIENCE DIRECT
Phytochemistry 66 (2005) 2766–2770
PHYTOCHEMISTRY
www.elsevier.com/locate/phytochem

Negative ion electrospray mass spectrometry of neoflavonoids

Alison N. Hulme [a,*], Hamish McNab [a,*], David A. Peggie [a,b], Anita Quye [b,*]

[a] School of Chemistry, The University of Edinburgh, West Mains Road, Edinburgh EH9 3JJ, UK
[b] National Museums of Scotland, Chambers Street, Edinburgh EH1 1JF, UK

Received 23 December 2003; received in revised form 31 August 2005
Available online 20 October 2005

Abstract

The electrospray ionisation mass spectra of the neoflavanoids brazilin and hematoxylin are reported in both their reduced (**1** and **2**, respectively) and their oxidised forms (**3** and **4**, respectively). In the reduced forms, breakdown pathways under collision induced decomposition (CID) conditions produce fragments characteristic of rings A and C; in their oxidised forms, the fragments are characteristic of rings B and D. The structural assignments of the fragments are substantiated by recording the spectra after deuterium exchange at the hydroxyl groups.

Keywords: Neoflavonoids; Mass spectrometry

1. Introduction

The neoflavonoid derivatives brazilin **1** and hematoxylin **2** are well-known constituents of the hard-woods *Caesalpinia* L. spp. and *Haematoxylum* L. spp., respectively. The structures of these compounds are very similar, with hematoxylin having an extra OH group in the A ring. In their oxidised forms brazilein **3** and hematein **4**, have been used for centuries as dyestuffs (Ferreira et al., 2004) and more recently as a nuclear stain for animal tissues (Bettinger and Zimmermann, 1991). The NMR spectra of brazilin have been previously reported in this journal (Kim et al., 1997) but there is little information on their mass spectra in the literature except for an isolated report of fragmentation under electron impact conditions (Bettinger and Zimmermann, 1991). However, with the advent of liquid chromatography–mass spectrometry (LC–MS), an understanding of the behaviour of neoflavonoids under electrospray conditions has become increasingly important (Cuyckens and Claeys, 2004). Accordingly, we report here an extension to neoflavonoids of our earlier work on the mass spectra of flavonoids under negative ion electrospray conditions (Ferreira et al., 1999, 2001).

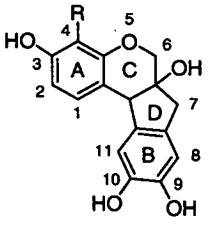

1, R = H, brazilin
2, R = OH, hematoxylin

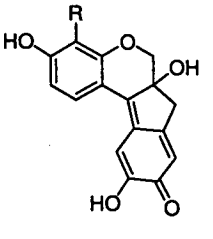

3, R = H, brazilein
4, R = OH, hematein

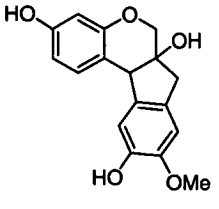

5

* Corresponding authors. Tel: +44 131 650 4711 (A.N. Hulme), +44 131 650 4718 (H. McNab), +44 131 247 4376 (A. Quye); fax: +44 131 650 4743 (A.N. Hulme), +44 131 650 4743 (H. McNab), +44 131 247 4306 (A. Quye).
E-mail addresses: Alison.Hulme@ed.ac.uk (A.N. Hulme), H.McNab@ed.ac.uk (H. McNab), a.quye@nms.ac.uk (A. Quye).

0031-9422/$ - see front matter © 2005 Elsevier Ltd. All rights reserved.
doi:10.1016/j.phytochem.2005.09.001

In undertaking this investigation, we hoped to identify collision induced decomposition (CID) conditions which would reveal partial structural information on neoflavonoid ring systems, in either their reduced or their oxidised forms. In this way it may be possible to obtain structural information on new neoflavonoid analogues from a few micrograms of material. Such compounds are known natural products; for example, Namikoshi et al. (1987) have isolated 9-*O*-methylbrazilin **5** from Sappan Lignum, the dried heartwood of *Caesalpinia sappan* L.

2. Results and discussion

Freshly prepared methanolic solutions of the neoflavonoids **1–4** gave good mass spectra under negative ion electrospray conditions. Ions due to deprotonated molecules at *m/z* $[M-H]^-$ were obtained in all cases; peaks corresponding to dimers and trimers of hematoxylin **2** ($[2M-H]^-$ and $[3M-H]^-$) were sometimes observed. Samples of the reduced forms (**1** and **2**) also showed the presence of the deprotonated molecules of the corresponding oxidised species (**3** and **4**), respectively. It was confirmed by CID of the $[M-H]^-$ ions of **1** and **2** that $[M-3H]^-$ peaks are not obtained and therefore the oxidised species are indeed present in the starting material and not formed in the mass spectrometer.

To provide further evidence of the nature of the breakdown pathways, spectra were also recorded using deuteriated methanol (MeOD) as solvent. Under these conditions, ion clusters were observed corresponding to deprotonated molecules with sequential replacement by deuterium of the hydrogen atom in each of the OH groups (with the exception of the ionised OH). In each case, the ion corresponding to the most fully deuteriated species was chosen for CID experiments (see below).

CID mass spectra of the reduced forms brazilin **1** and hematoxylin **2** show only 2 breakdown peaks (ca. >10% intensity) (Table 1). The first of these is a minor peak due to loss of H_2O; when MeOD was used as solvent, loss of HOD as well as H_2O was observed, indicating that at least one of the hydrogen atoms lost does not originate at the phenol group. It is therefore not possible to identify the position of this cleavage with any certainty; this is also commonly found in H_2O loss from the phenol groups of flavonoids (Ferreira et al., 2001).

The major peak in the spectra of both **1** and **2** is due to loss of a neutral fragment of 122 Da from the $[M-H]^-$ ion. This neutral fragment must originate from the C/D/B ring sections which are the same in both precursors. These results are best explained if the A-ring is the initial ionisation site, giving the deprotonated species **6** and **7**. Thereafter, the fragmentation can be rationalised as depicted in Scheme 1. This mechanism is supported by CID of the fully deuteriated species, which show that the major observed ion in both deuteriated samples corresponds to the A/C ring fragment with the available hydroxyl group(s) retaining their deuterium atoms.

We conclude that the CID mass spectra of the reduced forms **1** and **2** of neoflavonoids provide direct information on the substituents of rings A and C; the mass of the neutral fragment lost gives supporting information on the substituents of ring B and those of the methylene group of ring D.

CID mass spectra of the oxidised forms brazilein **3** and hematein **4** show many breakdown peaks (>10% intensity) which can act as useful fingerprints for these compounds (Fig. 1 and Table 2). It is likely that that the 10-hydroxyl group of the B-ring is the initial ionisation site (Lalor and Martin, 1959) to provide the deprotonated oxidised neoflavonoid species **10** and **11**, respectively. In both cases, the highest mass fragment, though of low intensity, is due to loss of *m/z* 15 (CH_3). When the spectrum was recorded in MeOD, it is clear that these fragments correspond to loss of CH_2D; presumably the carbon atom derives from that at C(6) or C(7), together with the deuterium from the 6a-OH group. The most intense breakdown peaks were found to be due to loss of H_2O; in the deuteriated case, the major peak was due to loss of HOD, but some loss of H_2O was also observed. Some loss of CO (*m/z* 28) is also found in both cases. These are common breakdown peaks in negative ion ESI mass spectra of flavonoids (Ferreira et al., 2001; Ferriera, 2002). More unusually, a significant peak is also observed in the spectra of both **3** and **4** due to loss of a fragment of 43 Da (probably CH_3CO). In the case of **3** the deuteriated species shows peaks due to loss of both *m/z* 43 (i.e., the fragment contains no deuterium) and 44 (i.e., the fragment contains one deuterium). In the case of **4**, the situation is complicated by the presence of other peaks (*e.g.* *m/z* 255, due to loss of CO_2) so that further analysis is not possible.

Table 1
Negative ion ESI mass spectra of brazilin and hematoxylin (reduced forms) under CID conditions

Brazilin (MeOH) *m/z* (%)	Brazilin (MeOD) *m/z* (%)	Hematoxylin (MeOH) *m/z* (%)	Hematoxylin (MeOD) *m/z* (%)	Fragment lost
285 (64%) $[M-H]^-$	288 (8%) $[M_D-D]^-$	301 (100%) $[M-H]^-$	305 (14%) $[M_D-D]^-$	
267 (8%) $[M-H-18]^-$	270 (10%) $[M_D-D-18]^-$	283 (19%) $[M-H-18]^-$	287 (8%) $[M_D-D-18]^-$	H_2O
	269 (11%) $[M_D-D-19]^-$		286 (16%) $[M_D-D-19]^-$	HOD
163 (100%) $[M-H-122]^-$	164 (100%) $[M_D-D-124]^-$	179 (100%) $[M-H-122]^-$	181 (100%) $[M_D-D-124]^-$	See Scheme 1
	165 (40%) $[M_D-D-123]^-$		182 (21%) $[M_D-D-123]^-$	
	163 (16%) $[M_D-D-125]^-$		180 (49%) $[M_D-D-125]^-$	

M_D corresponds to the molecular mass in which all exchangeable protons are replaced by deuterium (i.e., M + 4 in the case of brazilin; M + 5 in the case of hematoxylin).

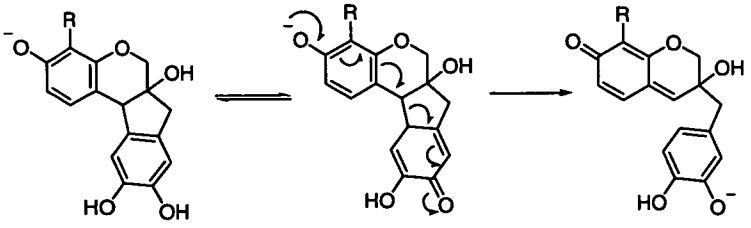

6, R = H, brazilin $[M-H]^-$
7, R = OH, hematoxylin $[M-H]^-$

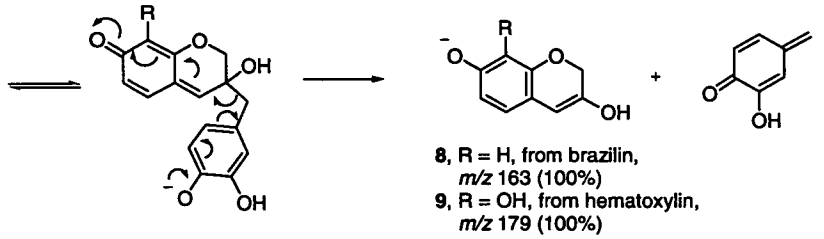

8, R = H, from brazilin, *m/z* 163 (100%)
9, R = OH, from hematoxylin, *m/z* 179 (100%)

Scheme 1.

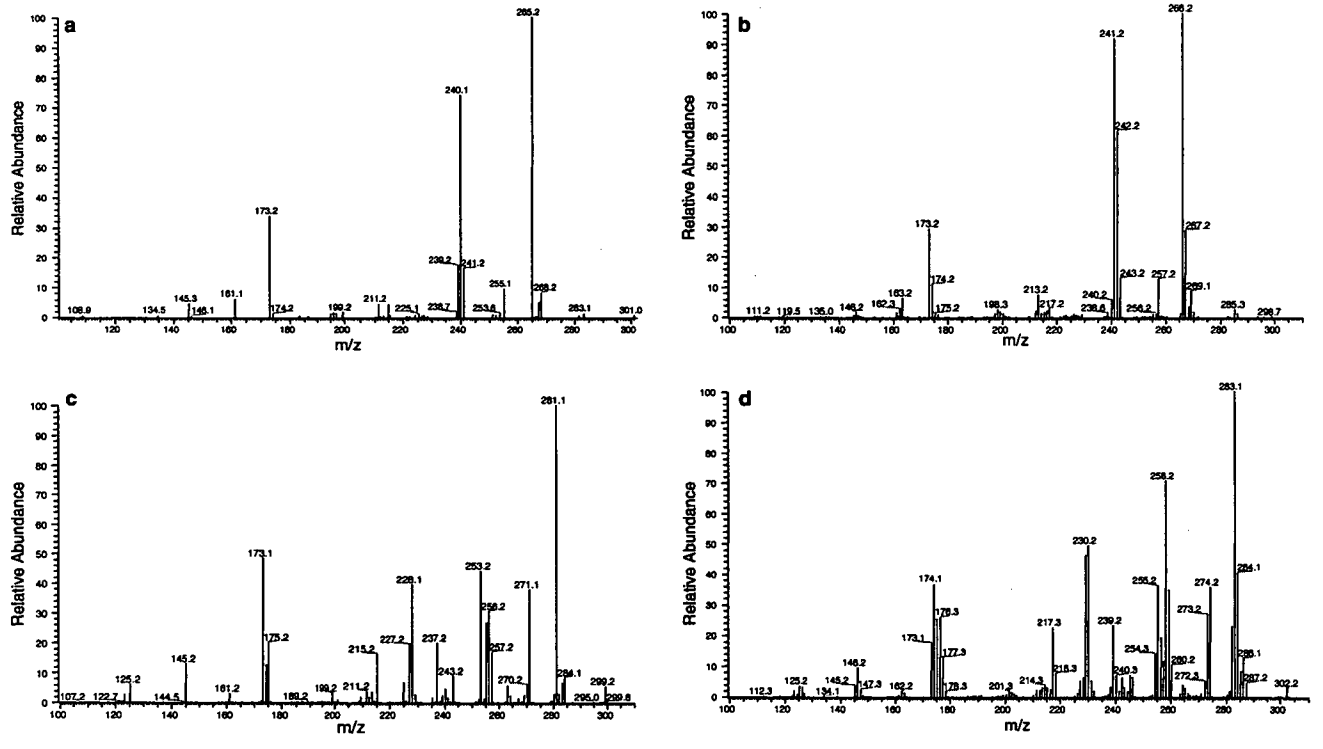

Fig. 1. (a) CID mass spectrum (MS^2) of brazilein **3** (*m/z* 283) in MeOH. (b) CID mass spectrum (MS^2) of deuteriated brazilein **3** (*m/z* 285) in MeOD. (c) CID mass spectrum (MS^2) of hematein **4** (*m/z* 299) in MeOH. (d) CID mass spectrum (MS^2) of deuteriated hematein **4** (*m/z* 302) in MeOD.

In the range *m/z* 180–240, the CID spectrum of hematein **4** is much more complex than that of brazilein (Fig. 1) presumably due to the juxtaposition of hydroxyl groups in ring A. Thus, peaks at *m/z* 253 $[M - H - H_2O - CO]^-$, 237 $[M - H - H_2O - CO_2]^-$, 228 $[M - H - C_3H_3O_2]^-$, 227 $[M - H - C_3H_4O_2]^-$ are only found in the spectrum of **4**.

The major low-mass fragment ion is found at *m/z* 173 in **3** and **4**. Since the same fragment is produced from both precursors, it is clear that, in contrast to the spectra of the reduced forms, the observed fragment cannot be derived from ring A. A suggested mechanism is shown in Scheme 2. Again, the mechanism is supported by the results of the MeOD deuterium labelling experiments, which,

Table 2
Negative ion ESI mass spectra of brazilein and hematein (oxidised forms) under CID conditions

Brazilein (MeOH) *m/z* (%)	Brazilein (MeOD) *m/z* (%)	Hematein (MeOH) *m/z* (%)	Hematein (MeOD) *m/z* (%)	Fragment lost
283 (77%) $[M - H]^-$	285 (100%) $[M_D - D]^-$	299 (100%) $[M - H]^-$	302 (100%) $[M_D - D]^-$	
268 (8%) $[M - H - 15]^-$	269 (8%) $[M_D - D - 16]^-$	284 (8%) $[M - H - 15]^-$	286 (12%) $[M_D - D - 16]^-$	CH_3/CH_2D
265 (100%) $[M - H - 18]^-$	267 (29%) $[M_D - D - 18]^-$	281 (100%) $[M - H - 18]^-$	284 (38%) $[M_D - D - 18]^-$	H_2O
	266 (100%) $[M_D - D - 19]^-$		283 (100%) $[M_D - D - 19]^-$	HOD
			282 (23%) $[M_D - D - 20]^-$	D_2O
255 (9%) $[M - H - 28]^-$	257 (13%) $[M_D - D - 28]^-$	271 (38%) $[M - H - 28]^-$	274 (36%) $[M_D - D - 28]^-$	CO
241 (17%) $[M - H - 42]^-$	243 (13%) $[M_D - D - 42]^-$	257 (16%) $[M - H - 42]^-$	260 (10%) $[M_D - D - 42]^-$	CH_2CO
240 (74%) $[M - H - 43]^-$	242 (62%) $[M_D - D - 43]^-$	256 (30%) $[M - H - 43]^-$	259 (35%) $[M_D - D - 43]^-$	CH_3CO
	241 (92%) $[M_D - D - 44]^-$		258 (71%) $[M_D - D - 44]^-$	CH_2DCO
239 (18%) $[M - H - 44]^-$		255 (26%) $[M - H - 44]^-$		CO_2
173 (34%) $[M - H - 110]^-$	173 (29%) $[M_D - D - 112]^-$	173 (48%) $[M - H - 126]^-$	173 (17%) $[M_D - D - 129]^-$	See Scheme 2
	174 (11%) $[M_D - D - 111]^-$			

M_D corresponds to the molecular mass in which all exchangeable protons are replaced by deuterium (i.e., M + 3 in the case of brazilein; M + 4 in the case of hematein).

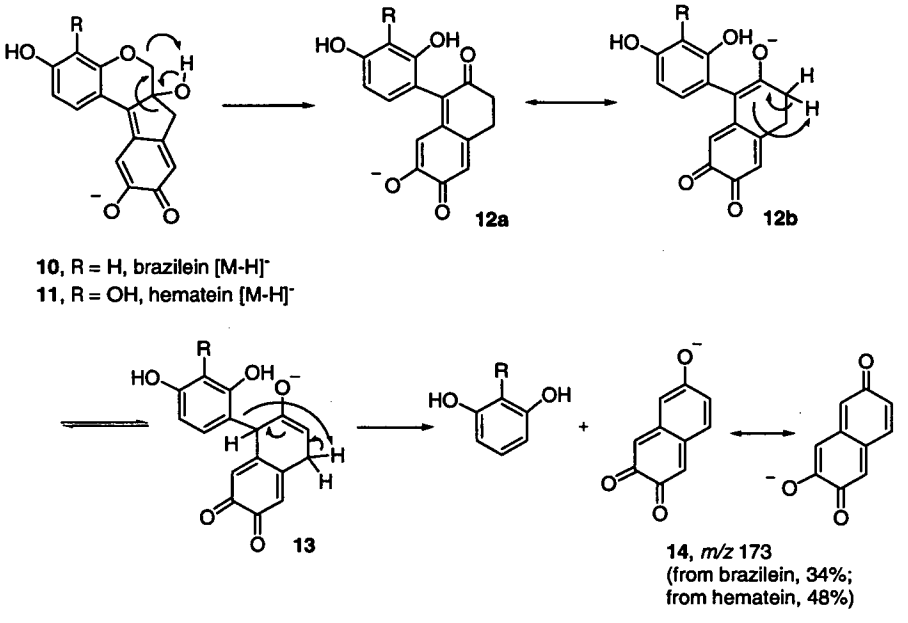

Scheme 2.

in the case of brazilein **3** show relatively little evidence of deuterium incorporation in the fragment ion. The scrambling which occurs (and which is more prevalent in the spectrum of the hematein **4**) may be explained by equilibration of hydroxyl groups and the anion centre in the intermediates **12** and **13**.

In conclusion, the CID mass spectra of the oxidised forms **3** and **4** of neoflavonoids provide information on the substituents of rings B, D and the methylene group of ring C; the mass of the neutral fragment lost gives information on the substituent pattern of ring A.

3. Experimental

Hematoxylin **2** was obtained from Fluka Chemika and hematein **4** from Acros, while brazilin **1** was purchased from Pfaltz and Bauer. The oxidised form brazilein **3** was present in the sample adventitiously.

Mass spectra were recorded on a Finnigan LCQ mass spectrometer operating in negative ion electrospray mode. Samples were directly injected into the source in solution in methanol or deuteriated methanol (MeOD) as appropriate. Peaks were selected for CID with a band-width of 1.0 Da and operating parameters were optimized by tuning the detector to the $[M - H]^-$ ion peak. Data were collected and processed by LCQ Navigator software.

Acknowledgements

This work was funded by the EC, contract number EVK4-CT-2001-00048. We are most grateful to Mr. A.T. Taylor for expert technical assistance.

References

Bettinger, C., Zimmermann, H.W., 1991. New investigations on hematoxylin, hematein and hematein–aluminium complexes. Histochemistry 95, 279–288.

Cuyckens, F., Claeys, M., 2004. Mass spectrometry in the structural analysis of flavonoids. J. Mass Spectrom. 39, 1–15.

Ferreira, E.S.B., Quye, A., McNab, H., Hulme, A.N., Wouters, J., Boon, J.J., 1999. The analytical characterisation of flavonoid photodegradation products: a novel approach to identifying natural yellow dyes in ancient textiles. In: Bridgeland, J. (Ed.), Preprints of the 12th triennial meeting of the ICOM committee for conservation, vol. 1. James and James (science) publishers, London, pp. 221–227.

Ferreira, E.S.B., Quye, A., McNab, H., Hulme, A.N., Wouters, J., Boon, J.J., 2001. Development of analytical techniques for the study of natural yellow dyes in historic textiles. Dyes Hist. Archaeol. 16/17, 179–186.

Ferriera, E.S.B., 2002. PhD Thesis, The University of Edinburgh.

Ferreira, E.S.B., Hulme, A.N., McNab, H., Quye, A., 2004. The natural constituents of historical textile dyes. Chem. Soc. Rev. 33, 329–336.

Kim, D.S., Baek, N.-I., Oh, S.R., Jung, K.Y., Lee, I.S., Lee, H.-K., 1997. NMR assignment of Brazilein. Phytochemistry 46, 177–178.

Lalor, G.C., Martin, S.L., 1959. Studies on haematoxylin and haematein, the colouring principles of logwood II – Behaviour in aqueous solutions at varying pH, and the pK values. J. Soc. Dyers Colour. 75, 517–521.

Namikoshi, M., Nakata, H., Yamada, H., Nagai, M., Saitoh, T., 1987. Homoisoflavonoids and related compounds II. Isolation and absolute configuration of 3,4-dihydroxylated homoisoflavans and brazilins from *Caesalpina sappan* L. Chem. Pharm. Bull. 35, 2761–2773.

Abstract

The standard sample preparation for the extraction of dye components on historical textiles usually involves a hydrolysis procedure with hydrochloric acid. However, photodiode array high-performance liquid chromatography traces obtained from textile samples dyed with logwood or redwood appear to show 'marker compounds' for the neoflavonoid components. These markers are chromatographically and spectroscopically different from the dye components themselves. Multidimensional nuclear magnetic resonance techniques were used to provide the unambiguous structural characterization of the 'marker compound' obtained when hematein was subjected to the standard hydrochloric acid extraction procedure, thus characterizing the compound found in the extract of an historical textile sample dyed with logwood.

Keywords

redwood, logwood, nuclear magnetic resonance, historical textiles, dye extracts

Analytical characterization of the main component found in logwood-dyed textile samples after extraction with hydrochloric acid

Alison N Hulme and Hamish McNab
School of Chemistry
University of Edinburgh
West Mains Road
Edinburgh
EH9 3JJ
United Kingdom

David A Peggie and Anita Quye*
National Museums of Scotland
Chambers Street
Edinburgh
EH1 1JF
United Kingdom

Ina Vanden Berghe and Jan Wouters
Royal Institute for Cultural Heritage (KIK/IRKPA)
Jubelpark 1
B-1000 Brussels
Belgium

*Author to whom correspondence should be addressed

Introduction

As part of the Monitoring of Damage in Historic Tapestries (MODHT) project[1], a study of two soluble redwood dyes, hematein and brazilein, has been initiated. Botanical sources containing these neoflavonoid molecules have been used in early European dye recipes for the dyeing of textile fibres (Brunello 1973). However, these dye molecules have been studied much less than the ubiquitous red anthraquinone plant and insect dyes. The analysis of the redwood and logwood dyes is problematic due to both the complex solution chemistry of the neoflavonoids (Arshid et al. 1954, Lalor and Martin 1959, Bettinger and Zimmermann 1991) and difficulties in the characterization of the biological species used to obtain these dyes (Nowik 2001).

Previous work in our laboratories has shown that photodiode array high performance liquid chromatography (PDA-HPLC) is a convenient method to identify many historical dyes. In the case of flavonoid yellow dyes, this technique has been augmented by the use of liquid chromatography–mass spectrometry (LC–MS), particularly using electrospray ionization (ESI), for the identification of unknown minor dye constituents and photo-degradation products (Ferreira et al. 2001). In addition, the use of MS^n experiments, obtained through the use of a quadrupole ion trap, provides structural information not available in other ways. In an initial study, the electrospray ionization mass spectra of pure samples of the neoflavonoids of interest have been obtained in both their reduced and oxidized forms. Fragmentation studies with ESI MS^n experiments have been employed to elucidate characteristic breakdown pathways (Hulme et al. 2005).

The standard sample preparation for the extraction of dye components on historical textiles is a hydrochloric acid hydrolysis procedure (Wouters and Verhecken 1989). However, any acid-sensitive dye molecules present may decompose under these conditions. In practice, the PDA HPLC traces obtained from textile samples dyed with redwood or logwood extracts appear to show 'marker compounds' for the neoflavonoid components. These markers are chromatographically and spectroscopically different from the main dyeing constituents.

For brazilwood, an alternative method of hydrolysis can also be used (Hofenk de Graaff 2004). The sample is hydrolysed using the standard method above, but with acetic acid replacing the hydrochloric acid. When the textile is hydrolysed in this way, the main colouring component, brazilein, can be detected, although recovery of the dye is low (Hofenk de Graaff 2004).

This paper provides a structural characterization of the 'marker compound' obtained from hematein when using the standard hydrochloric acid extraction method, thus characterizing the component found in the extracts of historical textile samples dyed with logwood.

Experimental

The National Museums of Scotland chromatographic method for the analysis of flavonoids used the following conditions. The column used was a Phenomenex Sphericlone ODS2 5 μm particle size (150 mm × 4.6 mm), reverse phase, with guard column. The total run time was 35 min at a flow rate of 1.2 mL/min and at a temperature of 25 °C. The volume injected was 20 μL. A tertiary solvent system was used (A = 20 per cent by volume MeOH(aq), B = MeOH, C = 5 per cent by volume ortho-phosphoric acid(aq)) and the gradient programme was isocratic for 3 min (67A : 23B : 10C) then a linear gradient from 3 min to 29 min (0A : 90B : 10C) before initial conditions recovery over 1 min and equilibration over 5 min.

For the preparation of the hematein elimination product, hematein (82 mg) was added to 100 mL HCl:MeOH:H_2O (2:1:1) hot solvent and allowed to reflux for 10 min before rapid cooling. After evaporating to dryness, the recovered solid, 3,4,10-trihydroxy-7*H*-indeno[2,1-*c*]chromen-9-one, could be dissolved in a methanol/DMSO mix. The ^{1}H NMR spectra were acquired on a Bruker ARX 250 MHz instrument, while all 2D work was performed on a Bruker DPX 360 MHz instrument (δ_H and δ_C data are shown in Table 1). The mass spectrum (FAB, NOBA conditions) showed a molecular ion $[M+H]^+$ at 283 (Found: $[M+H]^+$ 283.0600. $C_{16}H_{11}O_5$ requires 283.0607).

Table 1. ^{1}H and ^{13}C NMR chemical shifts (δ/ppm) and coupling constants (J/Hz) for the hematein elimination product in a DMSO/MeOH mix, performed on a Bruker ARX 250 MHz spectrometer

H/C – assignment	^{1}H Chemical shift (δ/ppm)	Coupling constant (J/Hz)	^{13}C Chemical shift (δ/ppm)
6	8.97	s	151.9
I	8.18	d, 9.2	117.0
II	7.88	s	111.4
2	7.40	d, 9.2	118.1
8	7.16	s	110.5
7	4.04	s	31.6

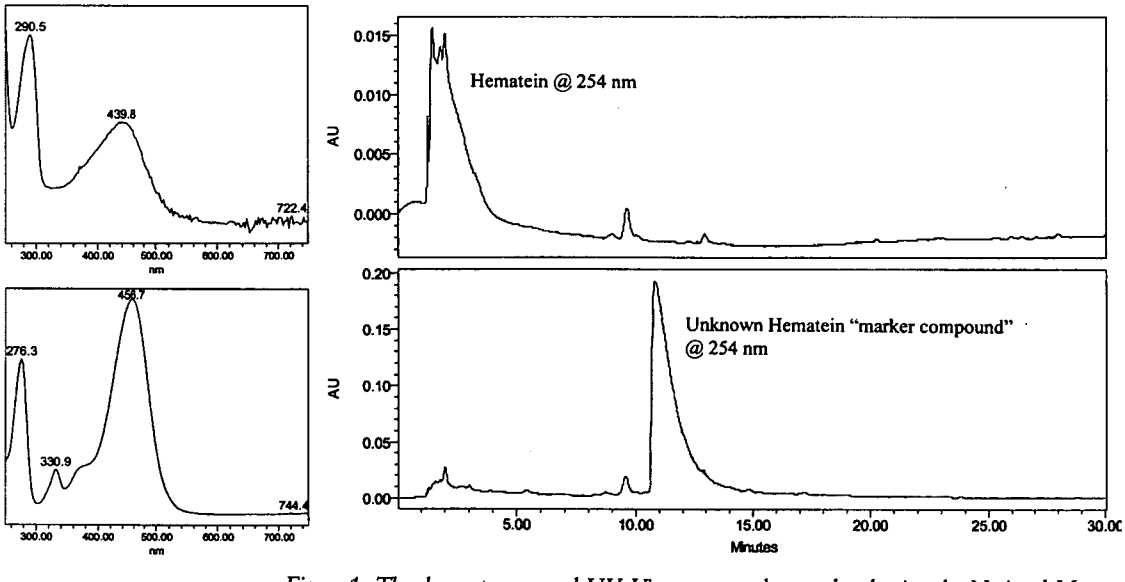

Figure 1. The chromatogram and UV-Vis spectrum when analysed using the National Museums of Scotland PDA HPLC method for flavonoid analysis (a) hematein and (b) hematein after treatment using the standard hydrochloric acid hydrolysis extraction procedure.

Results and Discussion

Hematein

When dissolved in MeOH:H_2O (1:1) and analysed using the National Museums of Scotland PDA HPLC method for flavonoid analysis (see Experimental section), hematein eluted between approximately 1 and 4 min and had an ultraviolet-visible (UV-Vis) spectrum as shown in Figure 1a. However, when hematein was treated using the standard hydrochloric acid hydrolysis extraction procedure, a new compound was observed, eluting at approximately 11 min and with a UV-Vis spectrum as shown in Figure 1b.

In an effort to elucidate the structure of this unknown compound, a series of NMR spectroscopic experiments was carried out. Firstly, a proton NMR spectrum of hematein was obtained for reference (Figure 2a) which agreed with previously published data (Bassoli et al. 1996). The standard acid hydrolysis procedure was then performed on a preparative scale to allow the recovery and analysis of the unknown product, obtained as a 'brick red' powder. For NMR spectroscopy, the solubility of the unknown compound in DMSO was poor. However, this was improved with the addition of a small amount of methanol.

The ^{1}H NMR spectrum of the unknown compound (Figure 2b) clearly shows a new two-proton singlet at 4.04 parts per million (ppm) and a further one-proton singlet at 8.97 ppm. The two pairs of doublets due to the H-6 and H-7 protons (the latter almost degenerate) in the hematein spectrum were no longer observed. All chemical shifts and coupling constants are shown in Table 1. The absence of the pair of doublets due to the CH_2 group at the 6-position suggests an elimination reaction involving the tertiary alcohol (6a) to produce either the $\Delta^{6,6a}$ or $\Delta^{6a,7}$ isomer (Figure 3). The structure was confirmed as the $\Delta^{6,6a}$ isomer by the use of 2D NMR techniques as described below.

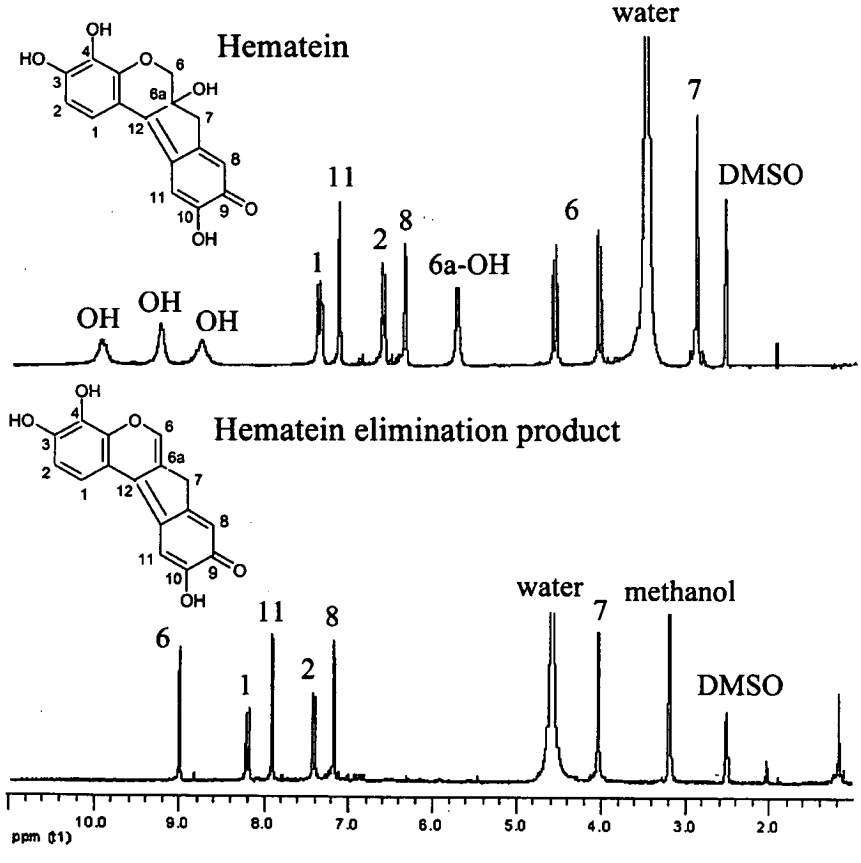

Figure 2. The ^{1}H NMR spectra of (a) hematein in DMSO and (b) the hematein elimination product in DMSO/MeOH.

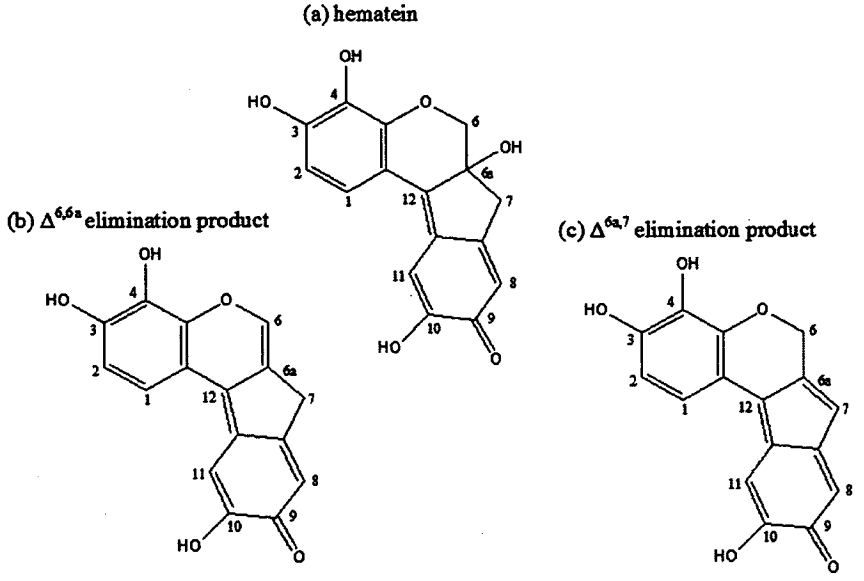

Figure 3. The structures of (a) hematein, and the two possible elimination products (b) $\Delta^{6,6a}$ isomer and (c) $\Delta^{6a,7}$ isomer

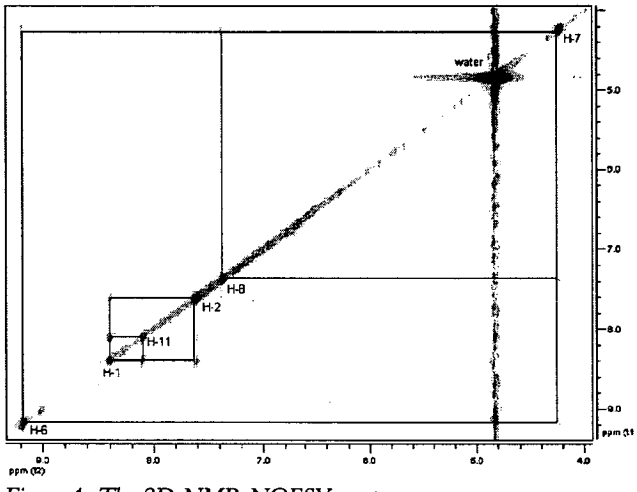

Figure 4. The 2D NMR NOESY spectrum

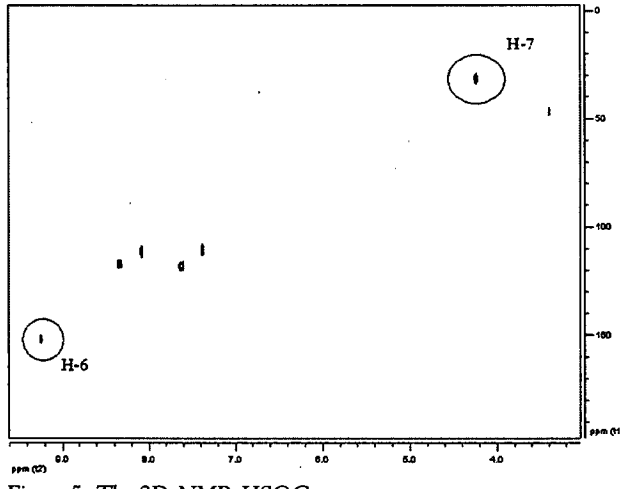

Figure 5. The 2D NMR HSQC spectrum

The first of these techniques, nuclear Overhauser effect spectroscopy (NOESY), correlates protons which are close to one another in space. In the $\Delta^{6,6a}$ isomer, the CH_2 signal originating from the H-7 protons should correlate both with the signal due to H-6 and that due to H-8. In contrast, the CH_2 group in the alternative $\Delta^{6a,7}$ isomer would show only one correlation, with the signal from the H-7 proton. The 2D NOESY spectrum shown in Figure 4 clearly indicates that the CH_2 singlet at 4.04 ppm correlates both to the signal at 7.16 ppm (H-8) and to the new singlet at 8.97 ppm (H-6) providing strong evidence for the formation of the $\Delta^{6,6a}$ isomer. This technique also allows the signal from H-1 and H-2 to be distinguished, since only H-1 is in close spatial proximity to H-11. Interpretation of the unknown as the $\Delta^{6,6a}$ isomer was also supported by a correlation spectroscopy (COSY) experiment, which correlates protons which are typically separated by up to 4 bonds within the molecule. Again, the signal from H-7 correlates with both H-6 and H-8.

The second technique, a heteronuclear single quantum coherence (HSQC) spectrum, correlates proton signals with the resonances due to the carbon atoms to which they are attached (Figure 5 and Table 1). Figure 5 shows the CH_2 signal at 4.04 ppm (assigned to H-7) correlates with a carbon whose chemical shift is 31.6 ppm, consistent with the shift expected for a benzylic CH_2 remote from a heteroatom. This further supports the formation of the $\Delta^{6,6a}$ isomer over the $\Delta^{6a,7}$

isomer. In addition, the singlet at 8.97 ppm correlates with a carbon chemical shift of just over 151.9 ppm, suggesting that it is next to a heteroatom (in this case, oxygen). The quality of the proton spectra obtained at the beginning and end of the experiments (about 18 h) indicated that the elimination product of hematein is unstable in solution for a prolonged length of time.

The observation of this peak in the chromatogram of a sample prepared using the standard hydrochloric acid hydrolysis procedure can now be directly related to the presence of hematein, the main neoflavonoid dyeing constituent of logwood.

Logwood in historical samples

Figure 6. A black wool sample taken from the reverse of Christ before Pilate (Brussels, ca. 1520), as part of the Monitoring of Damage in Historic Tapestries (MODHT) project.

Samples of threads taken from the sampling campaigns of historical tapestries initiated as part of the MODHT project were used to provide an historical perspective.

The characteristic 'marker compound' for hematein was observed in an historical fibre, taken from the reverse side of *Christ before Pilate*, woven in Brussels around 1520 (Figure 6). Dye analysis of this black wool fibre using PDA-HPLC found chromatographic peaks for the hematein elimination product, ellagic acid, quercetin and maclurin (Figure 7) suggesting that it was dyed with a combination of logwood, tannin and old fustic dye sources. Due to the date of manufacture of this tapestry, the presence of the peak characteristic for hematein suggests that this particular sample is an early restoration thread (Cardon 2003).

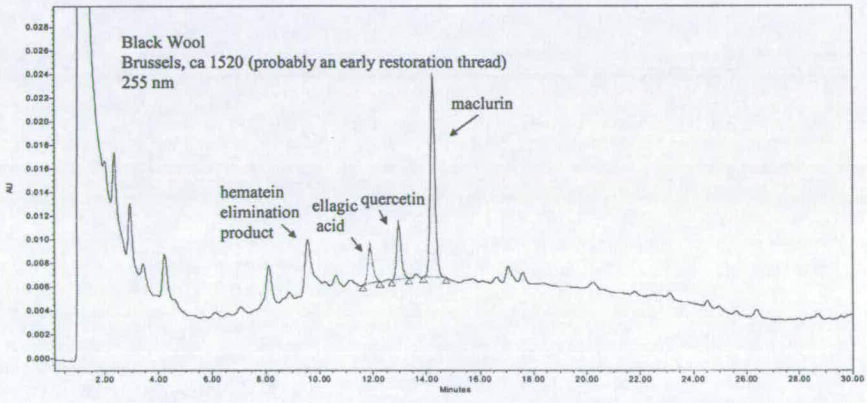

Figure 7. The HPLC chromatogram (at 255 nm) of the acid hydrolysed extract of the historical sample, showing the hematein elimination product, ellagic acid, quercetin and Maclurin

Conclusion

The 'marker compound' observed for hematein is a hitherto unreported species, structurally related to hematein, 3,4,10-trihydroxy-7*H*-indeno[2,1-*c*]chromen-9-one. Multidimensional nuclear magnetic resonance (NMR) spectroscopic studies have been used for unambiguous characterization. Further studies are underway to demonstrate if the analogous compound is formed when brazilein undergoes the hydrochloric acid extraction procedure. As the soluble redwood dyes are notoriously prone to fading, accelerated light ageing studies of wool and silk samples dyed with redwoods is also currently being investigated. These studies should provide a semi-quantitative picture of the rate of photodegradation, and allow the identification of any stable breakdown products.

Acknowledgements

We thank Stuart Wharton for his invaluable help in the acquiring and processing of the NMR data, Alan Taylor for the mass spectrometric analysis and the EC (Contract No. EV4K-CT-2001-00048) for funding.

Notes

1 MODHT is supported by the European Commission under the Fifth Framework Programme and contributing to the implementation of Key Action 4: 'The City of Tomorrow and Cultural Heritage', subsection 4.2.1 'Improved damage assessment of cultural heritage,' within the Energy, Environment and Sustainable Development. Contract No. EV4K-CT-2001-00048. The project website can be found at http://www.hrp.org.uk/webcode/content.asp?ID=706.

References

Arshid, F M, Desai, J N, Duff, D J, Giles, C H, Jain, S K and MacNeal, I R, 1954, 'A study of certain natural dyes-I', *Journal of the Society of Dyers and Colourists* 70, 392–401.

Bassoli, A, Borgonovo, G, Merlini, L and Scaglioni, L, 1996, 'On the structure of haematein', *Gazzetta Chimica Italiana* 126, 761–763.

Bettinger, Ch and Zimmermann, H W, 1991, 'New investigations on hematoxylin, hematein, and hematein–aluminium complexes', *Histochemistry* 95, 279–288.

Brunello, F, 1973, *The Art of Dyeing in the History of Mankind, first American edition*, Vicenza, 130–131.

Cardon, D, 2003, *Le monde des teintures naturelles*, Editions Belin, 209–216.

Ferreira, E S B, Quye, A, McNab, H, Hulme, A N, Wouters, J and Boon, J J, 2001, 'Development of analytical techniques for the study of natural yellow dyes in historic textiles', *Dyes in History and Archaeology* 16/17, 179–186.

Hofenk de Graaff, J H, 2004, *The Colourful Past, first edition*, Abegg-Stiftung and Archetype Publications, 147–149.

Hulme, A N, McNab, H, Peggie, D A and Quye, A, 2005, 'Negative ion electrospray mass spectrometry of neoflavonoids', *Phytochemistry*.

Lalor, G C and Martin, S L, 1959, 'Studies on haematoxylin and haematein, the colouring principles of logwood', *Journal of the Society of Dyers and Colourists* 75, 513–517.

Nowik, W, 2001, 'The possibility of differentiation and identification of red and blue 'soluble' dyewoods', *Dyes in History and Archaeology* 16/17, 129–144.

Wouters, J and Verhecken, A, 1989, 'The coccid insect dyes: HPLC and computerized diode array analysis of dyed yarns', *Studies in Conservation* 34, 189–200.

The application of liquid chromatography–mass spectrometry and accelerated light ageing for the analytical identification of yellow flavonoid dyes in historical tapestries

Alison N. Hulme, Hamish McNab, David A. Peggie and Anita Quye

ABSTRACT The chemical characterisation and identification of natural dyes using high-performance liquid chromatography coupled to a photodiode array detector (HPLC–PDA) and liquid chromatography–mass spectrometry (LC–MS) techniques are explored. The techniques have allowed the dye sources to be identified from many yellow and green historical fibres sampled from a collection of well-provenanced European tapestries as part of the Monitoring of Damage to Historic Tapestries (MODHT) project. These results are beginning to provide information regarding dyeing practices in different weaving centres at different times. The results from current accelerated ageing experiments to compare weld and sawwort are also reported.

Keywords: flavonoids, HPLC, mass spectrometry, accelerated ageing, weld, sawwort, dyer's greenweed

Introduction

High-performance liquid chromatography with photodiode array detection (HPLC–PDA) is now an established routine method for the analytical identification of natural dyes in historical textiles (Wouters 1989; Koren 2001). Interpretation of the results to identify the biological origin of the dye, for example, the plant species, relies on matching data for major and minor organic compounds in the sample with data from known chemical references and authentic botanical sources (Ferreira *et al.* 2004). The application of liquid chromatography–mass spectrometry (LC–MS) techniques to complement HPLC–PDA extends existing boundaries for the chemical characterisation and identification of natural dyes (Ferreira *et al.* 2003b; Szostek *et al.* 2003). The combined techniques have been applied successfully to the characterisation of yellow flavonoid dyes and their altered molecular composition caused by light-ageing effects (Ferreira *et al.* 2003a). This analytical approach is now being applied in the EC-funded project, Monitoring of Damage to Historic Tapestries (MODHT) to identify the dye sources in the tapestries under study and to relate the damage to the dyes with the overall damage to the objects.[1]

The MODHT project aims to create a scientific 'damage assessment' method for historical tapestries using physical and chemical markers at the macro- and micro-scale (Quye in press). A range of analytical techniques is being developed and applied to measure the chemical and physical properties of 17 well-provenanced tapestries from northern and southern European collections, about which the storage, display and conservation histories are known. Model tapestries replicated using authentic materials and methods, then subjected to accelerated ageing under controlled conditions, are also being analyzed to study relationships between the materials used to make tapestries, and the chemical changes to the dyes, wool, silk and metal threads and physical changes such as tensile strength caused by ageing. This novel approach to damage assessment will provide an objective evaluation method for conservators and curators when making decisions about the display, handling and conservation of tapestries, and indeed other historical textiles. This paper is concerned solely with the analytical study of flavonoid dyes for MODHT.

The basic technique of dye analysis using HPLC, although destructive, requires only a small amount of thread (approximately 1 mg or 5 mm in length). The fibres are broken down with acidified solvents, releasing the dyestuff into solution (Wouters 1989). Although this process has been optimised to leave many natural dye compounds largely unaltered molecularly, it must be appreciated that chemical changes have the potential to occur and may make the analysis of certain dyestuffs using this method problematic (Ferreira 2001).

Most natural dyestuffs contain several major and minor organic chemical compounds which attach to the fibre during dyeing, either directly or via a mordant, to impart the colour. For a large number of natural yellow dyes, the colouring components are flavonols and flavones which belong to the class of molecules known as the flavonoids (some of the most important flavonoids present in natural European dye sources are shown in Fig. 1). Although flavonoid molecules can be found in many plants, certain components are more

common than others due to both a high naturally occurring frequency and a molecular arrangement conferring an excellent ability to adhere to the fibre (or mordant). In many cases, different natural dye sources contain different flavonoids with differing relative concentrations. This can be the first clue in the identification of the botanical source used to dye an historical fibre.

The HPLC–PDA method allows dye components present in the solution to be separated and, in many cases, identified by comparing their retention times (HPLC) and response to light over a range of wavelengths (PDA). The elution programme used in the present study is a modification of previously reported methodology (Ferreira *et al.* 2003b) in an effort to maximise the flavonoid information (Table 1). Interpreting the results to identify the source of the dye relies not only on a good reference library of known chemical materials to match against both the major and minor organic compounds found in the sample, but also extensive knowledge regarding the chemical components (and sometimes their relative ratios) found on fibres dyed using authentic botanical sources. Figure 2 shows the chromatograms obtained from the acid-hydrolysed extracts of reference dyeings of weld (*Reseda luteola* L.), sawwort (*Serratula tinctoria* L.) and dyer's greenweed (*Genista tinctoria* L.). The flavonoids luteolin and apigenin are present in all three dyes, but they can be distinguished by other components: luteolin methyl ether in weld; quercetin and kaempferol in sawwort; and genistein in dyer's greenweed. In favourable cases, the

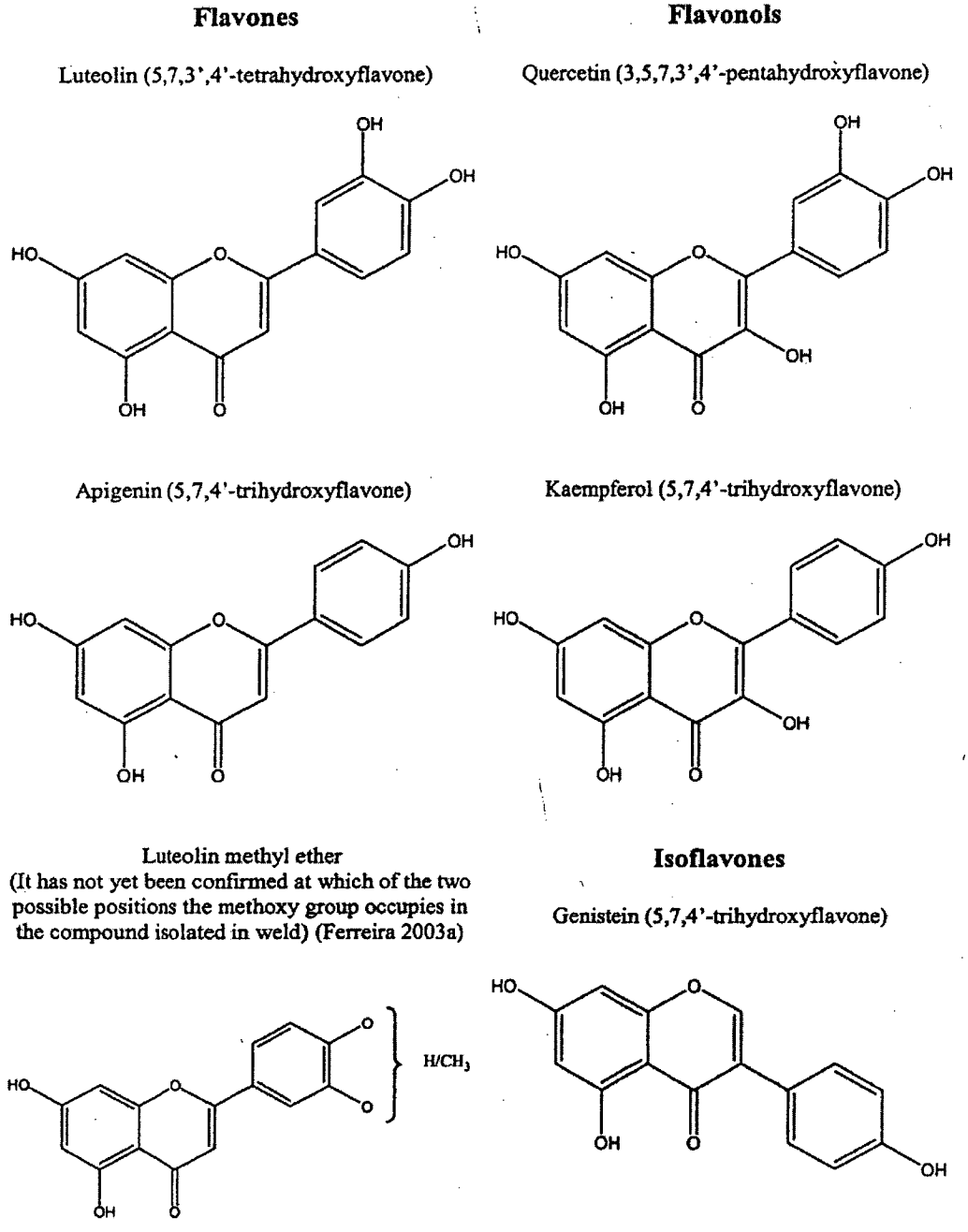

Figure 1 Flavonoids present in some historically important European dye plants.

Table 1 The analytical conditions for the identification of flavonoids using HPLC.

Column	Eluents	Eluent programme	Flow rate (mL min^{-1})
5 µm Sphericlone ODS2	A: 20% (v/v) MeOH(aq) B: MeOH C: 5% (w/v) ortho-phosphoric acid(aq)	0–3 min 67A:23B:10C (isocratic), 3–29 min 0A:90B:10C (linear), 29–30 min 67A:23B:10C (linear) then 5 min equilibration at starting conditions before next injection	1.2

detection of characteristic minor components allows the presence of different dyestuffs to be inferred.

The use of a mass spectrometer equipped with an 'ion trap' analyzer has further confirmed the presence of these species by enabling a molecular mass to be assigned to each of the chromatographed peaks. The ion trap enables yet more information to be gained by breaking the molecular species into smaller fragments by multistep fragmentation, typically in two stages, called MS-MS (or MS^2) or three stages (MS^3). This fragmentation involves loss of characteristic groups in a unique way, thus giving a structural 'fingerprint' for each component (Fig. 3). This technique is a powerful tool for enabling the full or partial chemical structure of previously unknown components to be elucidated. For example, the location of the methoxy group in the luteolin methyl ether was shown to be on the 'B' ring of the flavonoid (Fig. 1) (Ferreira *et al.* 2003a). The structure of unknown degradation products caused by light ageing can be found in a similar manner (Ferreira *et al.* 2002).

The application of HPLC–PDA and LC–MS has enabled the identification of the dye sources in many of the yellow or green yarns sampled from the back of the tapestries selected for MODHT as being weld or dyer's greenweed. From the results for the 14 historic tapestries analyzed so far (a total of 145 samples), some tentative trends for yellow dye sources are being explored (Table 2). For the nine tapestries originating from workshops in Brussels or Bruges in the first half of the 16th century, the use of both weld and dyer's greenweed has

Table 2 Emerging trends in the historical use of yellow dyestuffs.

	Date				
Workshop	<1500	1501–1550	1551–1600	1601–1650	1650–1700
Arras (1)	●	–	–	–	–
Brussels (8)	–	●◆	–	–	–
Bruges (1) (3)	–	●◆	–	●	–
Antwerp (1)	–	–	–	–	●

● Weld; ◆ Dyer's greenweed; (Number of tapestries)

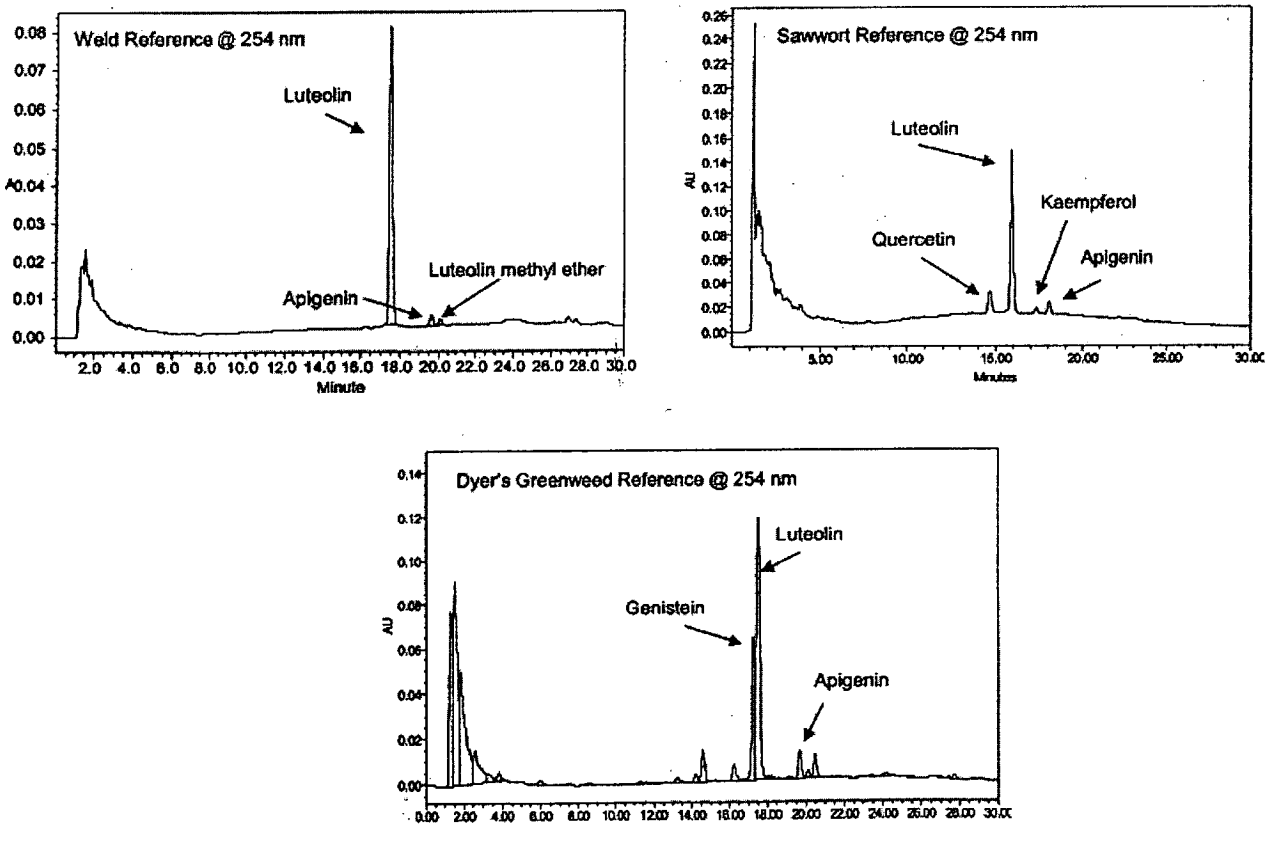

Figure 2 Chromatograms obtained from the acid-hydrolysed extracts of alum-mordanted wool reference dyeings of weld (*Reseda luteola* L.), sawwort (*Serratula tinctoria* L.) and dyer's greenweed (*Genista tinctoria* Gaud.).

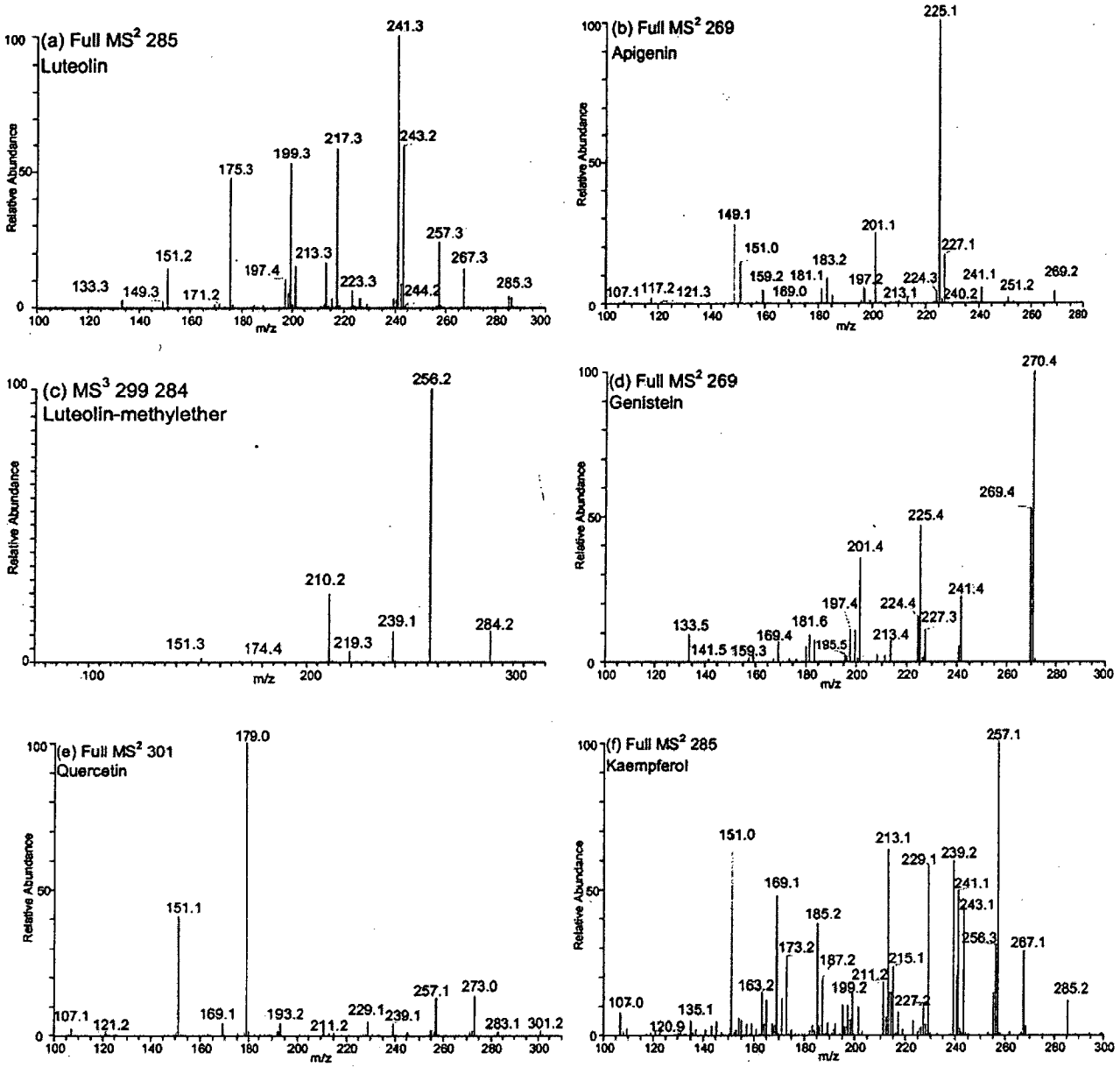

Figure 3 Ion trap fragmentation 'fingerprints' for luteolin, apigenin, luteolin methyl ether, genistein, quercetin and kaempferol.

been found. In the tapestries woven after 1600 from Bruges and Antwerp, and the tapestry woven in Arras before 1500, however, only weld was used with no evidence for dyer's greenweed. If this pattern continues with the analysis of further samples, previously unknown information regarding dyeing practices in different weaving centres at different times will emerge.

Dye source identification is not always so easy. Yellow flavonoid dyes can prove particularly challenging to identify because they are prone to fading caused by chemical damage when exposed to light. Experiments on authentic samples to examine how the dyestuff changes chemically upon ageing and what influences this process form an essential part of MODHT.

Recent research has shown that flavonols in flavonoid dyes on alum-mordanted wool degrade much faster than flavones when exposed to visible light (Ferreira *et al.* 2002). Caution should therefore be exercised when using HPLC–PDA results for the identification of historical dye sources. A study within the MODHT project employs accelerated conditions (experiments conducted at the National Gallery, London) (spectral characteristics of the light box given in Saunders and Kirby 2001) to light-age alum-mordanted wool dyed with weld and with sawwort. After exposure to approximately 10,000 lux of simulated daylight through glass for 4500 hours (equivalent, very approximately, to 60 years exposure at 250 lux for eight hours each day), the two distinguishing flavonols (quercetin and kaempferol) degrade, leaving the HPLC–PDA dye profile of sawwort looking very similar to that of weld (Fig. 4). It is therefore possible that sawwort, a dye plant historically documented as an important alternative to weld (Cardon 1994), has been overlooked analytically for some time. Although the photodegradation pathway is understood and the products of the reaction known to be detectable by HPLC–PDA (Ferreira *et*

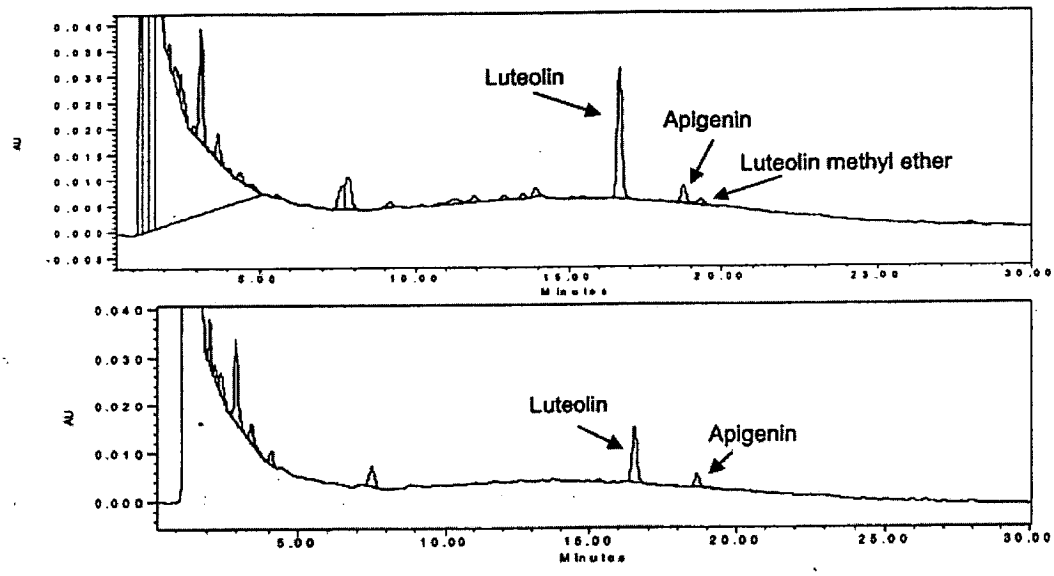

Figure 4 Comparative HPLC–PDA dye profiles for weld and sawwort after exposure to accelerated light-ageing conditions.

al. 2002), the initially small amounts of quercetin and kaempferol present in the MODHT samples make the detection of characteristic photodegradation products difficult. Currently, LC–MS analysis of light-aged tapestry models and historical samples are underway to find other potentially distinguishing features, for example, whether the methyl ether derivatives of luteolin and quercetin are likely to survive at a detectable level after 500 years and so distinguish between these two dye sources. In the context of MODHT, this is important because although extreme photogradation as modelled in the accelerated ageing studies is unlikely to have occurred in the historical samples, since they were taken from the reverse of the tapestries, several show the flavonoid components of weld with other minor coloured peaks. These minor peaks are, as yet, uncharacterised, but may relate to sawwort or other flavonoid dyes.

Accelerated ageing experiments are also in progress for a wide variety of dyes, including young fustic (*Cotinus coggygria* Scop.), identified in a number of dyed silk cores from tapestry metal threads. The development of an analytical method for the identification of neoflavonoid compounds in the fugitive red dyes from brazilwoods (*Caesalpinia* species) and the black dye from logwood (*Haematoxylum campechianum* L.) is also underway. With a better understanding of the chemical changes to dyes caused by light ageing and the ability to detect analytically the degradation products or processes comes the potential to use them as indicators of damage.

Acknowledgements

The authors would like to thank Alan Taylor (University of Edinburgh); Jo Kirby-Atkinson and David Saunders (National Gallery Scientific Department, London); Ester S. B. Ferreira (AMOLF, FOM Institute for Atomic and Molecular Physics, Amsterdam). Funding is gratefully acknowledged from the European Commission FP5.

Note

1. This research project is supported by the European Commission under the Fifth Framework Programme and contributed to the implementation of the Key Action, 'The City of Tomorrow and Cultural Heritage' through the subsection 4.2.1 Improved Damage Assessment of Cultural Heritage within the Energy, Environment and Sustainable Development Programme, contract number EVK4-CT-2001-00048. (The project website can be found at www.hrp.org.uk/webcode/content.asp?ID=706.)

References

Cardon, D. (1994) 'Yellow dyes of historical importance: beginnings of a long-term multi-disciplinary study', *Dyes in History and Archaeology* 13: 59–73.

Ferreira, E. S. B. (2001) *New Approaches Towards the Identification of Yellow Dyes in Ancient Textiles*. PhD thesis, University of Edinburgh.

Ferreira, E. S. B., Quye, A., McNab, H. and Hulme, A. N. (2002) 'Photo-oxidation products of quercetin and morin as markers for the characterisation of natural flavonoid yellow dyes in ancient textiles', *Dyes in History and Archaeology* 18: 63–72.

Ferreira, E. S. B., Quye, A., Hulme, A. N. and McNab, H. (2003a) 'LC–ion trap MS and PDA–HPLC – complementary techniques in the analysis of flavonoid dyes in historical textiles: the case study of an 18th-century herald's tabard', *Dyes in History and Archaeology* 19: 13–18.

Ferreira, E. S. B., Hulme, A. N., McNab, H. and Quye, A. (2003b) 'LC–ion trap MS and PDA–HPLC – complementary techniques in the analysis of different components of flavonoid dyes: the example of Persian berries (*Rhamnus* sp.)', *Dyes in History and Archaeology* 19: 19–24.

Ferreira, E. S. B., Hulme, A. N., McNab, H. and Quye, A. (2004) 'The natural constituents of historical textile dyes', *Chemical Society Reviews* 33: 329–36.

Koren, Z. C. (2001) 'A successful Talmudic-flavored high-performance liquid chromatographic analysis of carthamin from red safflower dyeings', *Dyes in History and Archaeology* 16/17: 158–78.

Quye, A. (in press) 'Monitoring of damage to historic tapestries (MODHT): a newly initiated EU project', *Dyes in History and Archaeology*.

Saunders, D. and Kirby, J. (2001) 'A comparison of light-accelerated ageing regimes in some galleries and museums', *The Conservator* 25: 95–104.

Szostek, B., Orska-Gawrys, J. J., Surowiec, I. and Trojanowicz, M. (2003) 'Investigation of natural dyes occurring in historical Coptic textiles by high-performance liquid chromatography with UV-vis and mass spectrometric detection', *Journal of Chromatography A* 1012: 179–92.

Wouters, J. and Verhecken, A. (1989) 'The coccid insect dyes: HPLC and computerized diode-array analysis of dyed yarns', *Studies in Conservation* 34: 189–200.

The authors

- Alison Hulme is a Senior Lecturer in Chemistry at the University of Edinburgh. Her research interests include the asymmetric synthesis of bioactive natural products, the development of new chiral catalysts, and the chemistry of natural and non-natural dyestuffs.
- Hamish McNab is Reader in Chemistry at the University of Edinburgh. His research has involved the synthetic applications of flash vacuum pyrolysis (FVP) and the chemistry of conjugated systems such as dyestuffs.
- David Peggie is currently working towards a PhD jointly supervised by Drs Hulme, McNab and Quye. His research focuses on the MODHT project, developing analytical methods for the identification of natural dyestuffs and exploring the effects of their degradation.
- Anita Quye works as an organic analytical scientist in the Department of Conservation and Analytical Research of the National Museums of Scotland, applying established and novel analytical techniques to the identification of organic materials in historical and archaeological artifacts. Her specialist research interests include the study of degradative ageing processes on the identification and preservation of natural textile dyes and man-made plastics in museum collections.

Addresses

- Corresponding author: Anita Quye, Department of Conservation and Analytical Research, National Museums of Scotland, Chambers Street, Edinburgh EH1 1JF, UK (a.quye@nms.ac.uk).
- Alison N. Hulme, School of Chemistry, The University of Edinburgh, West Mains Road, Edinburgh EH9 3JJ, UK.
- Hamish McNab, School of Chemistry, The University of Edinburgh, West Mains Road, Edinburgh EH9 3JJ, UK.
- David A. Peggie, Department of Conservation and Analytical Research, National Museums of Scotland, Chambers Street, Edinburgh EH1 1JF, UK.